

Lecture Notes on

# NUMERICAL ANALYSIS of OF NONLINEAR EQUATIONS

Eusebius Doedel

# Persistence of Solutions

We discuss the *persistence* of solutions to nonlinear equations.

- Newton’s method for solving a nonlinear equation

$$\mathbf{G}(\mathbf{u}) = \mathbf{0}, \quad \mathbf{G}(\cdot), \quad \mathbf{u} \in \mathbb{R}^n,$$

may not converge if the “initial guess” is not close to a solution.

- To alleviate this problem one can introduce an artificial “*homotopy*” parameter in the equation.
- Actually, most equations already have parameters.
- We discuss the *persistence* of solutions to such parameter-dependent equations.

# The Implicit Function Theorem

IFT

Let  $\mathbf{G} : \mathbb{R}^n \times \mathbb{R} \rightarrow \mathbb{R}^n$  satisfy  
*two inputs*

- (i)  $\mathbf{G}(\mathbf{u}_0, \lambda_0) = \mathbf{0}$  ,  $\mathbf{u}_0 \in \mathbb{R}^n$  ,  $\lambda_0 \in \mathbb{R}$  .
- (ii)  $\mathbf{G}_{\mathbf{u}}(\mathbf{u}_0, \lambda_0)$  is nonsingular (*i.e.*,  $\mathbf{u}_0$  is an *isolated solution*) ,
- (iii)  $\mathbf{G}$  and  $\mathbf{G}_{\mathbf{u}}$  are smooth near  $\mathbf{u}_0$  .

Then there exists a unique, smooth *solution family*  $\mathbf{u}(\lambda)$  such that

- $\mathbf{G}(\mathbf{u}(\lambda), \lambda) = \mathbf{0}$  , for all  $\lambda$  near  $\lambda_0$  ,
- $\mathbf{u}(\lambda_0) = \mathbf{u}_0$  .

PROOF : See a good Analysis book ...

EXAMPLE: (AUTO demo hom.)

Let

$$g(u, \lambda) = (u^2 - 1)(u^2 - 4) + \lambda u^2 e^{cu},$$

where  $c$  is fixed, e.g.,  $c = 0.1$ .

When  $\lambda = 0$  the equation

$$g(u, 0) = 0,$$

has *four* solutions, namely,

$$u = \pm 1, \quad \text{and} \quad u = \pm 2.$$

We have

$$g_u(u, \lambda) \Big|_{\lambda=0} \equiv \frac{d}{du}(u, \lambda) \Big|_{\lambda=0} = 4u^3 - 10u.$$

Since

$$g_u(u, 0) = 4u^3 - 10u ,$$

we have

$$g_u(-1, 0) = 6 , \quad g_u(1, 0) = -6 ,$$

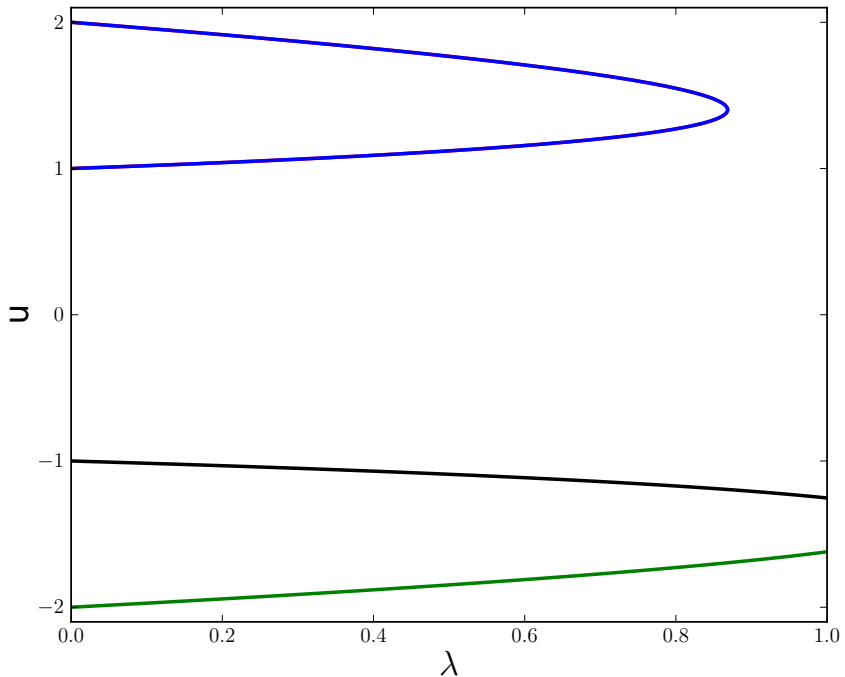
$$g_u(-2, 0) = -12 , \quad g_u(2, 0) = 12 ,$$

which are all nonzero.

Hence each of the four solutions when  $\lambda = 0$  is *isolated*.

Thus each of these solutions *persists* as  $\lambda$  becomes nonzero,

( at least for “small” values of  $|\lambda|$  ).



Four solution families of  $g(u, \lambda) = 0$ . Note the fold.

NOTE:

- Each of the four solutions at  $\lambda = 0$  is *isolated* .
- Thus each of these solutions *persists* as  $\lambda$  becomes nonzero.
- Only two of the four homotopies "reach"  $\lambda = 1$  .
- The two other homotopies meet at a *fold* .
- IFT condition (ii) is not satisfied at this fold. (Why not?)

Consider the equation

$$\mathbf{G}(\mathbf{u}, \lambda) = \mathbf{0}, \quad \mathbf{u}, \mathbf{G}(\cdot, \cdot) \in \mathbb{R}^n, \quad \lambda \in \mathbb{R}.$$

Let

$$\mathbf{x} \equiv (\mathbf{u}, \lambda).$$

Then the equation can be written

$$\mathbf{G}(\mathbf{x}) = \mathbf{0}, \quad \mathbf{G} : \mathbb{R}^{n+1} \rightarrow \mathbb{R}^n.$$

DEFINITION.

A solution  $\mathbf{x}_0$  of  $\mathbf{G}(\mathbf{x}) = \mathbf{0}$  is regular if the matrix

$$\mathbf{G}_{\mathbf{x}}^0 \equiv \mathbf{G}_{\mathbf{x}}(\mathbf{x}_0), \quad (\text{with } n \text{ rows and } n+1 \text{ columns})$$

has maximal rank, i.e., if

$$\text{Rank}(\mathbf{G}_{\mathbf{x}}^0) = n.$$

In the parameter formulation,

$$\mathbf{G}(\mathbf{u}, \lambda) = \mathbf{0} ,$$

we have

$$\text{Rank}(\mathbf{G}_x^0) = \text{Rank}(\mathbf{G}_u^0 | \mathbf{G}_\lambda^0) = n \iff \begin{cases} \text{(i) } \mathbf{G}_u^0 \text{ is nonsingular,} \\ \text{or} \\ \text{(ii) } \begin{cases} \dim \mathcal{N}(\mathbf{G}_u^0) = 1, \\ \text{and} \\ \mathbf{G}_\lambda^0 \notin \mathcal{R}(\mathbf{G}_u^0). \end{cases} \end{cases}$$

IF ↗

Above,

$\mathcal{N}(\mathbf{G}_u^0)$  denotes the *null space* of  $\mathbf{G}_u^0$ ,

and

$\mathcal{R}(\mathbf{G}_u^0)$  denotes the *range* of  $\mathbf{G}_u^0$ ,

i.e., the linear space spanned by the  $n$  columns of  $\mathbf{G}_u^0$ .

$\mathbf{G}_u^0$   $\mathbf{G}_x^0$   $\mathcal{N}$

 THEOREM. Let

$$\mathbf{x}_0 \equiv (\mathbf{u}_0, \lambda_0)$$

I see this page as  
a generalisation of the  
implicit function theorem

be a regular solution of

$$\mathbf{G}(\mathbf{x}) = \mathbf{0}.$$

Then, near  $\mathbf{x}_0$ , there exists a unique one-dimensional *solution family*

$$\mathbf{x}(s) \quad \text{with} \quad \mathbf{x}(0) = \mathbf{x}_0.$$

PROOF. Since

$$\text{Rank}(\mathbf{G}_{\mathbf{x}}^0) = \text{Rank}(\mathbf{G}_{\mathbf{u}}^0 | \mathbf{G}_{\lambda}^0) = n,$$

then either  $\mathbf{G}_{\mathbf{u}}^0$  is nonsingular and by the IFT we have

$$\mathbf{u} = \mathbf{u}(\lambda) \quad \text{near} \quad \mathbf{x}_0,$$

or else we can interchange columns in the Jacobian  $\mathbf{G}_{\mathbf{x}}^0$  to see that the solution can locally be parametrized by one of the components of  $\mathbf{u}$ .

Thus a unique solution family passes through a regular solution.

•

NOTE:

- Such a *solution family* is sometimes also called a *solution branch*.
- Case (ii) above is that of a *simple fold*, to be discussed later.
- Thus even near a simple fold there is a unique solution family.
- However, near such a fold, the family can **not** be parametrized by  $\lambda$ .

So What I get is that

The Case 1 is already that the  $G^0_u$  jacobian is rank n.

But the Case 2 is that the jacobian  $G^0_u$  has one null space (so rank is  $n-1$ ), but it is still in a solution family as the columns of the jacobian  $G^0_x$  can be arranged such that the first n of its columns span the space  $R^n$  (so still rank n).

This is when instead of lambda, one of the components of u is used as parameter.

I can see that, as the instantaneous vertical orientation on a solution family as a fold happens, does not generate a function since for a lambda value you get vertical function (!). However, when you look as the fold from the left, you actually accept the u as parameter and lambda as the variable. So you can still say that this is on a solution branch as the total rank is still n.

EXAMPLE: The  $A \rightarrow B \rightarrow C$  reaction. (AUTO demo abc.)

The equations are

$$u'_1 = -u_1 + D(1 - u_1)e^{u_3},$$

$$u'_2 = -u_2 + D(1 - u_1)e^{u_3} - D\sigma u_2 e^{u_3},$$

$$u'_3 = -u_3 - \beta u_3 + DB(1 - u_1)e^{u_3} + DB\alpha\sigma u_2 e^{u_3},$$

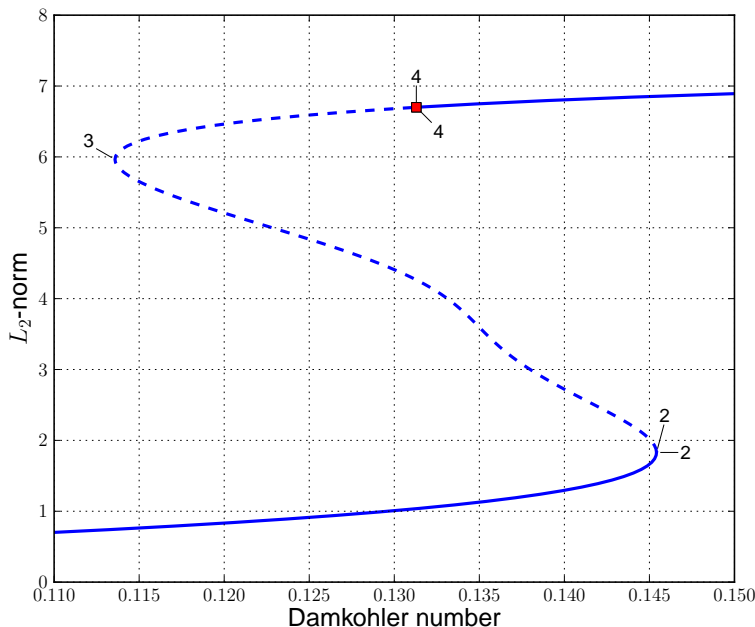
where

$1 - u_1$  is the concentration of  $A$  ,  $u_2$  is the concentration of  $B$  ,

$u_3$  is the temperature,  $\alpha = 1$  ,  $\sigma = 0.04$  ,  $B = 8$  ,

$D$  is the *Damkohler number* ,  $\beta = 1.21$  is the heat transfer coefficient .

We compute *stationary* solutions for varying  $D$ .



Stationary solution families of the  $A \rightarrow B \rightarrow C$  reaction for  $\beta = 1.15$ .

Solid/dashed lines denote stable/unstable solutions.

The red square denotes a Hopf bifurcation.

(`AUTO demo abc`). Note the *two folds*.

# Examples of IFT Application

*Here we give examples where the IFT shows that a given solution persists, at least locally, when a problem parameter is changed. We also identify some cases where the conditions of the IFT are not satisfied.*

# A Predator-Prey Model

(`AUTO demo pp2.`)

$$\begin{cases} u'_1 = 3u_1(1 - u_1) - u_1u_2 - \lambda(1 - e^{-5u_1}), \\ u'_2 = -u_2 + 3u_1u_2. \end{cases}$$

Here  $u_1$  may be thought of as “fish” and  $u_2$  as “sharks”, while the term

$$\lambda(1 - e^{-5u_1}),$$

represents “fishing”, with “fishing-quota”  $\lambda$ .

When  $\lambda = 0$  the *stationary solutions* are

$$\left. \begin{array}{rcl} 3u_1(1 - u_1) - u_1u_2 & = & 0 \\ -u_2 + 3u_1u_2 & = & 0 \end{array} \right\} \Rightarrow (u_1, u_2) = (0, 0), (1, 0), \left(\frac{1}{3}, 2\right).$$

The Jacobian matrix is

$$\mathbf{G}_{\mathbf{u}} = \begin{pmatrix} 3 - 6u_1 & -u_2 & -5\lambda e^{-5u_1} & -u_1 \\ 3u_2 & & & -1 + 3u_1 \end{pmatrix} = \mathbf{G}_{\mathbf{u}}(u_1, u_2; \lambda).$$

$$\mathbf{G}_{\mathbf{u}}(0, 0; 0) = \begin{pmatrix} 3 & 0 \\ 0 & -1 \end{pmatrix}; \text{ eigenvalues } 3, -1 \text{ (unstable)}.$$

$$\mathbf{G}_{\mathbf{u}}(1, 0; 0) = \begin{pmatrix} -3 & -1 \\ 0 & 2 \end{pmatrix}; \text{ eigenvalues } -3, 2 \text{ (unstable)}.$$

$$\mathbf{G}_{\mathbf{u}}\left(\frac{1}{3}, 2; 0\right) = \begin{pmatrix} -1 & -\frac{1}{3} \\ 6 & 0 \end{pmatrix}; \text{ eigenvalues } \begin{cases} (-1 - \mu)(-\mu) + 2 = 0 \\ \mu^2 + \mu + 2 = 0 \\ \mu_{\pm} = \frac{-1 \pm \sqrt{-7}}{2} \\ \text{Re}(\mu_{\pm}) < 0 \end{cases} \text{ (stable).}$$

$$-1/2$$

All three Jacobians at  $\lambda = 0$  are nonsingular.

Thus, by the IFT, all three stationary points persist for (small)  $\lambda \neq 0$ .

In this problem we can *explicitly* find all solutions (see Figure 1) :

Branch I :

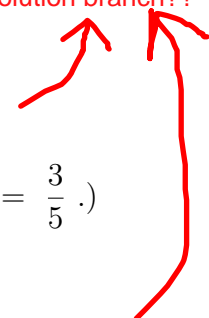
$$(u_1, u_2) = (0, 0).$$

How do I know that one of the dimensions will stay constant for a particular solution branch??

Branch II :

$$u_2 = 0, \quad \lambda = \frac{3u_1(1-u_1)}{1-e^{-5u_1}}.$$

$$\left(\text{Note that } \lim_{u_1 \rightarrow 0} \lambda = \lim_{u_1 \rightarrow 0} \frac{3(1-2u_1)}{5e^{-5u_1}} = \frac{3}{5}.\right)$$



Branch III :

$$u_1 = \frac{1}{3}, \quad \frac{2}{3} - \frac{1}{3}u_2 - \lambda(1-e^{-5/3}) = 0 \Rightarrow u_2 = 2 - 3\lambda(1-e^{-5/3}).$$

What if I substituted  $u_2$  here?

These solution families intersect at two branch points, one of which is

$$(u_1, u_2, \lambda) = (0, 0, 3/5).$$

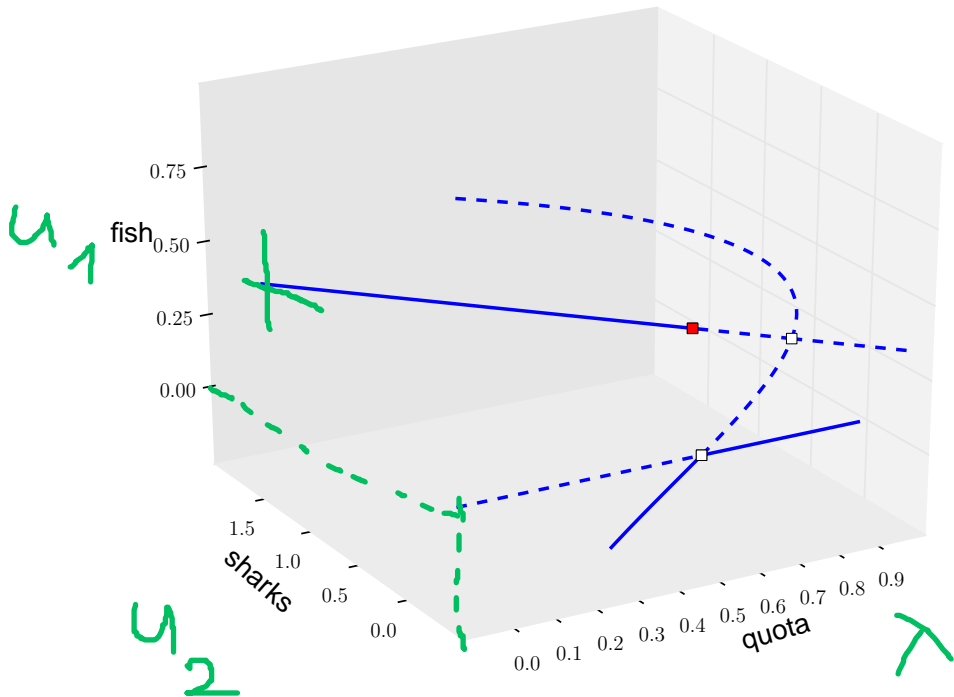


Figure 1: Stationary solution families of the predator-prey model. Solid/dashed lines denote stable/unstable solutions. Note the *fold*, the *bifurcations* (open squares), and the *Hopf bifurcation* (red square).

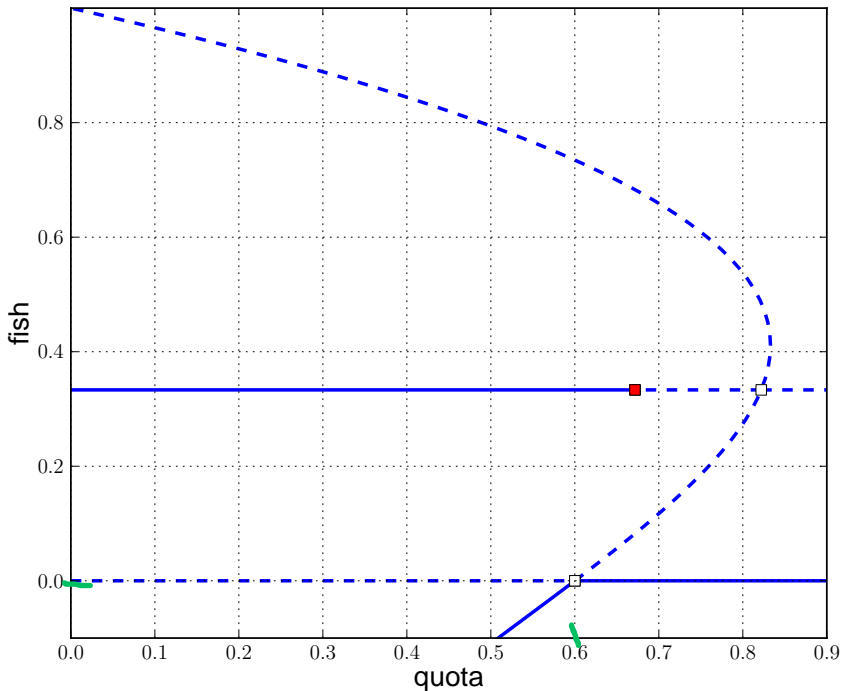


Figure 2: Stationary solution families of the predator-prey model, showing *fish* versus *quota*. Solid/dashed lines denote stable/unstable solutions.

- Stability of branch I :

$$\mathbf{G}_{\mathbf{u}}((0, 0); \lambda) = \begin{pmatrix} 3 - 5\lambda & 0 \\ 0 & -1 \end{pmatrix}; \quad \text{eigenvalues } 3 - 5\lambda, -1.$$

Hence the trivial solution is :

unstable if  $\lambda < 3/5$ ,

and

stable if  $\lambda > 3/5$ ,

as indicated in Figure 2.

- Stability of branch II :

This family has no stable positive solutions.

- Stability of branch III :

At

$$\lambda_H \approx 0.67 ,$$

(the red square in Figure 2) the complex eigenvalues cross the imaginary axis.

This crossing is a *Hopf bifurcation*, a topic to be discussed later.

Beyond  $\lambda_H$  there are *periodic solutions* whose period  $T$  increases as  $\lambda$  increases. (See Figure 4 for some representative periodic orbits.)

The period becomes infinite at  $\lambda = \lambda_\infty \approx 0.70$ .

This final orbit is called a *heteroclinic cycle*.

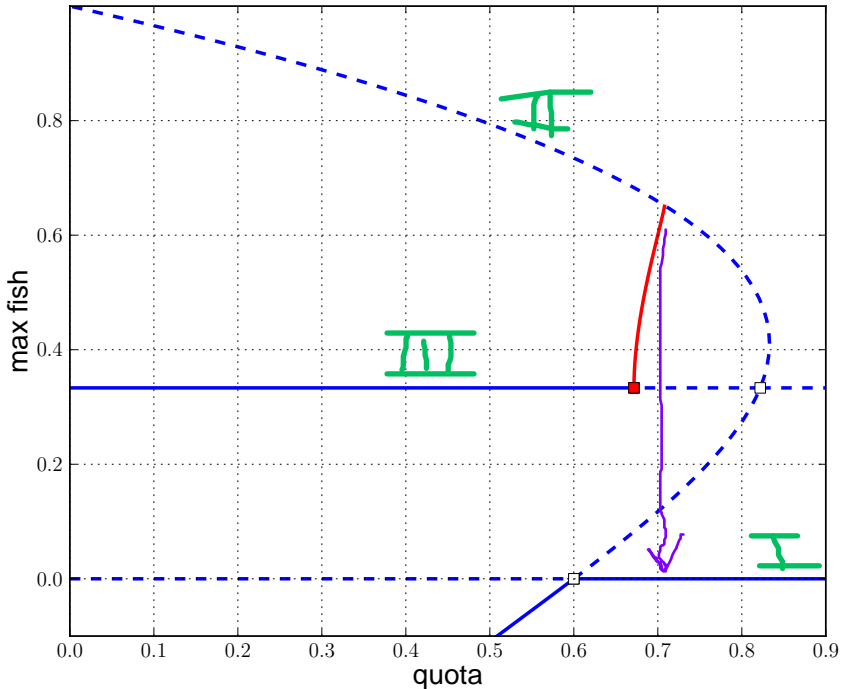


Figure 3: Stationary (blue) and periodic (red) solution families of the predator-prey model.

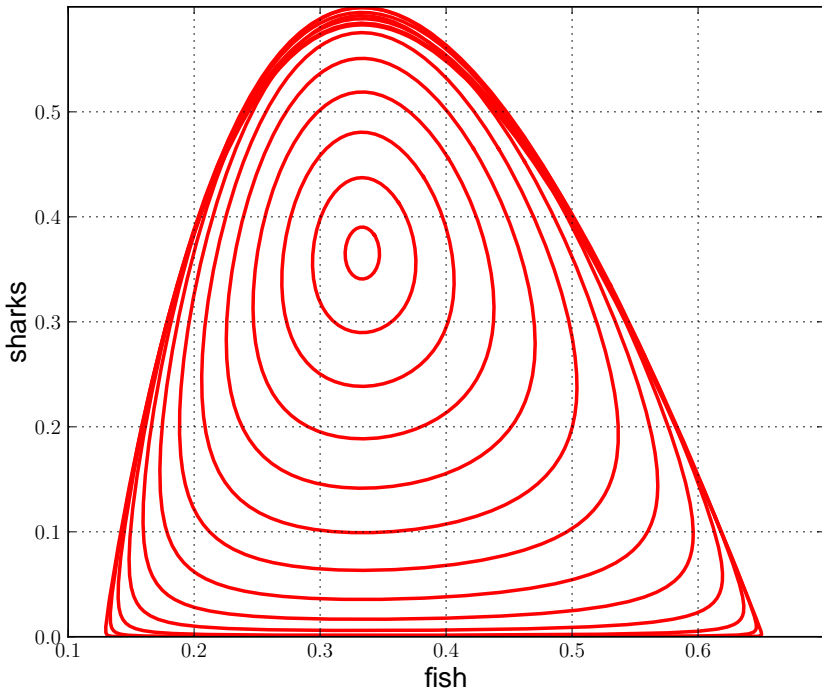


Figure 4: Some periodic solutions of the predator-prey model. The largest orbits are very close to a *heteroclinic cycle*.

From Figure 3 we can deduce the solution behavior for (slowly) increasing  $\lambda$  :

- Branch III is followed until  $\lambda_H \approx 0.67$  .
- Periodic solutions of increasing period until  $\lambda = \lambda_\infty \approx 0.70$  .
- Collapse to trivial solution (Branch I).

EXERCISE.

Use AUTO to repeat the numerical calculations (demo pp2) .

Sketch *phase plane diagrams* for  $\lambda = 0, 0.5, 0.68, 0.70, 0.71$  .

# The Gelfand-Bratu Problem

(AUTO demo exp.)

$$\begin{cases} u''(x) + \lambda e^{u(x)} = 0, & \forall x \in [0, 1], \\ u(0) = u(1) = 0. \end{cases}$$

If  $\lambda = 0$  then  $u(x) \equiv 0$  is a solution.



We'll prove that this solution is isolated, so that there is a continuation

$$u = \tilde{u}(\lambda), \quad \text{for } |\lambda| \text{ small}.$$

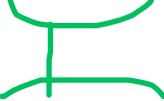
Consider

$$\left. \begin{array}{l} u''(x) + \lambda e^{u(x)} = 0, \\ u(0) = 0, \quad u'(0) = p, \end{array} \right\} \Rightarrow u = u(x; p, \lambda).$$

We want to solve

for  $|\lambda|$  small .

Here

$$\underbrace{u(1; p, \lambda)}_{\equiv G(p, \lambda)} = 0,$$

$$G(0, 0) = 0.$$

The solution with  $p$  and  $\lambda$  while keeping  $x 1$ . BN

This is our new assumed system, in place of the original system. BN

We must show (IFT) that

$$G_p(0, 0) \equiv u_p(1; 0, 0) \neq 0 :$$

$$\left. \begin{aligned} u_p''(x) + \lambda_0 e^{u_0(x)} u_p(x) &= 0, \\ u_p(0) = 0, \quad u_p'(0) &= 1, \end{aligned} \right\} \text{ where } u_0(x) \equiv 0.$$

Now  $u_p(x; 0, 0)$  satisfies

$$\left. \begin{aligned} u_p''(x) &= 0, \\ u_p(0) = 0, \quad u_p'(0) &= 1. \end{aligned} \right.$$

Hence

$$u_p(x; 0, 0) = x, \quad u_p(1; 0, 0) = 1 \neq 0.$$

EXERCISE. Compute the solution family of the Gelfand-Bratu problem as represented in Figures 5 and 6. (AUTO demo exp.)

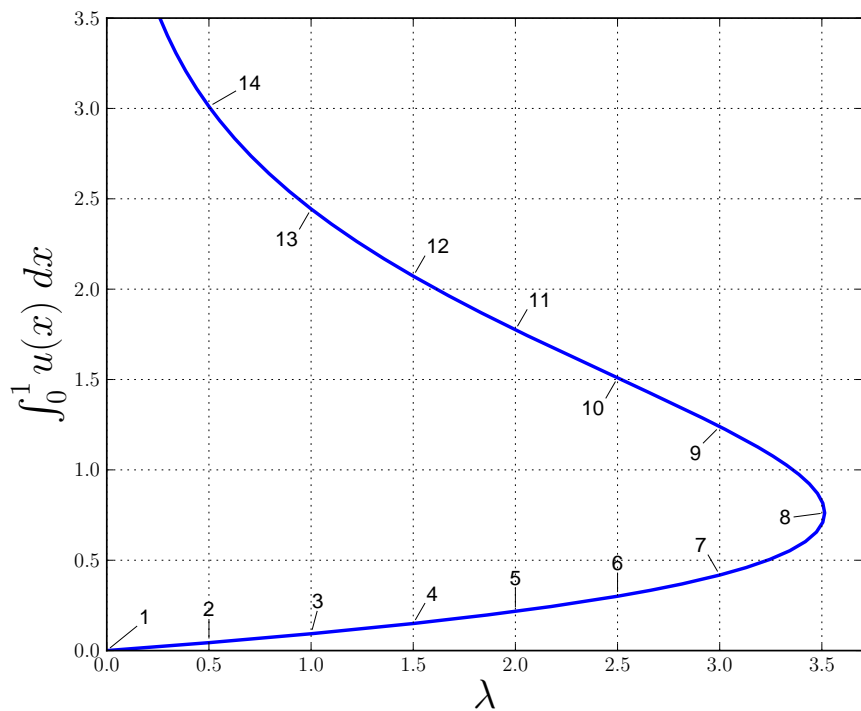


Figure 5: Bifurcation diagram of the Gelfand-Bratu equation.

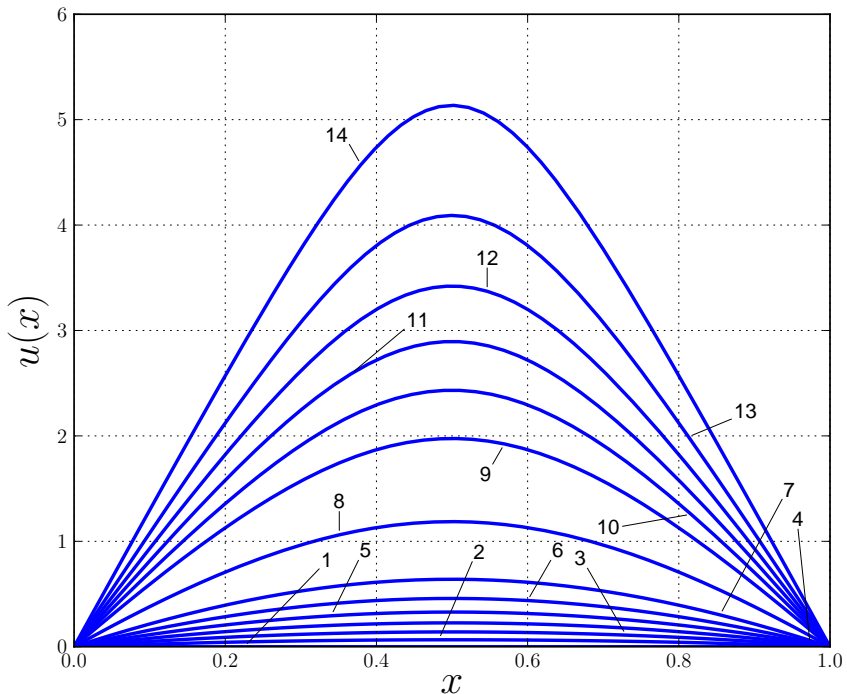


Figure 6: Some solutions to the Gelfand-Bratu equation.

# A Nonlinear Eigenvalue Problem

(AUTO demo nev.)

Consider the nonlinear boundary value problem

$$\begin{cases} u'' + \lambda(u + u^2) = 0, \\ u(0) = u(1) = 0, \end{cases}$$

which has  $u(t) \equiv 0$  as solution for all  $\lambda$ .

Equivalently, we want the solution

$$u = u(t; p, \lambda),$$

of the initial value problem

$$\begin{cases} u'' + \lambda(u + u^2) = 0, \\ u(0) = 0, \quad u'(0) = p, \end{cases}$$

that satisfies

$$G(p, \lambda) \equiv u(1; p, \lambda) = 0.$$

Here

$$G : \mathbb{R} \times \mathbb{R} \rightarrow \mathbb{R},$$

with

$$G(0, \lambda) = 0, \quad \text{for all } \lambda.$$

Let

$$u_p(t; p, \lambda) = \frac{du}{dp}(t; p, \lambda),$$

$$G_p(p, \lambda) = u_p(1; p, \lambda).$$

Then  $u_p$  ( $= u_p^0$ ) satisfies

$$\begin{cases} u_p'' + \lambda (1 + 2u) u_p = 0, \\ u_p(0) = 0, \quad u_p'(0) = 1, \end{cases}$$

which, about  $u \equiv 0$ , gives

$$\begin{cases} u_p'' + \lambda u_p = 0, \\ u_p(0) = 0, \quad u_p'(0) = 1. \end{cases}$$

By the variation of parameters formula

$$u_p(t; p, \lambda) = \frac{\sin \sqrt{\lambda} t}{\sqrt{\lambda}}, \quad \lambda \geq 0, \quad (\text{independent of } p).$$

$$G_p(0, \lambda) = u_p(1; p, \lambda) = \frac{\sin(\sqrt{\lambda})}{\sqrt{\lambda}} = 0, \quad \text{if } \lambda = \lambda_k \equiv (k\pi)^2.$$

Thus the conditions of the IFT fail to be satisfied at  $\lambda_k = (k\pi)^2$ .

(We will see that these solutions are branch points.)

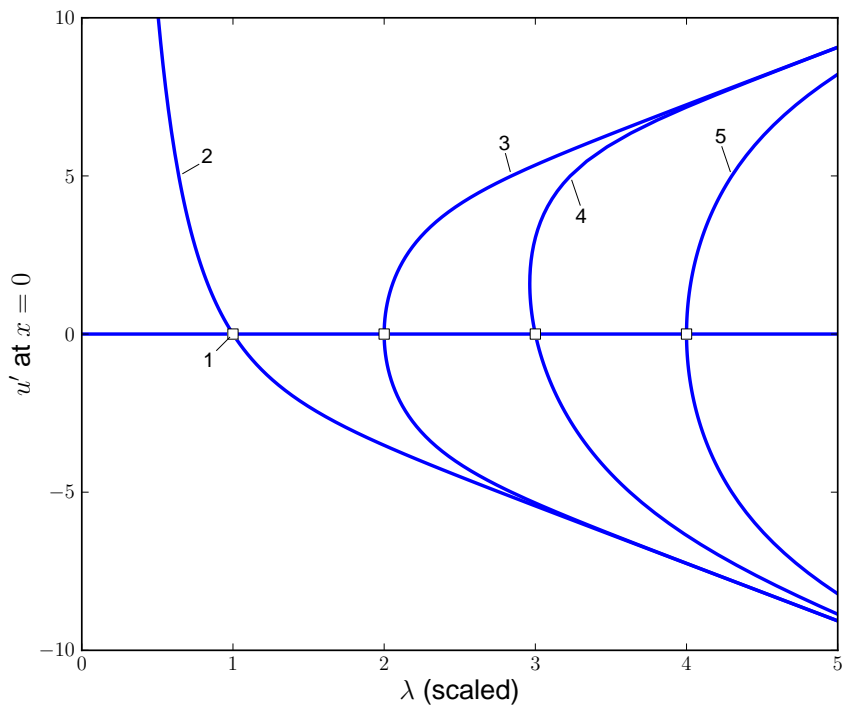


Figure 7: Solution families to the nonlinear eigenvalue problem.

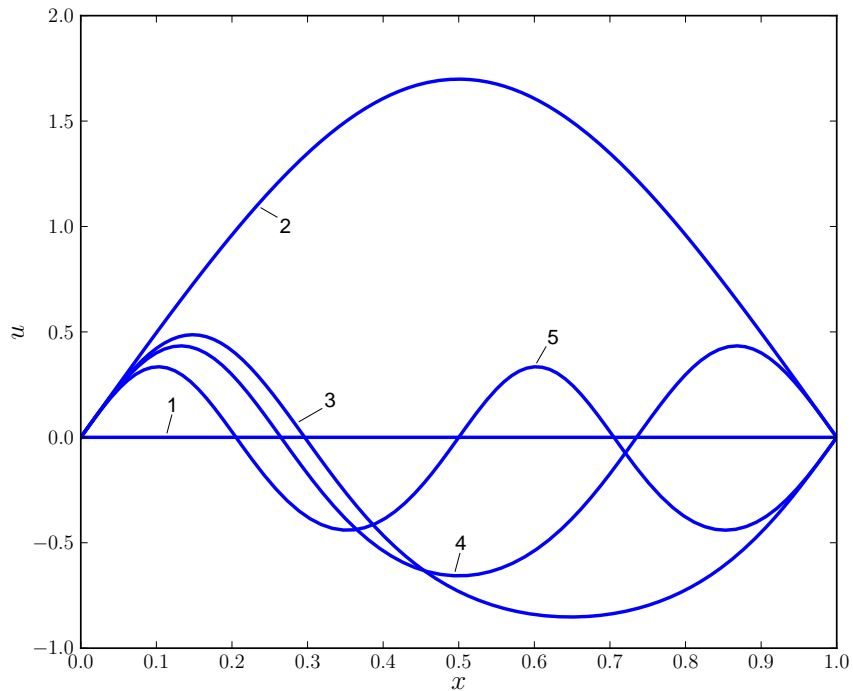


Figure 8: Some solutions to the nonlinear eigenvalue problem.



# Numerical Continuation

Here we discuss algorithms for computing families of solutions to nonlinear equations. The IFT is important in the design of such continuation methods.

- Newton’s method for solving a nonlinear equation

$$\mathbf{G}(\mathbf{u}) = \mathbf{0}, \quad \mathbf{G}(\cdot), \mathbf{u} \in \mathbb{R}^n,$$

may not converge if the “initial guess” is not close to a solution.

- To deal with this one can introduce a “*homotopy parameter*” .
- Most equations already naturally have parameters.
- We now discuss computing such *families of solutions*.

Consider the equation

$$\mathbf{G}(\mathbf{u}, \lambda) = \mathbf{0}, \quad \mathbf{u}, \mathbf{G}(\cdot, \cdot) \in \mathbb{R}^n, \quad \lambda \in \mathbb{R}.$$

Let

$$\mathbf{x} \equiv (\mathbf{u}, \lambda).$$

Then the equation can be written

$$\mathbf{G}(\mathbf{x}) = \mathbf{0}, \quad \mathbf{G} : \mathbb{R}^{n+1} \rightarrow \mathbb{R}^n.$$

DEFINITION.

A solution  $\mathbf{x}_0$  of  $\mathbf{G}(\mathbf{x}) = \mathbf{0}$  is *regular* if the  $n$  (rows) by  $n + 1$  (columns) matrix

$$\mathbf{G}_{\mathbf{x}}^0 \equiv \mathbf{G}_{\mathbf{x}}(\mathbf{x}_0),$$

has maximal rank, *i.e.*, if

$$\text{Rank}(\mathbf{G}_{\mathbf{x}}^0) = n.$$

In the parameter formulation,

$$\mathbf{G}(\mathbf{u}, \lambda) = \mathbf{0} ,$$

we have

$$\text{Rank}(\mathbf{G}_{\mathbf{x}}^0) = \text{Rank}(\mathbf{G}_{\mathbf{u}}^0 \mid \mathbf{G}_{\lambda}^0) = n \iff \begin{cases} \text{(i)} & \mathbf{G}_{\mathbf{u}}^0 \text{ is nonsingular,} \\ \text{or} \\ \text{(ii)} & \begin{cases} \dim \mathcal{N}(\mathbf{G}_{\mathbf{u}}^0) = 1, \\ \text{and} \\ \mathbf{G}_{\lambda}^0 \notin \mathcal{R}(\mathbf{G}_{\mathbf{u}}^0) . \end{cases} \end{cases}$$

Above,

$\mathcal{N}(\mathbf{G}_{\mathbf{u}}^0)$  denotes the *null space* of  $\mathbf{G}_{\mathbf{u}}^0$ ,

and

$\mathcal{R}(\mathbf{G}_{\mathbf{u}}^0)$  denotes the *range* of  $\mathbf{G}_{\mathbf{u}}^0$ ,

*i.e.*, the linear space spanned by the  $n$  columns of  $\mathbf{G}_{\mathbf{u}}^0$ .

**THEOREM.** Let

$$\mathbf{x}_0 \equiv (\mathbf{u}_0, \lambda_0)$$

be a regular solution of

$$\mathbf{G}(\mathbf{x}) = \mathbf{0}.$$

Then, near  $\mathbf{x}_0$ , there exists a unique one-dimensional continuum of solutions

$$\mathbf{x}(s) \quad \text{with} \quad \mathbf{x}(0) = \mathbf{x}_0.$$

**PROOF.** Since

$$\text{Rank}(\mathbf{G}_{\mathbf{x}}^0) = \text{Rank}(\mathbf{G}_{\mathbf{u}}^0 | \mathbf{G}_{\lambda}^0) = n,$$

then either  $\mathbf{G}_{\mathbf{u}}^0$  is nonsingular and by the IFT we have

$$\mathbf{u} = \mathbf{u}(\lambda) \quad \text{near} \quad \mathbf{x}_0,$$

or else we can interchange columns in the Jacobian  $\mathbf{G}_{\mathbf{x}}^0$  to see that the solution can locally be parametrized by one of the components of  $\mathbf{u}$ .

Thus a unique solution family passes through a regular solution. •

NOTE:

- Such a continuum of solutions is called a *solution family* or a *solution branch*.
- Case (ii) above, namely,

$$\dim \mathcal{N}(\mathbf{G}_{\mathbf{u}}^0) = 1 \quad \text{and} \quad \mathbf{G}_{\lambda}^0 \notin \mathcal{R}(\mathbf{G}_{\mathbf{u}}^0),$$

is that of a *simple fold*, to be discussed later.



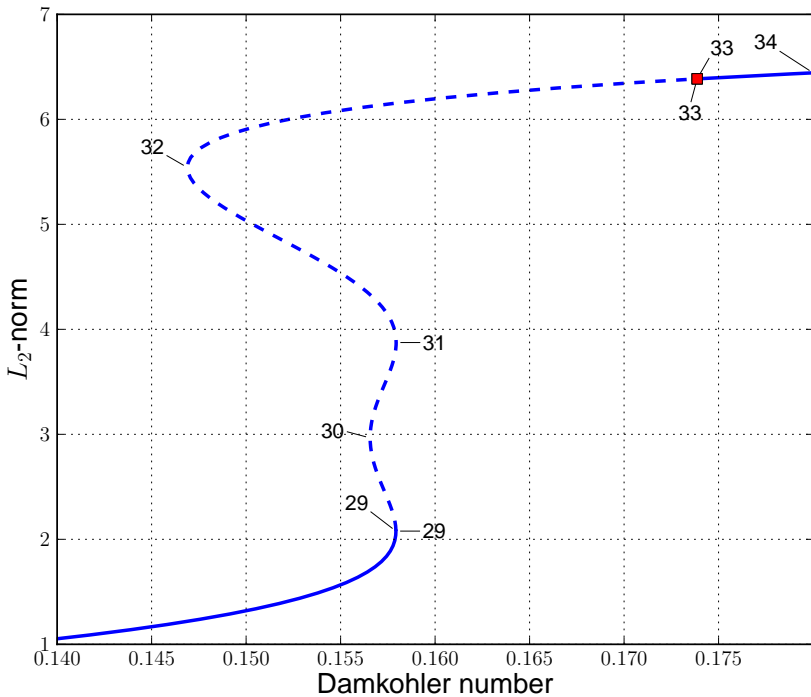


Figure 9: A solution family with four folds. (AUTO demo abc with  $\beta = 1.25$ .)

# Parameter Continuation

Here the continuation parameter is taken to be  $\lambda$ .

Suppose we have a solution  $(\mathbf{u}_0, \lambda_0)$  of

$$\mathbf{G}(\mathbf{u}, \lambda) = \mathbf{0},$$

as well as the direction vector  $\dot{\mathbf{u}}_0$ .

Here

$$\dot{\mathbf{u}} \equiv \frac{d\mathbf{u}}{d\lambda}.$$

We want to compute the solution  $\mathbf{u}_1$  at  $\lambda_1 \equiv \lambda_0 + \Delta\lambda$ .

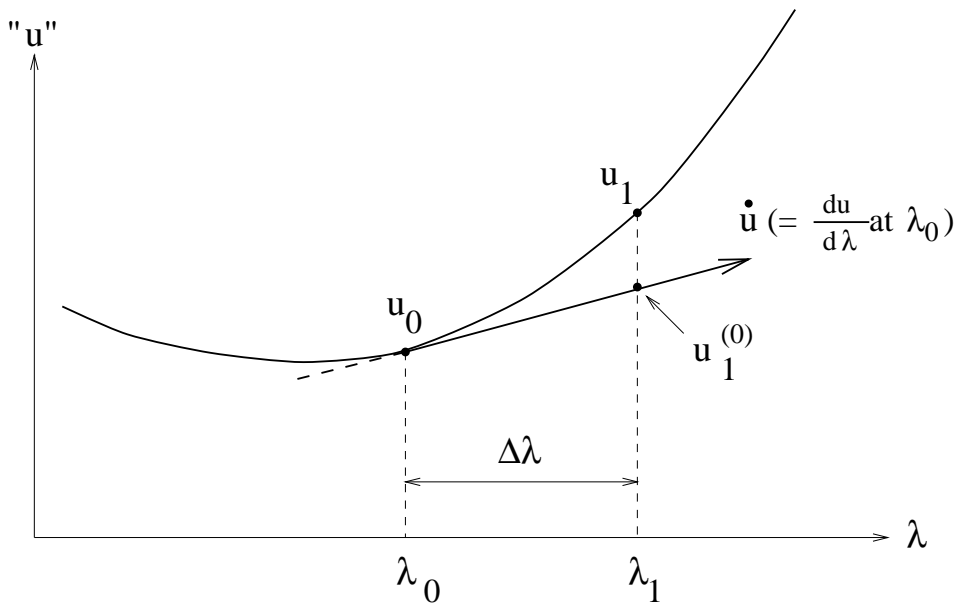


Figure 10: Graphical interpretation of parameter-continuation.

To solve the equation

$$\mathbf{G}(\mathbf{u}_1, \lambda_1) = \mathbf{0},$$

for  $\mathbf{u}_1$  (with  $\lambda = \lambda_1$  fixed) we use Newton's method

$$\begin{aligned}\mathbf{G}_{\mathbf{u}}(\mathbf{u}_1^{(\nu)}, \lambda_1) \Delta \mathbf{u}_1^{(\nu)} &= -\mathbf{G}(\mathbf{u}_1^{(\nu)}, \lambda_1), \\ \mathbf{u}_1^{(\nu+1)} &= \mathbf{u}_1^{(\nu)} + \Delta \mathbf{u}_1^{(\nu)}. \quad \nu = 0, 1, 2, \dots.\end{aligned}$$

As initial approximation use

$$\mathbf{u}_1^{(0)} = \mathbf{u}_0 + \Delta \lambda \dot{\mathbf{u}}_0.$$

If

$$\mathbf{G}_{\mathbf{u}}(\mathbf{u}_1, \lambda_1) \text{ is nonsingular ,}$$

and  $\Delta \lambda$  sufficiently small, then the Newton convergence theory guarantees that this iteration will converge.

After convergence, the new direction vector  $\dot{\mathbf{u}}_1$  can be computed by solving

$$\mathbf{G}_\mathbf{u}(\mathbf{u}_1, \lambda_1) \dot{\mathbf{u}}_1 = -\mathbf{G}_\lambda(\mathbf{u}_1, \lambda_1).$$

This equation follows from differentiating

$$\mathbf{G}(\mathbf{u}(\lambda), \lambda) = \mathbf{0},$$

with respect to  $\lambda$  at  $\lambda = \lambda_1$ .

NOTE:

- ☞  $\dot{\mathbf{u}}_1$  can be computed without another *LU*-factorization of  $\mathbf{G}_\mathbf{u}(\mathbf{u}_1, \lambda_1)$ .  
LU-factorisation was used here to take the inverse of the  $\mathbf{G}_\mathbf{u}$  during the iterations. With  $\mathbf{u}_1$  converged, you have the  $\mathbf{G}_\mathbf{u}(\mathbf{u}_1, \lambda_1)$  already, and its inverse is in your hand.
- ☞ Thus the extra work to find  $\dot{\mathbf{u}}_1$  is negligible.

EXAMPLE: The Gelfand-Bratu problem (AUTO demo exp) :

$$u''(x) + \lambda e^{u(x)} = 0 \quad \text{for } x \in [0, 1] , \quad u(0) = 0 , \quad u(1) = 0 .$$

If  $\lambda = 0$  then  $u(x) \equiv 0$  is an isolated solution.

Discretize by introducing a mesh ,

$$0 = x_0 < x_1 < \cdots < x_N = 1 ,$$

$$x_j - x_{j-1} = h , \quad (1 \leq j \leq N) , \quad h = 1/N .$$

The discrete equations are :

$$\frac{u_{j+1} - 2u_j + u_{j-1}}{h^2} + \lambda e^{u_j} = 0 , \quad j = 1, \dots, N-1 ,$$

with  $u_0 = u_N = 0$  .

Let

$$\mathbf{u} \equiv \begin{pmatrix} u_1 \\ u_2 \\ \vdots \\ u_{N-1} \end{pmatrix} .$$

Then we can write the above as

$$\mathbf{G}(\mathbf{u}, \lambda) = \mathbf{0},$$

where

$$\mathbf{G} : \mathbb{R}^n \times \mathbb{R} \rightarrow \mathbb{R}^n, \quad n \equiv N - 1.$$

**Parameter-continuation :** Suppose we have

$$\lambda_0, \mathbf{u}_0, \text{ and } \dot{\mathbf{u}}_0.$$

Set

$$\lambda_1 = \lambda_0 + \Delta\lambda.$$

Newton's method :

$$\mathbf{G}_{\mathbf{u}}(\mathbf{u}_1^{(\nu)}, \lambda_1) \Delta \mathbf{u}_1^{(\nu)} = -\mathbf{G}(\mathbf{u}_1^{(\nu)}, \lambda_1),$$
$$\mathbf{u}_1^{(\nu+1)} = \mathbf{u}_1^{(\nu)} + \Delta \mathbf{u}_1^{(\nu)},$$

$\nu = 0, 1, 2, \dots,$

with

$$\mathbf{u}_1^{(0)} = \mathbf{u}_0 + \Delta\lambda \dot{\mathbf{u}}_0.$$

After convergence find  $\dot{\mathbf{u}}_1$  from

$$\mathbf{G}_{\mathbf{u}}(\mathbf{u}_1, \lambda_1) \dot{\mathbf{u}}_1 = -\mathbf{G}_{\lambda}(\mathbf{u}_1, \lambda_1).$$

Repeat the above procedure to find  $\mathbf{u}_2, \mathbf{u}_3, \dots$ .

$$\mathbf{u}_1, \mathbf{u}_2, \mathbf{u}_3 = \begin{Bmatrix} \mathbf{u}_1 \\ \mathbf{u}_2 \\ \vdots \\ \mathbf{u}_3 \end{Bmatrix}$$

Here

$$\mathbf{G}_u(\mathbf{u}, \lambda) = \begin{pmatrix} -\frac{2}{h^2} + \lambda e^{u_1} & \frac{1}{h^2} & & \\ \frac{1}{h^2} & -\frac{2}{h^2} + \lambda e^{u_2} & \frac{1}{h^2} & \\ & \ddots & \ddots & \\ & & \ddots & \\ & & & \frac{1}{h^2} - \frac{2}{h^2} + \lambda e^{u_{N-1}} \end{pmatrix}.$$

Thus we must solve a tridiagonal system for each Newton iteration.

The solution family has a fold where the parameter-continuation method fails.  
(**AUTO** demo exp: See the earlier Figures 5 and 6).

# Keller's Pseudo-Arclength Continuation

Compare to the description in 2001 vonGroll Ewins.

This method allows continuation of a solution family past a fold.

Suppose we have a solution  $(\mathbf{u}_0, \lambda_0)$  of

$$\mathbf{G}(\mathbf{u}, \lambda) = \mathbf{0},$$

as well as the direction vector  $(\dot{\mathbf{u}}_0, \dot{\lambda}_0)$  of the solution branch.

$\dot{\mathbf{u}} = \frac{d\mathbf{u}}{d\alpha}$  ;  $\dot{\lambda} = \frac{d\lambda}{d\alpha}$

= Tangent vector  
von Groll-Ewins

Pseudo-arclength continuation solves the following equations for  $(\mathbf{u}_1, \lambda_1)$ :

$$\mathbf{G}(\mathbf{u}_1, \lambda_1) = \mathbf{0},$$

$$(\mathbf{u}_1 - \mathbf{u}_0)^* \dot{\mathbf{u}}_0 + (\lambda_1 - \lambda_0) \dot{\lambda}_0 - \Delta s = 0.$$

This equation is the same  
as the eq15 of 2001  
vonGroll Ewins article.

See Figure 11 for a graphical interpretation.

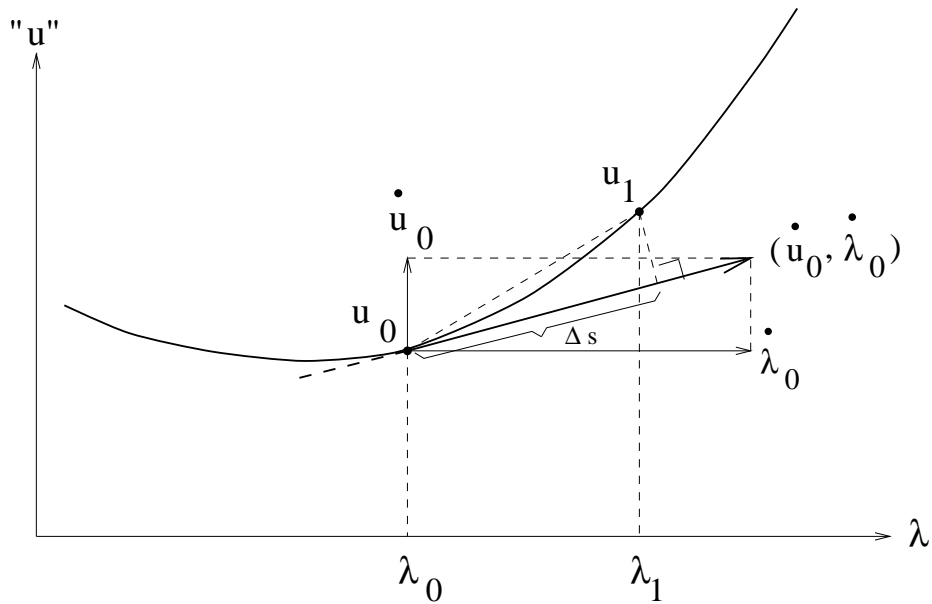


Figure 11: Graphical interpretation of pseudo-arclength continuation.

Solve the equations

$$\mathbf{G}(\mathbf{u}_1, \lambda_1) = \mathbf{0},$$

$$(\mathbf{u}_1 - \mathbf{u}_0)^* \dot{\mathbf{u}}_0 + (\lambda_1 - \lambda_0) \dot{\lambda}_0 - \Delta s = 0.$$

for  $(\mathbf{u}_1, \lambda_1)$  by Newton's method:

$$\begin{pmatrix} (\mathbf{G}_{\mathbf{u}}^1)^{(\nu)} & (\mathbf{G}_{\lambda}^1)^{(\nu)} \\ \dot{\mathbf{u}}_0^* & \dot{\lambda}_0 \end{pmatrix} \begin{pmatrix} \Delta \mathbf{u}_1^{(\nu)} \\ \Delta \lambda_1^{(\nu)} \end{pmatrix} = - \begin{pmatrix} \mathbf{G}(\mathbf{u}_1^{(\nu)}, \lambda_1^{(\nu)}) \\ (\mathbf{u}_1^{(\nu)} - \mathbf{u}_0)^* \dot{\mathbf{u}}_0 + (\lambda_1^{(\nu)} - \lambda_0) \dot{\lambda}_0 - \Delta s \end{pmatrix}.$$

Next direction vector :

$$\begin{pmatrix} \mathbf{G}_{\mathbf{u}}^1 & \mathbf{G}_{\lambda}^1 \\ \dot{\mathbf{u}}_0^* & \dot{\lambda}_0 \end{pmatrix} \begin{pmatrix} \dot{\mathbf{u}}_1 \\ \dot{\lambda}_1 \end{pmatrix} = \begin{pmatrix} \mathbf{0} \\ 1 \end{pmatrix}.$$

NOTE:

- In practice  $(\dot{\mathbf{u}}_1, \dot{\lambda}_1)$  can be computed with one extra backsubstitution.
- The orientation of the branch is preserved if  $\Delta s$  is sufficiently small.
- The direction vector must be rescaled, so that indeed  $\| \dot{\mathbf{u}}_1 \|^2 + \dot{\lambda}_1^2 = 1$ .

## THEOREM.

The *Jacobian* of the pseudo-arc length system is *nonsingular* at a *regular* solution point.

PROOF. Let

$$\mathbf{x} \equiv (\mathbf{u}, \lambda) \in \mathbb{R}^{n+1} .$$

Then pseudo-arc length continuation can be written as

$$\mathbf{G}(\mathbf{x}_1) = 0 ,$$

$$(\mathbf{x}_1 - \mathbf{x}_0)^* \dot{\mathbf{x}}_0 - \Delta s = 0 , \quad (\| \dot{\mathbf{x}}_0 \| = 1 ) .$$

(See Figure 12 for a graphical interpretation.)

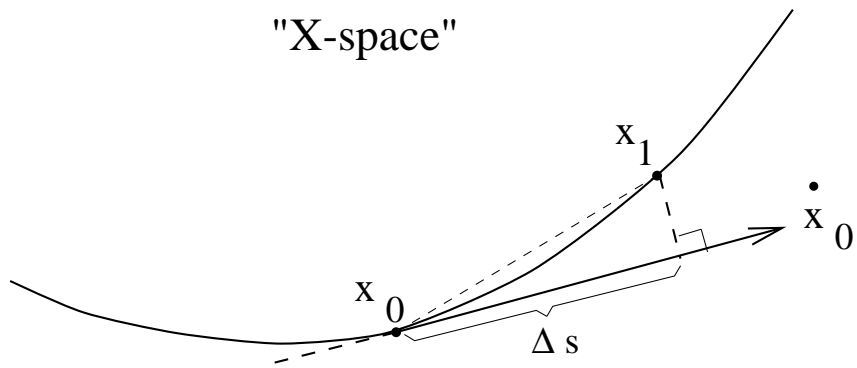


Figure 12: Parameter-independent pseudo-arc length continuation.

The matrix in Newton's method at  $\Delta s = 0$  is

$$\begin{pmatrix} \mathbf{G}_{\mathbf{x}}^0 \\ \dot{\mathbf{x}}_0^* \end{pmatrix}.$$

At a regular solution we have

$$\mathcal{N}(\mathbf{G}_{\mathbf{x}}^0) = \text{Span}\{\dot{\mathbf{x}}_0\}.$$

We must show that

$$\begin{pmatrix} \mathbf{G}_{\mathbf{x}}^0 \\ \dot{\mathbf{x}}_0^* \end{pmatrix}$$

is nonsingular at a regular solution.

If on the contrary

$$\begin{pmatrix} \mathbf{G}_{\mathbf{x}}^0 \\ \dot{\mathbf{x}}_0^* \end{pmatrix}$$

is singular then

$$\mathbf{G}_{\mathbf{x}}^0 \mathbf{z} = 0 \quad \text{and} \quad \dot{\mathbf{x}}_0^* \mathbf{z} = 0,$$

for some vector  $\mathbf{z} \neq \mathbf{0}$ .

Thus

$$\mathbf{z} = c \dot{\mathbf{x}}_0, \quad \text{for some constant } c.$$

But then

$$0 = \dot{\mathbf{x}}_0^* \mathbf{z} = c \dot{\mathbf{x}}_0^* \dot{\mathbf{x}}_0 = c \|\dot{\mathbf{x}}_0\|^2 = c,$$

so that  $\mathbf{z} = \mathbf{0}$ , which is a contradiction. •

## EXAMPLE:

Use pseudo-arclength continuation for the discretized Gelfand-Bratu problem.

Then the matrix

$$\begin{pmatrix} \mathbf{G}_x \\ \dot{\mathbf{x}}^* \end{pmatrix} = \begin{pmatrix} \mathbf{G}_u & \mathbf{G}_\lambda \\ \dot{\mathbf{u}}^* & \dot{\lambda} \end{pmatrix},$$

in Newton's method is a “bordered tridiagonal” matrix :

$$\begin{pmatrix} \circ & \circ & & & & & & & \circ \\ \circ & \circ & \circ & & & & & & \circ \\ & \circ & \circ & \circ & & & & & \circ \\ & & \circ & \circ & \circ & & & & \circ \\ & & & \circ & \circ & \circ & & & \circ \\ & & & & \circ & \circ & \circ & & \circ \\ & & & & & \circ & \circ & \circ & \circ \\ & & & & & & \circ & \circ & \circ \\ \circ & \circ \end{pmatrix}.$$

# Following Folds

When a parameter passes a fold, then the behavior of a system can change drastically. Thus it is useful to determine how the location of a fold changes when a second parameter changes, *i.e.*, we want to compute a “critical stability curve”, or a “locus of fold points”, in 2-parameter space.

# Simple Folds

A regular solution  $\mathbf{x}_0 \equiv (\mathbf{u}_0, \lambda_0)$  of  $\mathbf{G}(\mathbf{u}, \lambda) = \mathbf{0}$ , is called a *simple fold* if

$$\dim \mathcal{N}(\mathbf{G}_{\mathbf{u}}^0) = 1 \quad \text{and} \quad \mathbf{G}_{\lambda}^0 \notin \mathcal{R}(\mathbf{G}_{\mathbf{u}}^0).$$

From differentiating

$$\mathbf{G}(\mathbf{u}(s), \lambda(s)) = \mathbf{0},$$

we have

$$\mathbf{G}_{\mathbf{u}}(\mathbf{u}(s), \lambda(s)) \dot{\mathbf{u}}(s) + \mathbf{G}_{\lambda}(\mathbf{u}(s), \lambda(s)) \dot{\lambda}(s) = \mathbf{0}.$$

In particular,

$$\mathbf{G}_{\mathbf{u}}^0 \dot{\mathbf{u}}_0 = -\dot{\lambda}_0 \mathbf{G}_{\lambda}^0.$$

At a fold we have  $\mathbf{G}_{\lambda}^0 \notin \mathcal{R}(\mathbf{G}_{\mathbf{u}}^0)$ . Thus

$$\boxed{\dot{\lambda}_0 = 0}.$$

Hence  $\mathbf{G}_{\mathbf{u}}^0 \dot{\mathbf{u}}_0 = 0$ . Thus, since  $\dim \mathcal{N}(\mathbf{G}_{\mathbf{u}}^0) = 1$ , we have

$$\mathcal{N}(\mathbf{G}_{\mathbf{u}}^0) = \text{Span}\{\dot{\mathbf{u}}_0\}.$$

Differentiating again, we have

$$\mathbf{G}_{\mathbf{u}}^0 \ddot{\mathbf{u}}_0 + \mathbf{G}_\lambda^0 \ddot{\lambda}_0 + \mathbf{G}_{\mathbf{uu}}^0 \dot{\mathbf{u}}_0 \dot{\mathbf{u}}_0 + 2\mathbf{G}_{u\lambda}^0 \dot{\mathbf{u}}_0 \dot{\lambda}_0 + \mathbf{G}_{\lambda\lambda}^0 \dot{\lambda}_0 \dot{\lambda}_0 = 0.$$

At a simple fold  $(\mathbf{u}_0, \lambda_0)$  let

$$\mathcal{N}(\mathbf{G}_{\mathbf{u}}^0) = \text{Span}\{\phi\}, \quad (\phi = \dot{\mathbf{u}}_0),$$

and

$$\mathcal{N}((\mathbf{G}_{\mathbf{u}}^0)^*) = \text{Span}\{\psi\}.$$

Multiply by  $\psi^*$  and use  $\dot{\lambda}_0 = 0$  and  $\psi \perp \mathcal{R}(\mathbf{G}_{\mathbf{u}}^0)$  to find

$$\psi^* \mathbf{G}_\lambda^0 \ddot{\lambda}_0 + \psi^* \mathbf{G}_{\mathbf{uu}}^0 \phi \phi = 0.$$

Here  $\psi^* \mathbf{G}_\lambda^0 \neq 0$ , since  $\mathbf{G}_\lambda^0 \notin \mathcal{R}(\mathbf{G}_{\mathbf{u}}^0)$ . Thus

$$\ddot{\lambda}_0 = \frac{-\psi^* \mathbf{G}_{\mathbf{uu}}^0 \phi \phi}{\psi^* \mathbf{G}_\lambda^0}.$$

If the curvature  $\ddot{\lambda}_0 \neq 0$  then  $(\mathbf{u}_0, \lambda_0)$  is called a *simple quadratic fold*.

# The Extended System

To continue a fold in two parameters we use the *extended system*

$$\boxed{\begin{aligned}\mathbf{G}(\mathbf{u}, \lambda, \mu) &= \mathbf{0}, \\ \mathbf{G}_{\mathbf{u}}(\mathbf{u}, \lambda, \mu) \phi &= \mathbf{0}, \\ \phi^* \phi_0 - 1 &= 0.\end{aligned}}$$



Here  $\mu \in \mathbb{R}$  is a second parameter in the equations.

The vector  $\phi_0$  is from a “*reference solution*”  $(\mathbf{u}_0, \phi_0, \lambda_0, \mu_0)$ .

(In practice this is the latest computed solution point on the branch.)

The above system has the form

$$\mathbf{F}(\mathbf{U}, \mu) = \mathbf{0}, \quad \mathbf{U} \equiv (\mathbf{u}, \phi, \lambda), \quad \mathbf{F} : \mathbb{R}^{2n+1} \times \mathbb{R} \rightarrow \mathbb{R}^{2n+1},$$

or, using the “parameter-free” formulation,

$$\mathbf{F}(\mathbf{X}) = \mathbf{0}, \quad \mathbf{X} \equiv (\mathbf{U}, \mu), \quad \mathbf{F} : \mathbb{R}^{2n+2} \rightarrow \mathbb{R}^{2n+1}.$$

# Parameter Continuation

First consider continuing a solution

$$(\mathbf{u}_0, \phi_0, \lambda_0) \quad \text{at } \mu = \mu_0,$$

in  $\mu$  (although, in practice, we use pseudo-arc length continuation).

By the IFT there is a smooth solution family

$$\mathbf{U}(\mu) = (\mathbf{u}(\mu), \phi(\mu), \lambda(\mu)),$$

if the Jacobian

$$\mathbf{F}_{\mathbf{U}}^0 \equiv \frac{d\mathbf{F}}{d\mathbf{U}}(\mathbf{U}_0) = \begin{pmatrix} \mathbf{G}_{\mathbf{u}}^0 & \mathbf{O} & \mathbf{G}_{\lambda}^0 \\ \mathbf{G}_{\mathbf{uu}}^0 \phi_0 & \mathbf{G}_{\mathbf{u}}^0 & \mathbf{G}_{\mathbf{u}\lambda}^0 \phi_0 \\ \mathbf{0}^* & \phi_0^* & 0 \end{pmatrix},$$

is nonsingular.

THEOREM.

A simple quadratic fold with respect to  $\lambda$  can be continued locally, using the second parameter  $\mu$  as continuation parameter.

PROOF.

Suppose  $\mathbf{F}_U^0$  is singular. Then

$$(i) \quad \mathbf{G}_u^0 \mathbf{x} + z \mathbf{G}_\lambda^0 = \mathbf{0},$$

$$(ii) \quad \mathbf{G}_{uu}^0 \phi_0 \mathbf{x} + \mathbf{G}_u^0 \mathbf{y} + z \mathbf{G}_{u\lambda}^0 \phi_0 = \mathbf{0},$$

$$(iii) \quad \phi_0^* \mathbf{y} = 0,$$

for some

$$\mathbf{x}, \mathbf{y} \in \mathbf{R}^n, \quad z \in \mathbf{R}.$$

Since  $\mathbf{G}_\lambda^0 \notin \mathcal{R}(\mathbf{G}_{\mathbf{u}}^0)$  we have from (i) that  $z = 0$ , and hence

$$\mathbf{x} = c_1 \boldsymbol{\phi}_0, \quad \text{for some } c_1 \in \mathbb{R}.$$

Multiply (ii) on the left by  $\boldsymbol{\psi}_0^*$ , to get

$$c_1 \boldsymbol{\psi}_0^* \mathbf{G}_{\mathbf{u}\mathbf{u}}^0 \boldsymbol{\phi}_0 \boldsymbol{\phi}_0 = 0.$$

Thus  $c_1 = 0$ , because by assumption  $\boldsymbol{\psi}_0^* \mathbf{G}_{\mathbf{u}\mathbf{u}}^0 \boldsymbol{\phi}_0 \boldsymbol{\phi}_0 \neq 0$ .

Therefore  $\mathbf{x} = \mathbf{0}$ , and from (ii) we now have

$$\mathbf{G}_{\mathbf{u}}^0 \mathbf{y} = \mathbf{0}, \quad \text{i.e.}, \quad \mathbf{y} = c_2 \boldsymbol{\phi}_0.$$

But then by (iii)  $c_2 = 0$ . Thus

$$\mathbf{x} = \mathbf{y} = \mathbf{0}, \quad z = 0,$$

and hence  $\mathbf{F}_{\mathbf{U}}^0$  is nonsingular.  $\circ$

NOTE:

- The zero eigenvalue of  $\mathbf{G}_{\mathbf{u}}^0$  need not be algebraically simple.
- Thus, for example,  $\mathbf{G}_{\mathbf{u}}^0$  may have the form

$$\mathbf{G}_{\mathbf{u}}^0 = \begin{pmatrix} 0 & 1 \\ 0 & 0 \end{pmatrix},$$

provided the fold is simple and quadratic.

- Parameter-continuation fails at folds w.r.t  $\mu$  on a solution family to

$$\mathbf{F}(\mathbf{U}, \mu) = \mathbf{0}.$$

- Such points represent *cusps*, *branch points*, or *isola formation points*.

# Pseudo-Arclength Continuation of Folds

Treat  $\mu$  as one of the unknowns, and compute a solution family

$$\mathbf{X}(s) \equiv (\mathbf{u}(s), \phi(s), \lambda(s), \mu(s)),$$

to

$$\mathbf{F}(\mathbf{X}) \equiv \begin{cases} \mathbf{G}(\mathbf{u}, \lambda, \mu) = \mathbf{0}, \\ \mathbf{G}_{\mathbf{u}}(u, \lambda, \mu) \phi = \mathbf{0}, \\ \phi^* \phi_0 - 1 = 0, \end{cases} \quad (1)$$

and the added pseudo-arclength equation

$$(\mathbf{u} - \mathbf{u}_0)^* \dot{\mathbf{u}}_0 + (\phi - \phi_0)^* \dot{\phi}_0 + (\lambda - \lambda_0) \dot{\lambda}_0 + (\mu - \mu_0) \dot{\mu}_0 - \Delta s = 0. \quad (2)$$

As before,

$$(\dot{\mathbf{u}}_0, \dot{\phi}_0, \dot{\lambda}_0, \dot{\mu}_0),$$

is the direction of the branch at the current solution point

$$(\mathbf{u}_0, \phi_0, \lambda_0, \mu_0).$$

The Jacobian of  $\mathbf{F}$  with respect to  $\mathbf{u}$ ,  $\phi$ ,  $\lambda$ , and  $\mu$ , at

$$\mathbf{X}_0 = (\mathbf{u}_0, \phi_0, \lambda_0, \mu_0),$$

is now

$$\mathbf{F}_{\mathbf{X}}^0 \equiv \frac{d\mathbf{F}}{d\mathbf{X}}(\mathbf{X}_0) \equiv \begin{pmatrix} \mathbf{G}_{\mathbf{u}}^0 & \mathbf{O} & \mathbf{G}_{\lambda}^0 & \mathbf{G}_{\mu}^0 \\ \mathbf{G}_{\mathbf{u}\mathbf{u}}^0 \phi_0 & \mathbf{G}_{\mathbf{u}}^0 & \mathbf{G}_{\mathbf{u}\lambda}^0 \phi_0 & \mathbf{G}_{\mathbf{u}\mu}^0 \phi_0 \\ \mathbf{0}^* & \phi_0^* & 0 & 0 \end{pmatrix}.$$

For pseudo-arclength continuation we must check that  $\mathbf{F}_{\mathbf{X}}^0$  has full rank.

For a simple quadratic fold with respect to  $\lambda$  this follows from the Theorem.

Otherwise, if

$$\psi_0^* \mathbf{G}_{\mathbf{u}\mathbf{u}}^0 \phi_0 \phi_0 \neq 0,$$

and

$$\mathbf{G}_{\lambda}^0 \in \mathcal{R}(\mathbf{G}_{\mathbf{u}}^0), \quad \mathbf{G}_{\mu}^0 \notin \mathcal{R}(\mathbf{G}_{\mathbf{u}}^0),$$

i.e., if we have a simple quadratic fold with respect to  $\mu$ , then we can apply the theorem to  $\mathbf{F}_{\mathbf{X}}^0$  with the second last column struck out, to see that  $\mathbf{F}_{\mathbf{X}}^0$  still has full rank.

EXAMPLE: The  $A \rightarrow B \rightarrow C$  reaction. (AUTO demo abc.)

The equations are

$$u'_1 = -u_1 + D(1 - u_1)e^{u_3},$$

$$u'_2 = -u_2 + D(1 - u_1)e^{u_3} - D\sigma u_2 e^{u_3},$$

$$u'_3 = -u_3 - \beta u_3 + DB(1 - u_1)e^{u_3} + DB\alpha\sigma u_2 e^{u_3},$$

where

$1 - u_1$  is the concentration of  $A$  ,  $u_2$  is the concentration of  $B$  ,

$u_3$  is the temperature,  $\alpha = 1$  ,  $\sigma = 0.04$  ,  $B = 8$  ,

$D$  is the *Damkohler number* ,  $\beta$  is the heat transfer coefficient .

We will compute solutions for varying  $D$  and  $\beta$  .

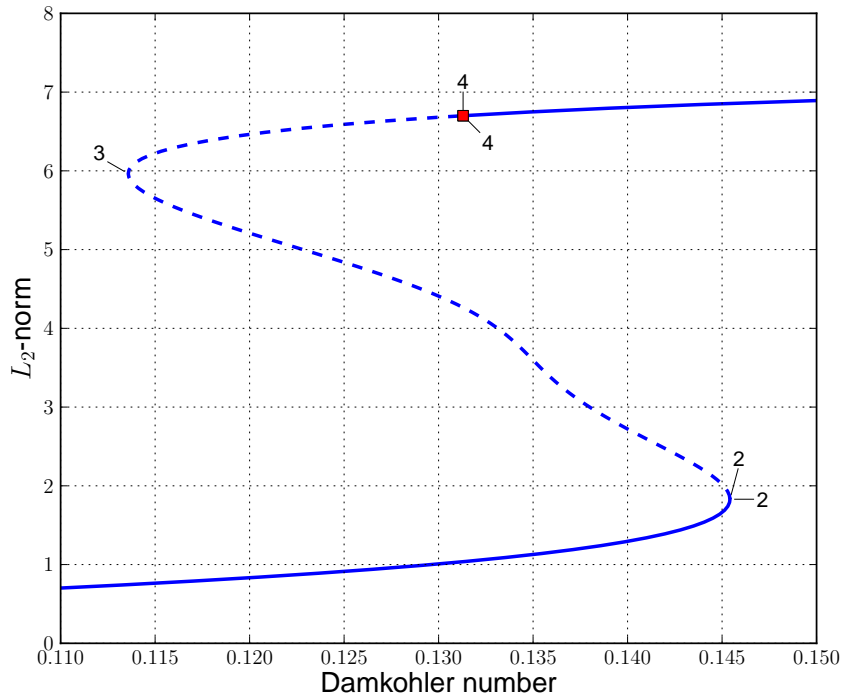


Figure 13: A stationary solution family of demo abc;  $\beta = 1.15$ .

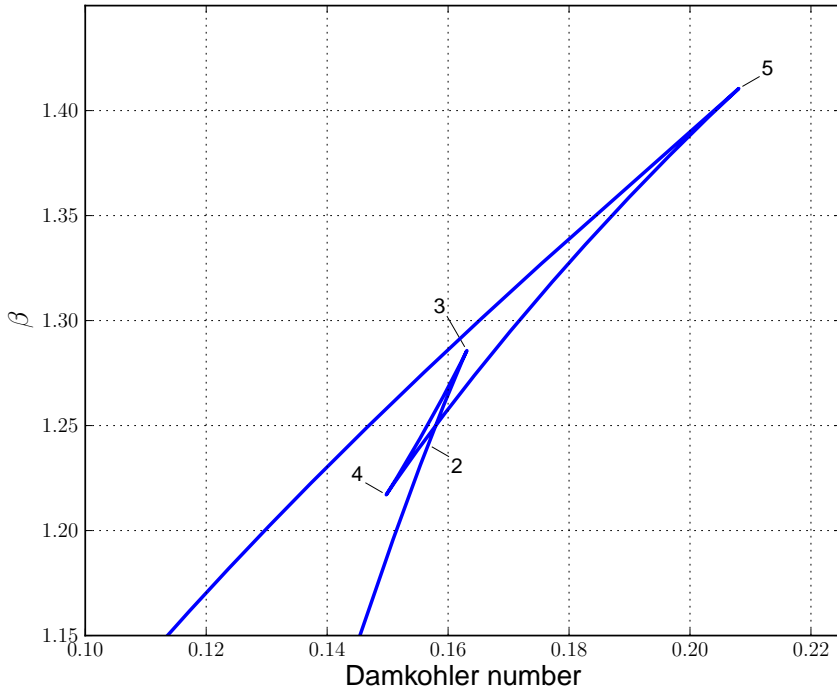


Figure 14: The locus of folds of demo abc.

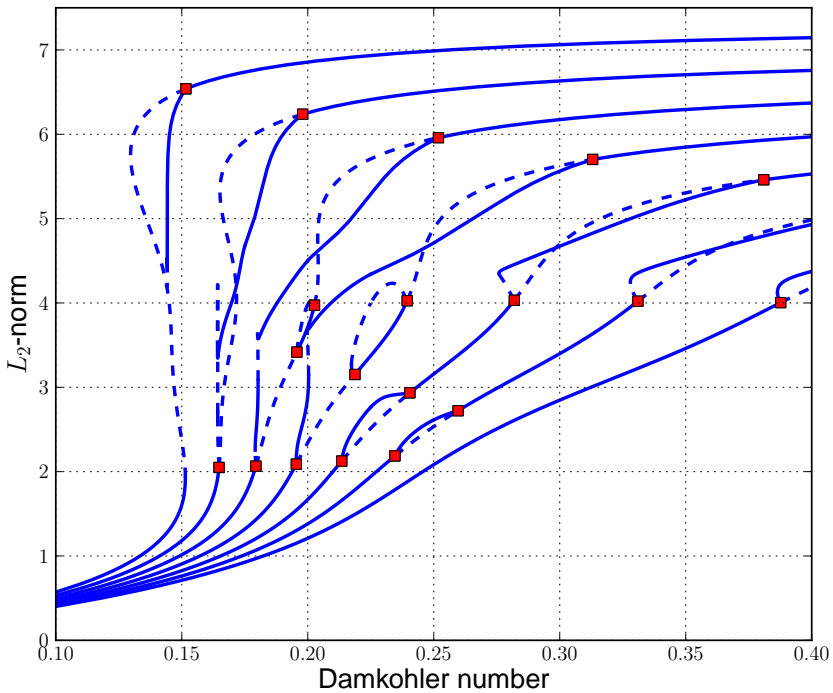


Figure 15: Stationary solution families for  $\beta = 1.15, 1.17, \dots, 1.39$ .

# Numerical Treatment of Bifurcations

Here we discuss branch switching, and the detection of branch points.

# Simple Singular Points

Let

$$\mathbf{G} : \mathbb{R}^{n+1} \rightarrow \mathbb{R}^n .$$

A solution

$$\mathbf{x}_0 \equiv \mathbf{x}(s_0) \quad \text{of} \quad \mathbf{G}(\mathbf{x}) = \mathbf{0} ,$$

is called a *simple singular point* if

$$\mathbf{G}_{\mathbf{x}}^0 \equiv \mathbf{G}_{\mathbf{x}}(\mathbf{x}_0) \quad \text{has rank } n - 1 .$$

In the parameter formulation, where

$$\mathbf{G}_{\mathbf{x}}^0 = (\mathbf{G}_u^0 \mid \mathbf{G}_\lambda^0) ,$$

we have that

$$\mathbf{x}_0 = (\mathbf{u}_0, \lambda_0) \quad \text{is a simple singular point}$$

if and only if

$$(i) \quad \dim \mathcal{N}(\mathbf{G}_{\mathbf{u}}^0) = 1 , \quad \mathbf{G}_\lambda^0 \in \mathcal{R}(\mathbf{G}_{\mathbf{u}}^0) ,$$

or

$$(ii) \quad \dim \mathcal{N}(\mathbf{G}_{\mathbf{u}}^0) = 2 , \quad \mathbf{G}_\lambda^0 \notin \mathcal{R}(\mathbf{G}_{\mathbf{u}}^0) .$$

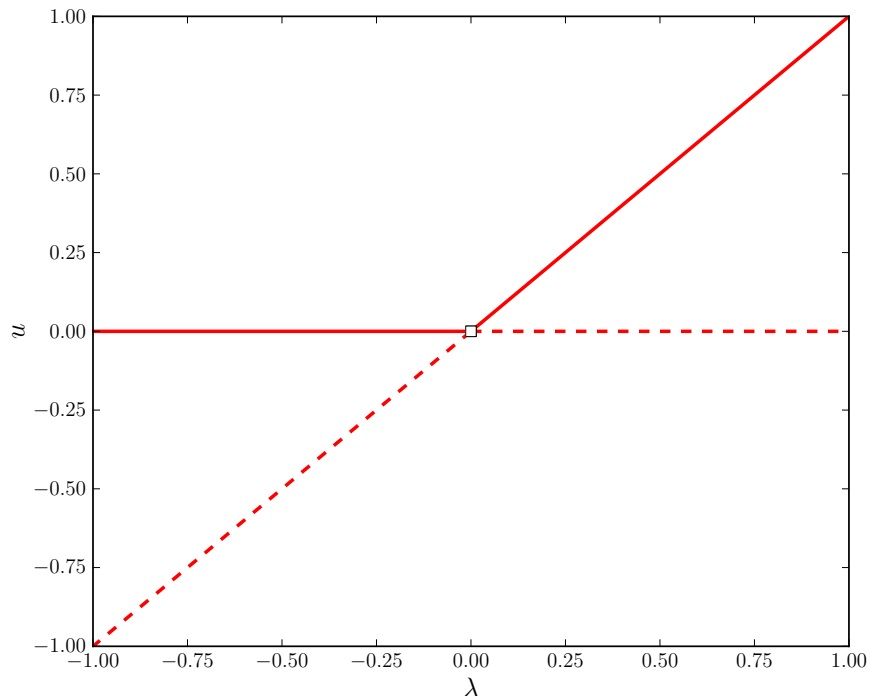


Figure 16: Solution curves of  $u(\lambda - u) = 0$ , with simple singular point.

An example of case (ii) is

$$\mathbf{G}(\mathbf{u}, \lambda) = \begin{pmatrix} \lambda - u_1^2 - u_2^2 \\ u_1 u_2 \end{pmatrix}, \quad \text{at} \quad \lambda = 0, \quad u_1 = u_2 = 0.$$

Here

$$\mathbf{G}_{\mathbf{u}}^0 = \begin{pmatrix} 0 & 0 \\ 0 & 0 \end{pmatrix}, \quad \text{and} \quad \mathbf{G}_\lambda^0 = \begin{pmatrix} 1 \\ 0 \end{pmatrix}.$$

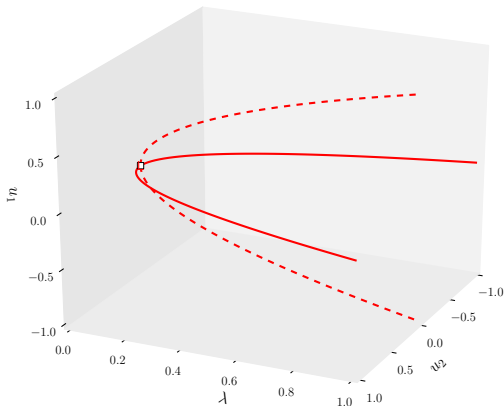


Figure 17: Solution curves of  $\mathbf{G}(\mathbf{u}, \lambda) = \mathbf{0}$ , with simple singular point.

Suppose we have a solution family  $\mathbf{x}(s)$  of

$$\mathbf{G}(\mathbf{x}) = \mathbf{0},$$

where  $s$  is some parametrization.

Let

$$\mathbf{x}_0 \equiv (\mathbf{u}_0, \lambda_0),$$

be a simple singular point.

Thus, by definition of simple singular point,

$$\mathcal{N}(\mathbf{G}_{\mathbf{x}}^0) = \text{Span}\{\phi_1, \phi_2\}, \quad \mathcal{N}(\mathbf{G}_{\mathbf{x}}^{0*}) = \text{Span}\{\psi\}.$$

We also have

$$\mathbf{G}(\mathbf{x}(s)) = \mathbf{0}, \quad \mathbf{G}^0 = \mathbf{G}(\mathbf{x}_0) = \mathbf{0},$$

$$\mathbf{G}_{\mathbf{x}}(\mathbf{x}(s)) \dot{\mathbf{x}}(s) = \mathbf{0}, \quad \mathbf{G}_{\mathbf{x}}^0 \dot{\mathbf{x}}_0 = \mathbf{0},$$

$$\mathbf{G}_{\mathbf{xx}}(\mathbf{x}(s)) \dot{\mathbf{x}}(s) \dot{\mathbf{x}}(s) + \mathbf{G}_{\mathbf{x}}(\mathbf{x}(s)) \ddot{\mathbf{x}}(s) = \mathbf{0}, \quad \mathbf{G}_{\mathbf{xx}}^0 \dot{\mathbf{x}}_0 \dot{\mathbf{x}}_0 + \mathbf{G}_{\mathbf{x}}^0 \ddot{\mathbf{x}}_0 = \mathbf{0}.$$

Thus  $\dot{\mathbf{x}}_0 = \alpha \phi_1 + \beta \phi_2$ , for some  $\alpha, \beta \in \mathbb{R}$ , and

$$\psi^* \mathbf{G}_{\mathbf{xx}}^0 (\alpha \phi_1 + \beta \phi_2) (\alpha \phi_1 + \beta \phi_2) + \underbrace{\psi^* \mathbf{G}_{\mathbf{x}}^0}_{=0} \ddot{\mathbf{x}}_0 = 0,$$

$$\boxed{\underbrace{(\psi^* \mathbf{G}_{\mathbf{xx}}^0 \phi_1 \phi_1)}_{c_{11}} \alpha^2 + 2 \underbrace{(\psi^* \mathbf{G}_{\mathbf{xx}}^0 \phi_1 \phi_2)}_{c_{12}} \alpha \beta + \underbrace{(\psi^* \mathbf{G}_{\mathbf{xx}}^0 \phi_2 \phi_2)}_{c_{22}} \beta^2 = 0}.$$

This is the Algebraic Bifurcation equation (ABE).

We want solution pairs

$$(\alpha, \beta),$$

of the ABE, with not both  $\alpha$  and  $\beta$  equal to zero.

If the *discriminant*

$$\Delta \equiv c_{12}^2 - c_{11} c_{22},$$

satisfies

$$\Delta > 0,$$

then the ABE has two real, distinct (*i.e.*, linearly independent) solutions,

$$(\alpha_1, \beta_1) \quad \text{and} \quad (\alpha_2, \beta_2),$$

which are unique up to scaling.

In this case we have a *bifurcation*, (or *branch point*), *i.e.*, two distinct branches pass through  $\mathbf{x}_0$ .

# Examples of Bifurcations

First we construct the Algebraic Bifurcation Equation (ABE) for our simple predator-prey model, in order to illustrate the necessary algebraic manipulations. Thereafter we present a more elaborate application to a nonlinear eigenvalue problem

# A Predator-Prey Model

In the 2-species predator-prey model

$$\begin{cases} u'_1 = 3u_1(1 - u_1) - u_1u_2 - \lambda(1 - e^{-5u_1}), \\ u'_2 = -u_2 + 3u_1u_2. \end{cases}$$

we have

$$\mathbf{G}_x = (\mathbf{G}_{u_1} | \mathbf{G}_{u_2} | \mathbf{G}_\lambda) = \begin{pmatrix} 3 - 6u_1 - u_2 - 5\lambda e^{-5u_1} & -u_1 & -(1 - e^{-5u_1}) \\ 3u_2 & -1 + 3u_1 & 0 \end{pmatrix},$$

and

$$\mathbf{G}_{xx} = \begin{pmatrix} (-6 + 25\lambda e^{-5u_1}, -1, -5e^{-5u_1}) & (-1, 0, 0) & (-5e^{-5u_1}, 0, 0) \\ (0, 3, 0) & (3, 0, 0) & (0, 0, 0) \end{pmatrix}.$$

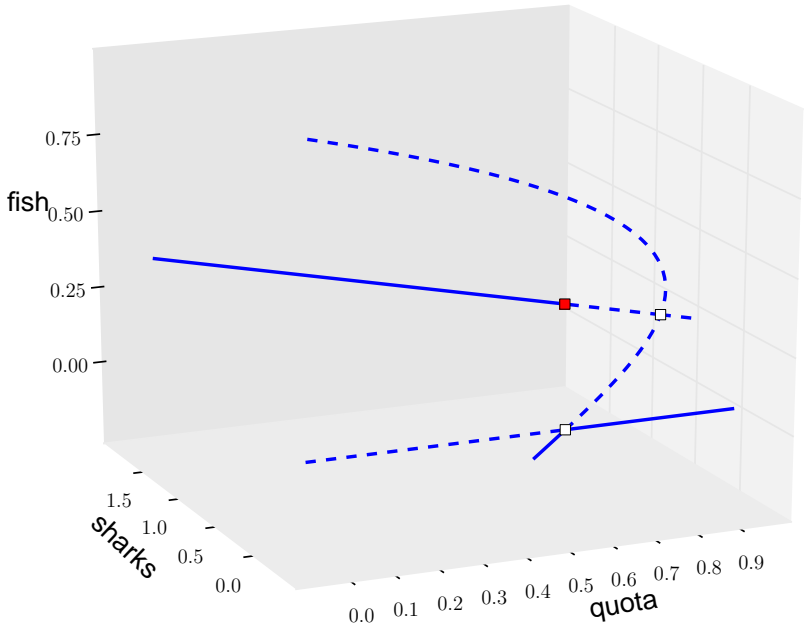


Figure 18: Two branch points (Solutions 2 and 4) in AUTO demo pp2.

At Solution 2 in Figure 18 we have  $u_1 = u_2 = 0$ ,  $\lambda = 3/5$ , so that

$$\mathbf{x}_0 = (0, 0, 3/5),$$

$$\mathbf{G}_{\mathbf{x}}^0 = \begin{pmatrix} 0 & 0 & 0 \\ 0 & -1 & 0 \end{pmatrix}, \quad \mathbf{G}_{\mathbf{x}}^{0*} = \begin{pmatrix} 0 & 0 \\ 0 & -1 \\ 0 & 0 \end{pmatrix},$$

$$\mathcal{N}(\mathbf{G}_{\mathbf{x}}^0) = \text{Span} \left\{ \begin{pmatrix} 0 \\ 0 \\ 1 \end{pmatrix}, \begin{pmatrix} 1 \\ 0 \\ 0 \end{pmatrix} \right\}, \quad \mathcal{N}(\mathbf{G}_{\mathbf{x}}^{0*}) = \text{Span} \left\{ \begin{pmatrix} 1 \\ 0 \\ 0 \end{pmatrix} \right\},$$

and

$$\mathbf{G}_{\mathbf{xx}}^0 = \begin{pmatrix} (9, -1, -5) & (-1, 0, 0) & (-5, 0, 0) \\ (0, 3, 0) & (3, 0, 0) & (0, 0, 0) \end{pmatrix}.$$

$$\mathbf{G}_{\mathbf{xx}}^0 \phi_1 = \begin{pmatrix} -5 & 0 & 0 \\ 0 & 0 & 0 \end{pmatrix}, \quad \mathbf{G}_{\mathbf{xx}}^0 \phi_2 = \begin{pmatrix} 9 & -1 & -5 \\ 0 & 3 & 0 \end{pmatrix}.$$

Thus

$$\psi^* \mathbf{G}_{\mathbf{xx}}^0 \phi_1 \phi_1 = \psi^* \begin{pmatrix} -5 & 0 & 0 \\ 0 & 0 & 0 \end{pmatrix} \phi_1 = \psi^* \begin{pmatrix} 0 \\ 0 \end{pmatrix} = 0,$$

$$\psi^* \mathbf{G}_{\mathbf{xx}}^0 \phi_1 \phi_2 = \psi^* \begin{pmatrix} -5 & 0 & 0 \\ 0 & 0 & 0 \end{pmatrix} \phi_2 = \psi^* \begin{pmatrix} -5 \\ 0 \end{pmatrix} = -5,$$

$$\psi^* \mathbf{G}_{\mathbf{xx}}^0 \phi_2 \phi_2 = \psi^* \begin{pmatrix} 9 & -1 & -5 \\ 0 & 3 & 0 \end{pmatrix} \phi_2 = \psi^* \begin{pmatrix} 9 \\ 0 \end{pmatrix} = 9.$$

Therefore the ABE is

$$-10 \alpha \beta + 9 \beta^2 = 0.$$

which has two linearly independent solutions, namely,

$$\begin{pmatrix} \alpha \\ \beta \end{pmatrix} = \begin{pmatrix} 1 \\ 0 \end{pmatrix}, \quad \begin{pmatrix} 9 \\ 10 \end{pmatrix}.$$

Thus the (non-normalized) directions of the two bifurcation families at  $\mathbf{x}_0$  are

$$\dot{\mathbf{x}}_0 = (1) \phi_1 + (0) \phi_2 = \begin{pmatrix} 0 \\ 0 \\ 1 \end{pmatrix} = \begin{pmatrix} \dot{u}_1 \\ \dot{u}_2 \\ \dot{\lambda} \end{pmatrix},$$

and

$$\dot{\mathbf{x}}_0 = (9) \phi_1 + (10) \phi_2 = \begin{pmatrix} 10 \\ 0 \\ 9 \end{pmatrix} = \begin{pmatrix} \dot{u}_1 \\ \dot{u}_2 \\ \dot{\lambda} \end{pmatrix}.$$

NOTE:

- The first direction is that of the zero solution family.
- The second direction is that of the bifurcating nonzero solution family.
- Since  $\dot{\lambda} \neq 0$  for the second direction, this is a *transcritical bifurcation*.
- (The case where  $\dot{\lambda} = 0$  may correspond to a *pitchfork bifurcation*.)

# A Nonlinear Eigenvalue Problem

*This example makes extensive use of the method of “Variation of Parameters” for solving linear differential equations. We first recall the use of this method.*

## Variation of Parameters

If

$$\mathbf{v}'(t) = A(t) \mathbf{v}(t) + \mathbf{f}(t),$$

then

$$\mathbf{v}(t) = V(t) [\mathbf{v}(0) + \int_0^t V(s)^{-1} \mathbf{f}(s) ds],$$

where  $V(t)$  is the solution (matrix) of

$$V'(t) = A(t) V(t),$$

$$V(0) = I.$$

Here  $V(t)$  is called the *fundamental solution matrix*.

EXAMPLE:

Apply Variation of Parameters to the equation

$$v'' + \lambda v = f,$$

rewritten as

$$\begin{cases} v'_1 = v_2, \\ v'_2 = -\lambda v_1 + f, \end{cases}$$

or

$$\begin{pmatrix} v'_1 \\ v'_2 \end{pmatrix} = \begin{pmatrix} 0 & 1 \\ -\lambda & 0 \end{pmatrix} \begin{pmatrix} v_1 \\ v_2 \end{pmatrix} + \begin{pmatrix} 0 \\ f \end{pmatrix}.$$

Then

$$V(t) = \begin{pmatrix} \cos \sqrt{\lambda}t & \sin \sqrt{\lambda}t / \sqrt{\lambda} \\ -\sqrt{\lambda} \sin \sqrt{\lambda}t & \cos \sqrt{\lambda}t \end{pmatrix}.$$

We find that

$$V^{-1}(t) = \begin{pmatrix} \cos \sqrt{\lambda}t & -\sin \sqrt{\lambda}t/\sqrt{\lambda} \\ \sqrt{\lambda} \sin \sqrt{\lambda}t & \cos \sqrt{\lambda}t \end{pmatrix},$$

$$V^{-1}(s) \begin{pmatrix} 0 \\ f \end{pmatrix} = \begin{pmatrix} -\sin \sqrt{\lambda}s f(s)/\sqrt{\lambda} \\ \cos \sqrt{\lambda}s f(s) \end{pmatrix},$$

so that  $\begin{pmatrix} v_1(t) \\ v_2(t) \end{pmatrix} =$

$$\begin{pmatrix} \cos \sqrt{\lambda}t & \sin \sqrt{\lambda}t/\sqrt{\lambda} \\ -\sqrt{\lambda} \sin \sqrt{\lambda}t & \cos \sqrt{\lambda}t \end{pmatrix} \left[ \begin{pmatrix} v_1(0) \\ v_2(0) \end{pmatrix} + \int_0^t \begin{pmatrix} -\sin \sqrt{\lambda}s f(s)/\sqrt{\lambda} \\ \cos \sqrt{\lambda}s f(s) \end{pmatrix} ds \right]$$

Hence

$$\begin{aligned} v_1(t) &= \cos(\sqrt{\lambda}t) v_1(0) + \frac{\sin(\sqrt{\lambda}t)}{\sqrt{\lambda}} v_2(0) \\ &\quad - \cos \sqrt{\lambda}t \int_0^t \frac{\sin \sqrt{\lambda}s f(s)}{\sqrt{\lambda}} ds + \frac{\sin \sqrt{\lambda}t}{\sqrt{\lambda}} \int_0^t \cos \sqrt{\lambda}s f(s) ds. \end{aligned}$$

For the specific initial value problem

$$\begin{cases} v'' + \lambda v = f, \\ v(0) = v'(0) = 0, \end{cases}$$

we have

$$v(t) = v_1(t) = \frac{\sin \sqrt{\lambda}t}{\sqrt{\lambda}} \int_0^t \cos \sqrt{\lambda}s f(s) ds - \frac{\cos \sqrt{\lambda}t}{\sqrt{\lambda}} \int_0^t \sin \sqrt{\lambda}s f(s) ds.$$

## Singular points

Consider the nonlinear boundary value problem

$$\begin{cases} u'' + \lambda(u + u^2) = 0, \\ u(0) = u(1) = 0, \end{cases}$$

which has  $u(t) \equiv 0$  as solution for all  $\lambda$ .

Equivalently, we want the solution

$$u = u(t; p, \lambda),$$

of the initial value problem

$$\begin{cases} u'' + \lambda(u + u^2) = 0, \\ u(0) = 0, \quad u'(0) = p, \end{cases}$$

that satisfies

$$G(p, \lambda) \equiv u(1; p, \lambda) = 0.$$

$$u'' + \lambda(u + u^2) = 0 , \quad u(0) = 0 , \quad u'(0) = p$$

$$G(p, \lambda) \equiv u(1; p, \lambda) = 0$$

We have that

$$G : \mathbb{R} \times \mathbb{R} \rightarrow \mathbb{R} ,$$

with

$$G(0, \lambda) = 0 , \quad \text{for all } \lambda .$$

Let

$$u_p(t; p, \lambda) = \frac{du}{dp}(t; p, \lambda) ,$$

$$G_p(p, \lambda) = u_p(1; p, \lambda) , \quad etc.$$

$$\boxed{u'' + \lambda(u + u^2) = 0 \quad u(0) = 0, \quad u'(0) = p}$$

Then  $u_p$  ( $= u_p^0$ ) satisfies

$$\begin{cases} u_p'' + \lambda(1+2u)u_p = 0, \\ u_p(0) = 0, \quad u'_p(0) = 1, \end{cases}$$

which, about  $u \equiv 0$ , gives

$$\begin{cases} u_p'' + \lambda u_p = 0, \\ u_p(0) = 0, \quad u'_p(0) = 1. \end{cases}$$

By the variation of parameters formula

$$u_p(t; p, \lambda) = \frac{\sin \sqrt{\lambda}t}{\sqrt{\lambda}}, \quad \lambda \geq 0, \quad (\text{independent of } p).$$

$$G_p(0, \lambda) = u_p(1; p, \lambda) = \frac{\sin(\sqrt{\lambda})}{\sqrt{\lambda}} = 0, \quad \text{if } \lambda = \lambda_k \equiv (k\pi)^2.$$

(We will see that the  $\lambda_k$  are branch points.)

$$\boxed{u'' + \lambda(u + u^2) = 0 \quad u(0) = 0, \quad u'(0) = p}$$

Next,  $u_\lambda$  satisfies

$$\begin{cases} u_\lambda'' + u + u^2 + \lambda(1+2u)u_\lambda = 0, \\ u_\lambda(0) = 0, \quad u'_\lambda(1) = 0, \end{cases}$$

which, about  $u \equiv 0$ , gives

$$\begin{cases} u_\lambda'' + \lambda u_\lambda = 0, \\ u_\lambda(0) = 0, \quad u'_\lambda(0) = 0. \end{cases}$$

from which,

$$u_\lambda(t; p, \lambda) \equiv 0, \quad G_\lambda(0, \lambda) = u_\lambda(1; 0, \lambda) = 0,$$

which holds, in particular, at

$$\lambda = \lambda_k = (k\pi)^2.$$

Thus, so far we know that

$$G(0, \lambda) = 0, \quad \text{for all } \lambda,$$

and if

$$\lambda = \lambda_k \equiv (k\pi)^2,$$

then, with

$$\mathbf{x} \equiv (p, \lambda),$$

we have

$$G_{\mathbf{x}}^0 \equiv (G_p(0, \lambda_k) \mid G_\lambda(0, \lambda_k)) = (0 \mid 0),$$

$$\mathcal{N}(G_{\mathbf{x}}^0) = \text{Span}\left\{\begin{pmatrix} 1 \\ 0 \end{pmatrix}, \begin{pmatrix} 0 \\ 1 \end{pmatrix}\right\}, \quad (2D),$$

$$\mathcal{N}(G_{\mathbf{x}}^{0*}) = \text{Span}\{(1)\}, \quad (1D).$$

Thus the solutions

$$p = 0, \quad \lambda = \lambda_k = (k\pi)^2,$$

correspond to simple singular points.

## Construction of the ABE

The ABE is

$$(\psi^* G_{\mathbf{xx}}^0 \phi_1 \phi_1) \alpha^2 + 2(\psi^* G_{\mathbf{xx}}^0 \phi_1 \phi_2) \alpha \beta + (\psi^* G_{\mathbf{xx}}^0 \phi_2 \phi_2) \beta^2 = 0 ,$$

where

$$\psi = 1 ,$$

$$G_{\mathbf{xx}}^0 = \left( \begin{array}{c|c} (G_{pp}^0 | G_{p\lambda}^0) & (G_{\lambda p}^0 | G_{\lambda\lambda}^0) \end{array} \right) ,$$

with

$$G_{pp}^0 = G_{pp}(0, \lambda_k) = u_{pp}(1; 0, \lambda_k) , \quad etc.$$

If the ABE has 2 independent solutions then the bifurcation directions are

$$\begin{pmatrix} \dot{p} \\ \dot{\lambda} \end{pmatrix} = \alpha_1 \begin{pmatrix} 1 \\ 0 \end{pmatrix} + \beta_1 \begin{pmatrix} 0 \\ 1 \end{pmatrix} = \begin{pmatrix} \alpha_1 \\ \beta_1 \end{pmatrix},$$

and

$$\begin{pmatrix} \dot{p} \\ \dot{\lambda} \end{pmatrix} = \alpha_2 \begin{pmatrix} 1 \\ 0 \end{pmatrix} + \beta_2 \begin{pmatrix} 0 \\ 1 \end{pmatrix} = \begin{pmatrix} \alpha_2 \\ \beta_2 \end{pmatrix}.$$

Since

$$p = 0,$$

is a solution for all  $\lambda$ , one direction is

$$\begin{pmatrix} \dot{p} \\ \dot{\lambda} \end{pmatrix} = \begin{pmatrix} 0 \\ 1 \end{pmatrix}.$$

$$\boxed{u'' + \lambda(u + u^2) = 0 \quad u(0) = 0, \quad u'(0) = p}$$

Now  $u_{pp}$  satisfies

$$\begin{cases} u_{pp}'' + 2\lambda u_p^2 + \lambda(1+2u) u_{pp} = 0, \\ u_{pp}(0) = u'_{pp}(0) = 0, \end{cases}$$

which, about

$$u \equiv 0, \quad \lambda = \lambda_k, \quad u_p(t; p, \lambda) = \frac{\sin \sqrt{\lambda}t}{\sqrt{\lambda}},$$

gives

$$\begin{cases} u_{pp}'' + \lambda_k u_{pp} = -2\lambda_k u_p^2 = -2 \sin^2 \sqrt{\lambda}t, \\ u_{pp}(0) = u'_{pp}(0) = 0. \end{cases}$$

that is,

$$\begin{cases} u_{pp}'' + (k\pi)^2 u_{pp} = -2 \sin^2(k\pi t), \\ u_{pp}(0) = u'_{pp}(0) = 0. \end{cases}$$

By the variation of parameters formula

$$u_{pp}(t; p, \lambda) =$$

$$\begin{aligned} & \frac{\sin k\pi t}{k\pi} \int_0^t \cos k\pi s (-2 \sin^2 k\pi s) \, ds - \frac{\cos k\pi t}{k\pi} \int_0^t \sin k\pi s (-2 \sin^2 k\pi s) \, ds \\ &= -\frac{2 \sin k\pi t}{k\pi} \int_0^t \sin^2 k\pi s \cos k\pi s \, ds + \frac{2 \cos k\pi t}{k\pi} \int_0^t \sin^3 k\pi s \, ds, \end{aligned}$$

and hence

$$G_{pp}(0, \lambda_k) = u_{pp}(1; 0, \lambda_k) = \frac{2}{3(k\pi)^2} [1 - (-1)^k] = \begin{cases} 0, & k \text{ even}, \\ \frac{4}{3(k\pi)^2}, & k \text{ odd}. \end{cases}$$

$$\boxed{u'' + \lambda(u + u^2) = 0 \quad u(0) = 0, \quad u'(0) = p}$$

Next,  $u_{p\lambda}$  satisfies

$$\begin{cases} u''_{p\lambda} + (1+2u) u_p + 2\lambda u_p u_\lambda + \lambda (1+2u) u_{p\lambda} = 0, \\ u_{p\lambda}(0) = u'_{p\lambda}(0) = 0. \end{cases}$$

which, about

$$u \equiv 0, \quad \lambda_k = (k\pi)^2, \quad u_p(t; p, \lambda) = \frac{\sin \sqrt{\lambda}t}{\sqrt{\lambda}}, \quad u_\lambda = 0,$$

gives

$$\begin{cases} u''_{p\lambda} + k^2 \pi^2 u_{p\lambda} = -u_p = -\frac{\sin k\pi t}{k\pi}, \\ u_{p\lambda}(0) = u'_{p\lambda}(0) = 0. \end{cases}$$

Using the variation of parameters formula

$$u_{p\lambda}(t; p, \lambda) =$$

$$\begin{aligned} & \frac{\sin k\pi t}{k\pi} \int_0^t \cos k\pi s \left( \frac{-\sin k\pi s}{k\pi} \right) ds - \frac{\cos k\pi t}{k\pi} \int_0^t \sin k\pi s \left( \frac{-\sin k\pi s}{k\pi} \right) ds \\ &= \frac{\sin k\pi t}{(k\pi)^2} \int_0^t \sin k\pi s \cos k\pi s ds + \frac{\cos k\pi t}{(k\pi)^2} \int_0^t \sin^2 k\pi s ds , \end{aligned}$$

and hence

$$G_{p\lambda}(0, \lambda_k) = u_{p\lambda}(1; 0, \lambda_k) = \frac{1}{2(k\pi)^2} (-1)^k = \begin{cases} \frac{1}{2(k\pi)^2} , & k \text{ even} , \\ \frac{-1}{2(k\pi)^2} , & k \text{ odd} . \end{cases}$$

$$\boxed{u'' + \lambda(u + u^2) = 0 \quad u(0) = 0, \quad u'(0) = p}$$

Finally  $u_{\lambda\lambda}$  satisfies

$$\begin{cases} u''_{\lambda\lambda} + (1+2u)u_\lambda + (1+2u)u_\lambda + 2\lambda u_\lambda^2 + \lambda(1+2u)u_{\lambda\lambda} = 0, \\ u_{\lambda\lambda}(0) = u'_{\lambda\lambda}(0) = 0, \end{cases}$$

which, about

$$u = 0, \quad u_\lambda = 0, \quad \lambda = \lambda_k = k^2\pi^2,$$

gives

$$\begin{cases} u''_{\lambda\lambda} + k^2\pi^2 u_{\lambda\lambda} = 0, \\ u_{\lambda\lambda}(0) = u'_{\lambda\lambda}(0) = 0, \end{cases}$$

so that

$$u_{\lambda\lambda}(t; p, \lambda) \equiv 0, \quad G_{\lambda\lambda}(0, \lambda_k) = u_{\lambda\lambda}(1; 0, \lambda_k) = 0.$$

Thus we have found that

$$G_{\mathbf{xx}}^0 = \left( \begin{array}{c} (G_{pp}^0 | G_{p\lambda}^0) \\ (G_{\lambda p}^0 | G_{\lambda\lambda}^0) \end{array} \right) = \begin{cases} \left( (0 | \frac{1}{2(k\pi)^2}) \mid (\frac{1}{2(k\pi)^2} | 0) \right) , k \text{ even}, \\ \left( (\frac{4}{3(k\pi)^2} | \frac{-1}{2(k\pi)^2}) \mid (\frac{-1}{2(k\pi)^2} | 0) \right) , k \text{ odd}. \end{cases}$$

The coefficients of the ABE are

$$\psi^* G_{\mathbf{xx}}^0 \phi_1 \phi_1 = \begin{cases} 0 , & k \text{ even}, \\ \frac{4}{3(k\pi)^2} , & k \text{ odd}, \end{cases} \quad \psi^* G_{\mathbf{xx}}^0 \phi_1 \phi_2 = \begin{cases} \frac{1}{2(k\pi)^2} , & k \text{ even}, \\ \frac{-1}{2(k\pi)^2} , & k \text{ odd}, \end{cases}$$

$$\psi^* G_{\mathbf{xx}}^0 \phi_2 \phi_2 = \begin{cases} 0 , & k \text{ even}, \\ 0 , & k \text{ odd}. \end{cases}$$

Thus the ABE is

$$\begin{cases} \alpha \beta = 0, & k \text{ even,} \\ \frac{4}{3} \alpha^2 - \frac{1}{2} \alpha \beta = 0, & k \text{ odd,} \end{cases} \quad \begin{array}{l} \text{Roots : } (\alpha, \beta) = (1, 0), (0, 1), \\ \text{Roots : } (\alpha, \beta) = (0, 1), (3, 8). \end{array}$$

The directions of the bifurcating families are:

$$\dot{\mathbf{x}} = \begin{pmatrix} \dot{p} \\ \dot{\lambda} \end{pmatrix} = \alpha \boldsymbol{\phi}_1 + \beta \boldsymbol{\phi}_2 = \alpha \begin{pmatrix} 1 \\ 0 \end{pmatrix} + \beta \begin{pmatrix} 0 \\ 1 \end{pmatrix},$$

where

$$\begin{pmatrix} \dot{p} \\ \dot{\lambda} \end{pmatrix} = \begin{cases} \begin{pmatrix} 0 \\ 1 \end{pmatrix}, \quad \begin{pmatrix} 1 \\ 0 \end{pmatrix}, & k \text{ even, ("pitch-fork bifurcation")}, \\ \begin{pmatrix} 0 \\ 1 \end{pmatrix}, \quad \begin{pmatrix} 3 \\ 8 \end{pmatrix}, & k \text{ odd, ("transcritical bifurcation")}. \end{cases}$$

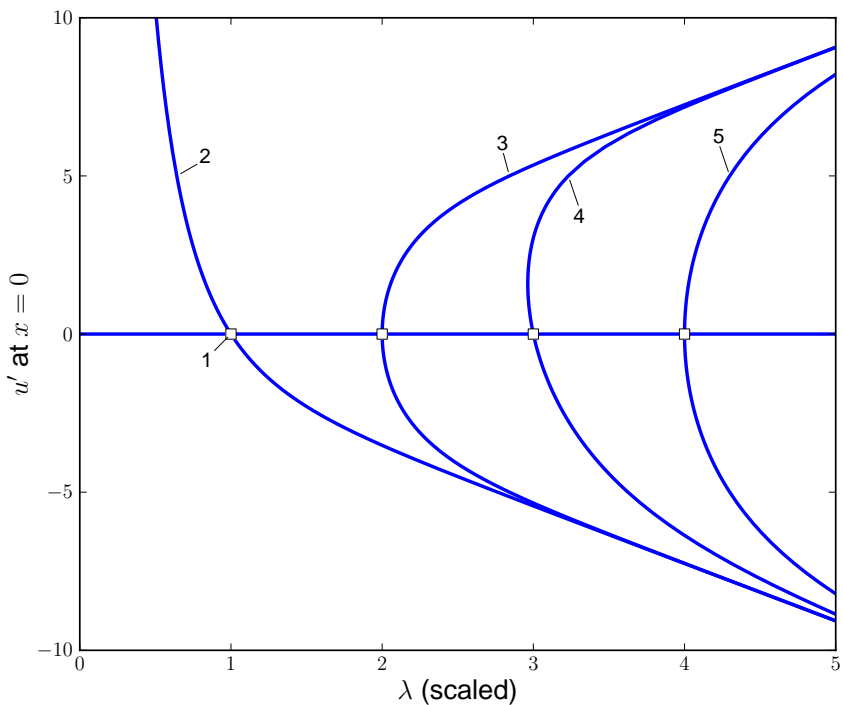


Figure 19: The bifurcating families of the nonlinear eigenvalue problem.

## EXERCISE.

- Check the above calculations (!).
- Use the **AUTO** demo `nev` to compute some bifurcating families.
- Do the numerical results support the analytical results?
- Also carry out the above analysis and **AUTO** computations for

$$\begin{cases} u'' + \lambda (u + u^3) = 0 , \\ u(0) = u(1) = 0 . \end{cases}$$

# Branch Switching

- Along a solution family we may find *branch points*.
- We give *two* methods for switching branches.
- We also give a method to detect branch points.

# Computing the bifurcation direction

Let

$$\mathbf{G} : \mathbb{R}^{n+1} \rightarrow \mathbb{R}^n .$$

Suppose that we have a solution family  $\mathbf{x}(s)$  of

$$\mathbf{G}(\mathbf{x}) = \mathbf{0} ,$$

and that

$$\mathbf{x}_0 \equiv \mathbf{x}(s_0) ,$$

is a simple singular point, i.e., the  $n$  by  $n + 1$  matrix

$$\mathbf{G}_{\mathbf{x}}^0 \equiv \mathbf{G}_{\mathbf{x}}(\mathbf{x}_0) \text{ has } \underline{\text{rank }} n - 1 ,$$

with

$$\mathcal{N}(\mathbf{G}_{\mathbf{x}}^0) = \text{Span}\{\boldsymbol{\phi}_1, \boldsymbol{\phi}_2\} , \quad \mathcal{N}(\mathbf{G}_{\mathbf{x}}^{0*}) = \text{Span}\{\boldsymbol{\psi}\} .$$

## NOTATION.

- $\dot{\mathbf{x}}_0 = \alpha_1 \phi_1 + \beta_1 \phi_2$  denotes the direction of the "given" family.
- $\mathbf{x}'_0 = \alpha_2 \phi_1 + \beta_2 \phi_2$  denotes the direction of the *bifurcating* family.

The two coefficient vectors

$$(\alpha_1, \beta_1) \quad \text{and} \quad (\alpha_2, \beta_2),$$

correspond to two *linearly independent* solutions of the ABE

$$c_{11} \alpha^2 + 2 c_{12} \alpha \beta + c_{22} \beta^2 = 0.$$

Assume that the *discriminant* is positive:

$$\Delta \equiv c_{12}^2 - c_{11} c_{22} > 0.$$

Since along the "given" family we have

$$\mathbf{G}_x^0 \dot{\mathbf{x}}_0 = \mathbf{0} ,$$

we can take

$$\phi_1 = \dot{\mathbf{x}}_0 , \quad (\dot{\mathbf{x}}_0 = \alpha_1 \phi_1 + \beta_1 \phi_2) .$$

Thus

$$(\alpha_1, \beta_1) = (1, 0)$$

is a solution of the ABE

$$c_{11} \alpha^2 + 2 c_{12} \alpha \beta + c_{22} \beta^2 = 0 .$$

Thus

$$c_{11} = 0 , \quad \text{and} \quad (\text{since } c_{12}^2 - c_{11} c_{22} > 0) \quad c_{12} \neq 0 .$$

The second solution then satisfies

$$2 c_{12} \alpha + c_{22} \beta = 0 ,$$

from which,

$$(\alpha_2, \beta_2) = (c_{22}, -2c_{12}) , \quad (\text{unique, up to scaling}) .$$

To evaluate  $c_{12}$  and  $c_{22}$ , we need the null vectors  $\phi_1$  and  $\phi_2$  of  $\mathbf{G}_{\mathbf{x}}^0$ .

$\phi_1$  : We already have chosen  $\phi_1 = \dot{\mathbf{x}}_0$ .

$\phi_2$  : Choose  $\phi_2 \perp \phi_1$ . Then  $\phi_2$  is a null vector of

$$\mathbf{F}_{\mathbf{x}}^0 = \begin{pmatrix} \mathbf{G}_{\mathbf{x}}^0 \\ \dot{\mathbf{x}}_0^* \end{pmatrix} \quad i.e., \quad F_{\mathbf{x}}^0 \phi_2 = \begin{pmatrix} \mathbf{G}_{\mathbf{x}}^0 \\ \dot{\mathbf{x}}_0^* \end{pmatrix} \phi_2 = \mathbf{0}.$$

Note that  $\mathbf{F}_{\mathbf{x}}^0$  is the Jacobian of the pseudo-arclength system at  $\mathbf{x}_0$ !

The null space of  $\mathbf{F}_x^0$  is indeed one-dimensional. (Check!)

$\psi$  : is the left null vector:  $(\mathbf{G}_{\mathbf{x}}^0)^* \psi = \mathbf{0}$ , so that also

$$(\mathbf{F}_{\mathbf{x}}^0)^* \begin{pmatrix} \psi \\ 0 \end{pmatrix} = ((\mathbf{G}_{\mathbf{x}}^0)^* | \dot{\mathbf{x}}_0) \begin{pmatrix} \psi \\ 0 \end{pmatrix} = \mathbf{0},$$

i.e.,  $\psi$  is also the left null vector of  $\mathbf{F}_{\mathbf{x}}^0$ .

NOTE:

- Left and right null vectors of a matrix can be computed *at little cost* , once the matrix has been *LU* decomposed.
- After determining the coefficients  $\alpha_2$  and  $\beta_2$  , scale the direction vector

$$\mathbf{x}'_0 \equiv \alpha_2 \boldsymbol{\phi}_1 + \beta_2 \boldsymbol{\phi}_2 ,$$

of the bifurcating family so that

$$\| \mathbf{x}'_0 \| = 1 .$$

## Switching branches

The *first* solution  $\mathbf{x}_1$  on the bifurcating family can be computed from :

$$\begin{aligned}\mathbf{G}(\mathbf{x}_1) &= \mathbf{0}, \\ (\mathbf{x}_1 - \mathbf{x}_0)^* \mathbf{x}'_0 - \Delta s &= 0,\end{aligned}\tag{3}$$

where

$\mathbf{x}'_0$  is the direction of the bifurcating branch.

As *initial approximation* in Newton's method take

$$\mathbf{x}_1^{(0)} = \mathbf{x}_0 + \Delta s \mathbf{x}'_0.$$

For a graphical interpretation see Figure 20.

NOTE: Computing  $\mathbf{x}'_0$  requires evaluation of  $\mathbf{G}_{\mathbf{xx}}^0$ .

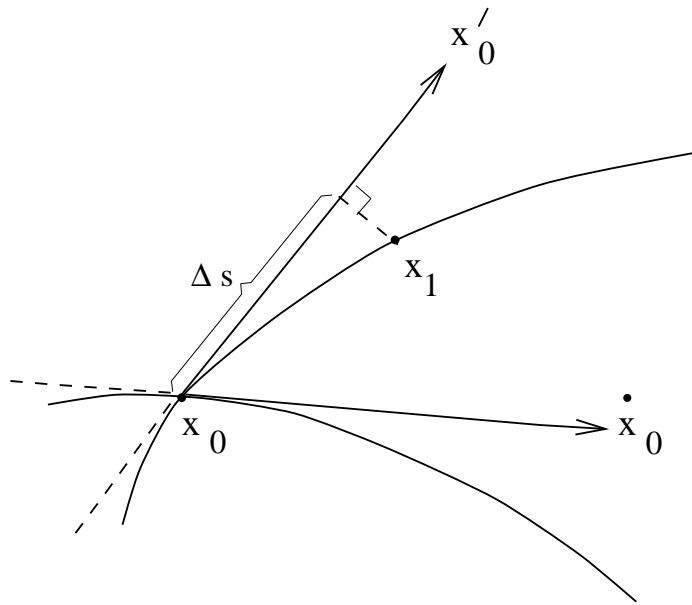


Figure 20: Switching branches using the *correct* bifurcation direction.

## Simplified branch switching

Instead of Eqn. (3) for the *first* solution on the bifurcating branch, use :

$$\mathbf{G}(\mathbf{x}_1) = \mathbf{0},$$

$$(\mathbf{x}_1 - \mathbf{x}_0)^* \phi_2 - \Delta s = 0.$$

where  $\phi_2$  is the second null vector of  $\mathbf{G}_{\mathbf{x}}^0$ , with, as before,

$$\phi_2 \perp \phi_1, \quad (\phi_1 = \dot{\mathbf{x}}_0),$$

i.e.,

$$\begin{pmatrix} \mathbf{G}_{\mathbf{x}}^0 \\ \dot{\mathbf{x}}_0^* \end{pmatrix} \phi_2 = 0, \quad \| \phi_2 \| = 1.$$

As initial approximation, now use

$$\mathbf{x}_1^{(0)} = \mathbf{x}_0 + \Delta s \phi_2.$$

For a graphical interpretation see Figure 21.

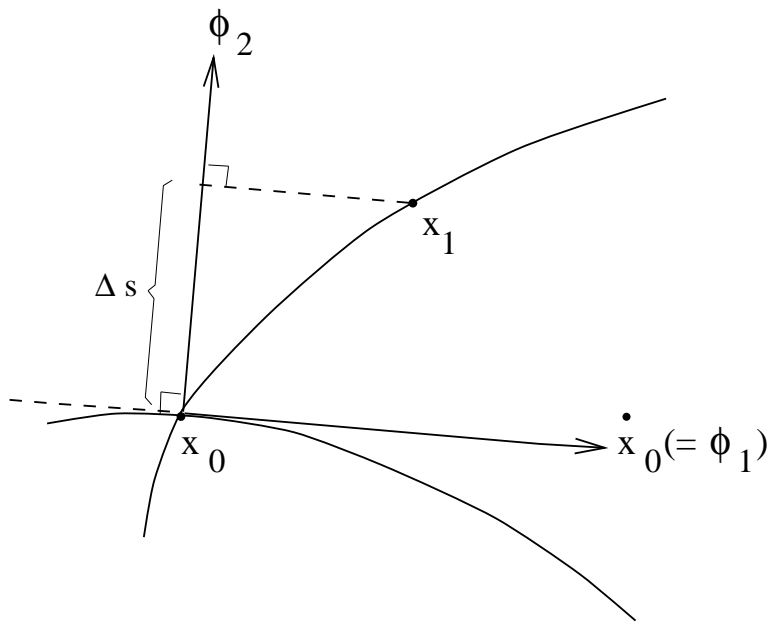


Figure 21: Switching branches using the *orthogonal* direction.

NOTE:

- The simplified branch switching method *may fail* in some situations.
- The advantage is that it *does not need second derivatives* .
- The orthogonal direction  $\phi_2$  can be computed at *little cost* .
- In fact,  $\phi_2$  is the *null vector* of the pseudo-arclength Jacobian

$$\begin{pmatrix} \mathbf{G}_{\mathbf{x}}^0 \\ \dot{\mathbf{x}}_0^* \end{pmatrix}$$

at the branch point.

# Detection of Branch Points

Let

$$\mathbf{G} : \mathbb{R}^{n+1} \rightarrow \mathbb{R}^n .$$

Recall that a solution

$$\mathbf{x}_0 \equiv \mathbf{x}(s_0) \quad \text{of} \quad \mathbf{G}(\mathbf{x}) = \mathbf{0} ,$$

is a *simple singular point* if

$$\mathbf{G}_{\mathbf{x}}^0 \equiv \mathbf{G}_{\mathbf{x}}(\mathbf{x}_0) \quad \text{has rank } n - 1 .$$

Suppose that we have a solution family  $\mathbf{x}(s)$  of

$$\mathbf{G}(\mathbf{x}) = \mathbf{0} ,$$

and that

$$\mathbf{x}_0 = \mathbf{x}(0) ,$$

is a simple singular point.

Let  $\dot{\mathbf{x}}_0$  be the unit tangent to  $\mathbf{x}(s)$  at  $\mathbf{x}_0$ .

Assume that  $\mathbf{x}(s)$  is parametrized by its projection onto  $\dot{\mathbf{x}}_0$ . (See Figure 22.)

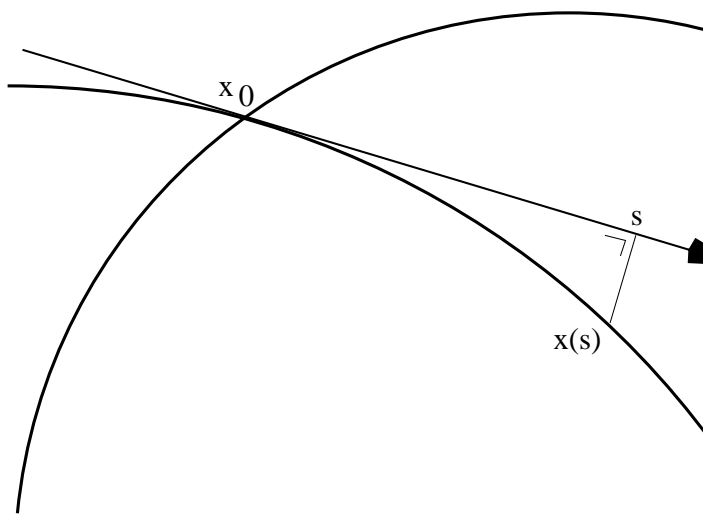


Figure 22: Parametrization of a solution family near a branch point.

Consider the pseudo-arc length system

$$\mathbf{F}(\mathbf{x}; s) \equiv \begin{pmatrix} \mathbf{G}(\mathbf{x}) \\ (\mathbf{x} - \mathbf{x}_0)^* \dot{\mathbf{x}}_0 - s \end{pmatrix}. \quad (4)$$

Then

$$\mathbf{F}_{\mathbf{x}}(\mathbf{x}; s) = \mathbf{F}_{\mathbf{x}}(\mathbf{x}) = \begin{pmatrix} \mathbf{G}_{\mathbf{x}}(\mathbf{x}) \\ \dot{\mathbf{x}}_0^* \end{pmatrix},$$

and

$$\mathbf{F}_{\mathbf{x}}^0 \equiv \mathbf{F}_{\mathbf{x}}(\mathbf{x}_0) = \begin{pmatrix} \mathbf{G}_{\mathbf{x}}^0 \\ \dot{\mathbf{x}}_0^* \end{pmatrix}.$$

NOTE:  $\mathbf{F}_{\mathbf{x}}$  does not explicitly depend on  $s$ .

Take

$$\phi_1 = \dot{\mathbf{x}}_0 ,$$

as the first null vector of  $\mathbf{G}_{\mathbf{x}}^0$ .

Thus

$$\mathbf{F}_{\mathbf{x}}^0 = \begin{pmatrix} \mathbf{G}_{\mathbf{x}}^0 \\ \phi_1^* \end{pmatrix} .$$

Choose the second null vector  $\phi_2$  of  $\mathbf{G}_{\mathbf{x}}^0$  such that

$$\phi_2^* \phi_1 = 0 .$$

Then

$$\mathbf{F}_{\mathbf{x}}^0 \phi_2 = \begin{pmatrix} \mathbf{G}_{\mathbf{x}}^0 \\ \phi_1^* \end{pmatrix} \phi_2 = 0 ,$$

so that  $\phi_2$  is also a null vector of  $\mathbf{F}_{\mathbf{x}}^0$ , while  $\phi_1$  is not.

In fact,  $\mathbf{F}_{\mathbf{x}}^0$  has a *one-dimensional nullspace*.

The null vector of

$$\mathbf{F}_x^{0*} = \begin{pmatrix} \mathbf{G}_x^0 \\ \phi_1^* \end{pmatrix}^* = ((\mathbf{G}_x^0)^* | \phi_1),$$

is given by

$$\Psi \equiv \begin{pmatrix} \psi \\ 0 \end{pmatrix},$$

where  $\psi$  is the null vector of  $(\mathbf{G}_x^0)^*$ .

NOTE: Since

$$\mathbf{G}_x^0 \text{ has } n \text{ rows and } n+1 \text{ columns ,}$$

and

$$\mathcal{N}(\mathbf{G}_x^0) = \text{Span}\{\phi_1, \phi_2\} \text{ is assumed two-dimensional ,}$$

it follows that

$$(\mathbf{G}_x^0)^* \text{ has } n+1 \text{ rows and } n \text{ columns ,}$$

and

$$\mathcal{N}(\mathbf{G}_x^{0*}) = \text{Span}\{\psi\} \text{ is one-dimensional .}$$

**THEOREM.** Let

$$\mathbf{x}_0 = \mathbf{x}(0),$$

be a *simple singular point* on a smooth solution family  $\mathbf{x}(s)$  of

$$\mathbf{G}(\mathbf{x}) = \mathbf{0}.$$

Let  $\mathbf{F}(\mathbf{x}; s)$  be as above, *i.e.*,  $\mathbf{F}(\mathbf{x}; s) \equiv \begin{pmatrix} \mathbf{G}(\mathbf{x}) \\ (\mathbf{x} - \mathbf{x}_0)^* \dot{\mathbf{x}}_0 - s \end{pmatrix}.$

Assume that

- the *discriminant*  $\Delta$  of the ABE is *positive*,
- 0 is an *algebraically* simple eigenvalue of

$$\mathbf{F}_{\mathbf{x}}^0 \equiv \begin{pmatrix} \mathbf{G}_{\mathbf{x}}^0 \\ \dot{\mathbf{x}}_0^* \end{pmatrix}.$$

Then

$$\det \mathbf{F}_{\mathbf{x}}(\mathbf{x}(s)) = \det \begin{pmatrix} \mathbf{G}_{\mathbf{x}}(\mathbf{x}(s)) \\ \dot{\mathbf{x}}_0^* \end{pmatrix},$$

*changes sign* at  $\mathbf{x}_0$ .

PROOF.

Consider the parametrized eigenvalue problem

$$\mathbf{F}_x(\mathbf{x}(s)) \phi(s) = \kappa(s) \phi(s),$$

where  $\kappa(s)$  and  $\phi(s)$  are smooth near  $s = 0$ , with

$$\kappa(0) = 0 \quad \text{and} \quad \phi(0) = \phi_2,$$

i.e., the eigen pair

$$(\kappa(s), \phi(s)),$$

is the continuation of  $(0, \phi_2)$ .

(This can be done because  $0$  is an algebraically simple eigenvalue.)

Differentiating

$$\mathbf{F}_{\mathbf{x}}(\mathbf{x}(s)) \phi(s) = \kappa(s) \phi(s),$$

gives

$$\mathbf{F}_{\mathbf{xx}}(\mathbf{x}(s)) \dot{\mathbf{x}}(s) \phi(s) + \mathbf{F}_{\mathbf{x}}(\mathbf{x}(s)) \dot{\phi}(s) = \dot{\kappa}(s) \phi(s) + \kappa(s) \dot{\phi}(s).$$

Evaluating at  $s = 0$ , using

$$\kappa(0) = 0,$$

and

$$\dot{\mathbf{x}}_0 = \phi_1 \quad \text{and} \quad \phi(0) = \phi_2,$$

gives

$$\mathbf{F}_{\mathbf{xx}}^0 \phi_1 \phi_2 + \mathbf{F}_{\mathbf{x}}^0 \dot{\phi}(0) = \dot{\kappa}_0 \phi_2.$$

$$\boxed{\mathbf{F}_{\mathbf{xx}}^0 \phi_1 \phi_2 + \mathbf{F}_x^0 \dot{\phi}(0) = \dot{\kappa}_0 \phi_2} .$$

Multiplying this on the left by  $\Psi^*$  we find

$$\dot{\kappa}_0 = \frac{\Psi^* \mathbf{F}_{\mathbf{xx}}^0 \phi_1 \phi_2}{\Psi^* \phi_2} = \frac{(\psi^*, 0) \begin{pmatrix} \mathbf{G}_{\mathbf{xx}}^0 \\ 0 \end{pmatrix} \phi_1 \phi_2}{\Psi^* \phi_2} = \frac{\psi^* \mathbf{G}_{\mathbf{xx}}^0 \phi_1 \phi_2}{\Psi^* \phi_2} .$$

The left and right null vectors ( $\Psi$  and  $\phi_2$ ) of  $\mathbf{F}_x^0$  *cannot be orthogonal* (because the eigenvalue 0 is assumed to be *algebraically simple*).

Thus

$$\Psi^* \phi_2 \neq 0 .$$

Note that

$$\psi^* \mathbf{G}_{\mathbf{x}\mathbf{x}}^0 \phi_1 \phi_2 = c_{12},$$

is a coefficient of the ABE.

By assumption, the discriminant satisfies

$$\Delta \neq 0.$$

As before this implies that

$$c_{12} \neq 0,$$

and hence

$$\dot{\kappa}_0 \neq 0 \quad \bullet$$

NOTE:

- The Theorem implies that  $\det \begin{pmatrix} \mathbf{G}_x(\mathbf{x}(s)) \\ \dot{\mathbf{x}}_0^* \end{pmatrix}$  changes sign .
- Note that  $\dot{\mathbf{x}}_0$  is kept fixed.
- We haven't proved that  $\det \mathbf{F}_x(\mathbf{x}(s)) = \det \begin{pmatrix} \mathbf{G}_x(\mathbf{x}(s)) \\ \dot{\mathbf{x}}(s)^* \end{pmatrix}$  changes sign.
- The latter follows from a similar, but more elaborate argument.
- Detection of simple singular points is based upon this fact.
- During continuation we monitor the determinant of the matrix  $\mathbf{F}_x$  .
- If a sign change is detected then an iterative method can be used to accurately locate the singular point.
- For large systems a scaled determinant avoids overflow .

The following theorem states that there must be a bifurcation at  $x_0$  .  
(This result can be proven by *degree theory* .)

## THEOREM.

Let  $\mathbf{x}(s)$  be a smooth solution family of

$$\mathbf{F}(\mathbf{x}; s) = \mathbf{0},$$

where

$$\mathbf{F} : \mathbb{R}^{n+1} \times \mathbb{R} \rightarrow \mathbb{R}^{n+1} \quad \text{is } C^1,$$

and assume that

$$\det \mathbf{F}_{\mathbf{x}}(\mathbf{x}(s); s) \text{ changes sign at } s = 0.$$

Then  $\mathbf{x}(0)$  is a *bifurcation point* , i.e., every open neighborhood of  $\mathbf{x}_0$  contains a solution of  $\mathbf{F}(\mathbf{x}; s) = \mathbf{0}$  that does not lie on  $\mathbf{x}(s)$  .

# Boundary Value Problems

# Boundary Value Problems.

Consider the first order system of ordinary differential equations

$$\mathbf{u}'(t) - \mathbf{f}(\mathbf{u}(t), \mu, \lambda) = \mathbf{0}, \quad t \in [0, 1],$$

where

$$\mathbf{u}(\cdot), \mathbf{f}(\cdot) \in \mathbb{R}^n, \quad \lambda \in \mathbb{R}, \quad \mu \in \mathbb{R}^{n_\mu},$$

subject to boundary conditions

$$\mathbf{b}(\mathbf{u}(0), \mathbf{u}(1), \mu, \lambda) = \mathbf{0}, \quad \mathbf{b}(\cdot) \in \mathbb{R}^{n_b},$$

and integral constraints

$$\int_0^1 \mathbf{q}(\mathbf{u}(s), \mu, \lambda) ds = \mathbf{0}, \quad \mathbf{q}(\cdot) \in \mathbb{R}^{n_q}.$$

This boundary value problem (BVP) is of the form

$$\mathbf{F}(\mathbf{X}) = \mathbf{0},$$

where

$$\mathbf{X} = (\mathbf{u}, \mu, \lambda),$$

to which we add the *pseudo-arclength* equation

$$\langle \mathbf{X} - \mathbf{X}_0, \dot{\mathbf{X}}_0 \rangle - \Delta s = 0,$$

where  $\mathbf{X}_0$  represents the preceding solution on the branch.

In detail, the pseudo-arclength equation is

$$\begin{aligned} \int_0^1 (\mathbf{u}(t) - \mathbf{u}_0(t))^* \dot{\mathbf{u}}_0(t) dt + (\mu - \mu_0) \dot{\mu}_0 \\ + (\lambda - \lambda_0) \dot{\lambda}_0 - \Delta s = 0. \end{aligned}$$

- We want to solve BVP for  $\mathbf{u}(\cdot)$  and  $\mu$ .
- We can think of  $\lambda$  as the *continuation parameter*.
- (In *pseudo-arc length continuation*, we don't distinguish  $\mu$  and  $\lambda$ .)
- In order for problem to be *formally well-posed* we must have

$$n_\mu = n_b + n_q - n \geq 0.$$

- A *simple case* is

$$n_q = 0, \quad n_b = n, \quad \text{for which } n_\mu = 0.$$

# Discretization

Here we discuss the method of “orthogonal collocation with piecewise polynomials”, for solving boundary value problems. This method is very accurate, and allows adaptive mesh-selection.

# Orthogonal Collocation

Introduce a mesh

$$\{ 0 = t_0 < t_1 < \cdots < t_N = 1 \} ,$$

where

$$h_j \equiv t_j - t_{j-1} , \quad (1 \leq j \leq N) ,$$

Define the space of (vector) *piecewise polynomials*  $\mathbf{P}_h^m$  as

$$\mathbf{P}_h^m \equiv \{ \mathbf{p}_h \in C[0, 1] : \mathbf{p}_h|_{[t_{j-1}, t_j]} \in \mathbf{P}^m \} ,$$

where  $\mathbf{P}^m$  is the space of (vector) polynomials of degree  $\leq m$ .

The collocation method consists of finding

$$\mathbf{p}_h \in \mathbf{P}_h^m , \quad \mu \in \mathbf{R}^{n_\mu} ,$$

such that the following *collocation equations* are satisfied:

$$\mathbf{p}'_h(z_{j,i}) = \mathbf{f}(\mathbf{p}_h(z_{j,i}), \mu, \lambda) , \quad j = 1, \dots, N , \quad i = 1, \dots, m ,$$

and such that  $\mathbf{p}_h$  satisfies the boundary and integral conditions.

The *collocation points*  $z_{j,i}$  in each subinterval

$$[t_{j-1}, t_j] ,$$

are the (scaled) roots of the  $m$ th-degree orthogonal polynomial (*Gauss points*) .

See Figure 23 for a graphical interpretation.

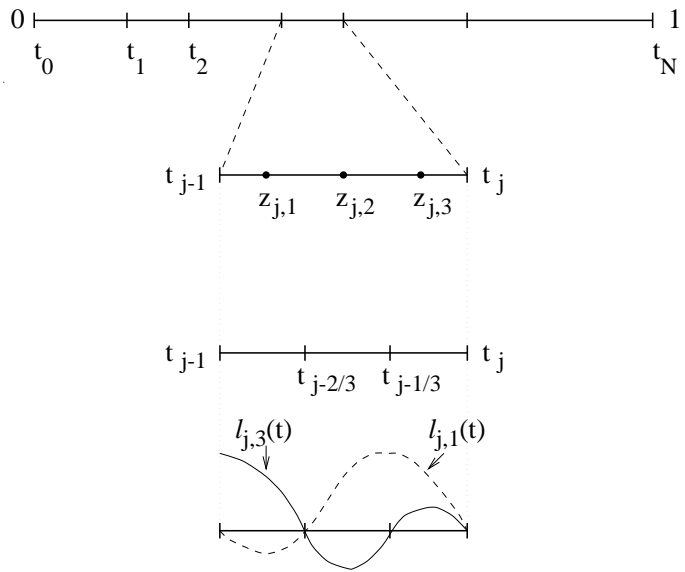


Figure 23: The mesh  $\{0 = t_0 < t_1 < \dots < t_N = 1\}$ . Collocation points and “extended-mesh points” are shown for the case  $m = 3$ , in the  $j$ th mesh interval. Also shown are two of the four local Lagrange basis polynomials.

Since each local polynomial is determined by

$$(m + 1) n ,$$

coefficients, the total number of degrees of freedom (considering  $\lambda$  as fixed) is

$$(m + 1) n N + n_\mu .$$

This is matched by the total number of equations :

$$\text{collocation} : m n N ,$$

$$\text{continuity} : (N - 1) n ,$$

$$\text{constraints} : n_b + n_q \quad (= n + n_\mu) .$$

Assume that the solution  $\mathbf{u}(t)$  of the BVP is sufficiently smooth.

Then the *order of accuracy* of the orthogonal collocation method is  $m$ , i.e.,

$$\| \mathbf{p}_h - \mathbf{u} \|_{\infty} = \mathcal{O}(h^m).$$

At the main meshpoints  $t_j$  we have *superconvergence*:

$$\max_j | \mathbf{p}_h(t_j) - \mathbf{u}(t_j) | = \mathcal{O}(h^{2m}).$$

The scalar variables  $\mu$  are also superconvergent.

# Implementation

For each subinterval  $[t_{j-1}, t_j]$ , introduce the Lagrange basis polynomials

$$\{\ell_{j,i}(t)\}, \quad j = 1, \dots, N, \quad i = 0, 1, \dots, m,$$

defined by

$$\ell_{j,i}(t) = \prod_{k=0, k \neq i}^m \frac{t - t_{j-\frac{k}{m}}}{t_{j-\frac{i}{m}} - t_{j-\frac{k}{m}}},$$

where

$$t_{j-\frac{i}{m}} \equiv t_j - \frac{i}{m} h_j.$$

The local polynomials can then be written

$$\mathbf{p}_j(t) = \sum_{i=0}^m \ell_{j,i}(t) \mathbf{u}_{j-\frac{i}{m}}.$$

With the above choice of basis

$$\mathbf{u}_j \sim \mathbf{u}(t_j) \quad \text{and} \quad \mathbf{u}_{j-\frac{i}{m}} \sim \mathbf{u}(t_{j-\frac{i}{m}}),$$

where  $\mathbf{u}(t)$  is the solution of the continuous problem.

The collocation equations are

$$\mathbf{p}_j'(z_{j,i}) = \mathbf{f}(\mathbf{p}_j(z_{j,i}), \mu, \lambda), \quad i = 1, \dots, m, \quad j = 1, \dots, N.$$

The *discrete boundary conditions* are

$$b_i(\mathbf{u}_0, \mathbf{u}_N, \mu, \lambda) = 0, \quad i = 1, \dots, n_b.$$

The *integral constraints* can be discretized as

$$\sum_{j=1}^N \sum_{i=0}^m \omega_{j,i} q_k(\mathbf{u}_{j-\frac{i}{m}}, \mu, \lambda) = 0, \quad k = 1, \dots, n_q,$$

where the  $\omega_{j,i}$  are the *Lagrange quadrature weights*.

The *pseudo-arc length equation* is

$$\int_0^1 (\mathbf{u}(t) - \mathbf{u}_0(t))^* \dot{\mathbf{u}}_0(t) dt + (\mu - \mu_0)^* \dot{\mu}_0 + (\lambda - \lambda_0) \dot{\lambda}_0 - \Delta s = 0,$$

where

$$(\mathbf{u}_0, \mu_0, \lambda_0),$$

is the *previous solution* on the solution branch, and

$$(\dot{\mathbf{u}}_0, \dot{\mu}_0, \dot{\lambda}_0),$$

is the *normalized direction* of the branch at the previous solution.

The *discretized pseudo-arc length equation* is

$$\begin{aligned} & \sum_{j=1}^N \sum_{i=0}^m \omega_{j,i} [ \mathbf{u}_{j-\frac{i}{m}} - (\mathbf{u}_0)_{j-\frac{i}{m}} ]^* (\dot{\mathbf{u}}_0)_{j-\frac{i}{m}} \\ & + (\mu - \mu_0)^* \dot{\mu}_0 + (\lambda - \lambda_0) \dot{\lambda}_0 - \Delta s = 0. \end{aligned}$$

# Numerical Linear Algebra

The complete discretization consists of

$$m \ n \ N \ + \ n_b \ + \ n_q \ + \ 1 ,$$

nonlinear equations, in the unknowns

$$\{\mathbf{u}_{j-\frac{i}{m}}\} \in \mathbb{R}^{mnN+n} , \quad \mu \in \mathbb{R}^{n_\mu} , \quad \lambda \in \mathbb{R} .$$

These equations can be solved by a *Newton-Chord iteration* .

We illustrate the *numerical linear algebra* for the case

$n = 2$  ODEs ,  $N = 4$  mesh intervals ,  $m = 3$  collocation points ,

$n_b = 2$  boundary conditions ,  $n_q = 1$  integral constraint ,

and the pseudo-arclength equation.

- The operations are also done on the *right hand side* , which is not shown.
- Entries marked “o” have been *eliminated* by Gauss elimination.
- Entries marked “.” denote *fill-in* due to *pivoting* .
- Most of the operations can be done *in parallel* .

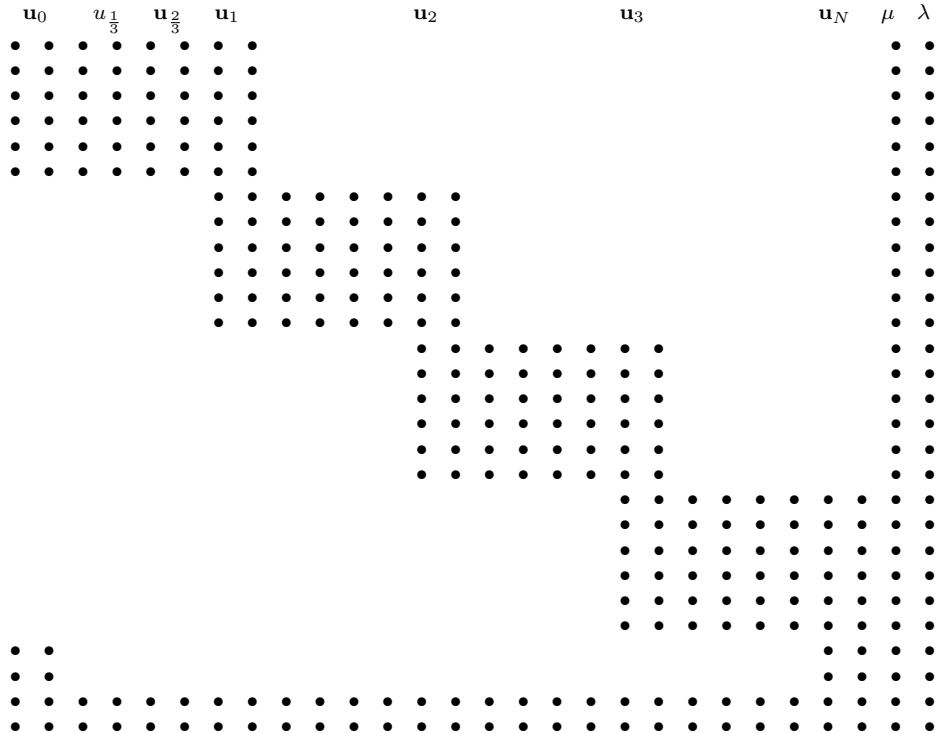


Figure 24: The structure of the Jacobian

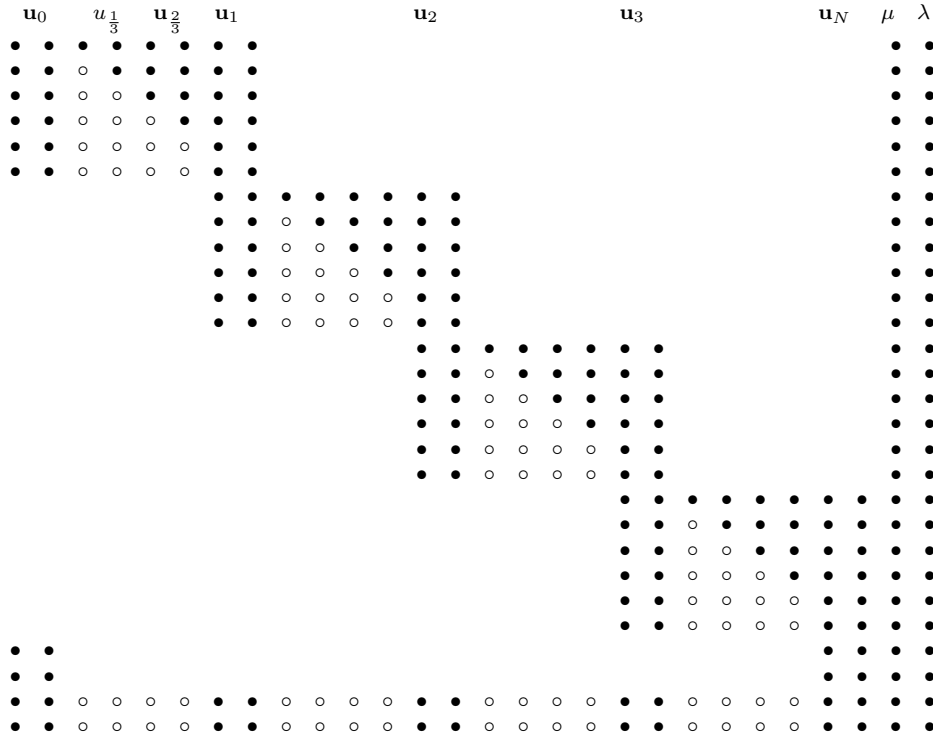


Figure 25: The system after *condensation of parameters*.

$\mathbf{u}_0$	$u_{\frac{1}{3}}$	$\mathbf{u}_{\frac{2}{3}}$	$\mathbf{u}_1$	$\mathbf{u}_2$	$\mathbf{u}_3$	$\mathbf{u}_N$	$\mu$	$\lambda$
• • •	• • •	• • •	• • •	• • •	• • •	• • •	• • •	• • •
• • •	○ • •	• • •	• • •	• • •	• • •	• • •	• • •	• • •
• • •	○ ○ ○	• • •	• • •	• • •	• • •	• • •	• • •	• • •
• • •	○ ○ ○	• • •	• • •	• • •	• • •	• • •	• • •	• • •
★ ★ ○ ○ ○	○ ○ ○	★ ★	★ ★				★ ★	
★ ★ ○ ○ ○	○ ○ ○	★ ★	★ ★				★ ★	
				• • •	• • •	• • •	• • •	• • •
				• ○ •	• • •	• • •	• • •	• • •
				• ○ ○	• • •	• • •	• • •	• • •
				• ○ ○	• • •	• • •	• • •	• • •
				★ ○ ○	○ ○ ○	★ ★	★ ★	
				★ ○ ○	○ ○ ○	★ ★	★ ★	
				★ ○ ○	○ ○ ○	★ ★	★ ★	
				★ ○ ○	○ ○ ○	★ ★	★ ★	
				• • •	• • •	• • •	• • •	• • •
				• ○ •	• • •	• • •	• • •	• • •
				• ○ ○	• • •	• • •	• • •	• • •
				• ○ ○	• • •	• • •	• • •	• • •
				★ ○ ○	○ ○ ○	★ ★	★ ★	
				★ ○ ○	○ ○ ○	★ ★	★ ★	
				★ ○ ○	○ ○ ○	★ ★	★ ★	
★ ★							★ ★	★ ★
★ ★							★ ★	★ ★
★ ★ ○ ○ ○	○ ○ ○	★ ★	○ ○ ○	○ ○ ○	★ ★	○ ○ ○	★ ★	★ ★
★ ★ ○ ○ ○	○ ○ ○	★ ★	○ ○ ○	○ ○ ○	★ ★	○ ○ ○	★ ★	★ ★

Figure 26: The preceding matrix, showing the decoupled  $\star$  sub-system.

$\mathbf{u}_0$	$u_{\frac{1}{3}}$	$\mathbf{u}_{\frac{2}{3}}$	$\mathbf{u}_1$	$\mathbf{u}_2$	$\mathbf{u}_3$	$\mathbf{u}_N$	$\mu$	$\lambda$
• • •	• • •	• • •	• • •	.	.	.	• •	• •
• • •	○ • •	• • •	• • •	.	.	.	• •	• •
• • •	○ ○ ○	• • •	• • •	.	.	.	• •	• •
• • •	○ ○ ○	• • •	• • •	.	.	.	• •	• •
★ ★ ○ ○ ○ ○	○ ○ ○ ○	★ ★	.	.	.	.	★ ★	.
★ ★ ○ ○ ○ ○	○ ○ ○ ○	○ ★	.	.	.	.	★ ★	.
• • •	• • •	• • •	• • •	• • •	• • •	• • •	• •	• •
• • •	• • ○	• • •	• • •	• • •	• • •	• • •	• •	• •
• • •	• ○ ○	• • ○	• • ○	• • ○	• • ○	• • ○	• •	• •
• • •	○ ○ ○	• ○ ○	• ○ ○	• ○ ○	• ○ ○	• ○ ○	• •	• •
• • •	○ ○ ○	○ ○ ○	• ○ ○	• ○ ○	• ○ ○	• ○ ○	• •	• •
★ ★	○ ○ ○ ○ ○ ○	○ ○ ○ ○ ○ ○	★ ★	.	.	.	★ ★	.
★ ★	○ ○ ○ ○ ○ ○	○ ○ ○ ○ ○ ○	★ ★	.	.	.	★ ★	.
• • •	• • •	• • •	• • •	• • •	• • •	• • •	• •	• •
• • •	• • ○	• • •	• • •	• • •	• • •	• • •	• •	• •
• • •	• ○ ○	• • ○	• • ○	• • ○	• • ○	• • ○	• •	• •
• • •	○ ○ ○	• ○ ○	• ○ ○	• ○ ○	• ○ ○	• ○ ○	• •	• •
• • •	○ ○ ○	○ ○ ○	• ○ ○	• ○ ○	• ○ ○	• ○ ○	• •	• •
★ ★ ○ ○ ○ ○	○ ○ ○ ○ ○ ○	★ ★	.	.	.	.	★ ★	★ ★
★ ★ ○ ○ ○ ○	○ ○ ○ ○ ○ ○	○ ★	.	.	.	.	★ ★	★ ★
• • •	• • •	• • •	• • •	• • •	• • •	• • •	• •	• •
• • •	• • ○	• • •	• • •	• • •	• • •	• • •	• •	• •
• • •	• ○ ○	• • ○	• • ○	• • ○	• • ○	• • ○	• •	• •
• • •	○ ○ ○	• ○ ○	• ○ ○	• ○ ○	• ○ ○	• ○ ○	• •	• •
• • •	○ ○ ○	○ ○ ○	• ○ ○	• ○ ○	• ○ ○	• ○ ○	• •	• •
★ ★	○ ○ ○ ○ ○ ○	○ ○ ○ ○ ○ ○	★ ★	.	.	.	★ ★	.
★ ★	○ ○ ○ ○ ○ ○	○ ○ ○ ○ ○ ○	★ ★	.	.	.	★ ★	.
★ ★ ○ ○ ○ ○	○ ○ ○ ○ ○ ○	★ ★	.	.	.	.	★ ★	★ ★
★ ★ ○ ○ ○ ○	○ ○ ○ ○ ○ ○	○ ★	.	.	.	.	★ ★	★ ★

Figure 27: Stage 1 of the *nested dissection* to solve the decoupled  $\star$  system.



Figure 29: The preceding matrix showing the final decoupled + sub-system.

$\mathbf{u}_0$	$u_{\frac{1}{3}}$	$\mathbf{u}_{\frac{2}{3}}$	$\mathbf{u}_1$	$\mathbf{u}_2$	$\mathbf{u}_3$	$\mathbf{u}_N$	$\mu$	$\lambda$
•	•	•	•	•	•	•	•	•
•	•	○	•	•	•	•	•	•
•	•	○	○	•	•	•	•	•
•	•	○	○	○	•	•	•	•
★	★	○	○	○	○	★	★	★
★	★	○	○	○	○	★	★	★
★	★	○	○	○	○	★	★	★
★	★	○	○	○	○	○	★	★
A	A	○	○	○	○	B	B	+
A	A	○	○	○	○	B	B	+
+	+	+	+	+	+	+	+	+
+	+	+	+	+	+	+	+	+
+	+	○	○	○	○	○	+	+
+	+	○	○	○	○	○	+	+

Figure 30: The Floquet Multipliers are the eigenvalues of  $-B^{-1}A$ .

# Accuracy Test

The Table shows the *location of the fold* in the Gelfand-Bratu problem for

- 4 Gauss *collocation points* per mesh interval
- $N$  *mesh intervals*

$N$	Fold location
2	3.5137897550
4	3.5138308601
8	3.5138307211
16	3.5138307191
32	3.5138307191

# A Singularly-Perturbed BVP

$$\epsilon u''(x) = u(x) u'(x) (u(x)^2 - 1) + u(x) .$$

with boundary conditions

$$u(0) = \frac{3}{2} , \quad u(1) = \gamma .$$

Computational formulation

$$u'_1 = u_2 ,$$

$$u'_2 = \frac{\lambda}{\epsilon} ( u_1 u_2 (u_1^2 - 1) + u_1 ) ,$$

with boundary conditions

$$u_1(0) = 3/2 , \quad u_1(1) = \gamma .$$

When  $\lambda = 0$  an *exact solution* is

$$u_1(x) = \frac{3}{2} + (\gamma - \frac{3}{2}) x , \quad u_2(x) = \gamma - \frac{3}{2} .$$

## COMPUTATIONAL STEPS:

- $\lambda$  is a *homotopy parameter* to locate a starting solution.
- In the *first run*  $\lambda$  varies from 0 to 1 .
- In the *second run*  $\epsilon$  is decreased by continuation.
- In the *third run*  $\epsilon = 10^{-3}$  , and the solution is continued in  $\gamma$  .
- This third run takes many continuation steps if  $\epsilon$  is very small.

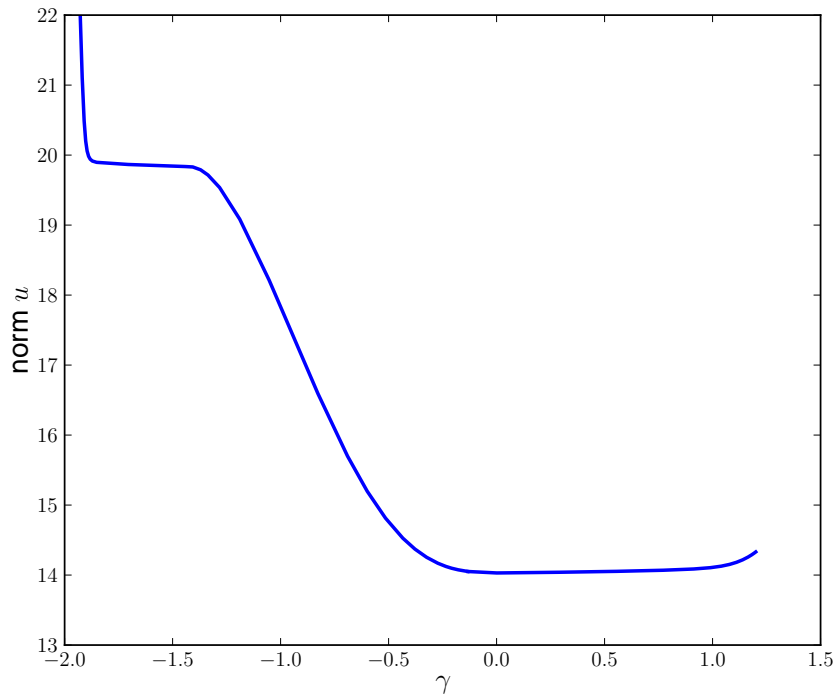


Figure 31: Bifurcation diagram of the singularly-perturbed BVP.

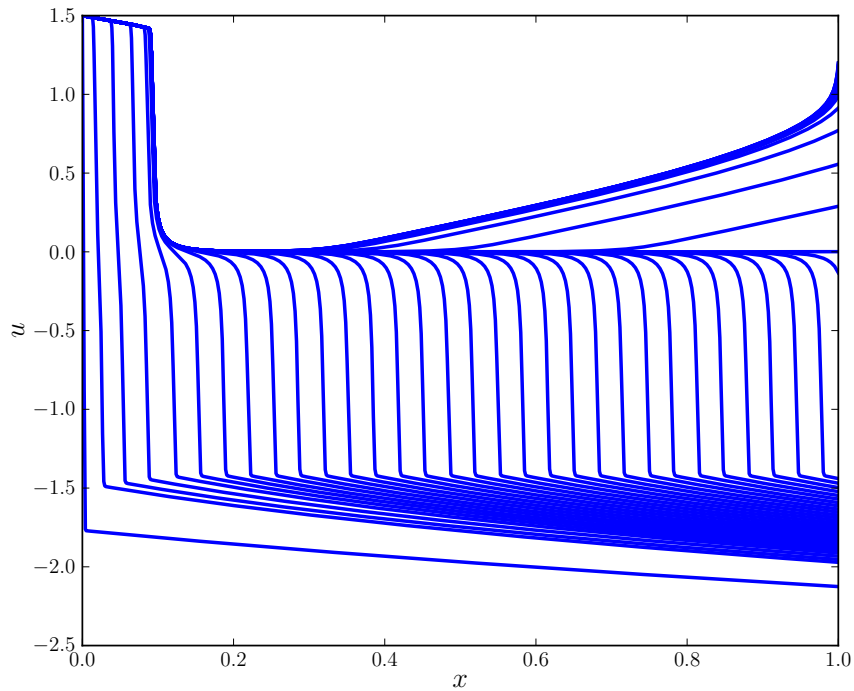


Figure 32: Some solutions along the solution family.

# Hopf Bifurcation and Periodic Solutions

We first introduce the concept of Hopf bifurcation for a “linear” problem. Then we state the Hopf Bifurcation Theorem (without proof), and we give examples of periodic solutions emanating from Hopf bifurcation points.

# A Linear Example

The linear problem :

$$\begin{cases} u'_1 = \lambda u_1 - u_2 , \\ u'_2 = u_1 , \end{cases} \quad (5)$$

which can also be written as

$$\begin{pmatrix} u'_1 \\ u'_2 \end{pmatrix} = \begin{pmatrix} \lambda & -1 \\ 1 & 0 \end{pmatrix} \begin{pmatrix} u_1 \\ u_2 \end{pmatrix} ,$$

is of the form

$$\mathbf{u}'(t) = A(\lambda) \mathbf{u}(t) \equiv \mathbf{G}(\mathbf{u}, \lambda) ,$$

with stationary solutions,

$$u_1 = u_2 = 0 , \quad \text{for all } \lambda .$$

The eigenvalues  $\mu$  of the Jacobian matrix

$$\mathbf{G}_{\mathbf{u}}(\mathbf{u}, \lambda) = A(\lambda) = \begin{pmatrix} \lambda & -1 \\ 1 & 0 \end{pmatrix} = \mathbf{G}_{\mathbf{u}}(\mathbf{0}, \lambda),$$

satisfy

$$\det(A(\lambda) - \mu I) = \mu^2 - \lambda \mu + 1 = 0,$$

from which

$$\mu_{1,2} = \frac{\lambda \pm \sqrt{\lambda^2 - 4}}{2}.$$

Consider the initial value problem

$$\mathbf{u}'(t) = A(\lambda) \mathbf{u}(t) \equiv \mathbf{G}(\mathbf{u}, \lambda),$$

with

$$\mathbf{u}(0) = \begin{pmatrix} u_1(0) \\ u_2(0) \end{pmatrix} = \begin{pmatrix} p_1 \\ p_2 \end{pmatrix} \equiv \mathbf{p}.$$

Then

$$\begin{aligned}\mathbf{u}(t) &= e^{tA(\lambda)} \mathbf{p} = V(\lambda) e^{t\Lambda(\lambda)} V^{-1}(\lambda) \mathbf{p} \\ &= V(\lambda) \begin{pmatrix} e^{t\mu_1(\lambda)} & 0 \\ 0 & e^{t\mu_2(\lambda)} \end{pmatrix} V^{-1}(\lambda) \mathbf{p},\end{aligned}\tag{6}$$

where

$$A(\lambda) V(\lambda) = V(\lambda) \Lambda(\lambda), \quad A(\lambda) = V(\lambda) \Lambda(\lambda) V^{-1}(\lambda),$$

and

$$\Lambda(\lambda) = \begin{pmatrix} \mu_1(\lambda) & 0 \\ 0 & \mu_2(\lambda) \end{pmatrix}, \quad V(\lambda) = \begin{pmatrix} v_{11}(\lambda) & v_{12}(\lambda) \\ v_{21}(\lambda) & v_{22}(\lambda) \end{pmatrix}.$$

Assume that

$$-2 < \lambda < 2 ,$$

and recall that

$$\mathbf{u}(t) = V(\lambda) \begin{pmatrix} e^{t\mu_1(\lambda)} & 0 \\ 0 & e^{t\mu_2(\lambda)} \end{pmatrix} V^{-1}(\lambda) \mathbf{p} ,$$

and

$$\mu_{1,2} = \frac{\lambda \pm \sqrt{\lambda^2 - 4}}{2} .$$

Thus we see that

$$\mathbf{u}(t) \rightarrow \mathbf{0} \quad \text{if } \lambda < 0 ,$$

and

$$\mathbf{u}(t) \rightarrow \infty \quad \text{if } \lambda > 0 ,$$

i.e., the zero solution is stable if  $\lambda$  is negative, and unstable if  $\lambda$  is positive.

However, if  $\lambda = 0$ , then

$$A_0 \equiv A(0) = \begin{pmatrix} 0 & -1 \\ 1 & 0 \end{pmatrix},$$

and

$$\begin{aligned} \mu_1 &= i, & \mu_2 &= -i, \\ V_0 &\equiv V(0) = \begin{pmatrix} 1 & -i \\ -i & 1 \end{pmatrix}, \\ V_0^{-1} &= \frac{1}{2} \begin{pmatrix} 1 & i \\ i & 1 \end{pmatrix}, \end{aligned}$$

so that

$$\begin{aligned} \mathbf{u}(t) &= V_0 e^{t\Lambda} V_0^{-1} \mathbf{p} = \frac{1}{2} \begin{pmatrix} 1 & -i \\ -i & 1 \end{pmatrix} \begin{pmatrix} e^{it} & 0 \\ 0 & e^{-it} \end{pmatrix} \begin{pmatrix} 1 & i \\ i & 1 \end{pmatrix} \begin{pmatrix} p_1 \\ p_2 \end{pmatrix} \\ &= \frac{1}{2} \begin{pmatrix} e^{it} + e^{-it} & i(e^{it} - e^{-it}) \\ -i(e^{it} - e^{-it}) & e^{it} + e^{-it} \end{pmatrix} \begin{pmatrix} p_1 \\ p_2 \end{pmatrix}. \end{aligned}$$

Thus, if  $\lambda = 0$ , then

$$\begin{pmatrix} u_1(t) \\ u_2(t) \end{pmatrix} = \begin{pmatrix} \cos(t) & -\sin(t) \\ \sin(t) & \cos(t) \end{pmatrix} \begin{pmatrix} p_1 \\ p_2 \end{pmatrix} = \begin{pmatrix} p_1 \cos(t) - p_2 \sin(t) \\ p_1 \sin(t) + p_2 \cos(t) \end{pmatrix},$$

and we see that

- This solution is periodic, with period  $2\pi$ , for any  $p_1, p_2$ .
- $u_1(t)^2 + u_2(t)^2 = p_1^2 + p_2^2$ , (The orbits are circles.) ,
- We can fix the phase by setting, for example,  $p_2 = 0$  .
- (Then  $u_2(0) = 0$  .)
- This leaves a one-parameter family of periodic solutions.  
(See Figures 33 and 34.).
- For nonlinear problems the family is generally not “vertical”.

EXERCISE. (Demo 1hb .)

Use **AUTO** to compute the zero stationary solution family, a Hopf bifurcation, and the emanating family of periodic solutions, of the “linear” Hopf bifurcation problem, *i.e.*, of

$$\begin{cases} u'_1 = \lambda u_1 - u_2 , \\ u'_2 = u_1 . \end{cases} \quad (7)$$

NOTE:

- The family of periodic solutions is “vertical”, *i.e.*,  $\lambda = 0$  along it.
- This is not “typical” (not “*generic*”) for Hopf bifurcation.
- For the numerically computed family,  $\lambda = 0$  up to numerical accuracy.
- The period is constant, namely,  $2\pi$ , along the family.
- This is also not generic for periodic solutions from a Hopf bifurcation.
- The numerical computation of periodic solutions will be considered later.

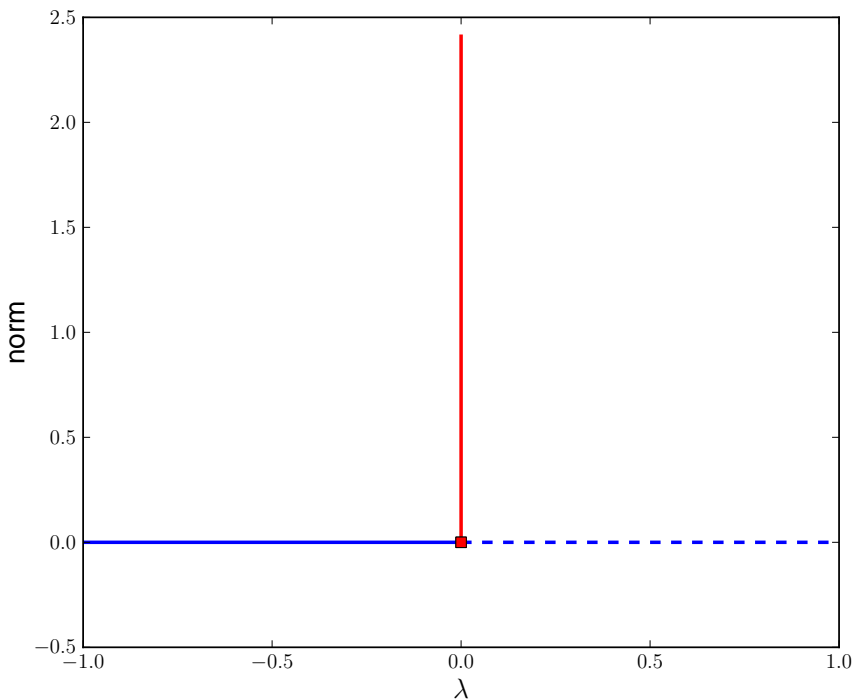


Figure 33: Bifurcation diagram of the “linear” Hopf bifurcation problem.

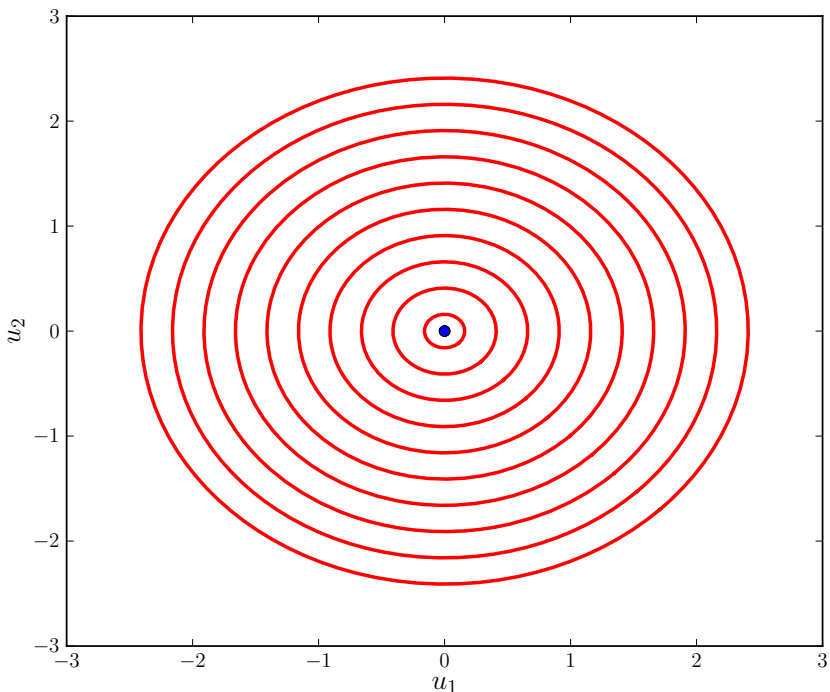


Figure 34: A phase plot of some periodic solutions.

# The Hopf Bifurcation Theorem

THEOREM. Suppose that along a stationary solution family  $(\mathbf{u}(\lambda), \lambda)$ , of

$$\mathbf{u}' = \mathbf{f}(\mathbf{u}, \lambda) ,$$

a complex conjugate pair of eigenvalues

$$\alpha(\lambda) \pm i \beta(\lambda) ,$$

of  $f_{\mathbf{u}}(\mathbf{u}(\lambda), \lambda)$  crosses the imaginary axis transversally, *i.e.*, for some  $\lambda_0$ ,

$$\alpha(\lambda_0) = 0 , \quad \beta(\lambda_0) \neq 0 , \quad \text{and} \quad \dot{\alpha}(\lambda_0) \neq 0 .$$

Also assume that there are no other eigenvalues on the imaginary axis.

Then there is a *Hopf bifurcation*, *i.e.*, a family of periodic solutions bifurcates from the stationary solution at  $(\mathbf{u}_0, \lambda_0)$ .       $\circ$

NOTE: The assumptions also imply that  $\mathbf{f}_{\mathbf{u}}^0$  is nonsingular, so that the stationary solution family can indeed be parametrized locally using  $\lambda$ .

EXERCISE. (AUTO Demo vhb.)

Use **AUTO** to compute the zero stationary solution family, a Hopf bifurcation, and the emanating family of periodic solutions for the equation

$$\begin{cases} u'_1 = \lambda u_1 - u_2, \\ u'_2 = u_1 (1 - u_1). \end{cases} \quad (8)$$

NOTE:

- $\mathbf{u}(t) \equiv \mathbf{0}$  is a stationary solution for all  $\lambda$ .
- $\mathbf{u}(t) \equiv \begin{pmatrix} 1 \\ \lambda \end{pmatrix}$  is another stationary solution.

NOTE:

The Jacobian along the solution family  $\mathbf{u}(t) \equiv \mathbf{0}$  is

$$\begin{pmatrix} \lambda & -1 \\ 1 & 0 \end{pmatrix},$$

with eigenvalues

$$\frac{\lambda \pm \sqrt{\lambda^2 - 4}}{2}.$$

- The eigenvalues are complex for  $\lambda \in (-2, 2)$ .
- The eigenvalues cross the imaginary axis when  $\lambda$  passes through zero.
- Thus there is a Hopf bifurcation along  $\mathbf{u} \equiv \mathbf{0}$  at  $\lambda = 0$ .
- A family of periodic solutions bifurcates from  $\mathbf{u} = \mathbf{0}$  at  $\lambda = 0$ .

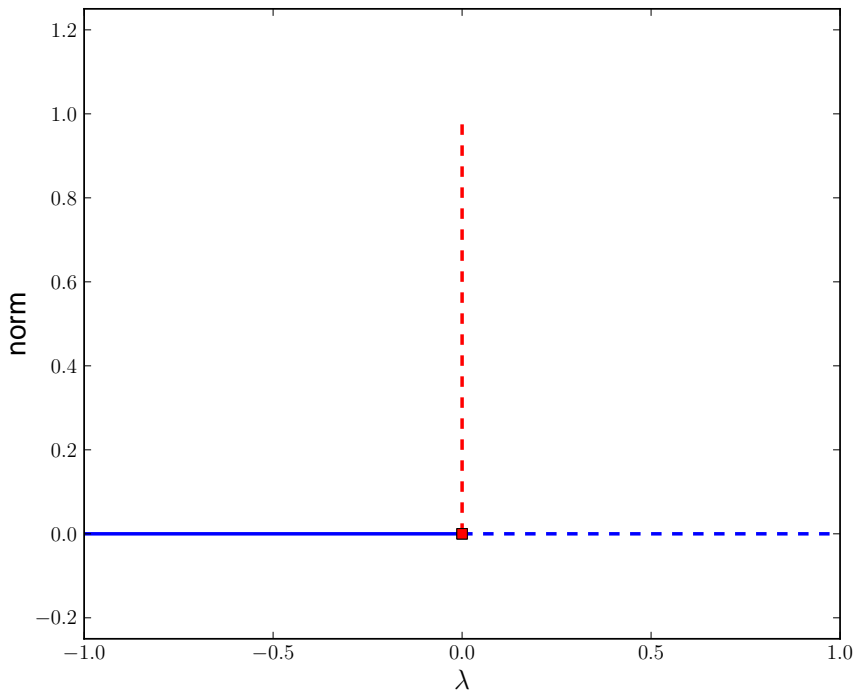


Figure 35: Bifurcation diagram for Equation (8).

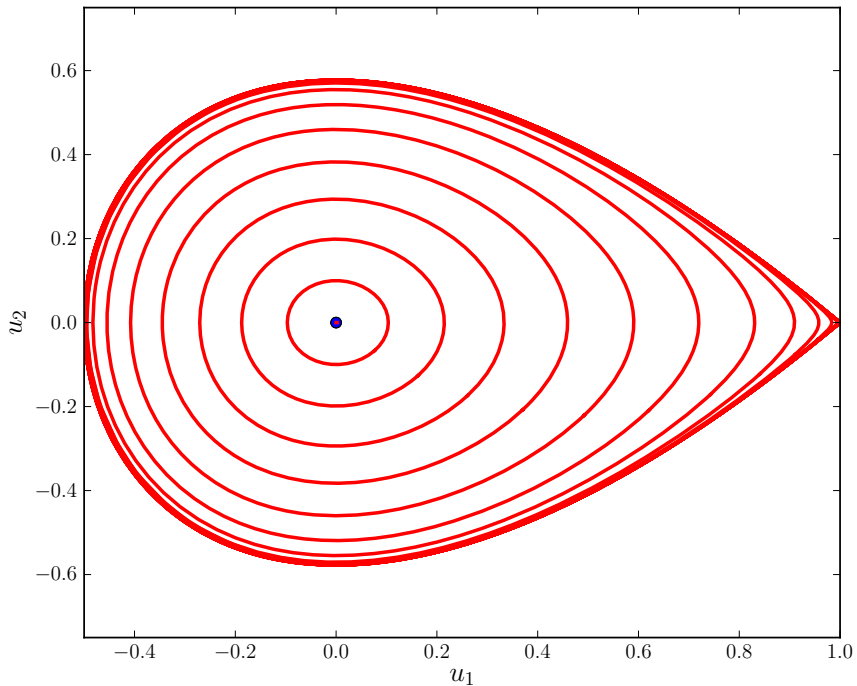


Figure 36: A phase plot of some periodic solutions to Equation (8).

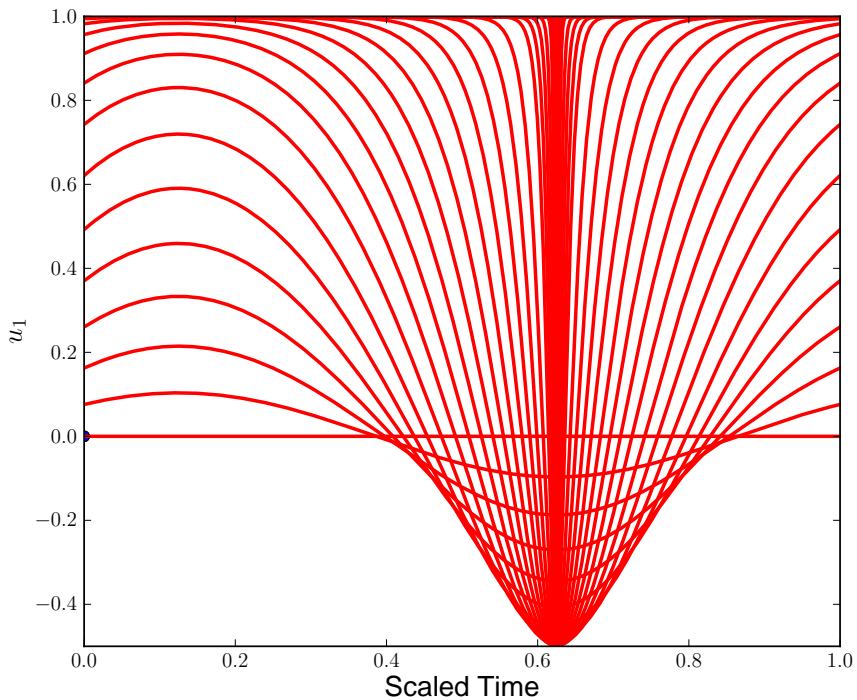


Figure 37:  $u_1$  as a function of the scaled time variable  $t$  for Equation (8).

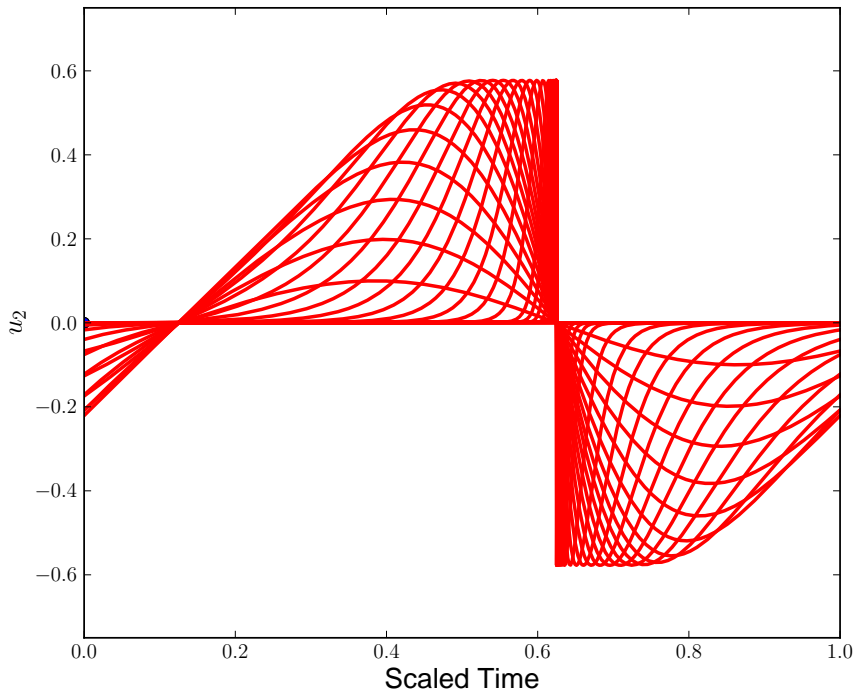


Figure 38:  $u_2$  as a function of the scaled time variable  $t$  for Equation (8).

NOTE:

- The family of periodic solutions is also “vertical” (non-generic).
- The period changes along this family; in fact, the period tends to infinity.
- The terminating infinite period orbit is an example of a *homoclinic orbit*.
- This homoclinic orbit contains the stationary point  $(u_1, u_2) = (1, 0)$  .
- In the solution diagrams, showing  $u_1$  and  $u_2$  versus time  $t$  , note how the “peak” in the solution remains in the same location.
- This is a result of the numerical “phase-condition”, to be discussed later.

EXERCISE. (Demo het.)

Use **AUTO** to compute the zero stationary solution family, a Hopf bifurcation, and the emanating family of periodic solutions, of the equation

$$\begin{cases} u'_1 = \lambda u_1 - u_2, \\ u'_2 = u_1 (1 - u_1^2). \end{cases} \quad (9)$$

NOTE:

- $\mathbf{u}(t) \equiv \mathbf{0}$  is a stationary solution for all  $\lambda$ .
- There is a Hopf bifurcation along  $\mathbf{u} \equiv \mathbf{0}$  at  $\lambda = 0$ .
- $\mathbf{u}(t) \equiv \begin{pmatrix} 1 \\ \lambda \end{pmatrix}, \begin{pmatrix} -1 \\ \lambda \end{pmatrix}$  are two more stationary solutions.

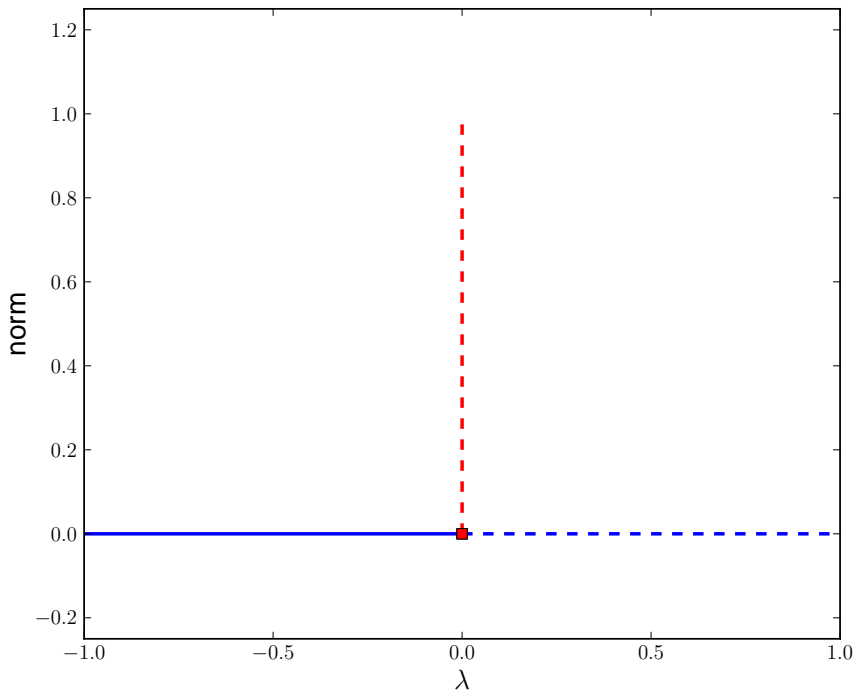


Figure 39: Bifurcation diagram for Equation (9).

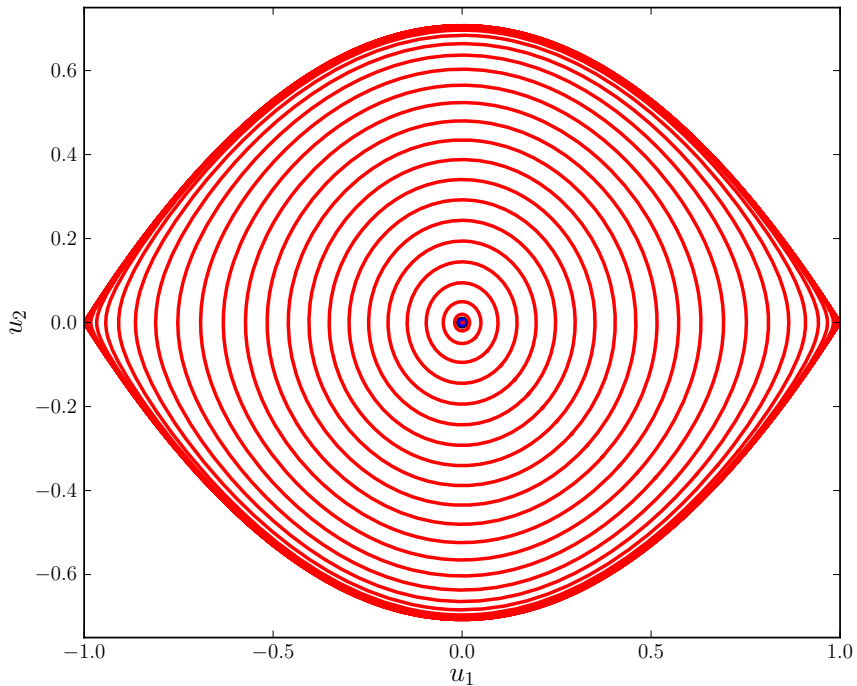


Figure 40: A phase plot of some periodic solutions to Equation (9).

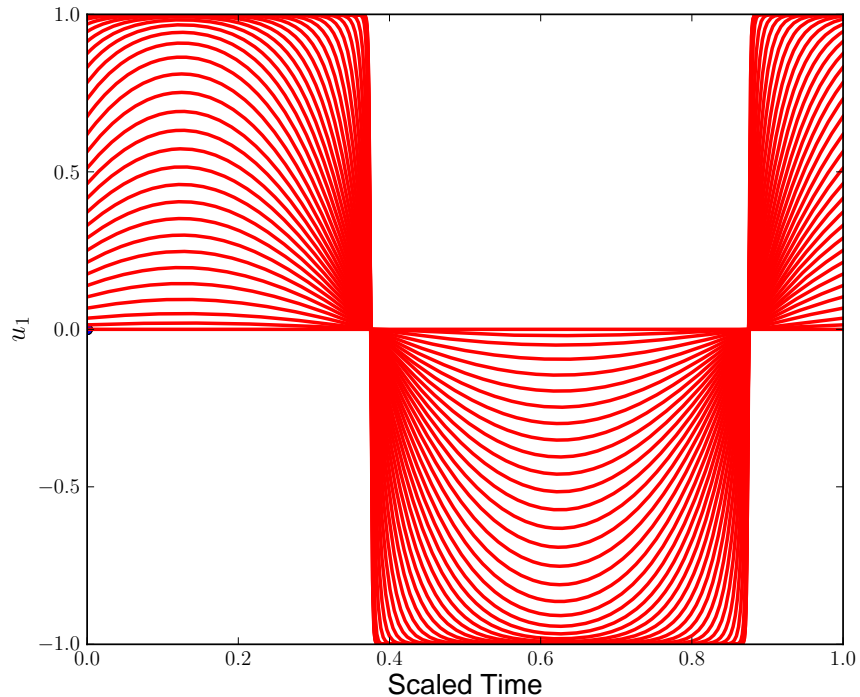


Figure 41:  $u_1$  as a function of the scaled time variable  $t$  for Equation (9).

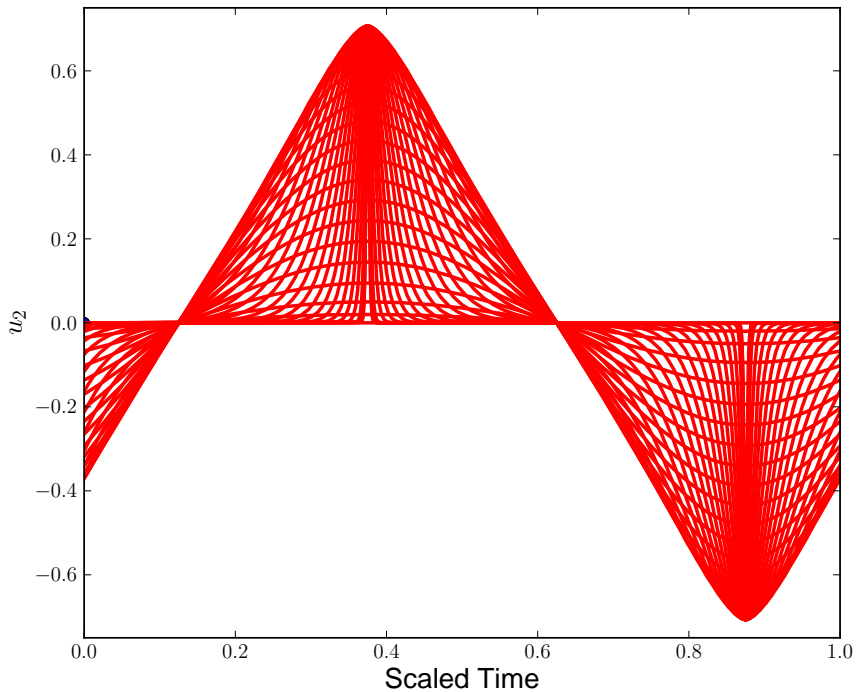


Figure 42:  $u_2$  as a function of the scaled time variable  $t$  for Equation (9).

NOTE:

- This family of periodic solutions is also “vertical” (non-generic).
- The period along this family also tends to infinity.
- The terminating infinite period orbit is an example of a *heteroclinic cycle*.
- This heteroclinic cycle is made up of two *heteroclinic orbits*.
- The heteroclinic orbits contains the stationary points

$$(u_1, u_2) = (1, 0) \quad \text{and} \quad (u_1, u_2) = (-1, 0) .$$

EXERCISE. (AUTO demo pp3.)

Compute the families of periodic solutions that bifurcate from the four Hopf bifurcation points in the following system; taking  $p_4 = 4$ .

$$u'_1(t) = u_1 (1 - u_1) - p_4 u_1 u_2 ,$$

$$u'_2(t) = -\frac{1}{4} u_2 + p_4 u_1 u_2 - 3 u_2 u_3 - p_1 (1 - e^{-5u_2}) ,$$

$$u'_3(t) = -\frac{1}{2} u_3 + 3 u_2 u_3 .$$

This is a simple predator-prey model where, say,

$$u_1 = \text{plankton}, \quad u_2 = \text{fish}, \quad u_3 = \text{sharks}, \quad \lambda \equiv p_1 = \text{fishing quota}.$$

The factor

$$(1 - e^{-5u_2}) ,$$

models that the quota cannot be met if the fish population is small.

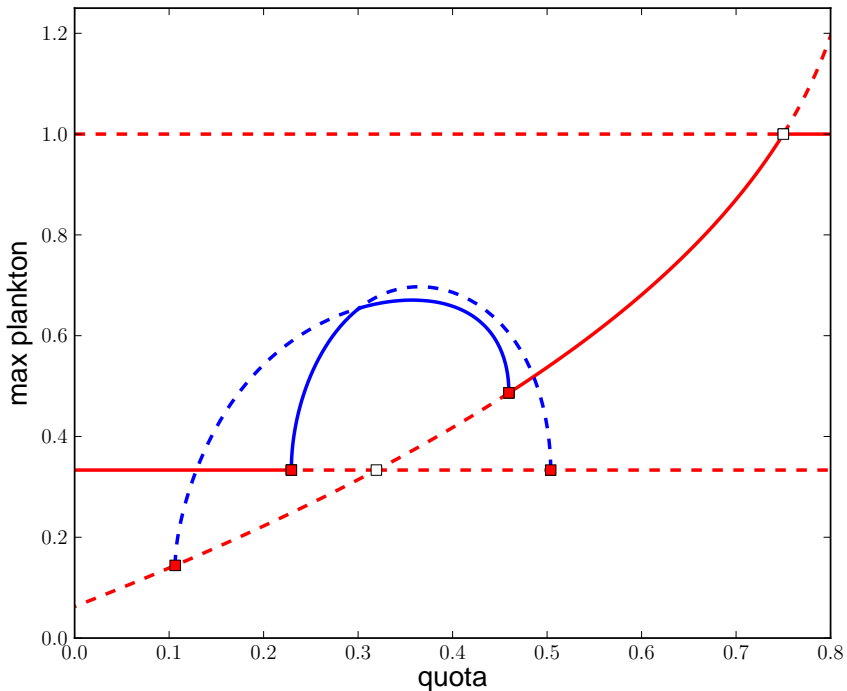


Figure 43: A bifurcation diagram for the 3-species model; with  $p_4 = 4$ .

NOTE:

- These periodic solution families are not “vertical”. (The generic case.)
- One family connects the two Hopf points along the stationary family along which  $u_1$  is constant.
- The second family connects the two Hopf points along the stationary family along which  $u_1$  is not constant.
- These two families of periodic solutions “intersect” at a branch point of periodic solutions, at  $\lambda \approx 0.3012$ .
- At this point there is an “interchange of stability” between the families.
- Stable periodic orbits are denoted by solid circles in the diagram.
- Unstable periodic orbits are denoted by open circles in the diagram.

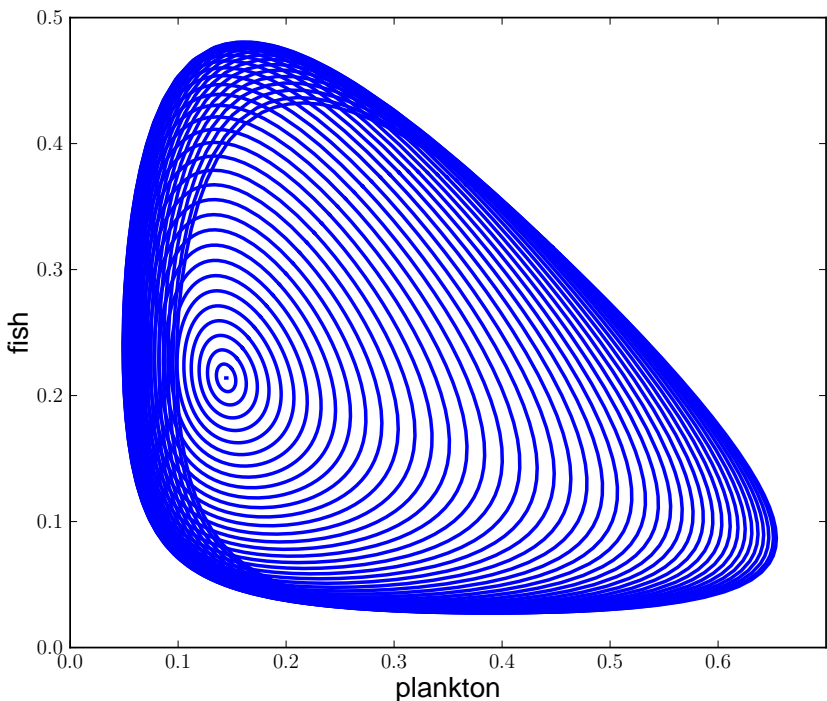


Figure 44: Part of the planar orbit family for the 3-species model;  $p_4 = 4$ .

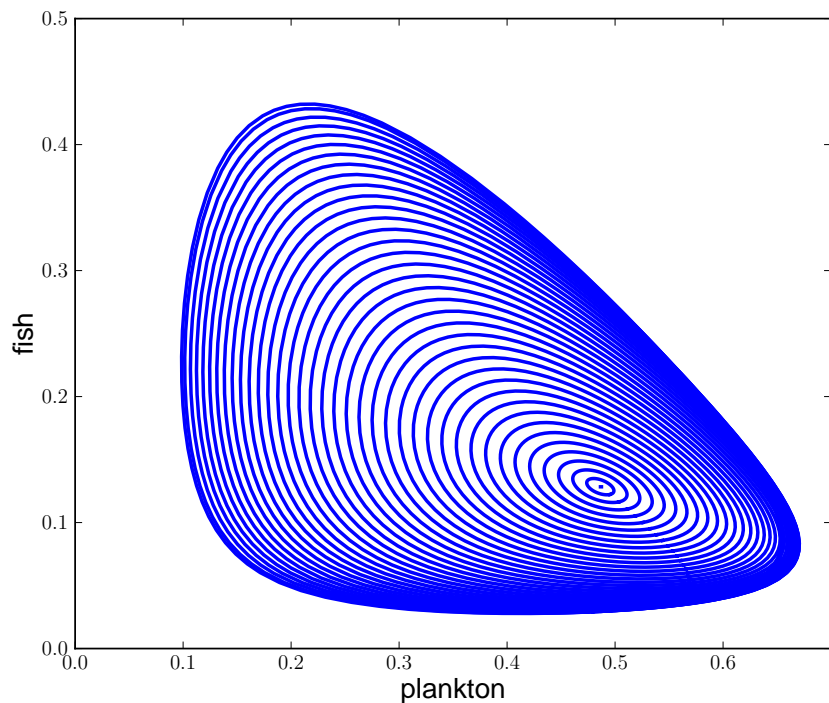


Figure 45: The remainder of the planar orbit family;  $p_4 = 4$ .

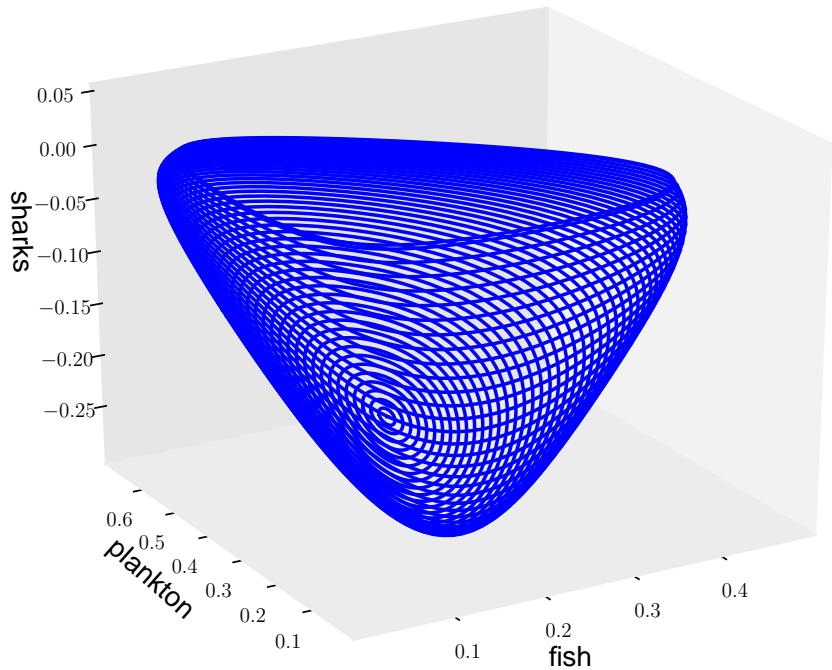


Figure 46: Part of the 3D orbit family for the 3-species model;  $p_4 = 4$ .

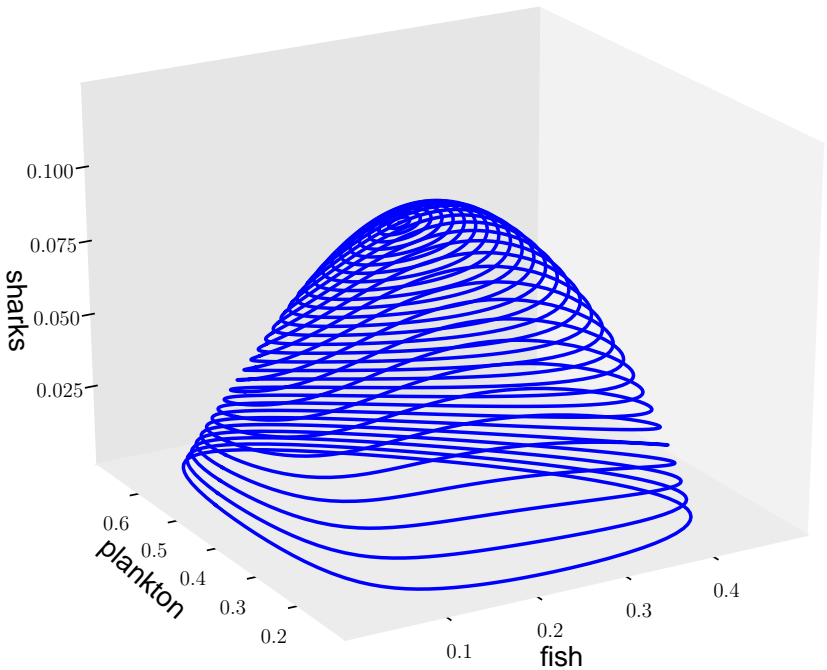


Figure 47: The remainder of the 3D orbit family;  $p_4 = 4$ .

# Computing Periodic Solutions

Periodic solutions can be computed very effectively using a boundary value approach. This method also determines the period very accurately. Moreover, the technique allows asymptotically unstable periodic orbits to be computed as easily as asymptotically stable ones.

# The BVP Approach.

Consider

$$\mathbf{u}'(t) = \mathbf{f}(\mathbf{u}(t), \lambda), \quad \mathbf{u}(\cdot), \mathbf{f}(\cdot) \in \mathbb{R}^n, \quad \lambda \in \mathbb{R}.$$

Fix the interval of periodicity by the transformation

$$t \rightarrow \frac{t}{T}.$$

Then the equation becomes

$$\boxed{\mathbf{u}'(t) = T \mathbf{f}(\mathbf{u}(t), \lambda)}, \quad \mathbf{u}(\cdot), \mathbf{f}(\cdot) \in \mathbb{R}^n, \quad T, \lambda \in \mathbb{R}.$$

and we seek solutions of period 1, *i.e.*,

$$\boxed{\mathbf{u}(0) = \mathbf{u}(1)}.$$

Note that the period  $T$  is one of the unknowns.

The above equations do not uniquely specify  $\mathbf{u}$  and  $T$ :

Assume that we have computed

$$(\mathbf{u}_{k-1}(\cdot), T_{k-1}, \lambda_{k-1}),$$

and we want to compute the next solution

$$(\mathbf{u}_k(\cdot), T_k, \lambda_k).$$

Specifically,  $\mathbf{u}_k(t)$  can be translated freely in time:

If  $\mathbf{u}_k(t)$  is a periodic solution, then so is

$$\mathbf{u}_k(t + \sigma),$$

for any  $\sigma$ .

Thus, a “*phase condition*” is needed.

An example is the Poincaré orthogonality condition

$$(\mathbf{u}_k(0) - \mathbf{u}_{k-1}(0))^* \mathbf{u}'_{k-1}(0) = 0.$$

(Below we derive a numerically more suitable phase condition.)

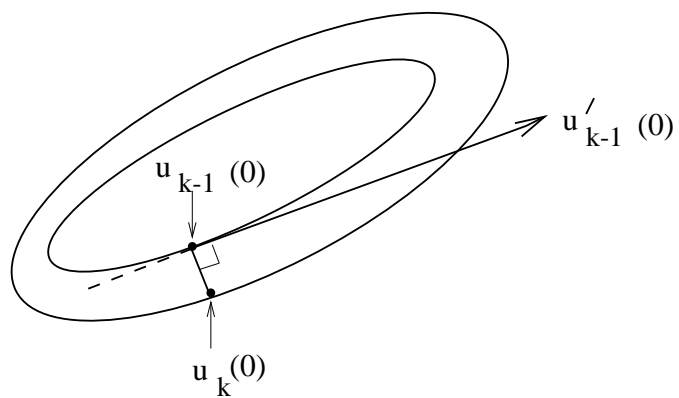


Figure 48: Graphical interpretation of the Poincaré phase condition.

# Integral Phase Condition

If  $\tilde{\mathbf{u}}_k(t)$  is a solution then so is

$$\tilde{\mathbf{u}}_k(t + \sigma) ,$$

for any  $\sigma$ .

We want the solution that minimizes

$$D(\sigma) \equiv \int_0^1 \| \tilde{\mathbf{u}}_k(t + \sigma) - \mathbf{u}_{k-1}(t) \|_2^2 dt .$$

The optimal solution

$$\tilde{\mathbf{u}}_k(t + \hat{\sigma}) ,$$

must satisfy the necessary condition

$$D'(\hat{\sigma}) = 0 .$$

Differentiation gives the necessary condition

$$\int_0^1 (\tilde{\mathbf{u}}_k(t + \hat{\sigma}) - \mathbf{u}_{k-1}(t))^* \tilde{\mathbf{u}}'_k(t + \hat{\sigma}) dt = 0.$$

Writing

$$\mathbf{u}_k(t) \equiv \tilde{\mathbf{u}}_k(t + \hat{\sigma}),$$

gives

$$\int_0^1 (\mathbf{u}_k(t) - \mathbf{u}_{k-1}(t))^* \mathbf{u}'_k(t) dt = 0.$$

Integration by parts, using periodicity, gives

$$\boxed{\int_0^1 \mathbf{u}_k(t)^* \mathbf{u}'_{k-1}(t) dt = 0}.$$

This is the *integral phase condition*.

# Pseudo-Arclength Continuation

We use pseudo-arclength continuation to follow a family of periodic solutions.

This allows calculation past folds along a family of periodic solutions.

It also allows calculation of a “vertical family” of periodic solutions.

For periodic solutions the pseudo-arclength equation is

$$\int_0^1 (\mathbf{u}_k(t) - \mathbf{u}_{k-1}(t))^* \dot{\mathbf{u}}_{k-1}(t) dt + (T_k - T_{k-1}) \dot{T}_{k-1} + (\lambda_k - \lambda_{k-1}) \dot{\lambda}_{k-1} = \Delta s .$$

In summary, we have the following equations for continuing periodic solutions:

$$\mathbf{u}'_k(t) = T \mathbf{f}(\mathbf{u}_k(t), \lambda_k),$$

$$\mathbf{u}_k(0) = \mathbf{u}_k(1),$$

$$\int_0^1 \mathbf{u}_k(t)^* \mathbf{u}'_{k-1}(t) dt = 0,$$

with pseudo-arc length continuation equation

$$\int_0^1 (\mathbf{u}_k(t) - \mathbf{u}_{k-1}(t))^* \dot{\mathbf{u}}_{k-1}(t) dt + (T_k - T_{k-1}) \dot{T}_{k-1} + (\lambda_k - \lambda_{k-1}) \dot{\lambda}_{k-1} = \Delta s.$$

Here

$$\mathbf{u}(\cdot), \mathbf{f}(\cdot) \in \mathbb{R}^n, \quad \lambda, T \in \mathbb{R}.$$

# Starting at a Hopf Bifurcation

Let

$$(\mathbf{u}_0, \lambda_0),$$

be a Hopf bifurcation point, *i.e.*,

$$\mathbf{f}_{\mathbf{u}}(\mathbf{u}_0, \lambda_0),$$

has a simple conjugate pair of purely imaginary eigenvalues

$$\pm i \omega_0, \quad \omega_0 \neq 0,$$

and no other eigenvalues on the imaginary axis.

Also, the pair crosses the imaginary axis transversally with respect to  $\lambda$ .

By the Hopf Bifurcation Theorem, a family of periodic solutions bifurcates.

Asymptotic estimates for periodic solutions near the Hopf bifurcation :

$$\mathbf{u}(t; \epsilon) = \mathbf{u}_0 + \epsilon \phi(t) + \mathcal{O}(\epsilon^2),$$

$$T(\epsilon) = T_0 + \mathcal{O}(\epsilon^2),$$

$$\lambda(\epsilon) = \lambda_0 + \mathcal{O}(\epsilon^2).$$

Here  $\epsilon$  locally parametrizes the family of periodic solutions.

$T(\epsilon)$  denotes the period, and

$$T_0 = \frac{2\pi}{\omega_0}.$$

The function  $\phi(t)$  is the normalized nonzero periodic solution of the linearized, constant coefficient problem

$$\phi'(t) = \mathbf{f}_{\mathbf{u}}(\mathbf{u}_0, \lambda_0) \phi(t).$$

To compute a first periodic solution

$$(\mathbf{u}_1(\cdot), T_1, \lambda_1),$$

near a Hopf bifurcation  $(\mathbf{u}_0, \lambda_0)$ , we still have

$$\boxed{\mathbf{u}'_1(t) = T \mathbf{f}(\mathbf{u}_1(t), \lambda_1)}, \quad (10)$$

$$\boxed{\mathbf{u}_1(0) = \mathbf{u}_1(1)}. \quad (11)$$

Initial estimates for Newton's method are

$$\mathbf{u}_1^{(0)}(t) = \mathbf{u}_0 + \Delta s \phi(t), \quad T_1^{(0)} = T_0, \quad \lambda_1^{(0)} = \lambda_0.$$

Above,  $\phi(t)$  is a nonzero solution of the time-scaled, linearized equations

$$\phi'(t) = T_0 \mathbf{f}_\mathbf{u}(\mathbf{u}_0, \lambda_0) \phi(t), \quad \phi(0) = \phi(1),$$

namely,

$$\phi(t) = \sin(2\pi t) \mathbf{w}_s + \cos(2\pi t) \mathbf{w}_c,$$

where

$$(\mathbf{w}_s, \mathbf{w}_c),$$

is a null vector in

$$\begin{pmatrix} -\omega_0 I & \mathbf{f}_\mathbf{u}(\mathbf{u}_0, \lambda_0) \\ \mathbf{f}_\mathbf{u}(\mathbf{u}_0, \lambda_0) & \omega_0 I \end{pmatrix} \begin{pmatrix} \mathbf{w}_s \\ \mathbf{w}_c \end{pmatrix} = \begin{pmatrix} \mathbf{0} \\ \mathbf{0} \end{pmatrix}, \quad \omega_0 = \frac{2\pi}{T_0}.$$

The nullspace is generically two-dimensional since

$$\begin{pmatrix} -\mathbf{w}_c \\ \mathbf{w}_s \end{pmatrix},$$

is also a null vector.

For the phase equation we “align”  $\mathbf{u}_1$  with  $\phi(t)$ , i.e.,

$$\boxed{\int_0^1 \mathbf{u}_1(t)^* \phi'(t) dt = 0}.$$

Since

$$\dot{\lambda}_0 = \dot{T}_0 = 0,$$

the pseudo-arc length equation for the first step reduces to

$$\boxed{\int_0^1 (\mathbf{u}_1(t) - \mathbf{u}_0(t))^* \phi(t) dt = \Delta s}.$$

## Accuracy Test

EXERCISE.

A simple accuracy test is to treat the linear equation

$$u'_1(t) = \lambda u_1 - u_2 ,$$

$$u'_2(t) = u_1 ,$$

as a bifurcation problem.

- It has a Hopf bifurcation point at  $\lambda = 0$  from the zero solution family.
- The bifurcating family of periodic solutions is vertical.
- Along the family, the period remains constant, namely,  $T = 2\pi$ .

For the above problem:

- Compute the family of periodic solutions, for different choices of the number of mesh points and the number of collocation points.
- Determine *the error in the period* for the computed solutions.

Typical results are shown in Table 1.

ntst	ncol = 2		ncol = 3		ncol = 4	
4	0.47e-1	(5.5)	0.85e-3	(7.9)	0.85e-5	(8.9)
8	0.32e-2	(4.0)	0.14e-4	(6.0)	0.35e-7	(8.0)
16	0.20e-3	(4.0)	0.22e-6	(6.0)	0.14e-9	(8.0)
32	0.13e-4		0.35e-8		0.54e-11	

Table 1: Accuracy of T for the linear problem

EXAMPLE: (AUTO demo fhn.)

The FitzHugh-Nagumo model

$$\begin{aligned} u'_1 &= u_1 - \frac{u_1^3}{3} - u_2 + I, \\ u'_2 &= a(u_1 + b - cu_2). \end{aligned}$$

is a model of spike generation in squid giant axons, where

$u_1$  is the *membrane potential* ,

$u_2$  is a *recovery variable* ,

$I$  is the *stimulus current* .

Take  $I$  as bifurcation parameter, and

$$a = 0.08, \quad b = 0.7, \quad c = 0.8.$$

If  $I = 0$  then  $(u_1, u_2) = (-1.19941, -0.62426)$  is a stationary solution.

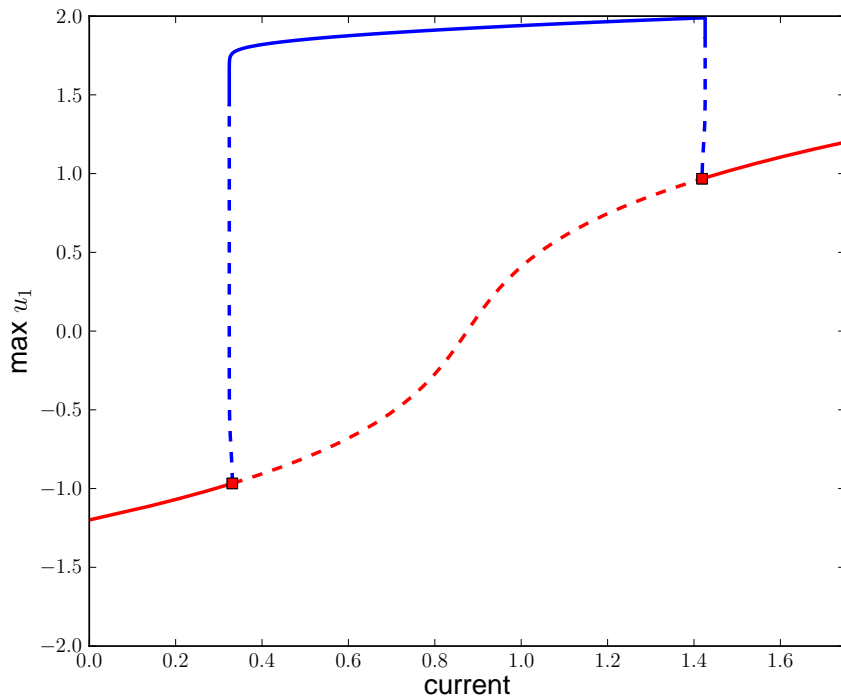


Figure 49: Bifurcation diagram of the Fitzhugh-Nagumo equations.

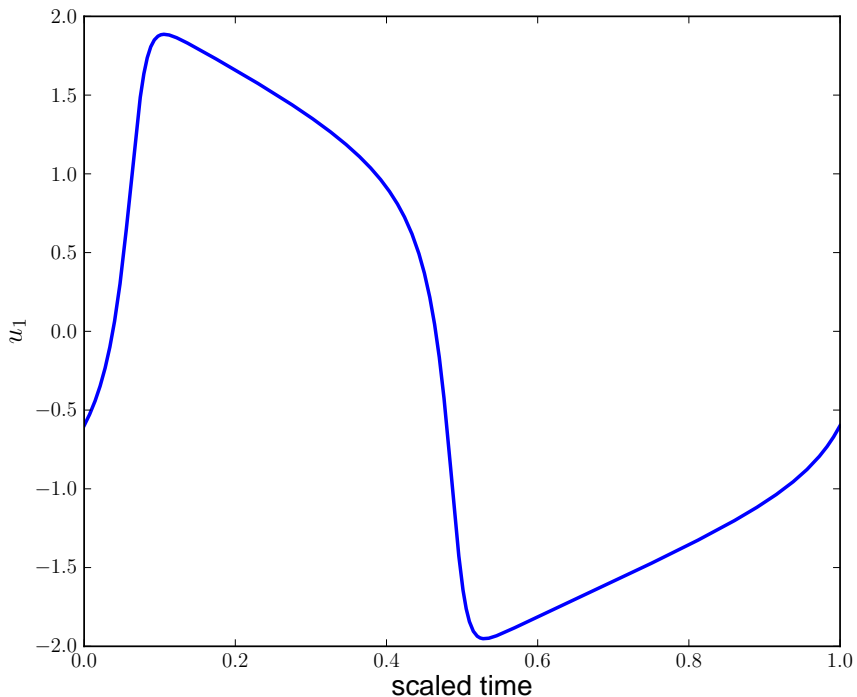


Figure 50: A stable periodic solutions .

# Periodically Forced Systems

Here we illustrate computing periodic solutions to a periodically forced system.

In AUTO this can be done by adding a nonlinear oscillator with the desired periodic forcing as one of its solution components.

An example of such an oscillator is

$$x' = x + \beta y - x(x^2 + y^2),$$

$$y' = -\beta x + y - y(x^2 + y^2),$$

which has the asymptotically stable solution

$$x = \sin(\beta t), \quad y = \cos(\beta t).$$

EXAMPLE. (AUTO demo **ffn**.)

Couple the oscillator

$$\begin{aligned}x' &= x + \beta y - x(x^2 + y^2), \\y' &= -\beta x + y - y(x^2 + y^2),\end{aligned}$$

to the Fitzhugh-Nagumo equations :

$$\begin{aligned}v' &= c(v - \frac{v^3}{3} + w - r y), \\w' &= -(v - a + b * w)/c,\end{aligned}$$

where

$$b = 0.8, \quad c = 3, \quad \text{and} \quad \beta = 10.$$

Note that if

$$a = 0 \quad \text{and} \quad r = 0,$$

then a solution is

$$x = \sin(\beta t), \quad y = \cos(\beta t), \quad v(t) \equiv 0, \quad w(t) \equiv 0,$$

Continue this solution from  $r = 0$  to, say,  $r = 10$ .

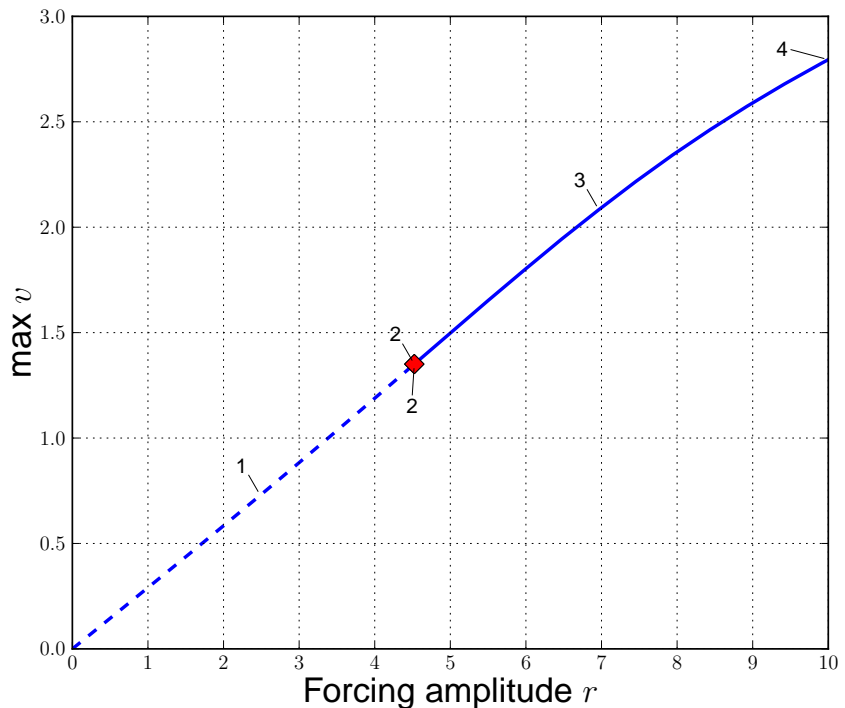


Figure 51: Continuation from  $r = 0$  to  $r = 10$ . Solution 1 is unstable. Solution 2 corresponds to a torus bifurcation.

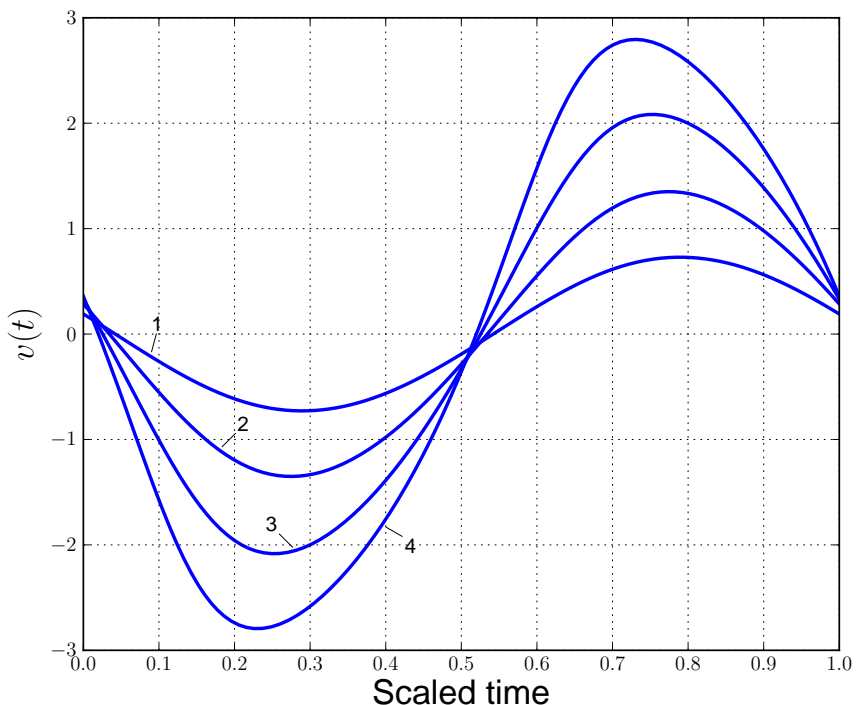


Figure 52: Some solutions along the path from  $r = 0$  to  $r = 10$ .

NOTE:

- The starting solution at  $r = 0$ , with  $v = w = 0$ , is unstable.
- The oscillation becomes stable when  $r$  passes the value  $r_T \approx 4.52$ .
- At  $r = r_T$  there is a *torus bifurcation*.

# General Non-Autonomous Systems

If the forcing is not periodic, or difficult to model by an autonomous oscillator, then the equations can be rewritten in autonomous form as follows:

$$\mathbf{u}'(t) = \mathbf{f}(t, \mathbf{u}(t)) , \quad \mathbf{u}(\cdot), \mathbf{f}(\cdot) \in \mathbb{R}^n , \quad t \in [0, 1] ,$$

$$\mathbf{b}(\mathbf{u}(0), \mathbf{u}(1)) = \mathbf{0} , \quad \mathbf{b}(\cdot) \in \mathbb{R}^n ,$$

can be transformed into

$$\mathbf{u}'(t) = \mathbf{f}(\mathbf{v}(t), \mathbf{u}(t)) ,$$

$$v'(t) = 1 , \quad v(\cdot) \in \mathbb{R} ,$$

$$\mathbf{b}(\mathbf{u}(0), \mathbf{u}(1)) = \mathbf{0} ,$$

$$v(0) = 0 ,$$

which is autonomous, with  $n + 1$  ODEs and  $n + 1$  boundary conditions.

# Periodic Solutions of Conservative Systems

EXAMPLE:

$$u'_1 = - u_2 ,$$

$$u'_2 = u_1 (1 - u_1) .$$

PROBLEM:

- This equation has a family of periodic solutions, but no parameter !
- This system has a constant of motion, namely the Hamiltonian

$$H(u_1, u_2) = -\frac{1}{2} u_1^2 - \frac{1}{2} u_2^2 + \frac{1}{3} u_1^3 .$$

REMEDY:

Introduce an “unfolding term” with “unfolding parameter”  $\lambda$  :

$$u'_1 = \lambda u_1 - u_2 ,$$

$$u'_2 = u_1 (1 - u_1) .$$

Then there is a “vertical” Hopf bifurcation from the trivial solution at  $\lambda = 0$  .

(This is **AUT0** demo **1hb**; see Figures 33 and 34.)

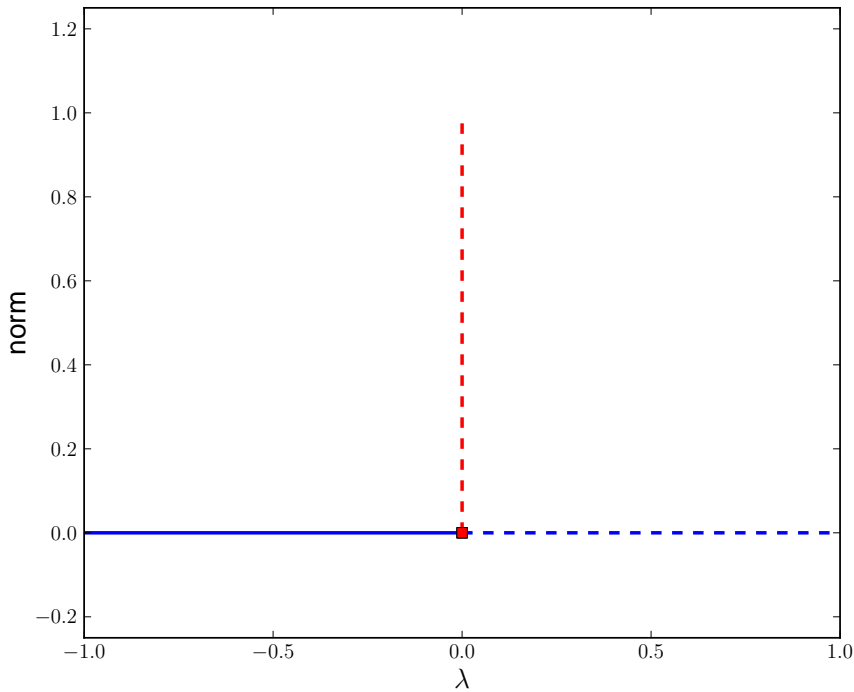


Figure 53: Bifurcation diagram of the “linear” Hopf bifurcation problem.

NOTE:

- The family of periodic solutions is “vertical”.
- The parameter  $\lambda$  is solved for in each continuation step.
- Upon solving,  $\lambda$  is found to be zero, up to numerical precision.
- One can use “standard” BVP continuation and bifurcation software.

EXAMPLE : The Circular Restricted 3-Body Problem (CR3BP).

$$\begin{aligned}x'' &= 2y' + x - \frac{(1-\mu)(x+\mu)}{r_1^3} - \frac{\mu(x-1+\mu)}{r_2^3}, \\y'' &= -2x' + y - \frac{(1-\mu)y}{r_1^3} - \frac{\mu y}{r_2^3}, \\z'' &= -\frac{(1-\mu)z}{r_1^3} - \frac{\mu z}{r_2^3},\end{aligned}$$

where

$$r_1 = \sqrt{(x + \mu)^2 + y^2 + z^2}, \quad r_2 = \sqrt{(x - 1 + \mu)^2 + y^2 + z^2}.$$

and

$$(x, y, z),$$

denotes the position of the zero-mass body.

For the Earth-Moon system  $\mu \approx 0.01215$ .

The CR3BP has one integral of motion, namely, the “*Jacobi-constant*”:

$$J = \frac{x'^2 + y'^2 + z'^2}{2} - U(x, y, z) - \mu \frac{1-\mu}{2},$$

where

$$U = \frac{1}{2}(x^2 + y^2) + \frac{1-\mu}{r_1} + \frac{\mu}{r_2},$$

where

$$r_1 = \sqrt{(x+\mu)^2 + y^2 + z^2}, \quad r_2 = \sqrt{(x-1+\mu)^2 + y^2 + z^2}.$$

## BOUNDARY VALUE FORMULATION:

$$x' = T v_x ,$$

$$y' = T v_y ,$$

$$z' = T v_z ,$$

$$v'_x = T [ 2v_y + x - (1-\mu)(x+\mu)r_1^{-3} - \mu(x-1+\mu)r_2^{-3} + \lambda v_x ] ,$$

$$v'_y = T [ -2v_x + y - (1-\mu)yr_1^{-3} - \mu yr_2^{-3} + \lambda v_y ] ,$$

$$v'_z = T [ -(1-\mu)zr_1^{-3} - \mu zr_2^{-3} + \lambda v_z ] ,$$

with periodicity boundary conditions

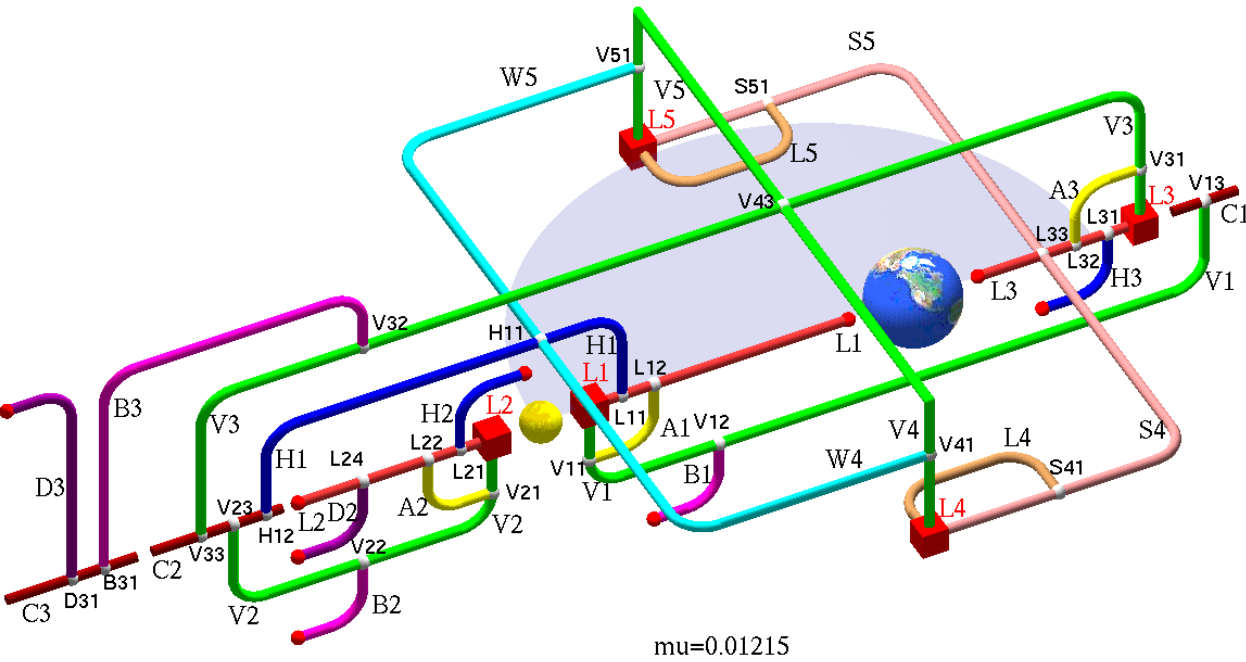
$$x(1) = x(0) , \quad y(1) = y(0) , \quad z(1) = z(0) ,$$

$$v_x(1) = v_x(0) , \quad v_y(1) = v_y(0) , \quad v_z(1) = v_z(0) ,$$

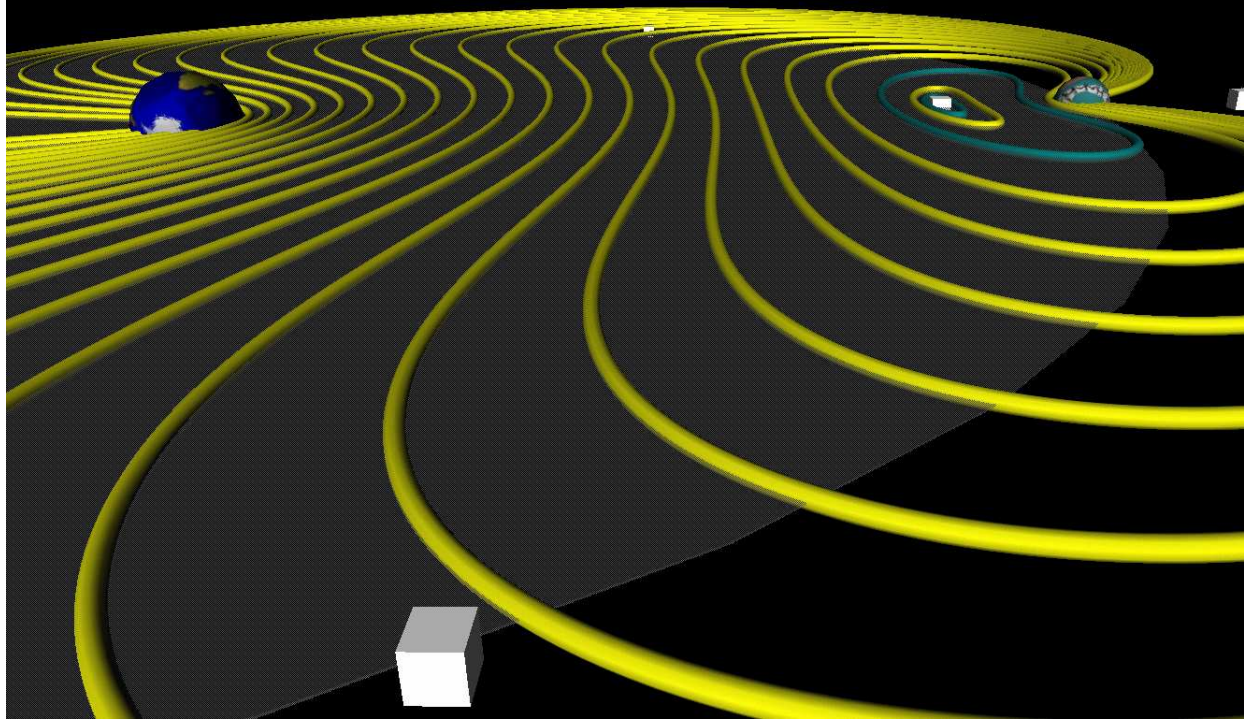
+ phase constraint + pseudo-arclength equation.

NOTE:

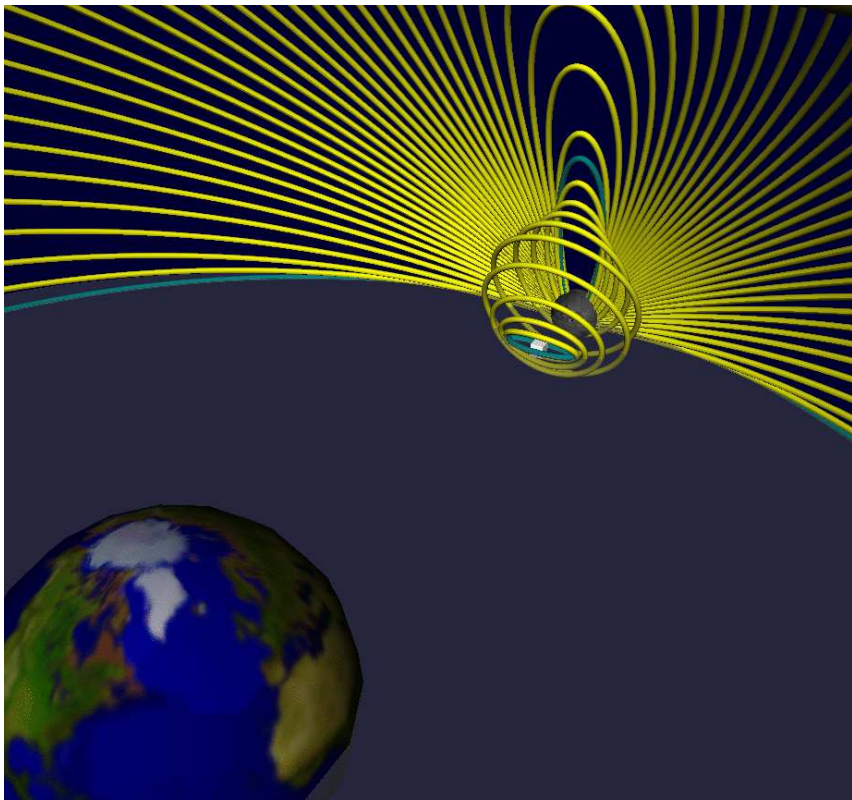
- One can use standard BVP continuation and bifurcation software.
- The “unfolding term”  $\lambda \nabla v$  regularizes the continuation.
- $\lambda$  will be ”zero”, once solved for.
- Other unfolding terms are possible.



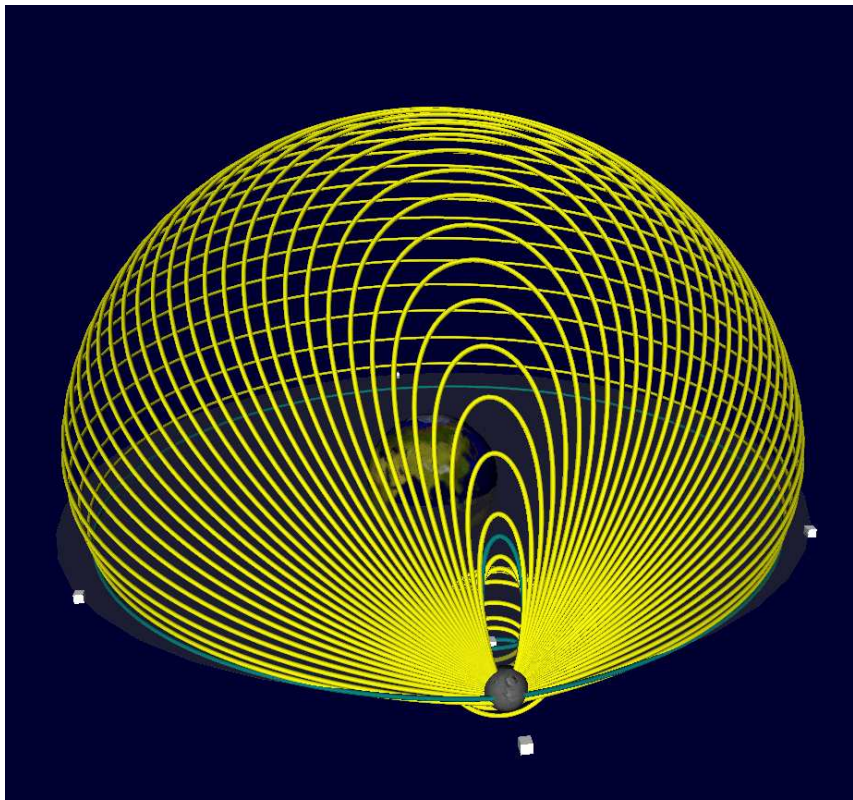
Families of Periodic Solutions of the Earth-Moon system.



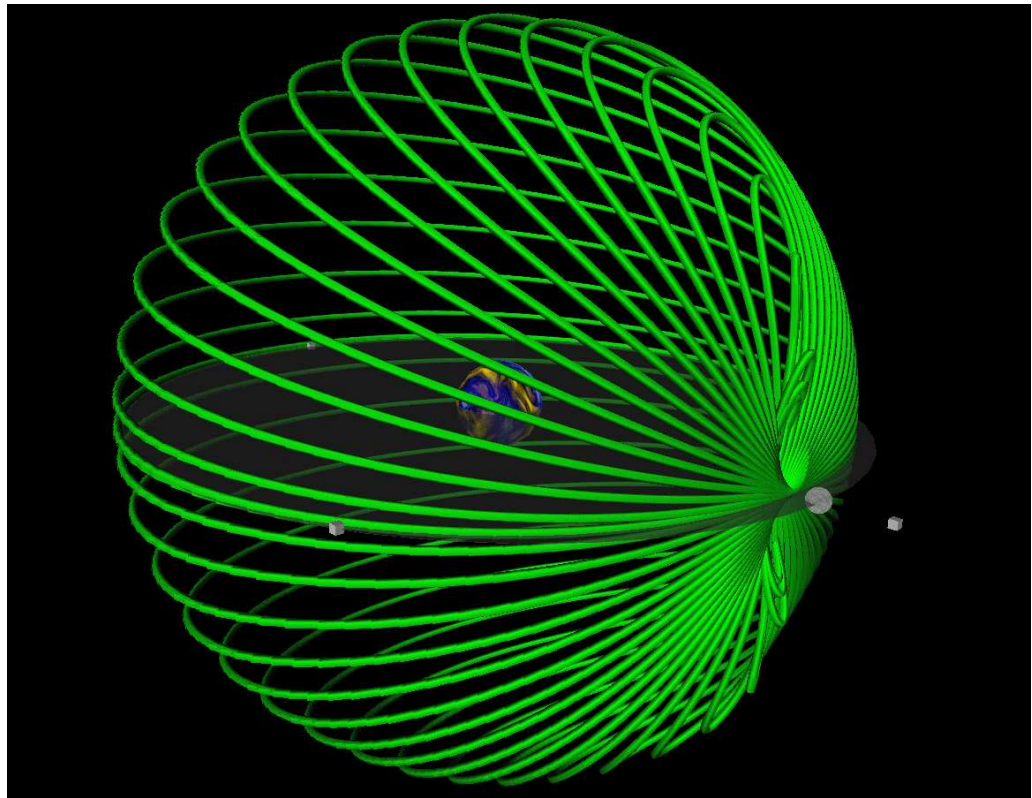
The planar Lyapunov family L1.



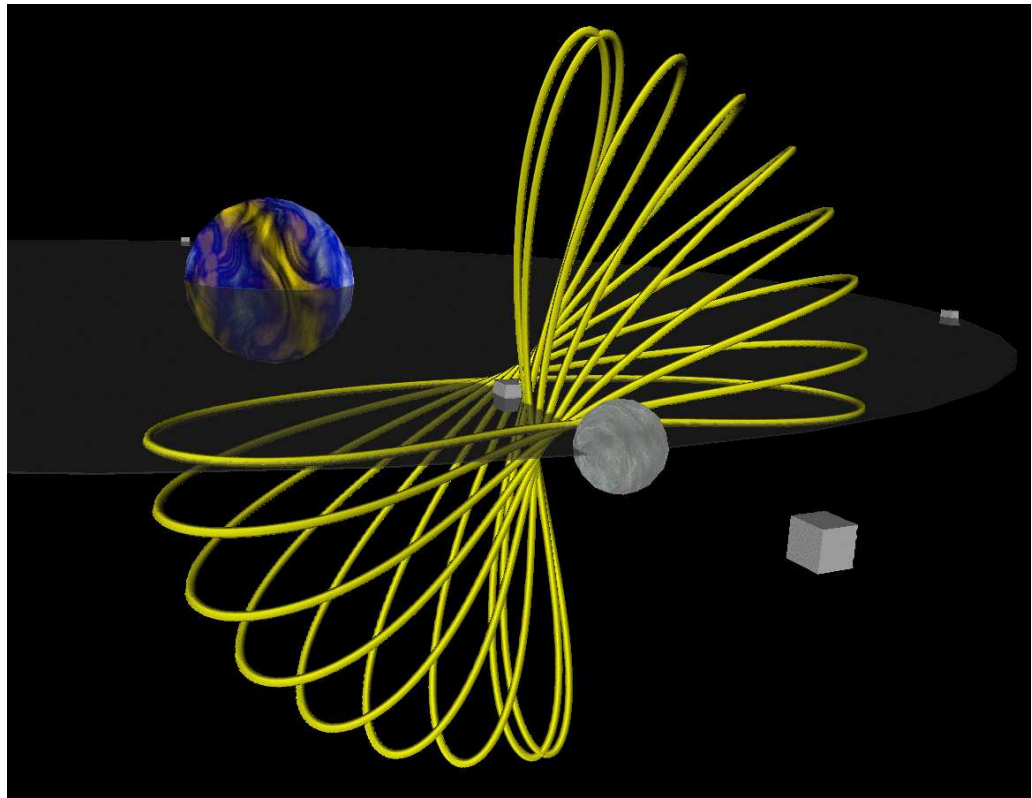
The Halo family H1.



The Halo family H1.



The Vertical family V1.



The Axial family A1.

## Following Periodic Orbit Folds

Fold-following algorithms also apply to folds along solution families of boundary value problems and, in particular, folds along families of periodic solutions.

EXAMPLE: The  $A \rightarrow B \rightarrow C$  reaction. (AUTO demo abc.)

The equations are

$$u'_1 = -u_1 + D(1 - u_1)e^{u_3},$$

$$u'_2 = -u_2 + D(1 - u_1)e^{u_3} - D\sigma u_2 e^{u_3},$$

$$u'_3 = -u_3 - \beta u_3 + DB(1 - u_1)e^{u_3} + DB\alpha\sigma u_2 e^{u_3},$$

with

$$\alpha = 1 , \quad \sigma = 0.04 , \quad B = 8 .$$

We will compute solutions for varying  $D$  and  $\beta$ .

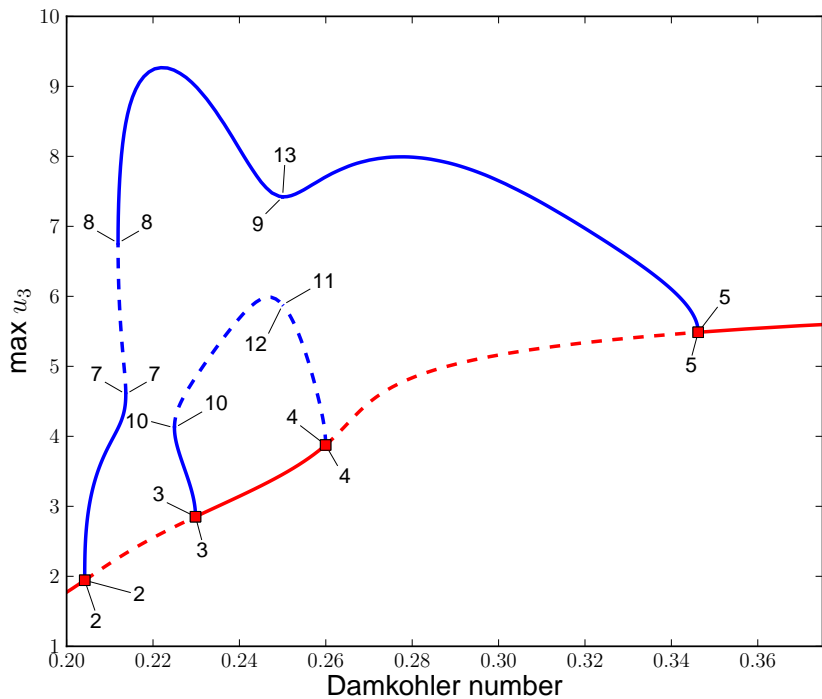


Figure 54: Stationary and periodic solutions of demo abc;  $\beta = 1.55$ .

Recall that periodic orbits families can be computed using the equations

$$\mathbf{u}'(t) - T \mathbf{f}(\mathbf{u}(t), \lambda) = \mathbf{0},$$

$$\mathbf{u}(0) - \mathbf{u}(1) = \mathbf{0},$$

$$\int_0^1 \mathbf{u}(t)^* \mathbf{u}'_0(t) dt = 0,$$

where  $\mathbf{u}_0$  is a reference orbit, typically the latest computed orbit.

The above boundary value problem is of the form

$$\mathbf{F}(\mathbf{X}, \lambda) = \mathbf{0},$$

where

$$\mathbf{X} = (\mathbf{u}, T).$$

At a fold with respect to  $\lambda$  we have

$$\mathbf{F}_X(\mathbf{X}, \lambda) \Phi = \mathbf{0},$$

$$\langle \Phi, \Phi \rangle = 1.$$

where

$$\mathbf{X} = (\mathbf{u}, T), \quad \Phi = (\mathbf{v}, S),$$

or, written in detail,

$$\mathbf{v}'(t) - T \mathbf{f}_{\mathbf{u}}(\mathbf{u}(t), \lambda) \mathbf{v} - S \mathbf{f}(\mathbf{u}(t), \lambda) = \mathbf{0},$$

$$\mathbf{v}(0) - \mathbf{v}(1) = \mathbf{0},$$

$$\int_0^1 \mathbf{v}(t)^* \mathbf{u}'_0(t) dt = 0,$$

$$\int_0^1 \mathbf{v}(t)^* \mathbf{v}(t) dt + S^2 = 1.$$

The complete *extended system* to follow a fold is

$$\mathbf{F}(\mathbf{X}, \lambda, \mu) = \mathbf{0},$$

$$\mathbf{F}_{\mathbf{X}}(\mathbf{X}, \lambda, \mu) \Phi = \mathbf{0},$$

$$\langle \Phi, \Phi \rangle - 1 = 0,$$

with two free problem parameters  $\lambda$  and  $\mu$ .

To the above we add the pseudo-arclength equation

$$\langle \mathbf{X} - \mathbf{X}_0, \dot{\mathbf{X}}_0 \rangle + \langle \Phi - \Phi_0, \dot{\Phi}_0 \rangle + (\lambda - \lambda_0) \dot{\lambda}_0 + (\mu - \mu_0) \dot{\mu}_0 - \Delta s = 0.$$

In detail:

$$\mathbf{u}'(t) - T \mathbf{f}(\mathbf{u}(t), \lambda, \mu) = \mathbf{0},$$

$$\mathbf{u}(0) - \mathbf{u}(1) = \mathbf{0},$$

$$\int_0^1 \mathbf{u}(t)^* \mathbf{u}'_0(t) dt = 0,$$

$$\mathbf{v}'(t) - T \mathbf{f}_{\mathbf{u}}(\mathbf{u}(t), \lambda, \mu) \mathbf{v} - S \mathbf{f}(\mathbf{u}(t), \lambda, \mu) = \mathbf{0},$$

$$\mathbf{v}(0) - \mathbf{v}(1) = \mathbf{0},$$

$$\int_0^1 \mathbf{v}(t)^* \mathbf{u}'_0(t) dt = 0,$$

with normalization

$$\int_0^1 \mathbf{v}(t)^* \mathbf{v}(t) dt + S^2 - 1 = 0,$$

and pseudo-arclength equation

$$\begin{aligned} & \int_0^1 (\mathbf{u}(t) - \mathbf{u}_0(t))^* \dot{\mathbf{u}}_0(t) dt + \int_0^1 (\mathbf{v}(t) - \mathbf{v}_0(t))^* \dot{\mathbf{v}}_0(t) dt + \\ & + (T_0 - T) \dot{T}_0 + (S_0 - S) \dot{S}_0 + (\lambda - \lambda_0) \dot{\lambda}_0 + (\mu - \mu_0) \dot{\mu}_0 - \Delta s = 0. \end{aligned}$$

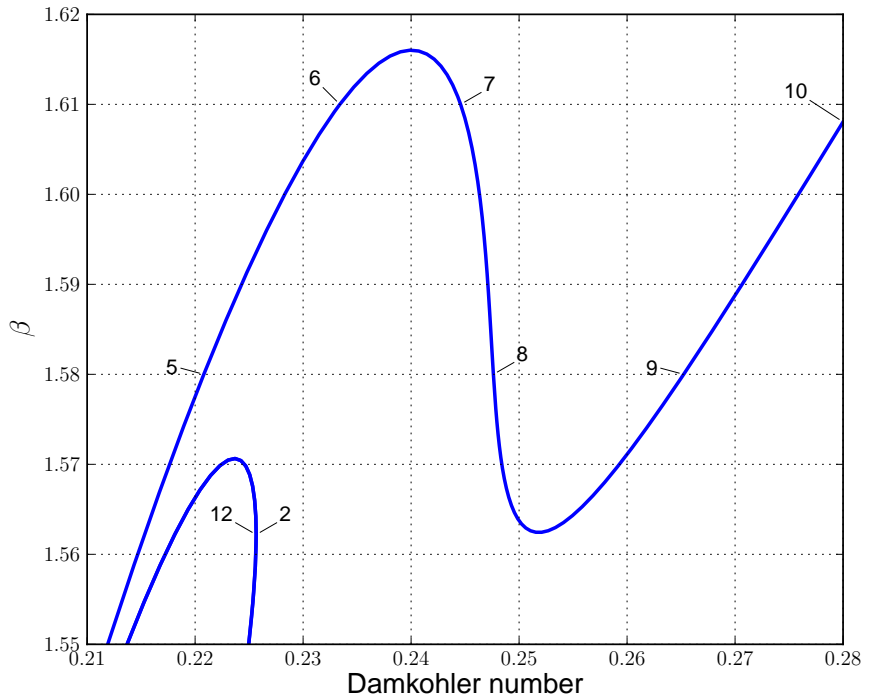


Figure 55: The locus of periodic solution folds of demo abc.

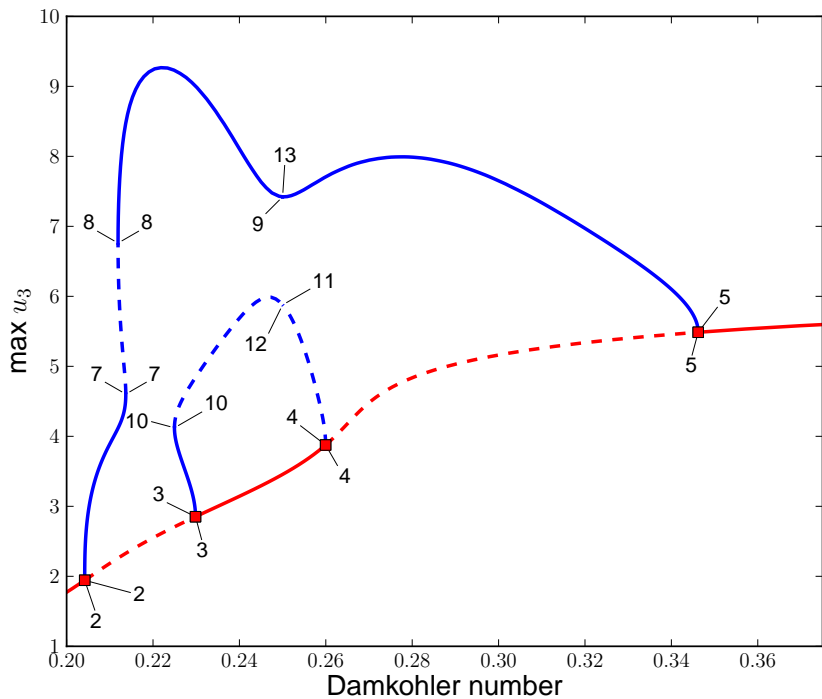


Figure 56: Stationary and periodic solutions of demo abc;  $\beta = 1.55$ .

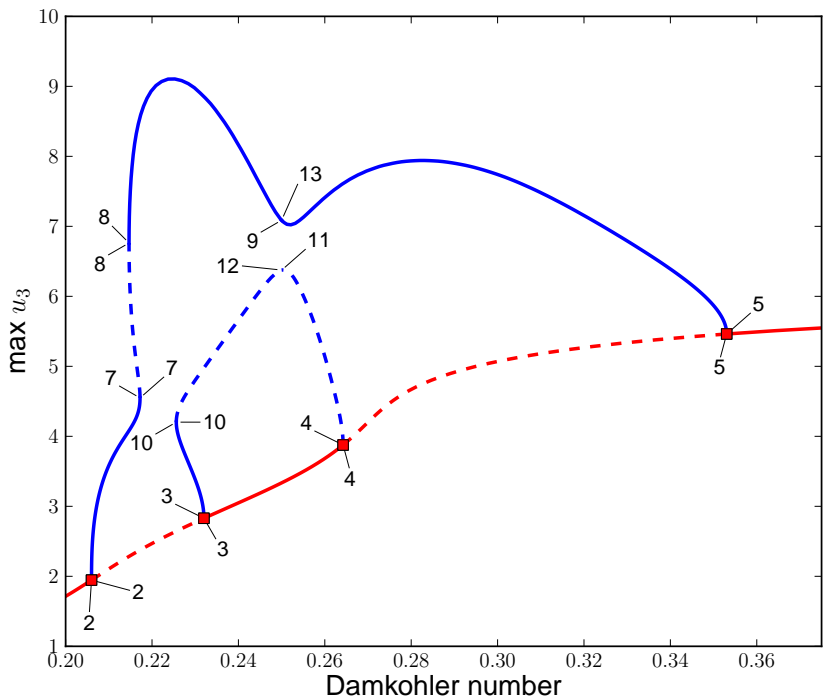


Figure 57: Stationary and periodic solutions of demo abc;  $\beta = 1.56$ .

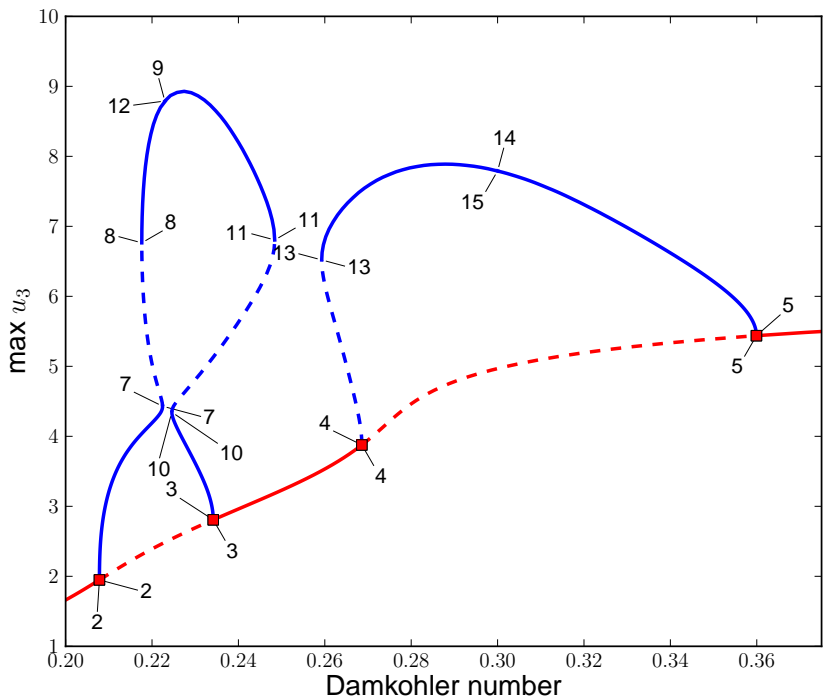


Figure 58: Stationary and periodic solutions of demo abc;  $\beta = 1.57$ .

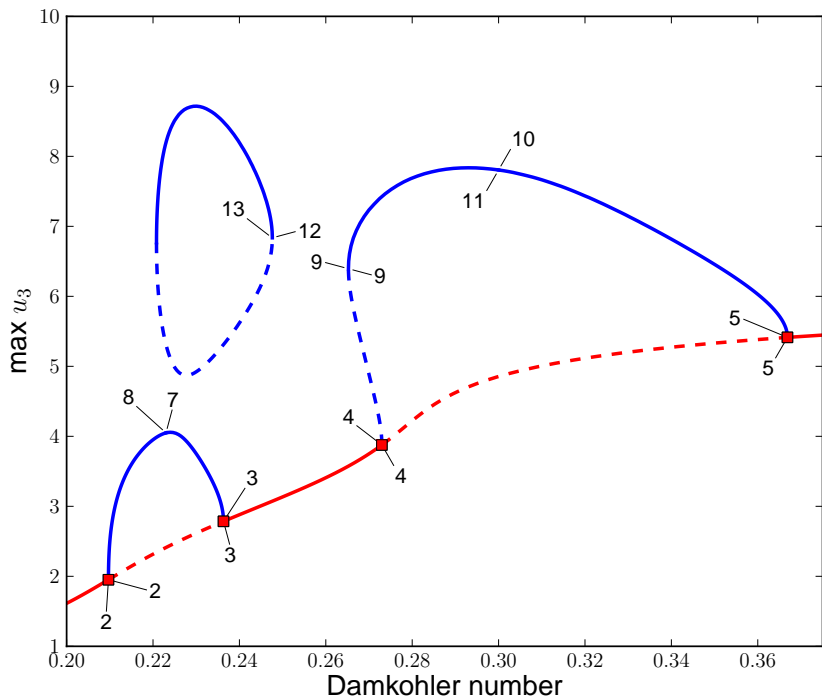


Figure 59: Stationary and periodic solutions of demo abc;  $\beta = 1.58$ .

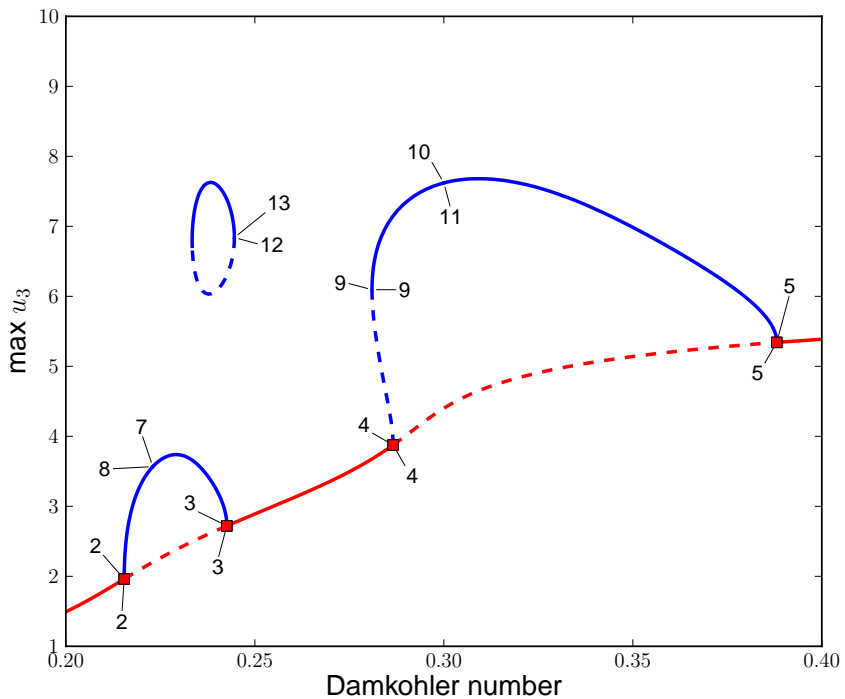


Figure 60: Stationary and periodic solutions of demo abc;  $\beta = 1.61$ .

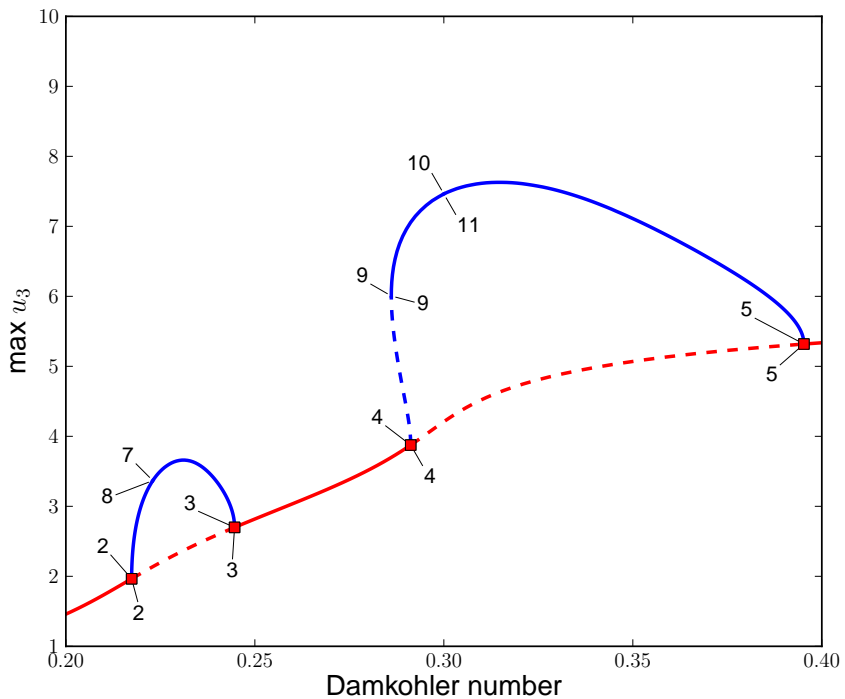


Figure 61: Stationary and periodic solutions of demo abc;  $\beta = 1.62$ .

# Following Hopf Bifurcations

We consider the persistence of a Hopf bifurcation as a second parameter is varied, and we give an algorithm for computing a 2-parameter locus of Hopf bifurcation points.

A Hopf bifurcation along a stationary solution family  $(\mathbf{u}(\lambda), \lambda)$ , of

$$\mathbf{u}' = \mathbf{f}(\mathbf{u}, \lambda) ,$$

occurs when a complex conjugate pair of eigenvalues

$$\alpha(\lambda) \pm i \beta(\lambda) ,$$

of  $f_{\mathbf{u}}(\mathbf{u}(\lambda), \lambda)$  crosses the imaginary axis *transversally*, *i.e.*, for some  $\lambda_0$ ,

$$\alpha(\lambda_0) = 0 , \quad \dot{\alpha}(\lambda_0) \neq 0 , \quad \text{and} \quad \beta_0 = \beta(\lambda_0) \neq 0 ,$$

also assuming there are no other eigenvalues on the imaginary axis.

The assumptions imply that  $\mathbf{f}_{\mathbf{u}}^0$  is *nonsingular*, so that stationary solution family can indeed be parametrized locally using  $\lambda$ .

The right and left complex eigenvectors of  $\mathbf{f}_{\mathbf{u}}^0 = f_{\mathbf{u}}(\mathbf{u}(\lambda_0), \lambda_0)$  are defined by

$$\mathbf{f}_{\mathbf{u}}^0 \boldsymbol{\phi}_0 = i \beta_0 \boldsymbol{\phi}_0 , \quad (\mathbf{f}_{\mathbf{u}}^0)^* \boldsymbol{\psi}_0 = -i \beta_0 \boldsymbol{\psi}_0 .$$

# Transversality and Persistence

THEOREM. The eigenvalue crossing in the Hopf Bifurcation Theorem is transversal if

$$\operatorname{Re} (\psi_0^* [f_{uu}^0 (f_u^0)^{-1} f_\lambda^0 - f_{u\lambda}^0] \phi_0) \neq 0.$$

PROOF. Since the eigenvalue

$$i \beta_0,$$

is algebraically simple, there is a smooth solution family (at least locally) to the parametrized right and left eigenvalue-eigenvector equations :

$$(a) \quad f_u(\mathbf{u}(\lambda), \lambda) \phi(\lambda) = \kappa(\lambda) \phi(\lambda),$$

$$(b) \quad \psi(\lambda)^* f_u(\mathbf{u}(\lambda), \lambda) = \kappa(\lambda) \psi^*(\lambda),$$

$$(c) \quad \psi(\lambda)^* \phi(\lambda) = 1, \quad (\text{and also } \phi(\lambda)^* \phi(\lambda) = 1),$$

with

$$\kappa(\lambda_0) = i \beta_0.$$

(Above, \* denotes conjugate transpose.)

$$\mathbf{f}_{\mathbf{u}}(\mathbf{u}(\lambda), \lambda) \phi(\lambda) = \kappa(\lambda) \phi(\lambda) , \quad \psi(\lambda)^* \mathbf{f}_{\mathbf{u}}(\mathbf{u}(\lambda), \lambda) = \kappa(\lambda) \psi^*(\lambda) , \quad \psi(\lambda)^* \phi(\lambda) = 1$$

Differentiation with respect to  $\lambda$  gives

$$(a) \quad \mathbf{f}_{\mathbf{uu}} \dot{\mathbf{u}} \phi + \mathbf{f}_{\mathbf{u}\lambda} \phi + \mathbf{f}_{\mathbf{u}} \dot{\phi} = \dot{\kappa} \phi + \kappa \dot{\phi} ,$$

$$(b) \quad \psi^* \mathbf{f}_{\mathbf{uu}} \dot{\mathbf{u}} + \psi^* \mathbf{f}_{\mathbf{u}\lambda} + \dot{\psi}^* \mathbf{f}_{\mathbf{u}} = \dot{\kappa} \psi^* + \kappa \dot{\psi}^* ,$$

$$(c) \quad \dot{\psi}^* \phi + \psi^* \dot{\phi} = 0 .$$

Multiply

$$(a) \quad \text{on the left by } \psi^* ,$$

and

$$(b) \quad \text{on the right by } \phi ,$$

to get

$$(a) \quad \psi^* \mathbf{f}_{\mathbf{uu}} \dot{\mathbf{u}} \phi + \psi^* \mathbf{f}_{\mathbf{u}\lambda} \phi + \psi^* \mathbf{f}_{\mathbf{u}} \dot{\phi} = \dot{\kappa} \psi^* \phi + \kappa \psi^* \dot{\phi} ,$$

$$(b) \quad \psi^* \mathbf{f}_{\mathbf{uu}} \dot{\mathbf{u}} \phi + \psi^* \mathbf{f}_{\mathbf{u}\lambda} \phi + \dot{\psi}^* \mathbf{f}_{\mathbf{u}} \phi = \dot{\kappa} \psi^* \phi + \kappa \dot{\psi}^* \phi .$$

$$\psi^* \mathbf{f}_{\mathbf{uu}} \dot{\mathbf{u}} \phi + \psi^* \mathbf{f}_{\mathbf{u}\lambda} \phi + \psi^* \mathbf{f}_{\mathbf{u}} \dot{\phi} = \dot{\kappa} \psi^* \phi + \kappa \psi^* \dot{\phi}$$

$$\psi^* \mathbf{f}_{\mathbf{uu}} \dot{\mathbf{u}} \phi + \psi^* \mathbf{f}_{\mathbf{u}\lambda} \phi + \dot{\psi}^* \mathbf{f}_{\mathbf{u}} \phi = \dot{\kappa} \psi^* \phi + \kappa \dot{\psi}^* \phi$$

Adding the above, and using

$$\underbrace{\psi^* \mathbf{f}_{\mathbf{u}} \dot{\phi}}_{=\kappa \psi^*} + \underbrace{\dot{\psi}^* \mathbf{f}_{\mathbf{u}} \phi}_{=\kappa \phi} = \kappa (\psi^* \dot{\phi} + \dot{\psi}^* \phi) = \kappa \frac{d}{d\lambda} (\underbrace{\psi^* \phi}_{=1}) = 0,$$

we find

$$\dot{\kappa} = \psi^* [\mathbf{f}_{\mathbf{uu}} \dot{\mathbf{u}} + \mathbf{f}_{\mathbf{u}\lambda}] \phi.$$

$$\dot{\kappa} = \psi^*[\mathbf{f}_{\mathbf{uu}} \dot{\mathbf{u}} + \mathbf{f}_{\mathbf{u}\lambda}] \phi$$

From differentiating

$$\mathbf{f}(\mathbf{u}(\lambda), \lambda) = \mathbf{0},$$

with respect to  $\lambda$ , we have

$$\dot{\mathbf{u}} = -(\mathbf{f}_{\mathbf{u}})^{-1} \mathbf{f}_\lambda,$$

so that

$$\dot{\kappa} = \psi^*[-\mathbf{f}_{\mathbf{uu}} (\mathbf{f}_{\mathbf{u}})^{-1} \mathbf{f}_\lambda + \mathbf{f}_{\mathbf{u}\lambda}] \phi.$$

Thus the eigenvalue crossing is transversal if

$$\dot{\alpha}(0) = \operatorname{Re}(\dot{\kappa}_0) = \operatorname{Re}(\psi_0^*[\mathbf{f}_{\mathbf{uu}}^0 (\mathbf{f}_{\mathbf{u}}^0)^{-1} \mathbf{f}_\lambda^0 - \mathbf{f}_{\mathbf{u}\lambda}^0] \phi_0) \neq 0. \bullet$$

NOTE:

The *transversality condition* of the Theorem, *i.e.*,

$$\operatorname{Re} (\psi_0^* [f_{uu}^0(f_u^0)^{-1} f_\lambda^0 - f_{u\lambda}^0] \phi_0) \neq 0,$$

is also needed for *persistence* of the Hopf bifurcation, as discussed below.

The *extended system* for following Hopf bifurcations is

$$\mathbf{F}(\mathbf{u}, \boldsymbol{\phi}, \beta, \lambda; \mu) \equiv \begin{cases} \mathbf{f}(\mathbf{u}, \lambda, \mu) = \mathbf{0} , \\ \mathbf{f}_{\mathbf{u}}(\mathbf{u}, \lambda, \mu) \boldsymbol{\phi} - i \beta \boldsymbol{\phi} = \mathbf{0} , \\ \boldsymbol{\phi}^* \boldsymbol{\phi}_0 - 1 = 0 , \end{cases}$$

where

$$\mathbf{F} : \mathbf{R}^n \times \mathbf{C}^n \times \mathbf{R}^2 \times \mathbf{R} \rightarrow \mathbf{R}^n \times \mathbf{C}^n \times \mathbf{C} ,$$

and to which we want to compute a solution family

$$(\mathbf{u}, \boldsymbol{\phi}, \beta, \lambda, \mu) ,$$

with

$$\mathbf{u} \in \mathbf{R}^n, \quad \boldsymbol{\phi} \in \mathbf{C}^n, \quad \beta, \lambda, \mu \in \mathbf{R} .$$

Above  $\boldsymbol{\phi}_0$  belongs to a “reference solution”

$$(\mathbf{u}_0, \boldsymbol{\phi}_0, \beta_0, \lambda_0, \mu_0) ,$$

which typically is the latest computed solution point of a family.

First consider parametrizing in the second parameter  $\mu$ , i.e., we seek a family

$$(\mathbf{u}(\mu), \phi(\mu), \beta(\mu), \lambda(\mu)).$$

(In practice, pseudo-arc length continuation is used.)

The derivative with respect to

$$(\mathbf{u}, \phi, \beta, \lambda),$$

at the solution point

$$(\mathbf{u}_0, \phi_0, \beta_0, \lambda_0, \mu_0),$$

is

$$\begin{pmatrix} \mathbf{f}_{\mathbf{u}}^0 & O & \mathbf{0} & \mathbf{f}_{\lambda}^0 \\ \mathbf{f}_{\mathbf{uu}}^0 \phi_0 & \mathbf{f}_{\mathbf{u}}^0 - i\beta_0 I & -i\phi_0 & \mathbf{f}_{\mathbf{u}\lambda}^0 \phi_0 \\ \mathbf{0}^* & \phi_0^* & 0 & 0 \end{pmatrix}. \quad (12)$$

The Jacobian is of the form

$$\begin{pmatrix} A & O & \mathbf{0} & c_1 \\ C & D & -i\phi_0 & c_2 \\ \mathbf{0}^* & \phi_0^* & 0 & 0 \end{pmatrix},$$

where

$$A = \mathbf{f}_{\mathbf{u}}^0 \quad (\text{nonsingular}), \quad C = \mathbf{f}_{\mathbf{u}\mathbf{u}}^0 \phi_0, \quad D = \mathbf{f}_{\mathbf{u}}^0 - i \beta_0 I,$$

and

$$c_1 = \mathbf{f}_{\lambda}^0, \quad c_2 = \mathbf{f}_{\mathbf{u}\lambda}^0 \phi_0,$$

with

$$\mathcal{N}(D) = \text{Span}\{\phi_0\}, \quad \mathcal{N}(D^*) = \text{Span}\{\psi_0\},$$

where

$$\psi_0^* \phi_0 = 1, \quad \phi_0^* \phi_0 = 1.$$

## THEOREM.

If the eigenvalue crossing is *transversal*, *i.e.*, if

$$\operatorname{Re}(\dot{\kappa}_0) \neq 0,$$

then the Jacobian matrix (12) is nonsingular.

Hence there locally exists a solution family

$$(\mathbf{u}(\mu), \phi(\mu), \beta(\mu), \lambda(\mu))$$

to the extended system

$$\mathbf{F}(\mathbf{u}, \phi, \beta, \lambda; \mu) = \mathbf{0},$$

*i.e.*, the Hopf bifurcation persists under small perturbations of  $\mu$ .

PROOF. We prove this by constructing a solution

$$\mathbf{x} \in \mathbb{R}^n , \quad \mathbf{y} \in \mathbb{C}^n , \quad z_1 , z_2 \in \mathbb{R} ,$$

to

$$\begin{pmatrix} A & O & \mathbf{0} & \mathbf{c}_1 \\ C & D & -i\phi_0 & \mathbf{c}_2 \\ \mathbf{0}^* & \phi_0^* & 0 & 0 \end{pmatrix} \begin{pmatrix} \mathbf{x} \\ \mathbf{y} \\ z_1 \\ z_2 \end{pmatrix} = \begin{pmatrix} \mathbf{f} \\ \mathbf{g} \\ h \end{pmatrix} ,$$

where

$$\mathbf{f} \in \mathbb{R}^n , \quad \mathbf{g} \in \mathbb{C}^n , \quad h \in \mathbb{C} .$$

From the first equation

$$A\mathbf{x} + z_2 \mathbf{c}_1 = \mathbf{f} ,$$

we have

$$\mathbf{x} = A^{-1}\mathbf{f} - z_2 A^{-1} \mathbf{c}_1 .$$

The second equation can then be written

$$C A^{-1}\mathbf{f} - z_2 C A^{-1} \mathbf{c}_1 + D \mathbf{y} - z_1 i \phi_0 + z_2 \mathbf{c}_2 = \mathbf{g} .$$

$$C A^{-1} \mathbf{f} - z_2 C A^{-1} \mathbf{c}_1 + D \mathbf{y} - z_1 i \boldsymbol{\phi}_0 + z_2 \mathbf{c}_2 = \mathbf{g}.$$

Multiply on the left by  $\boldsymbol{\psi}_0^*$  to get

$$\boldsymbol{\psi}_0^* C A^{-1} \mathbf{f} - z_2 \boldsymbol{\psi}_0^* C A^{-1} \mathbf{c}_1 - z_1 i \boldsymbol{\psi}_0^* \boldsymbol{\phi}_0 + z_2 \boldsymbol{\psi}_0^* \mathbf{c}_2 = \boldsymbol{\psi}_0^* \mathbf{g}.$$

Recall that

$$\boldsymbol{\psi}_0^* \boldsymbol{\phi}_0 = 1.$$

Defining

$$\tilde{\mathbf{f}} \equiv C A^{-1} \mathbf{f}, \quad \tilde{\mathbf{c}}_1 \equiv C A^{-1} \mathbf{c}_1.$$

we have

$$i z_1 + \boldsymbol{\psi}_0^* (\tilde{\mathbf{c}}_1 - \mathbf{c}_2) z_2 = \boldsymbol{\psi}_0^* (\tilde{\mathbf{f}} - \mathbf{g}).$$

Computationally  $\tilde{\mathbf{f}}$  and  $\tilde{\mathbf{c}}_1$  are obtained from

$$A \hat{\mathbf{f}} = \mathbf{f}, \quad A \hat{\mathbf{c}}_1 = \mathbf{c}_1,$$

$$\tilde{\mathbf{f}} = C \hat{\mathbf{f}}, \quad \tilde{\mathbf{c}}_1 = C \hat{\mathbf{c}}_1.$$

$$i z_1 + \psi_0^* (\tilde{\mathbf{c}}_1 - \mathbf{c}_2) z_2 = \psi_0^* (\tilde{\mathbf{f}} - \mathbf{g})$$

Separate real and imaginary part of this equation, and use the fact that

$$z_1 \text{ and } z_2 \text{ are real ,}$$

to get

$$\operatorname{Re}(\psi_0^* [\tilde{\mathbf{c}}_1 - \mathbf{c}_2]) z_2 = \operatorname{Re}(\psi_0^* [\tilde{\mathbf{f}} - \mathbf{g}]),$$

$$z_1 + \operatorname{Im}(\psi_0^* [\tilde{\mathbf{c}}_1 - \mathbf{c}_2]) z_2 = \operatorname{Im}(\psi_0^* [\tilde{\mathbf{f}} - \mathbf{g}]),$$

from which

$$z_2 = \frac{\operatorname{Re}(\psi_0^* [\tilde{\mathbf{f}} - \mathbf{g}])}{\operatorname{Re}(\psi_0^* [\tilde{\mathbf{c}}_1 - \mathbf{c}_2])},$$

$$z_1 = -z_2 \operatorname{Im}(\psi_0^* [\tilde{\mathbf{c}}_1 - \mathbf{c}_2]) + \operatorname{Im}(\psi_0^* [\tilde{\mathbf{f}} - \mathbf{g}]).$$

Now solve for  $\mathbf{x}$  in

$$\boxed{A \mathbf{x} = \mathbf{f} - z_2 \mathbf{c}_1},$$

and compute a particular solution  $\mathbf{y}_p$  to

$$\boxed{D \mathbf{y} = \mathbf{g} - C \mathbf{x} + i z_1 \phi_0 - z_2 \mathbf{c}_2}.$$

Then

$$\mathbf{y} = \mathbf{y}_p + \alpha \phi_0, \quad \alpha \in \mathbb{C}.$$

The third equation is

$$\phi_0^* \mathbf{y} = \phi_0^* \mathbf{y}_p + \alpha \phi_0^* \phi_0 = h,$$

from which, using  $\phi_0^* \phi_0 = 1$ ,

$$\boxed{\alpha = h - \phi_0^* \mathbf{y}_p}.$$

The above construction can be carried out if

$$\operatorname{Re}(\psi_0^* [\tilde{\mathbf{c}}_1 - \mathbf{c}_2]) \neq 0.$$

However, using the definition of  $\tilde{\mathbf{c}}_1$  and  $\mathbf{c}_2$ , we have

$$\begin{aligned}\operatorname{Re}(\psi_0^* [\tilde{\mathbf{c}}_1 - \mathbf{c}_2]) &= \operatorname{Re}(\psi_0^* [C A^{-1} \mathbf{c}_1 - \mathbf{c}_2]) \\&= \operatorname{Re}(\psi_0^* [\mathbf{f}_{\mathbf{uu}}^0 \phi_0 (\mathbf{f}_{\mathbf{u}}^0)^{-1} \mathbf{f}_{\lambda}^0 - \mathbf{f}_{\mathbf{u}\lambda}^0 \phi_0]) \\&= \operatorname{Re}(\psi_0^* [\mathbf{f}_{\mathbf{uu}}^0 (\mathbf{f}_{\mathbf{u}}^0)^{-1} \mathbf{f}_{\lambda}^0 - \mathbf{f}_{\mathbf{u}\lambda}^0] \phi_0) \\&= \operatorname{Re}(\dot{\kappa}_0) \neq 0. \quad \bullet\end{aligned}$$

# Practical Continuation of Hopf Bifurcations

Recall that the *extended system* for following Hopf bifurcations is

$$\mathbf{F}(\mathbf{u}, \phi, \beta, \lambda; \mu) \equiv \begin{cases} \mathbf{f}(\mathbf{u}, \lambda, \mu) = \mathbf{0} , \\ \mathbf{f}_{\mathbf{u}}(\mathbf{u}, \lambda, \mu) \phi - i \beta \phi = \mathbf{0} , \\ \phi^* \phi_0 - 1 = 0 , \end{cases}$$

where

$$\mathbf{F} : \mathbb{R}^n \times \mathbb{C}^n \times \mathbb{R}^2 \times \mathbb{R} \rightarrow \mathbb{R}^n \times \mathbb{C}^n \times \mathbb{C} ,$$

and to which we want to compute a solution family

$$(\mathbf{u}, \phi, \beta, \lambda, \mu), \quad \text{with } \mathbf{u} \in \mathbb{R}^n, \quad \phi \in \mathbb{C}^n, \quad \beta, \lambda, \mu \in \mathbb{R} .$$

In practice, we treat  $\mu$  as an unknown, and add the continuation equation

$$(\mathbf{u} - \mathbf{u}_0)^* \dot{\mathbf{u}}_0 + (\phi - \phi_0)^* \dot{\phi}_0 + (\beta - \beta_0) \dot{\beta}_0 + (\lambda - \lambda_0) \dot{\lambda}_0 + (\mu - \mu_0) \dot{\mu}_0 - \Delta s = 0 .$$

## EXERCISE.

Investigate the Hopf bifurcations in the system

$$u'_1(t) = u_1 (1 - u_1) - p_4 u_1 u_2 ,$$

$$u'_2(t) = -\frac{1}{4} u_2 + p_4 u_1 u_2 - 3 u_2 u_3 - p_1 (1 - e^{-5u_2}) ,$$

$$u'_3(t) = -\frac{1}{2} u_3 + 3 u_2 u_3 .$$

This is the predator-prey model where,

$u_1 \sim$  plankton,     $u_2 \sim$  fish,     $u_3 \sim$  sharks,     $\lambda \equiv p_1 \sim$  fishing quota.

(See also Figure 43.)

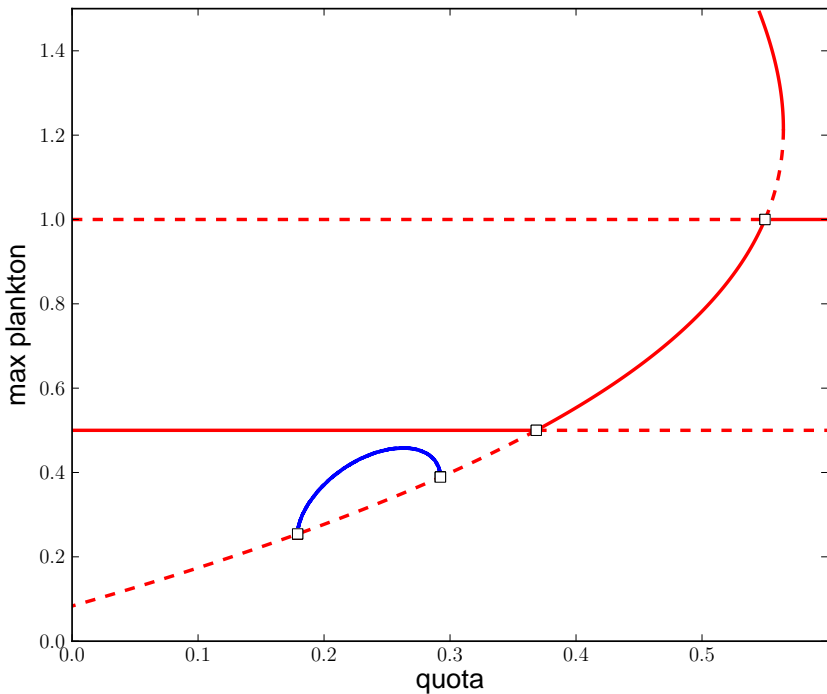


Figure 62: A bifurcation diagram for the 3-species model; with  $p_4 = 3$ .

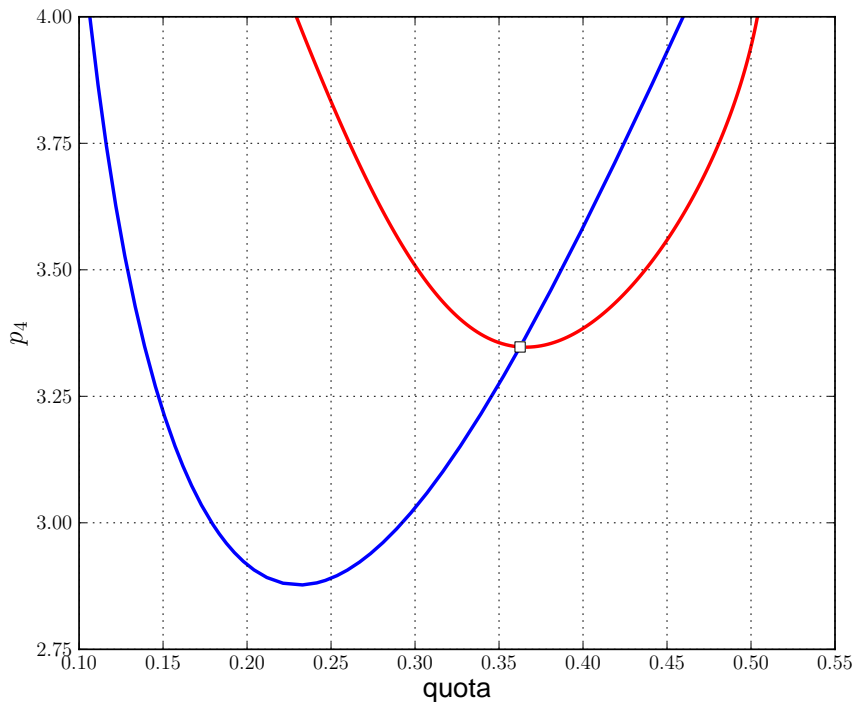


Figure 63: Loci of Hopf bifurcations for the 3-species model.

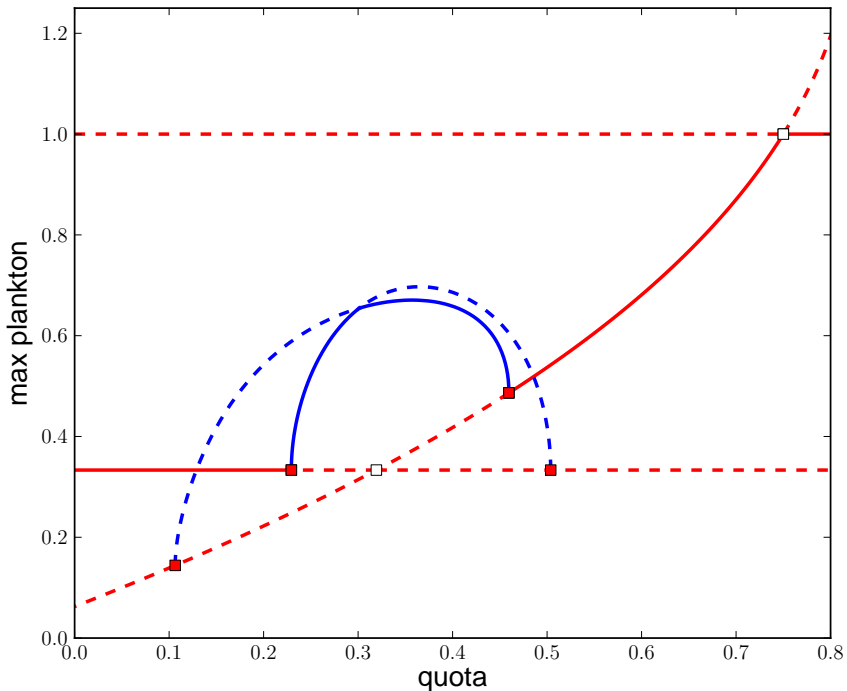


Figure 64: A bifurcation diagram for the 3-species model; with  $p_4 = 4$ .

EXERCISE. (AUTO demo abc-hb.)

Compute loci of Hopf bifurcation points for the  $A \rightarrow B \rightarrow C$  reaction

$$u'_1 = -u_1 + D(1 - u_1)e^{u_3} ,$$

$$u'_2 = -u_2 + D(1 - u_1)e^{u_3} - D\sigma u_2 e^{u_3} ,$$

$$u'_3 = -u_3 - \beta u_3 + DB(1 - u_1)e^{u_3} + DB\alpha\sigma u_2 e^{u_3} ,$$

with

$$\alpha = 1 , \quad \sigma = 0.04 , \quad B = 8 ,$$

and varying  $D$  and  $\beta$ .

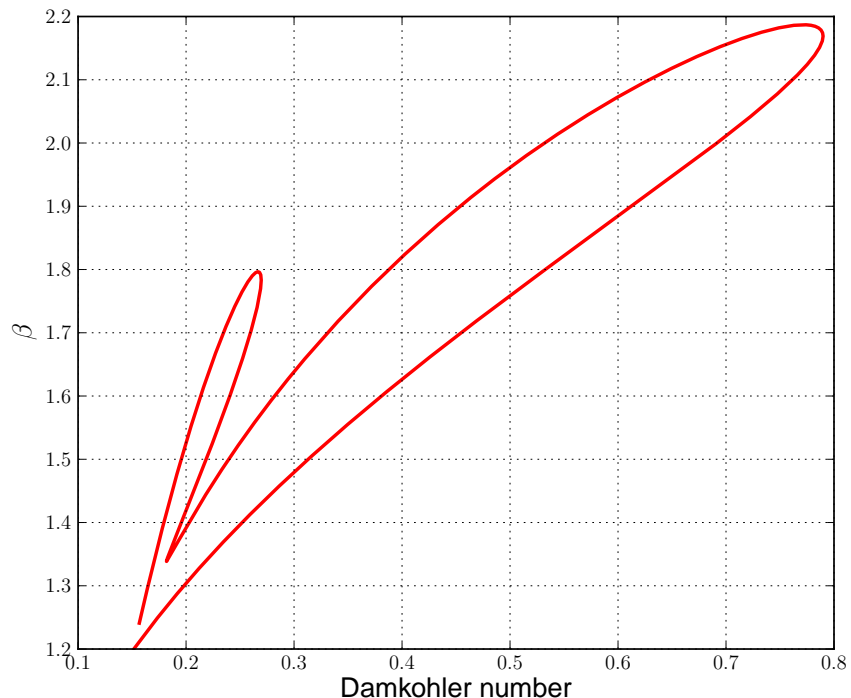


Figure 65: A locus of Hopf bifurcations.

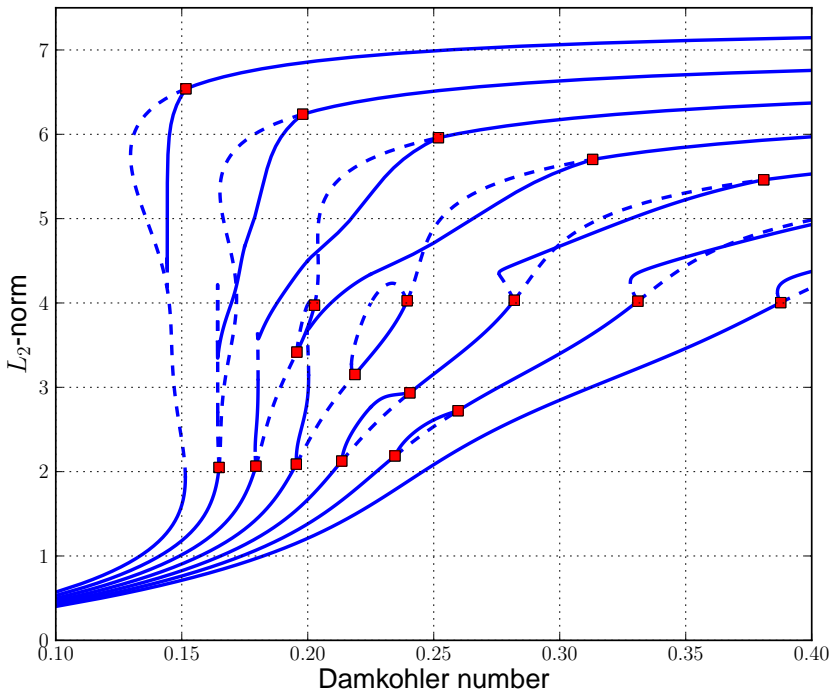


Figure 66: Diagrams for  $\beta = 1.2, 1.3, 1.4, 1.5, 1.6, 1.7, 1.8$ .

# Stable and Unstable Manifolds

- One can also use continuation to compute solution families of IVP.
- In particular, one can compute *stable and unstable manifolds* .

EXAMPLE: The Lorenz Equations. (AUTO demos `lor`, `lrz`, `man`.)

$$x' = \sigma (y - x) ,$$

$$y' = \rho x - y - x z ,$$

$$z' = x y - \beta z ,$$

where

$$\sigma = 10 \quad \text{and} \quad \beta = 8/3 .$$

### The Lorenz Equations

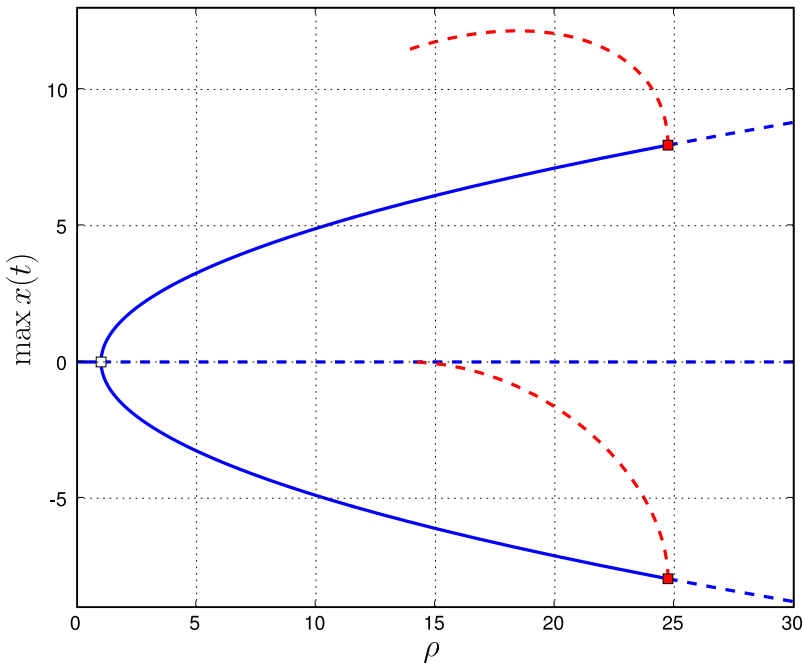


Figure 67: Bifurcation diagram of the Lorenz equations.

NOTE:

- The zero solution is unstable for  $\rho > 1$ .
- Two nonzero stationary solutions bifurcate at  $\rho = 1$ .
- The nonzero stationary solutions become unstable for  $\rho > \rho_H$ .
- At  $\rho_H$  ( $\rho_H \approx 24.7$ ) there are Hopf bifurcations.
- Unstable periodic solutions emanate from each Hopf bifurcation.
- These families end in *homoclinic orbits* (infinite period) at  $\rho \approx 13.9$ .
- For  $\rho > \rho_H$  there is the famous *Lorenz attractor*.

### The Lorenz Equations

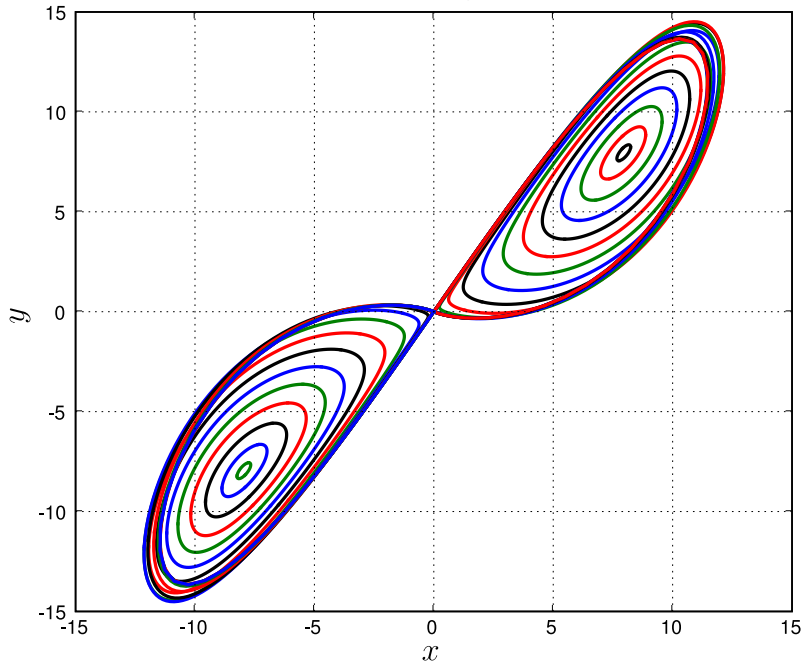


Figure 68: Unstable periodic orbits of the Lorenz equations.

# The Lorenz Manifold

- For  $\rho > 1$  the origin is a *saddle point* .
- The Jacobian has two negative eigenvalues and one positive eigenvalue.
- The two negative eigenvalues give rise to a 2D *stable manifold* .
- This manifold is known as the *Lorenz Manifold* .
- 
- The Lorenz Manifold helps us understand the *Lorenz attractor* .

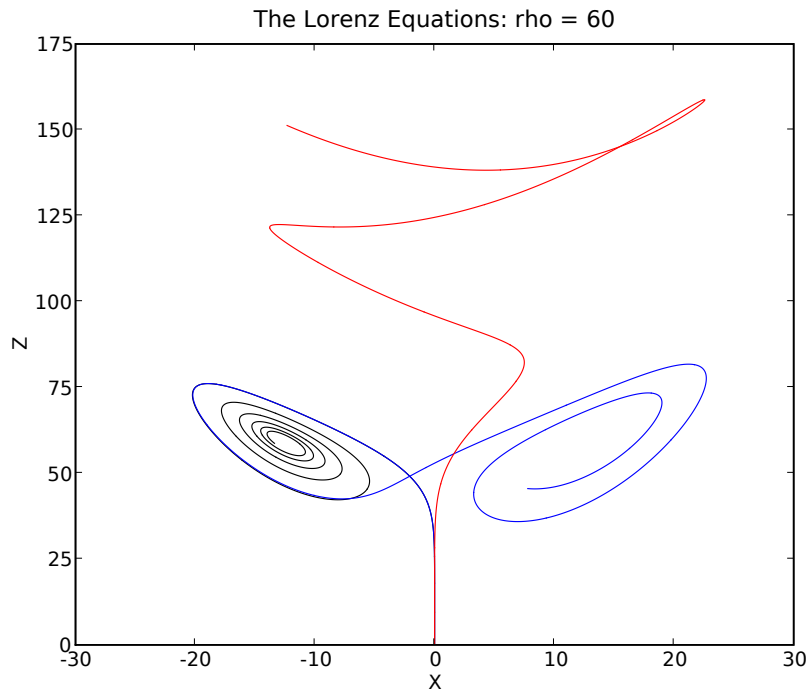


Figure 69: Three orbits whose initial conditions agree to  $>11$  decimal places !

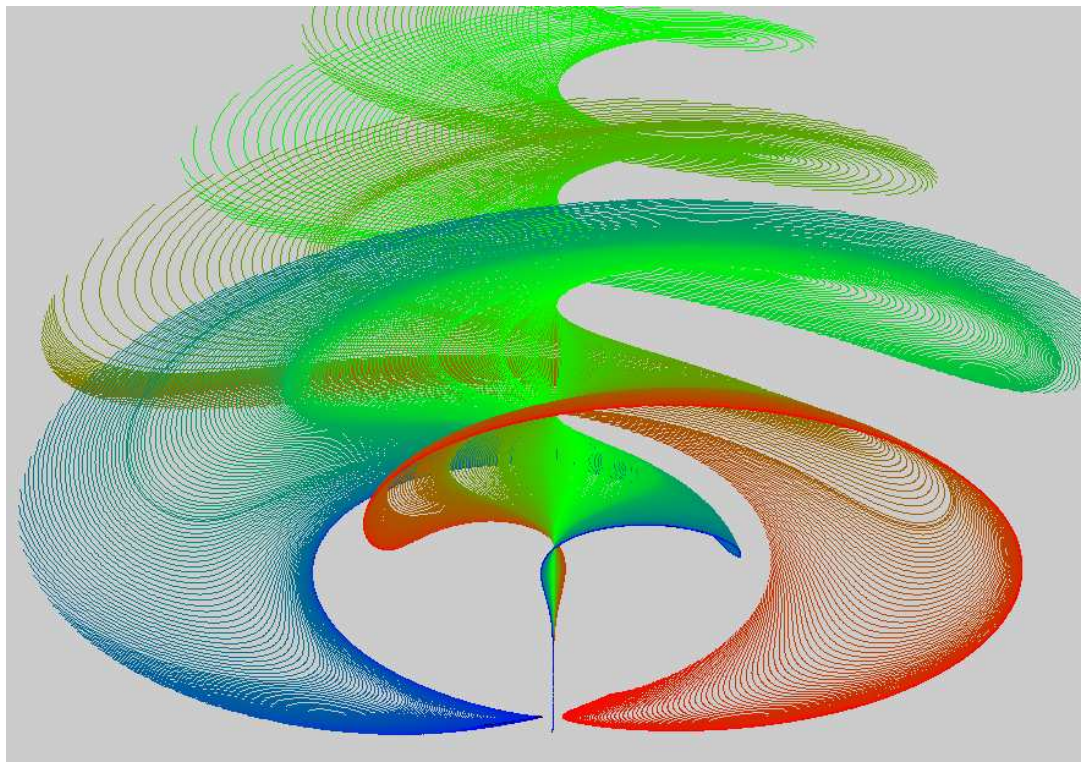


Figure 70: A small portion of a Lorenz Manifold ...

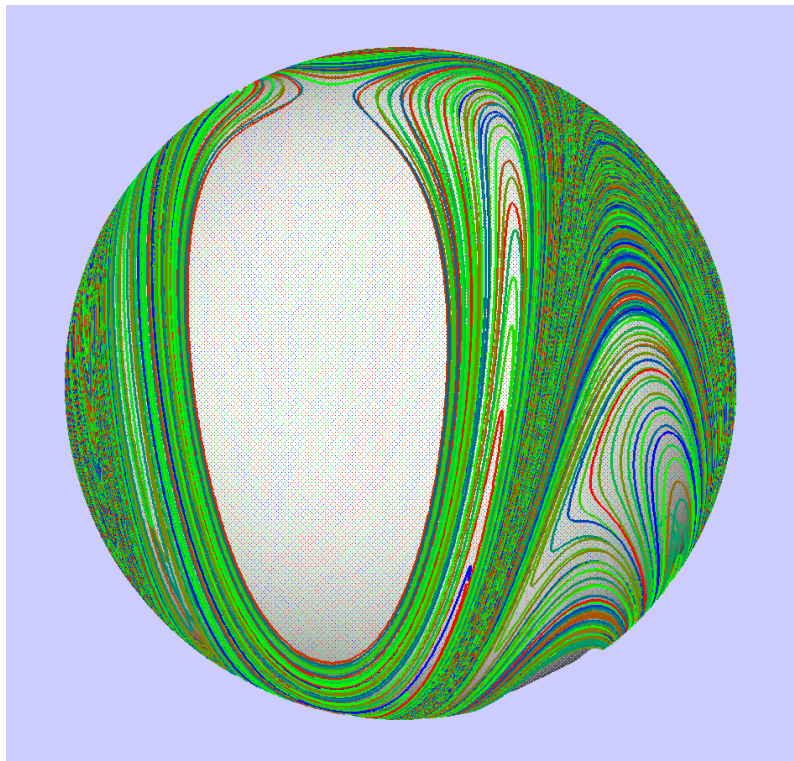


Figure 71: Intersection of a Lorenz Manifold with a sphere ( $\rho = 35$ ,  $R = 100$ ).

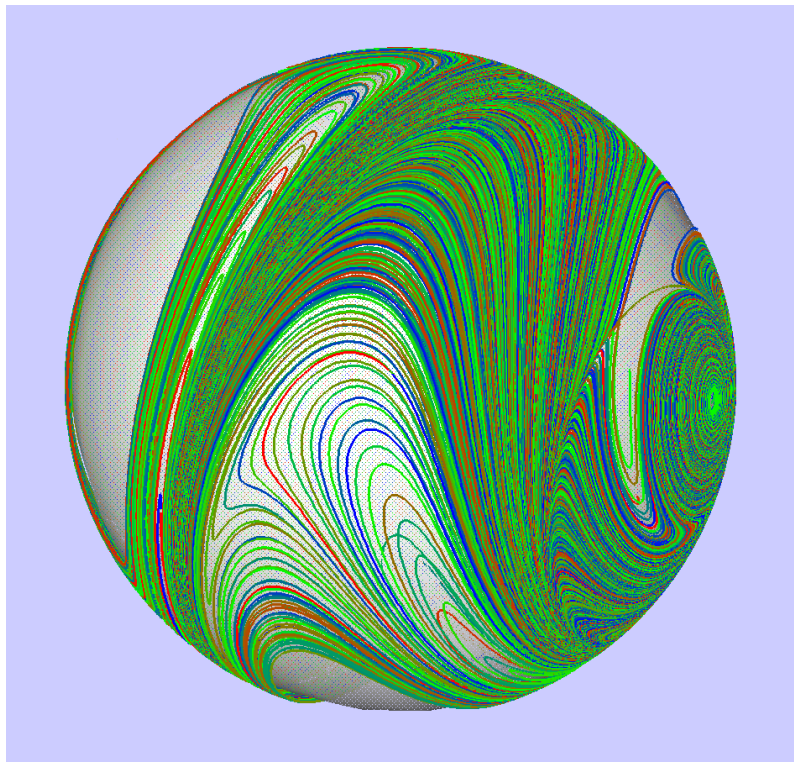


Figure 72: Intersection of a Lorenz Manifold with a sphere ( $\rho = 35$ ,  $R = 100$ ).

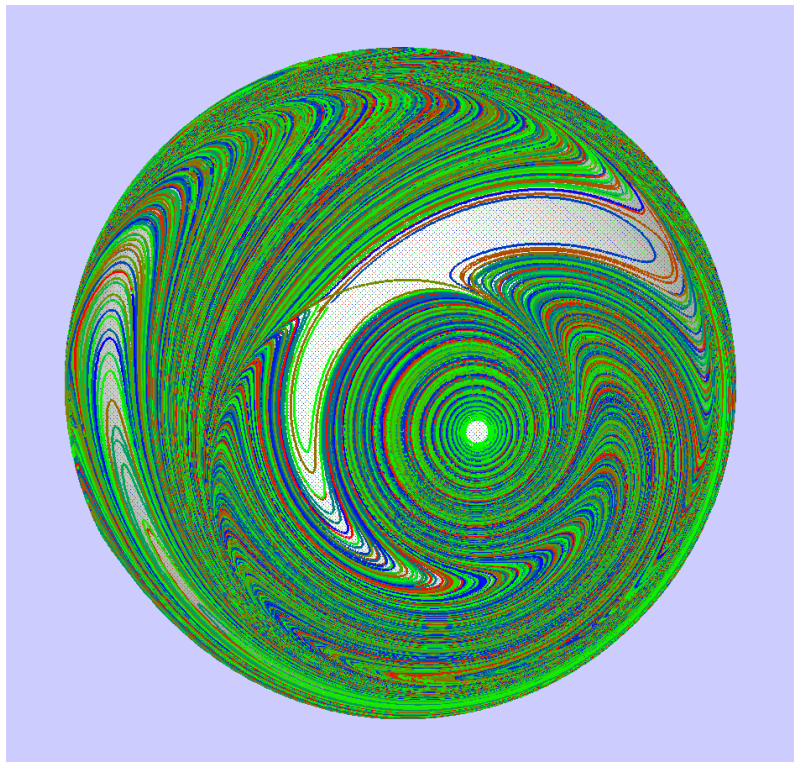


Figure 73: Intersection of a Lorenz Manifold with a sphere ( $\rho = 35$ ,  $R = 100$ ).

# How was the Lorenz Manifold computed?

First compute an orbit  $\mathbf{u}_0(t)$ , for  $t$  from 0 to  $T_0$  (where  $T_0 < 0$ ), with

$\mathbf{u}_0(0)$  close to the origin  $\mathbf{0}$ ,

and

$\mathbf{u}_0(0)$  in the stable eigenspace spanned by  $\mathbf{v}_1$  and  $\mathbf{v}_2$ ,

that is,

$$\mathbf{u}_0(0) = \mathbf{0} + \epsilon \left( \frac{\cos(2\pi\theta)}{|\mu_1|} \mathbf{v}_1 - \frac{\sin(2\pi\theta)}{|\mu_2|} \mathbf{v}_2 \right),$$

for, say,  $\theta = 0$ .

Scale time

$$t \quad \rightarrow \quad \frac{t}{T_0} \quad ,$$

Then the initial orbit satisfies

$$\mathbf{u}'_0(t) = T_0 \mathbf{f}(\mathbf{u}_0(t)) , \quad \text{for } 0 \leq t \leq 1 ,$$

and

$$\mathbf{u}_0(0) = \frac{\epsilon}{|\mu_1|} \mathbf{v}_1 .$$

The initial orbit has length

$$L = T_0 \int_0^1 \|\mathbf{f}(\mathbf{u}_0(s))\| ds .$$

Thus the initial orbit corresponds to a solution  $\mathbf{X}_0$  of the equation

$$\mathbf{F}(\mathbf{X}) = \mathbf{0},$$

where

$$\mathbf{F}(\mathbf{X}) \equiv \begin{cases} \mathbf{u}'(t) - T \mathbf{f}(\mathbf{u}(t)) \\ \mathbf{u}(0) - \epsilon \left( \frac{\cos(\theta)}{|\mu_1|} \mathbf{v}_1 - \frac{\sin(\theta)}{|\mu_2|} \mathbf{v}_2 \right) \\ T \int_0^1 \|\mathbf{f}(\mathbf{u})\| ds - L \end{cases}$$

with  $\mathbf{X} = (\mathbf{u}(\cdot), \theta, T)$ , (for given  $L$  and  $\epsilon$ ),

and

$$\mathbf{X}_0 = (\mathbf{u}_0(\cdot), 0, T_0).$$

As before, the continuation system is

$$\mathbf{F}(\mathbf{X}_k) = 0,$$

$$\langle \mathbf{X}_k - \mathbf{X}_{k-1}, \dot{\mathbf{X}}_{k-1} \rangle - \Delta s = 0, \quad (\|\dot{\mathbf{X}}_{k-1}\| = 1),$$

and

$$\mathbf{X} = (\mathbf{u}(\cdot), \theta, T), \quad (\text{keeping } L \text{ and } \epsilon \text{ fixed}),$$

or

$$\mathbf{X} = (\mathbf{u}(\cdot), \theta, L), \quad (\text{keeping } T \text{ and } \epsilon \text{ fixed}),$$

or (for computing the starting orbit  $\mathbf{u}_0(t)$ ),

$$\mathbf{X} = (\mathbf{u}(\cdot), L, T), \quad (\text{keeping } \theta \text{ and } \epsilon \text{ fixed}).$$

Other variations are possible . . . .

NOTE:

- We do not just change the initial point (*i.e.*,  $\theta$ ) and integrate !
- Every continuation step requires solving a “*boundary value problem*”.
- The continuation stepsize  $\Delta s$  controls the change in  $\mathbf{X}$  .
- $\mathbf{X}$  cannot suddenly change a lot in any continuation step.
- This allows the ”*entire manifold*” to be computed.

NOTE:

- Crossings of the Lorenz manifold with the plane  $z = \rho - 1$  can be located.
- Connections between the origin and the nonzero equilibria can be located.
- There are subtle variations on the algorithm !

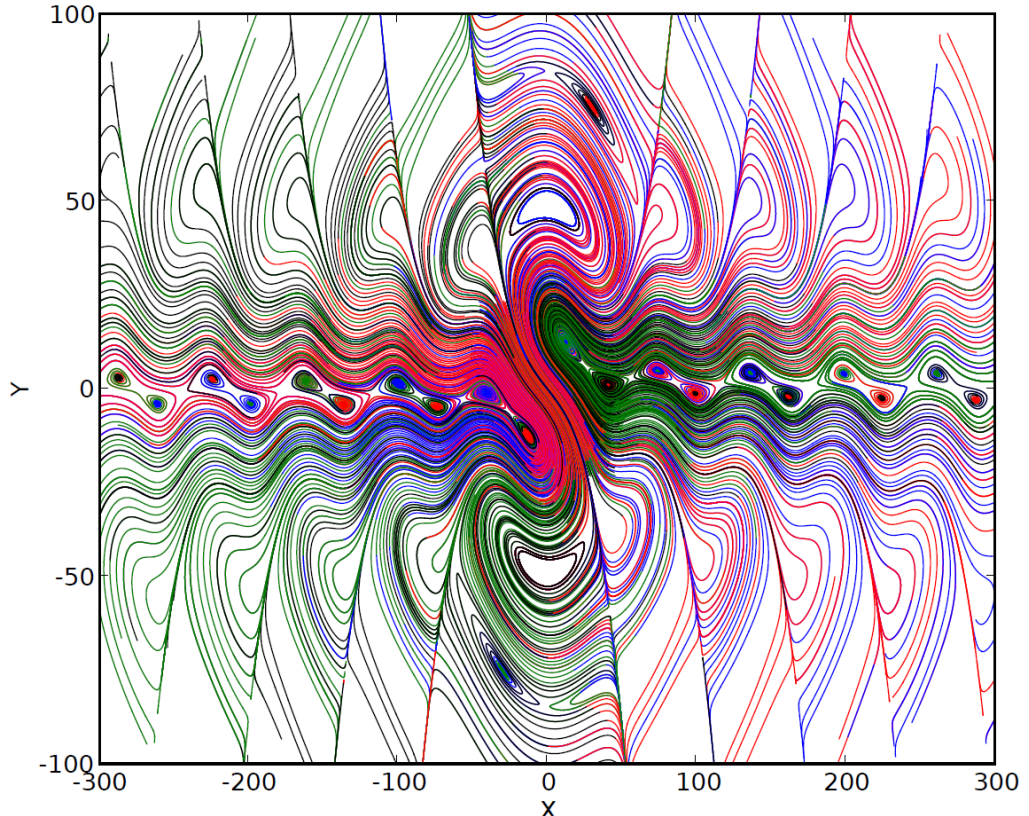


Figure 74: Crossings of the Lorenz Manifold with the plane  $z = \rho - 1$   
282

## Heteroclinic connections

- During the computation of the 2D stable manifold of the origin one can locate *heteroclinic orbits* between the origin and the nonzero equilibria.
- The same heteroclinic orbits can be detected during the computation of the 2D unstable manifold of the nonzero equilibria.

NORM

29.

28.

27.

26.

25.

24.

1.070

1.080

1.090

1.100

1.110

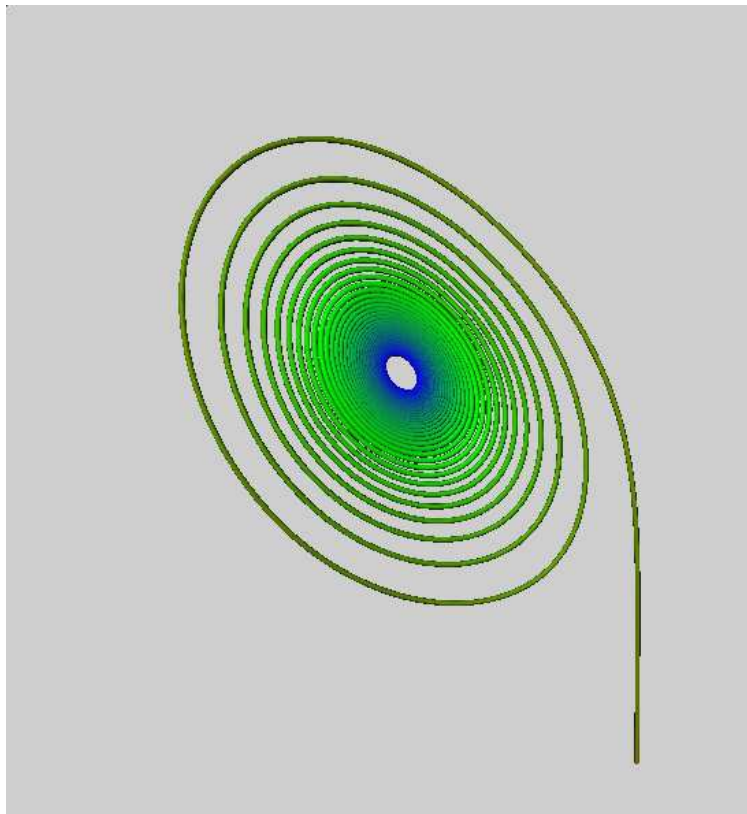
1.120

1.130

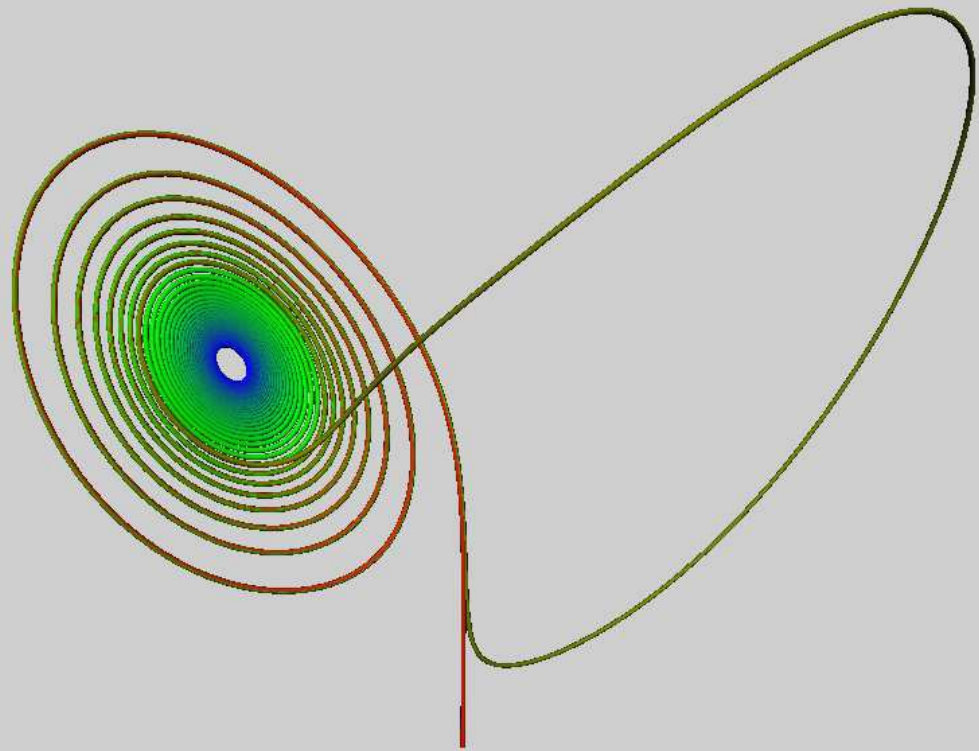
1.140

RADIUS

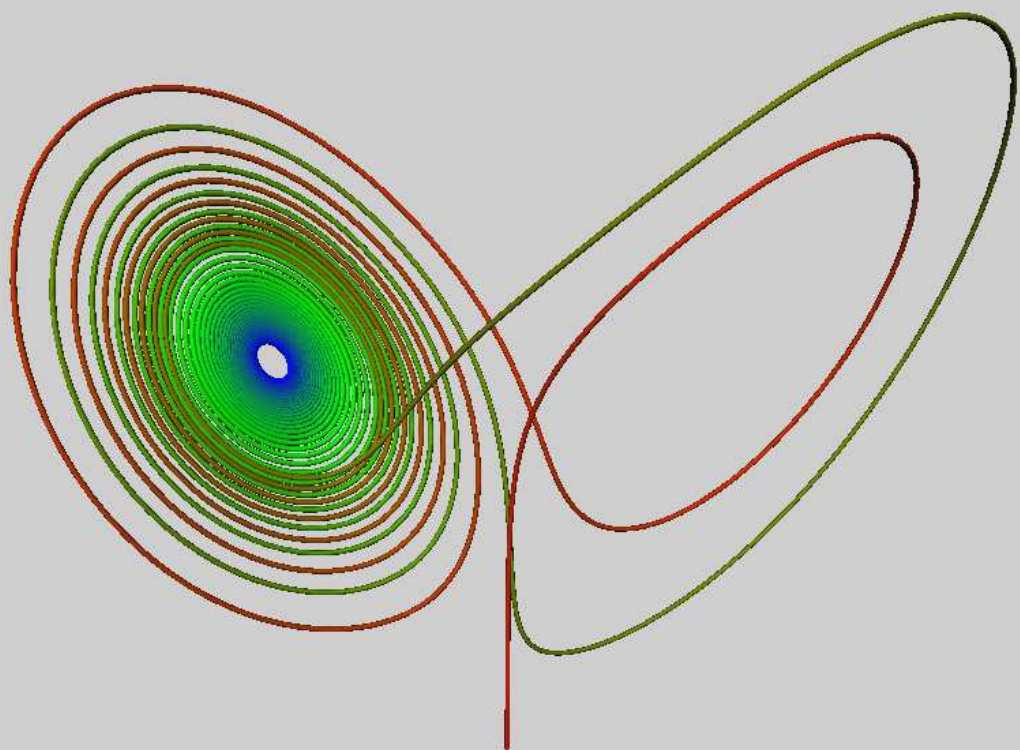
Representation of the orbit family in the stable manifold.



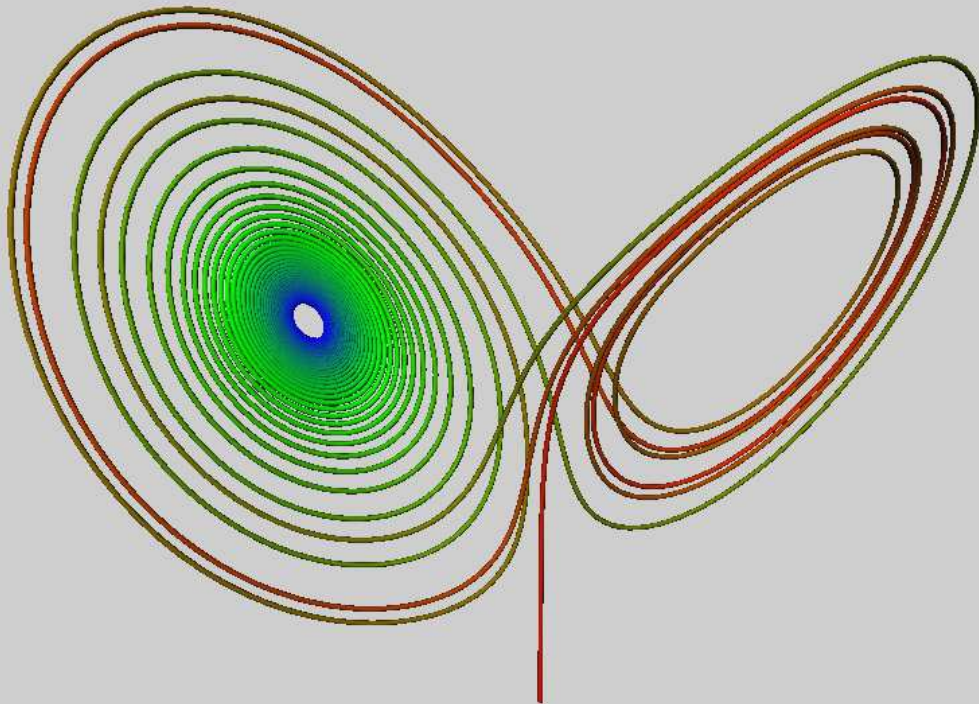
A heteroclinic connection in the Lorenz equations.



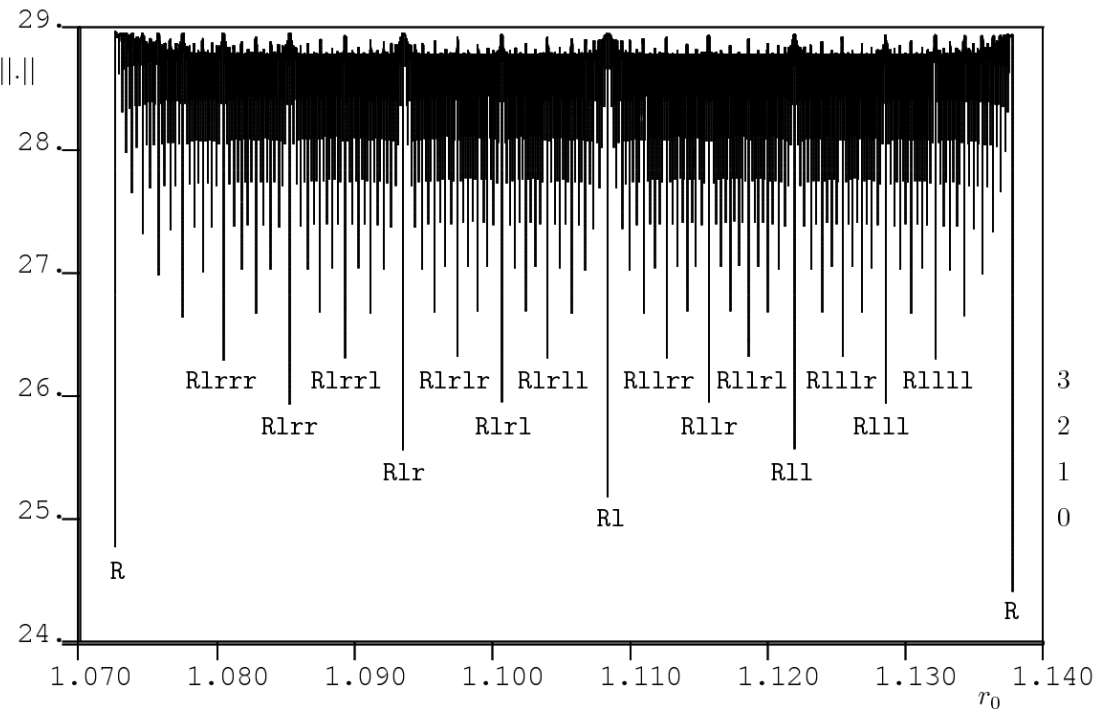
Another heteroclinic connection in the Lorenz equations.



... and another ...



... and another ...



This continuation located 512 connections!

NOTE:

- The heteroclinic connections have a combinatorial structure.
- We can also continue each heteroclinic connection as  $\rho$  varies.
- They spawns homoclinic orbits, having their own combinatorial structure.
- These results shed some light on the Lorenz attractor as  $\rho$  changes.

More details:

E. J. Doedel, B. Krauskopf, H. M. Osinga, Global bifurcations of the Lorenz model, Nonlinearity 19, 2006, 2947-2972.

## Example: The Circular Restricted 3-Body Problem

$$\begin{aligned}x'' &= 2y' + x - \frac{(1-\mu)(x+\mu)}{r_1^3} - \frac{\mu(x-1+\mu)}{r_2^3}, \\y'' &= -2x' + y - \frac{(1-\mu)y}{r_1^3} - \frac{\mu y}{r_2^3}, \\z'' &= -\frac{(1-\mu)z}{r_1^3} - \frac{\mu z}{r_2^3},\end{aligned}$$

where

$$(x, y, z),$$

is the position of the zero-mass body, and

$$r_1 = \sqrt{(x + \mu)^2 + y^2 + z^2}, \quad r_2 = \sqrt{(x - 1 + \mu)^2 + y^2 + z^2}.$$

For the Earth-Moon system  $\mu \approx 0.01215$ .

The CR3BP has one integral of motion, namely, the *Jacobi-constant* :

$$J = \frac{(x')^2 + (y')^2 + (z')^2}{2} - U(x, y, z) - \mu \frac{1-\mu}{2},$$

where

$$U = \frac{1}{2}(x^2 + y^2) + \frac{1-\mu}{r_1} + \frac{\mu}{r_2},$$

and

$$r_1 = \sqrt{(x+\mu)^2 + y^2 + z^2}, \quad r_2 = \sqrt{(x-1+\mu)^2 + y^2 + z^2}.$$

## BOUNDARY VALUE FORMULATION:

$$x' = T v_x ,$$

$$y' = T v_y ,$$

$$z' = T v_z ,$$

$$v'_x = T [ 2v_y + x - (1-\mu)(x+\mu)r_1^{-3} - \mu(x-1+\mu)r_2^{-3} + \lambda v_x ] ,$$

$$v'_y = T [ -2v_x + y - (1-\mu)yr_1^{-3} - \mu yr_2^{-3} + \lambda v_y ] ,$$

$$v'_z = T [ -(1-\mu)zr_1^{-3} - \mu zr_2^{-3} + \lambda v_z ] ,$$

with periodicity boundary conditions

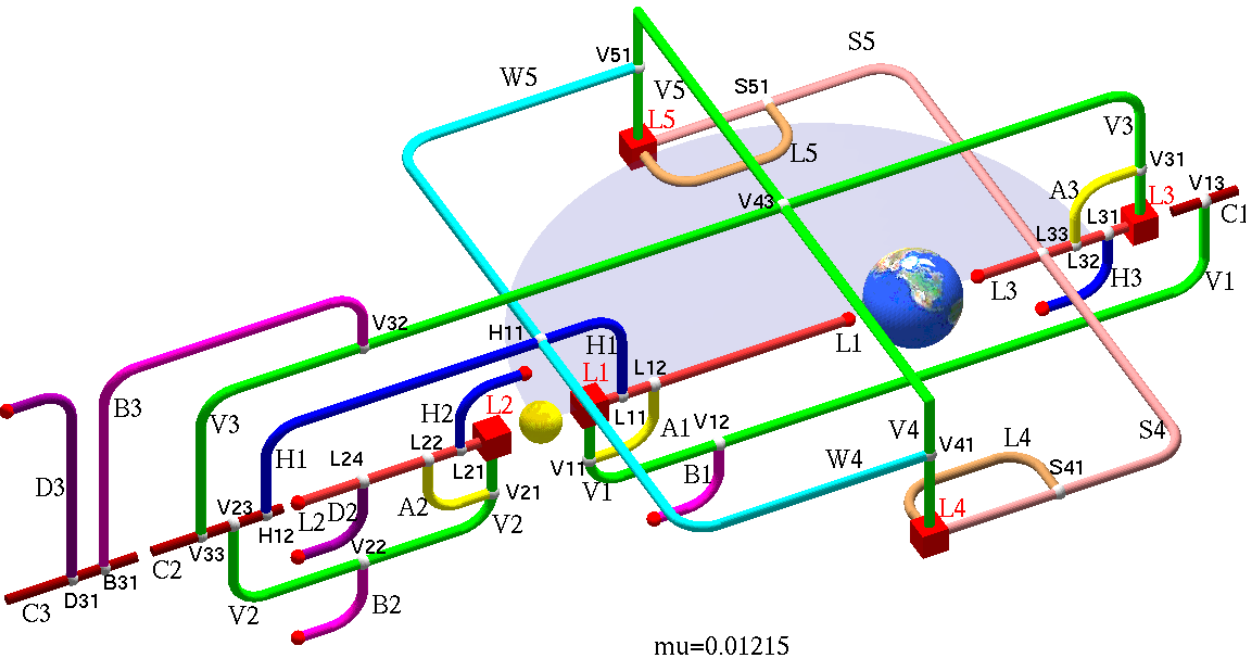
$$x(1) = x(0) , \quad y(1) = y(0) , \quad z(1) = z(0) ,$$

$$v_x(1) = v_x(0) , \quad v_y(1) = v_y(0) , \quad v_z(1) = v_z(0) ,$$

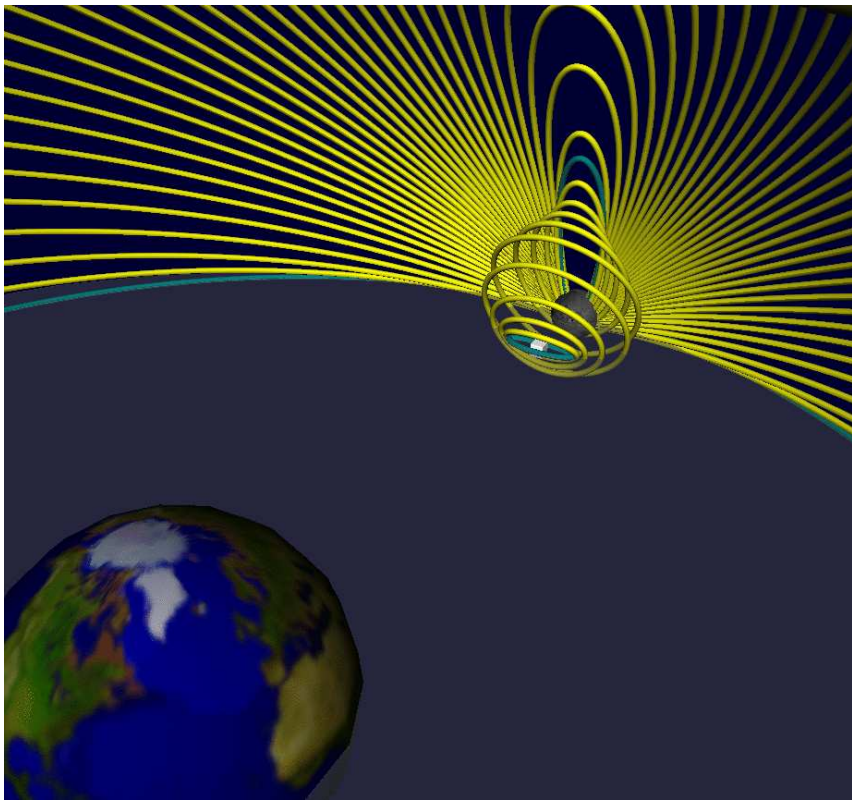
+ phase constraint + continuation equation.

NOTE:

- The “unfolding term”  $\lambda \nabla v$  regularizes the continuation.
- $\lambda$  will be ”zero”, once solved for.
- Other unfolding terms are possible.
- The unfolding term allows using BVP continuation.



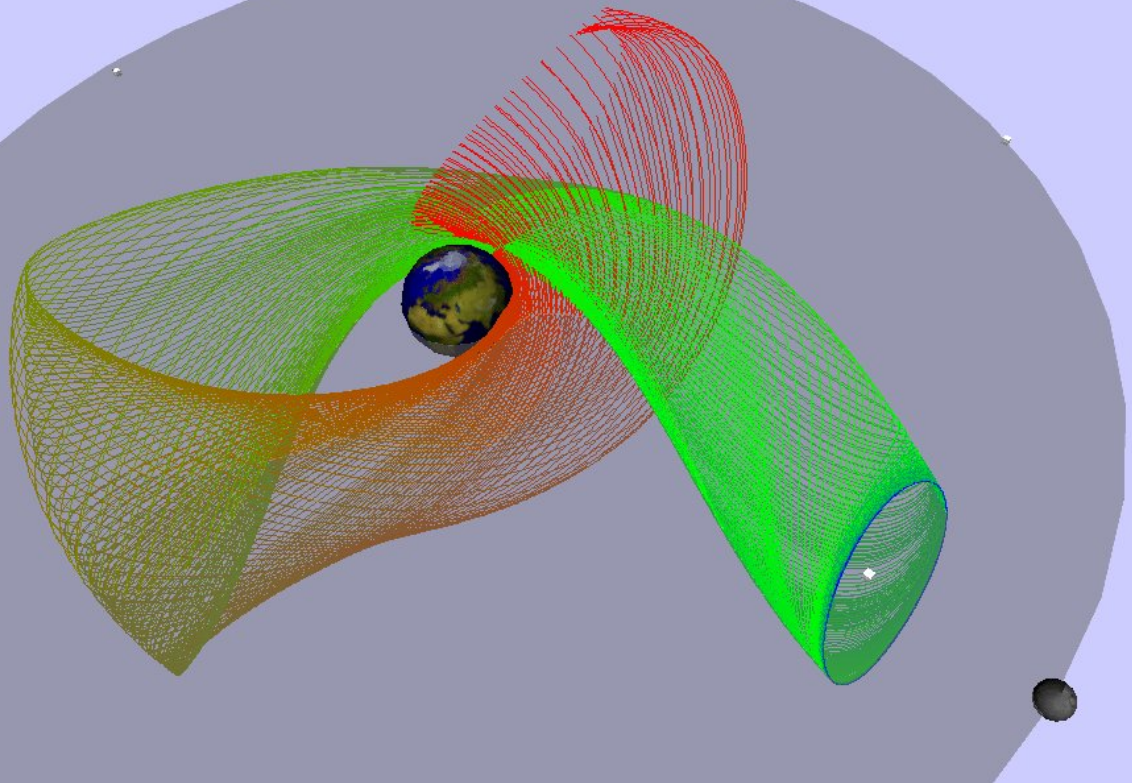
Families of Periodic Solutions of the Earth-Moon system.



A family of Halo orbits.

NOTE:

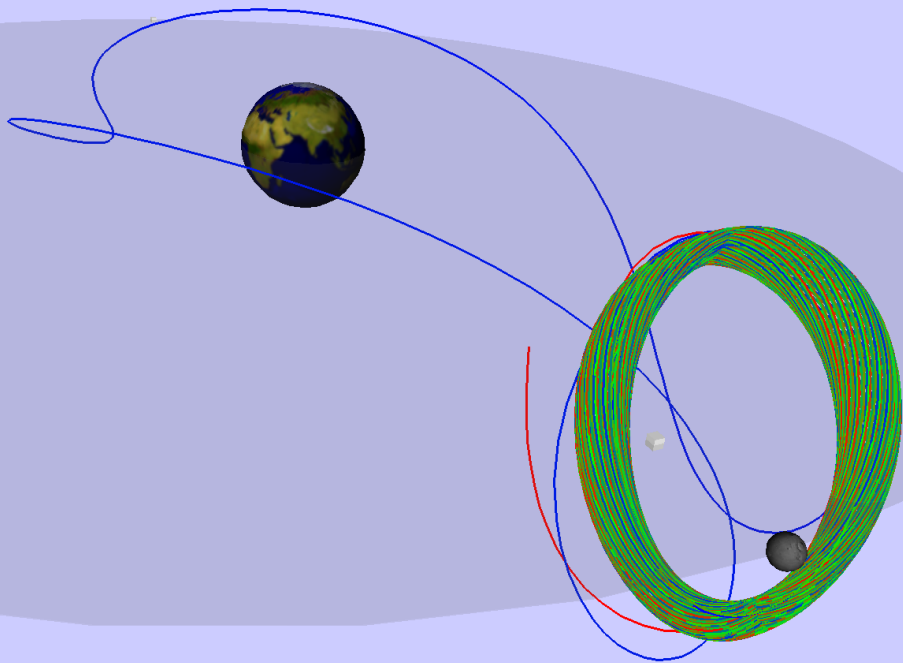
- "Small" Halo orbits have one real Floquet multiplier outside the unit circle.
- Such Halo orbits are *unstable* .
- They have a 2D *unstable manifold* .



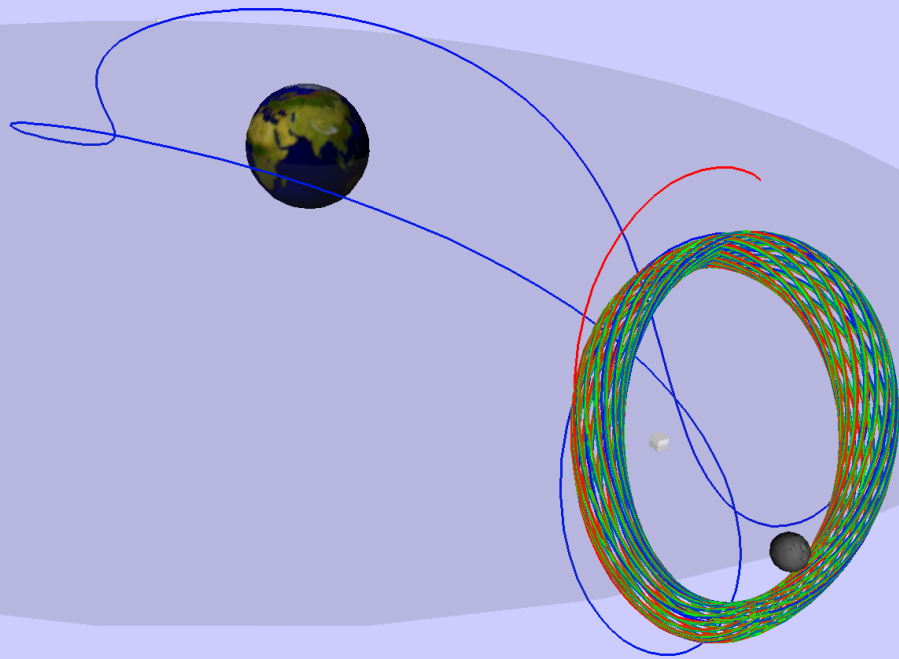
Continuation, keeping the endpoint  $x(1)$  fixed.

NOTE:

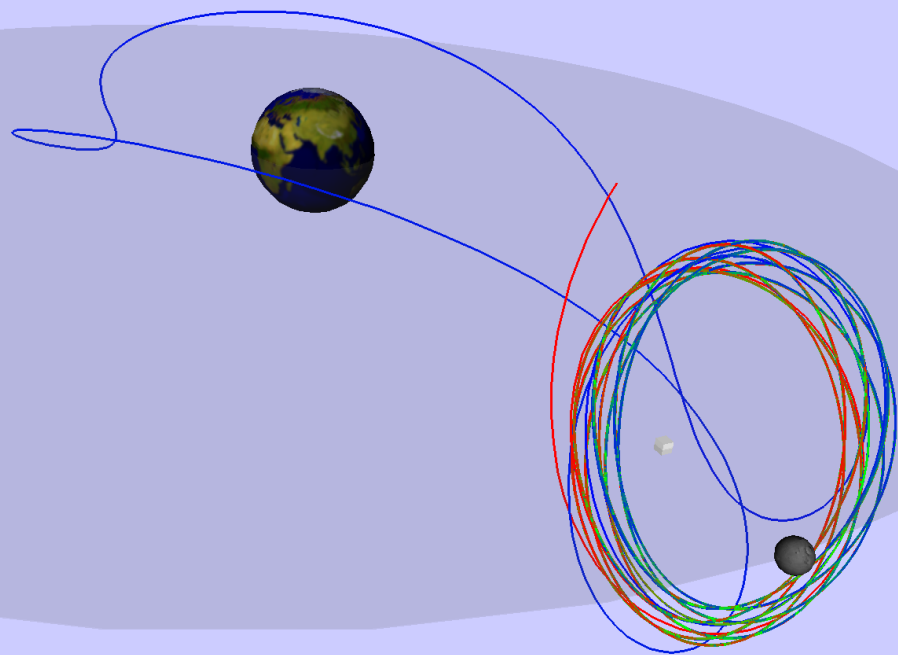
- The unstable manifold can be computed by *continuation* .
- First compute a *starting orbit* in the manifold.
- Then continue the orbit keeping, for example,  $x(1)$  *fixed* .



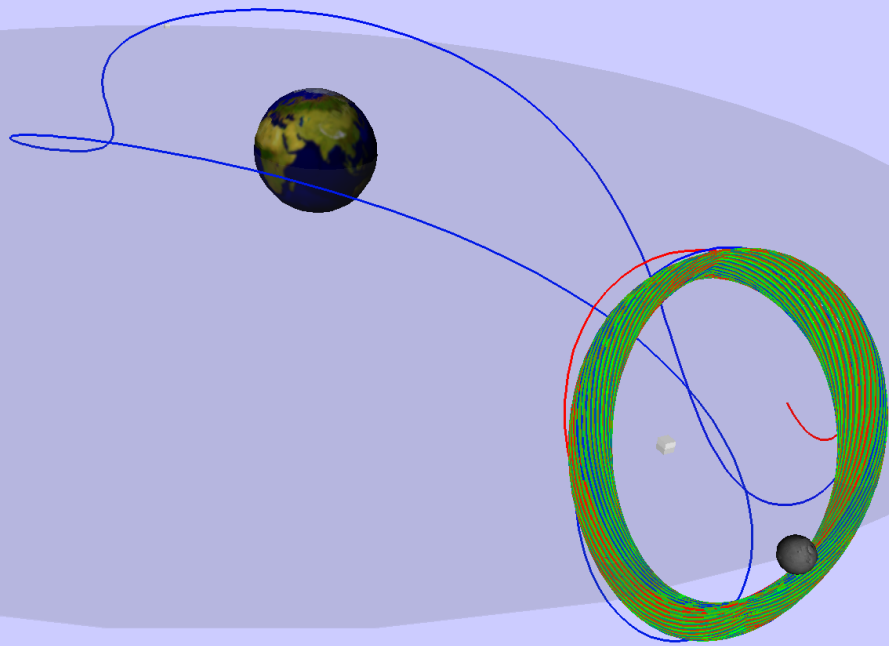
NEW1:Continuation, keeping the endpoint  $x(1)$  fixed.



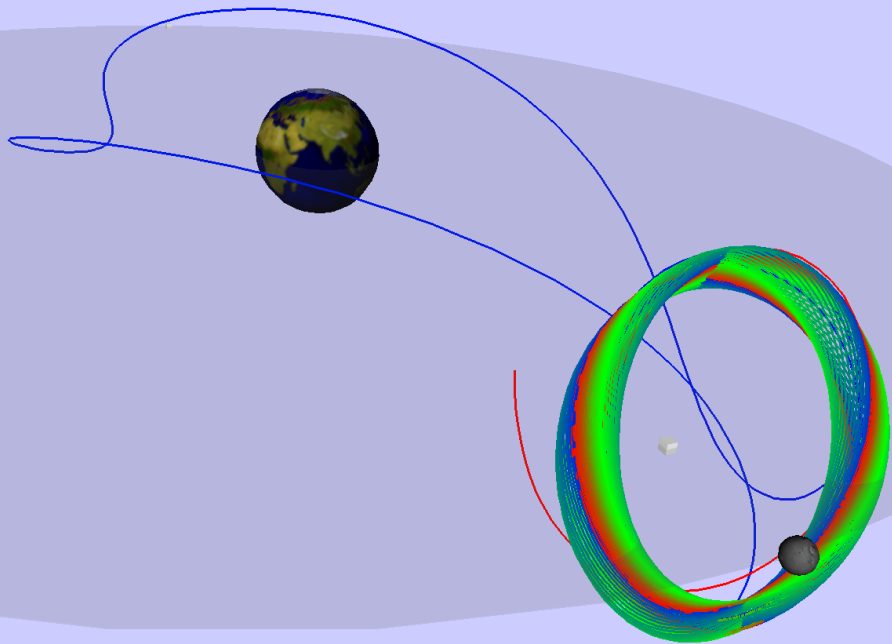
NEW1:Continuation, keeping the endpoint  $x(1)$  fixed.



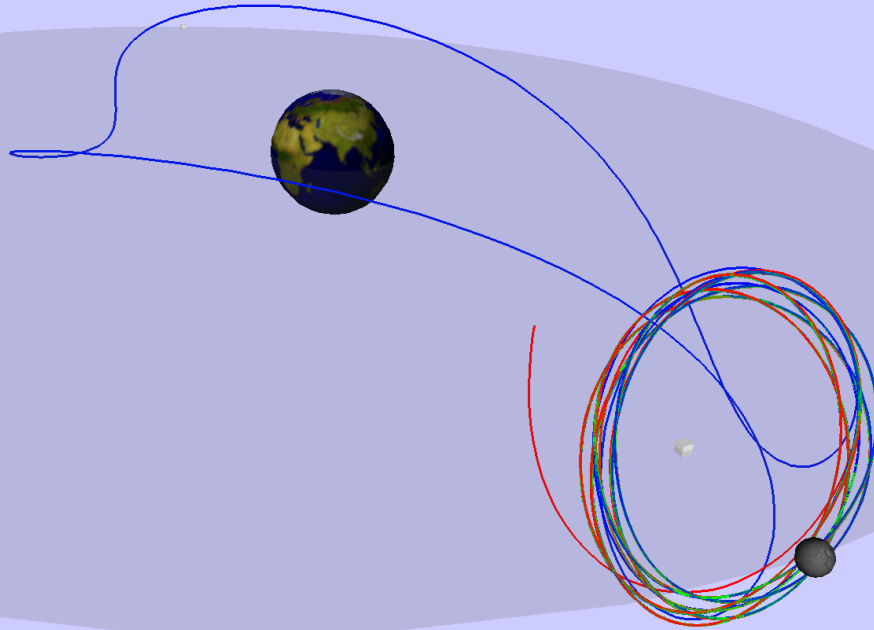
NEW1:Continuation, keeping the endpoint  $x(1)$  fixed.



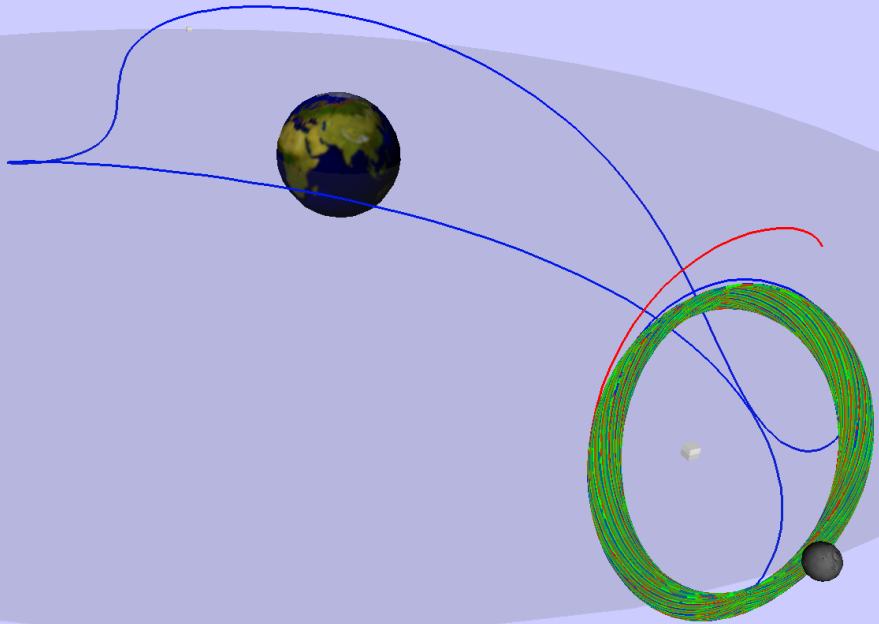
NEW1:Continuation, keeping the endpoint  $x(1)$  fixed.



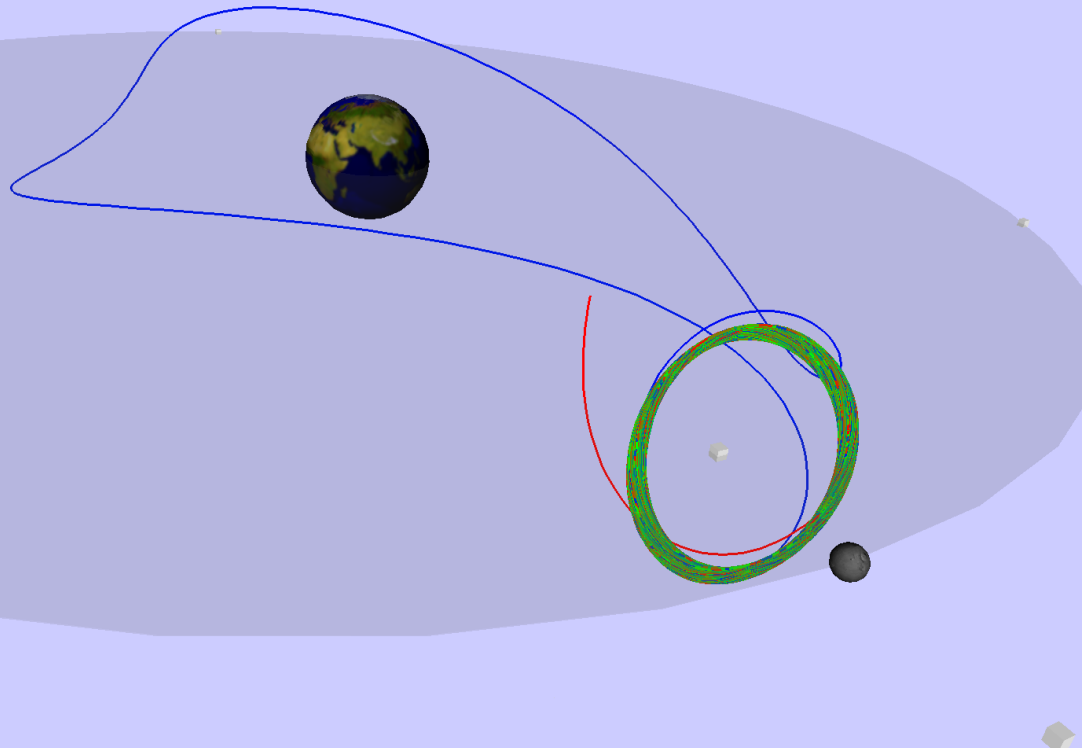
NEW1:Continuation, keeping the endpoint  $x(1)$  fixed.



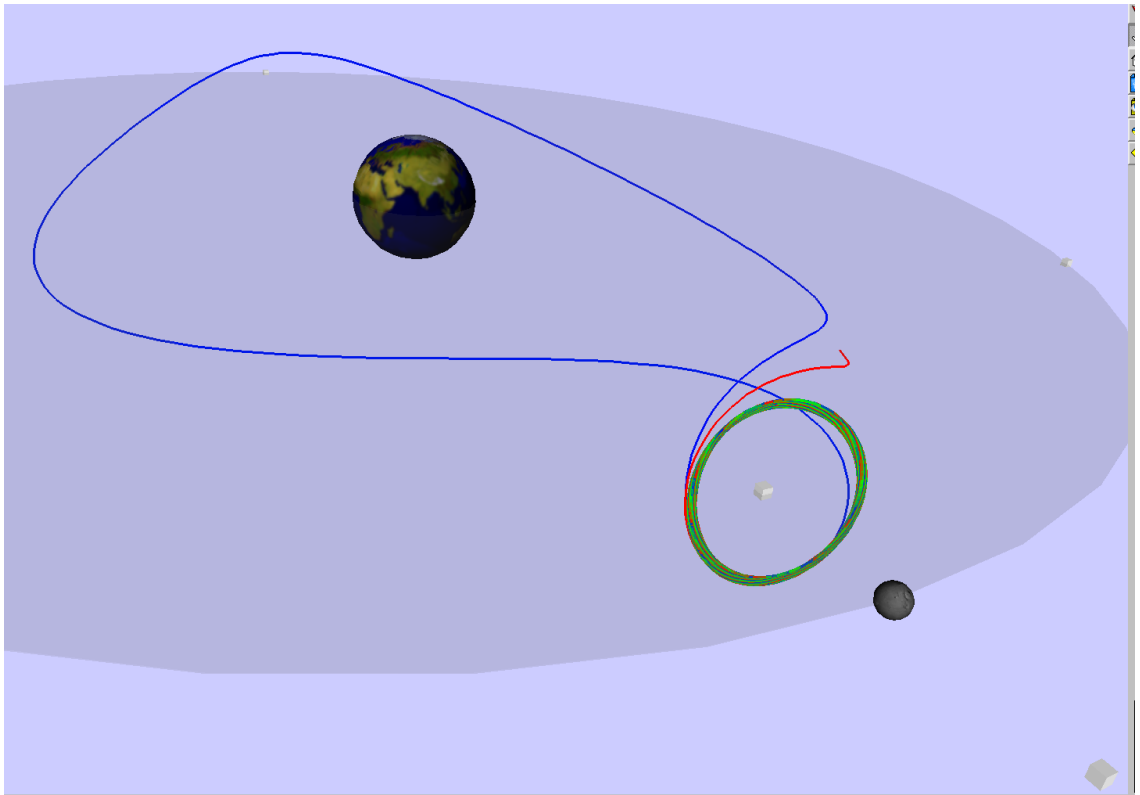
NEW1:Continuation, keeping the endpoint  $x(1)$  fixed.



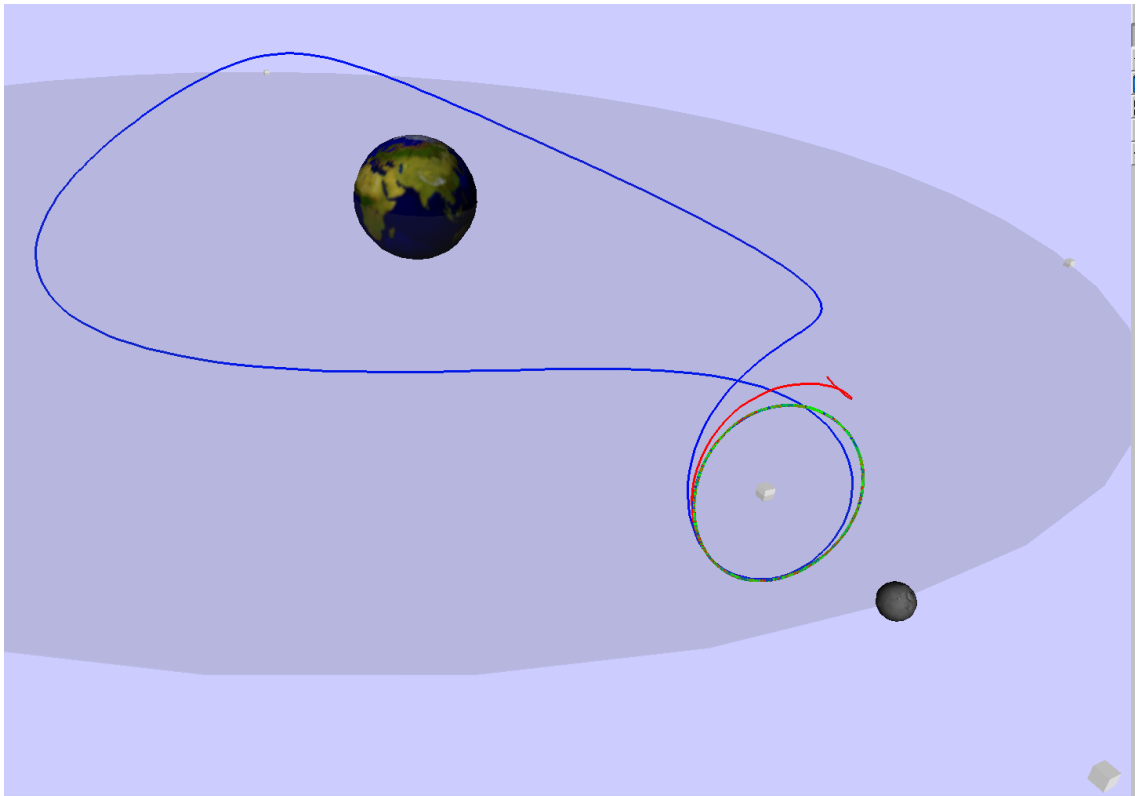
NEW1:Continuation, keeping the endpoint  $x(1)$  fixed.



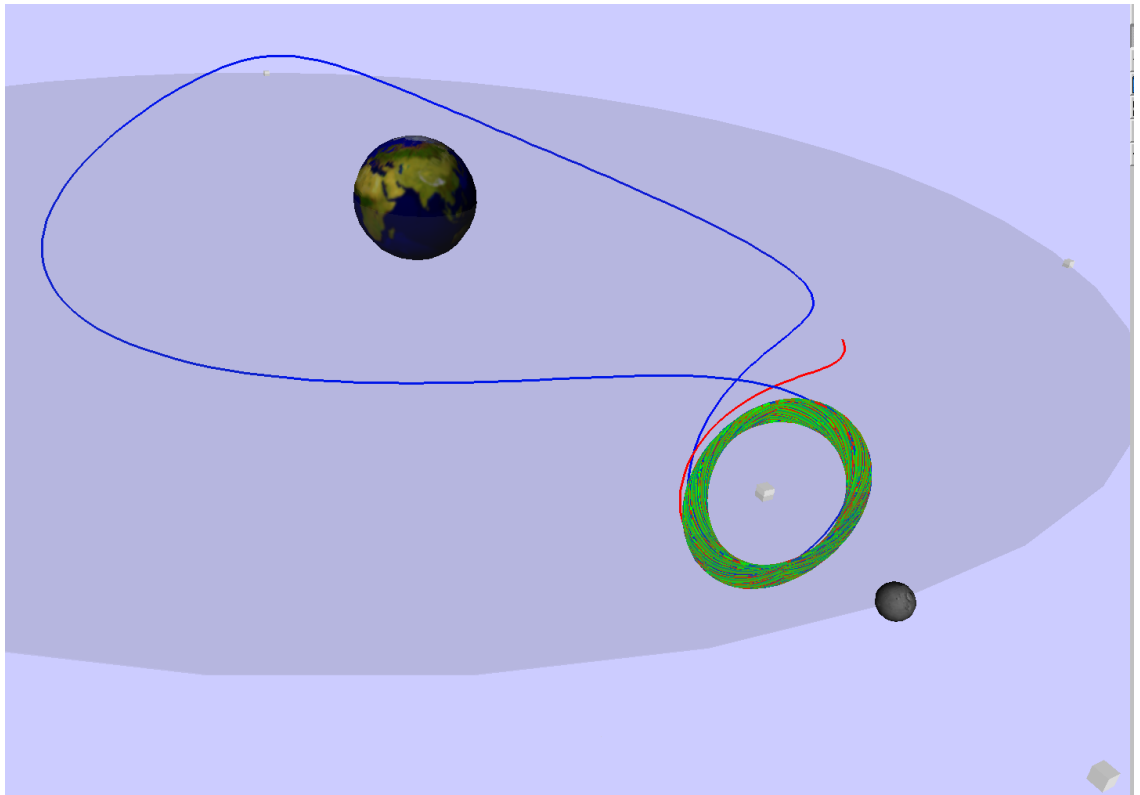
NEW1:Continuation, keeping the endpoint  $x(1)$  fixed.



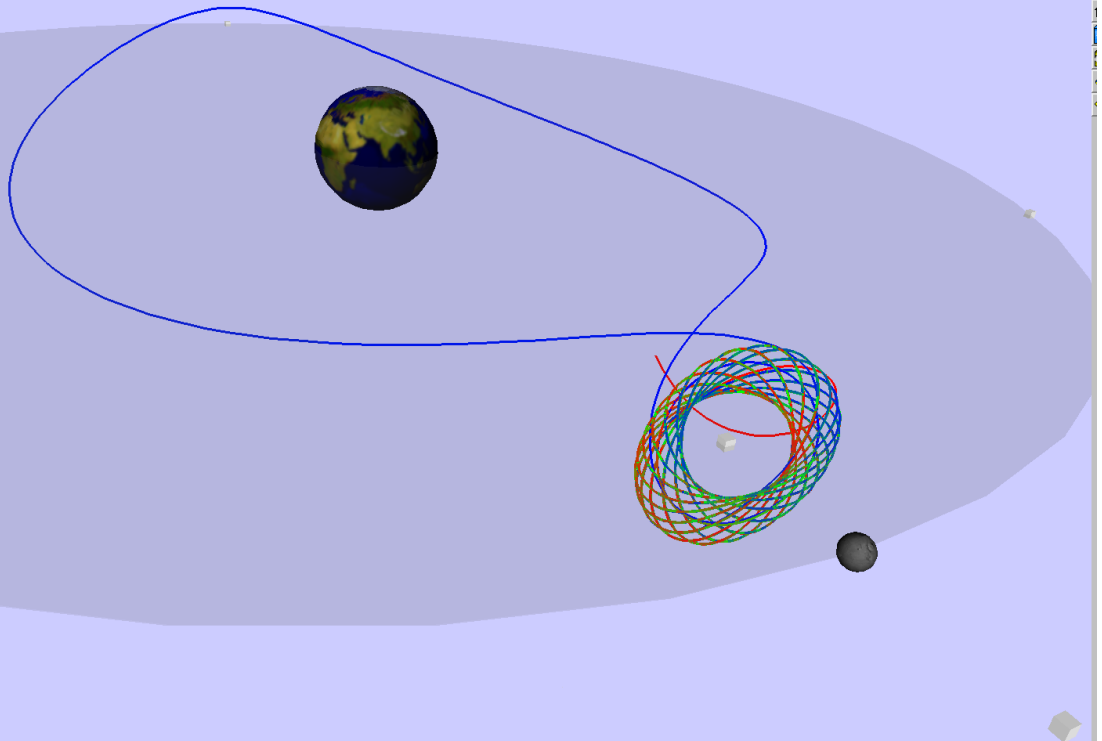
NEW1:Continuation, keeping the endpoint  $x(1)$  fixed.



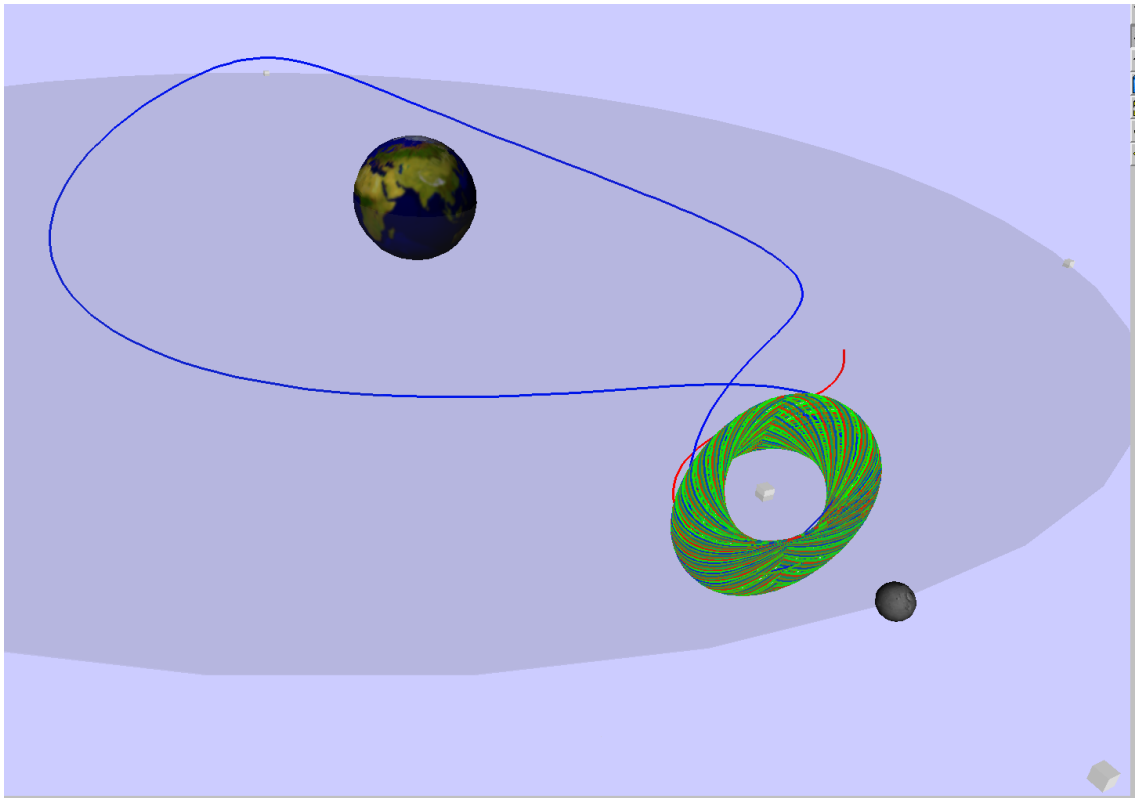
NEW1:Continuation, keeping the endpoint  $x(1)$  fixed.



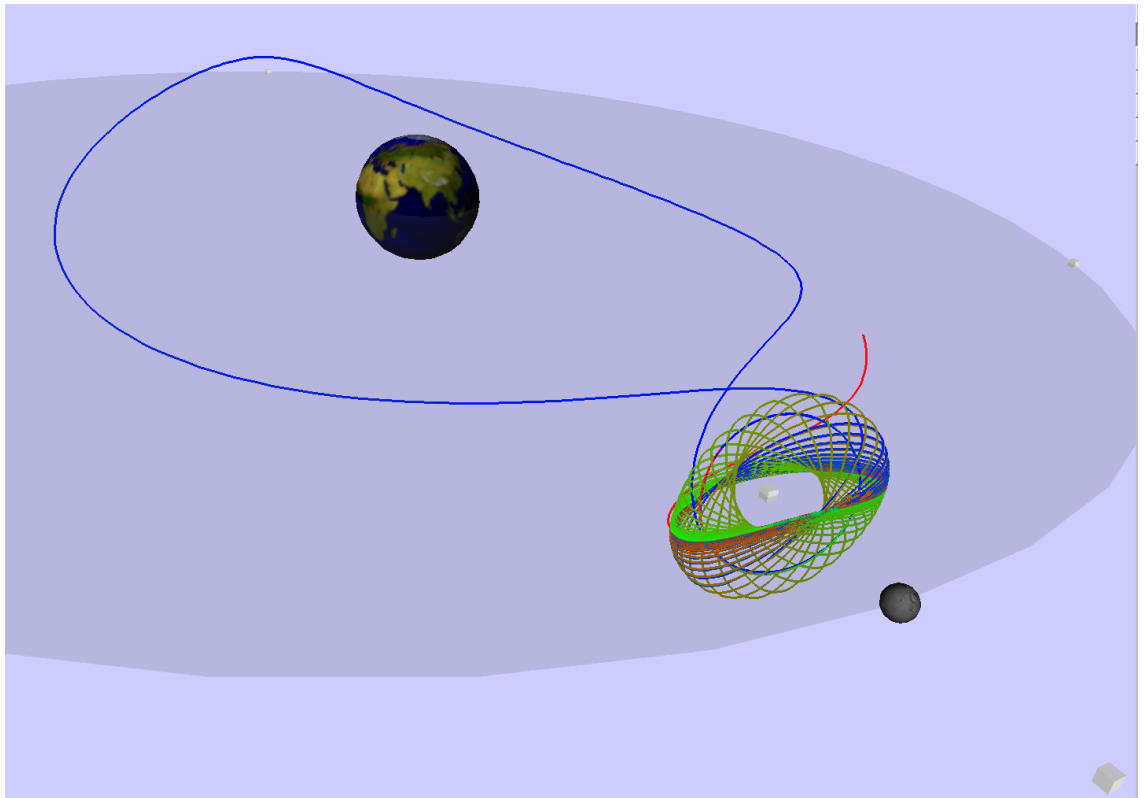
NEW1:Continuation, keeping the endpoint  $x(1)$  fixed.



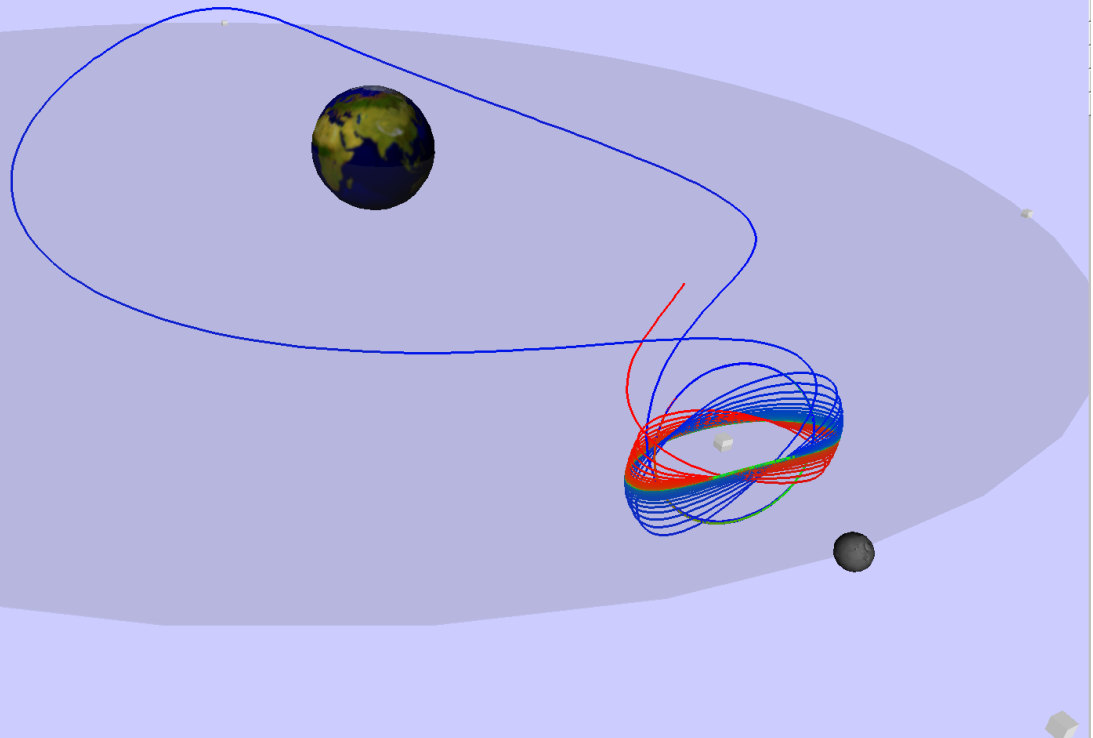
NEW1:Continuation, keeping the endpoint  $x(1)$  fixed.



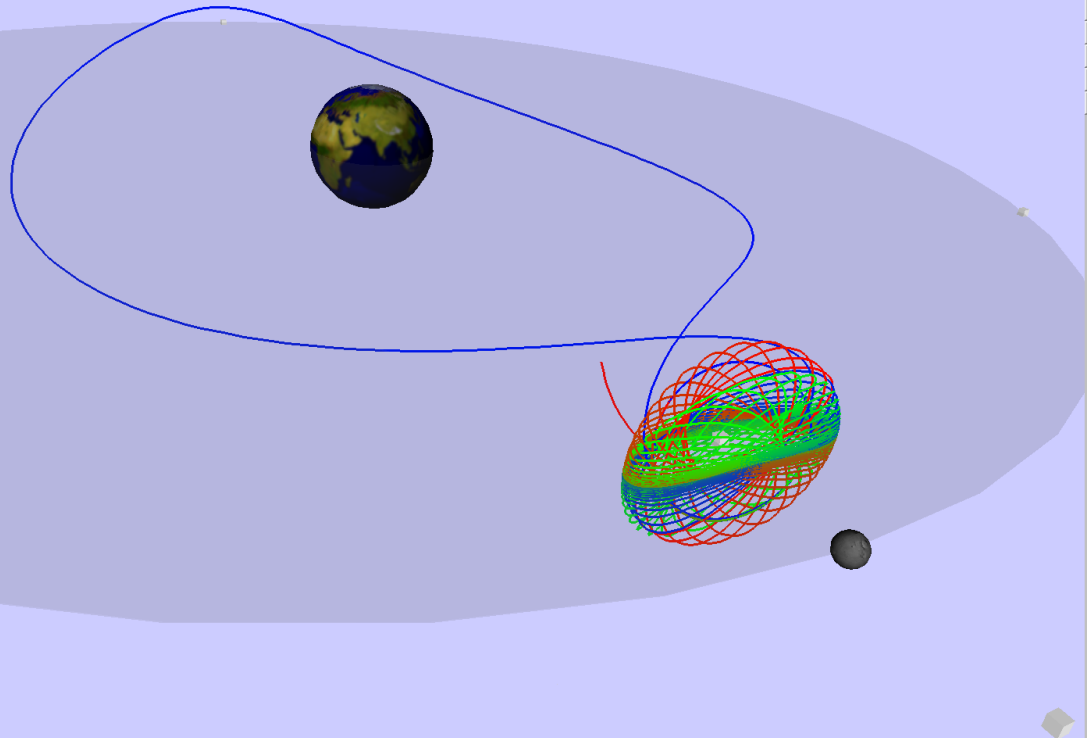
NEW1:Continuation, keeping the endpoint  $x(1)$  fixed.



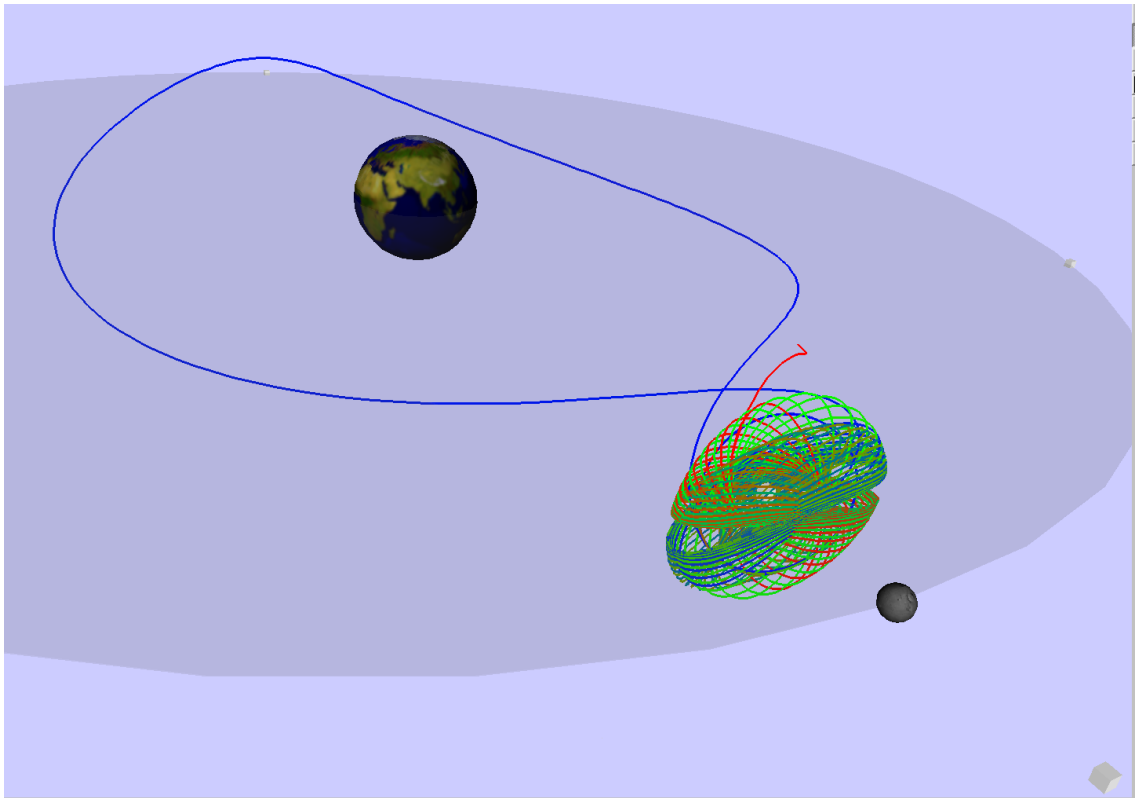
NEW1:Continuation, keeping the endpoint  $x(1)$  fixed.



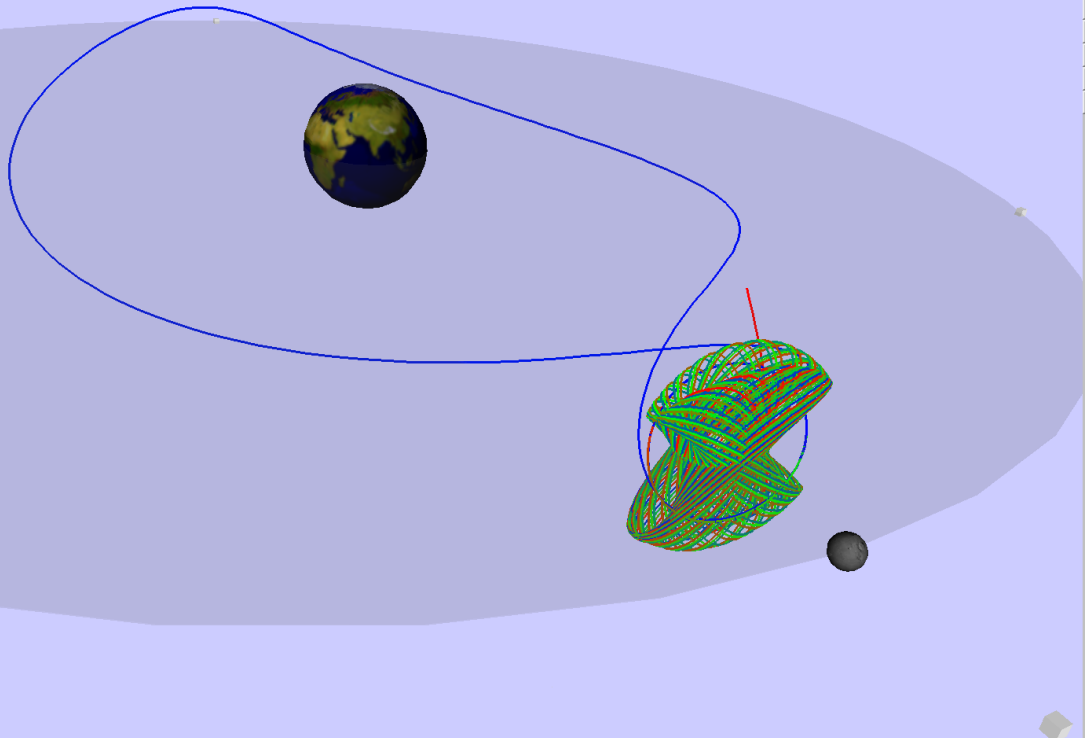
NEW1:Continuation, keeping the endpoint  $x(1)$  fixed.



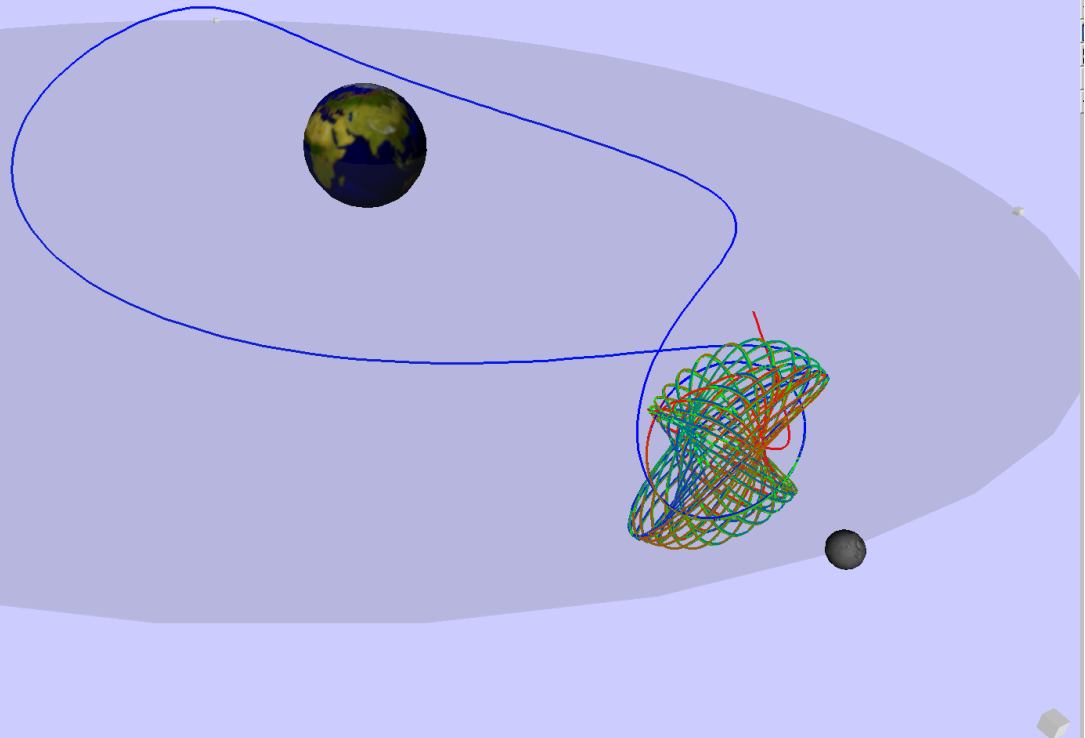
NEW1:Continuation, keeping the endpoint  $x(1)$  fixed.



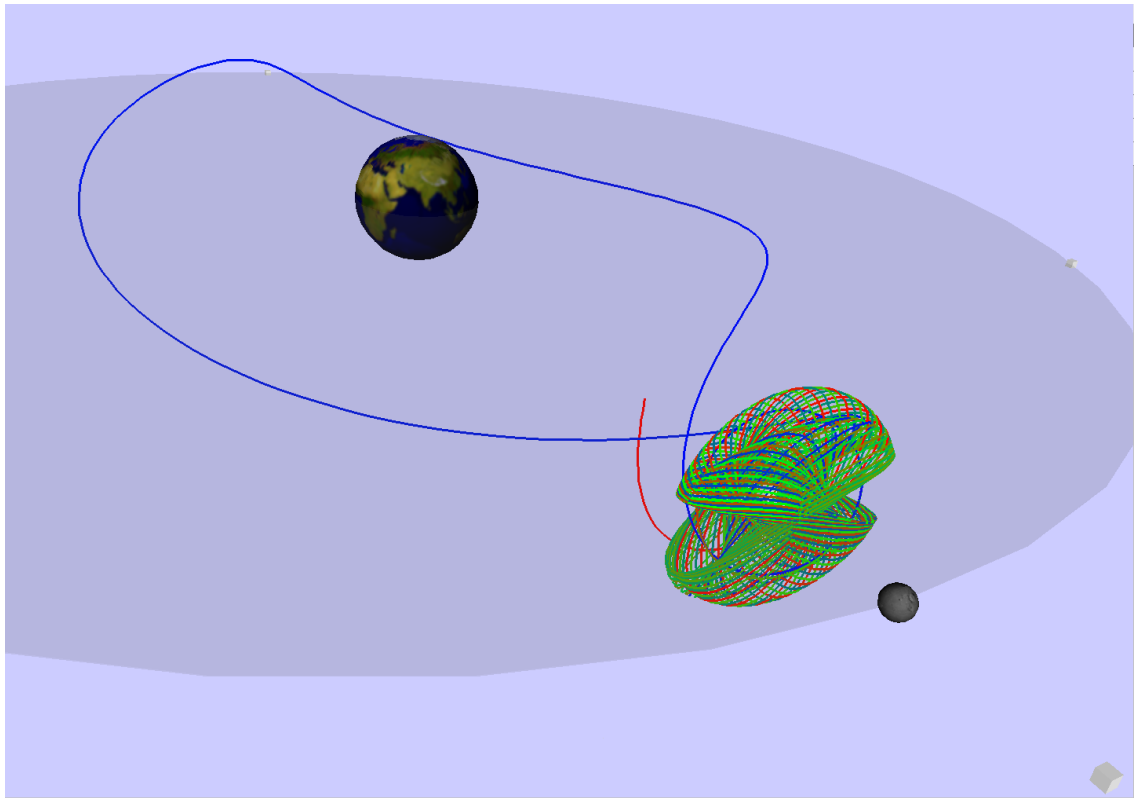
NEW1:Continuation, keeping the endpoint  $x(1)$  fixed.



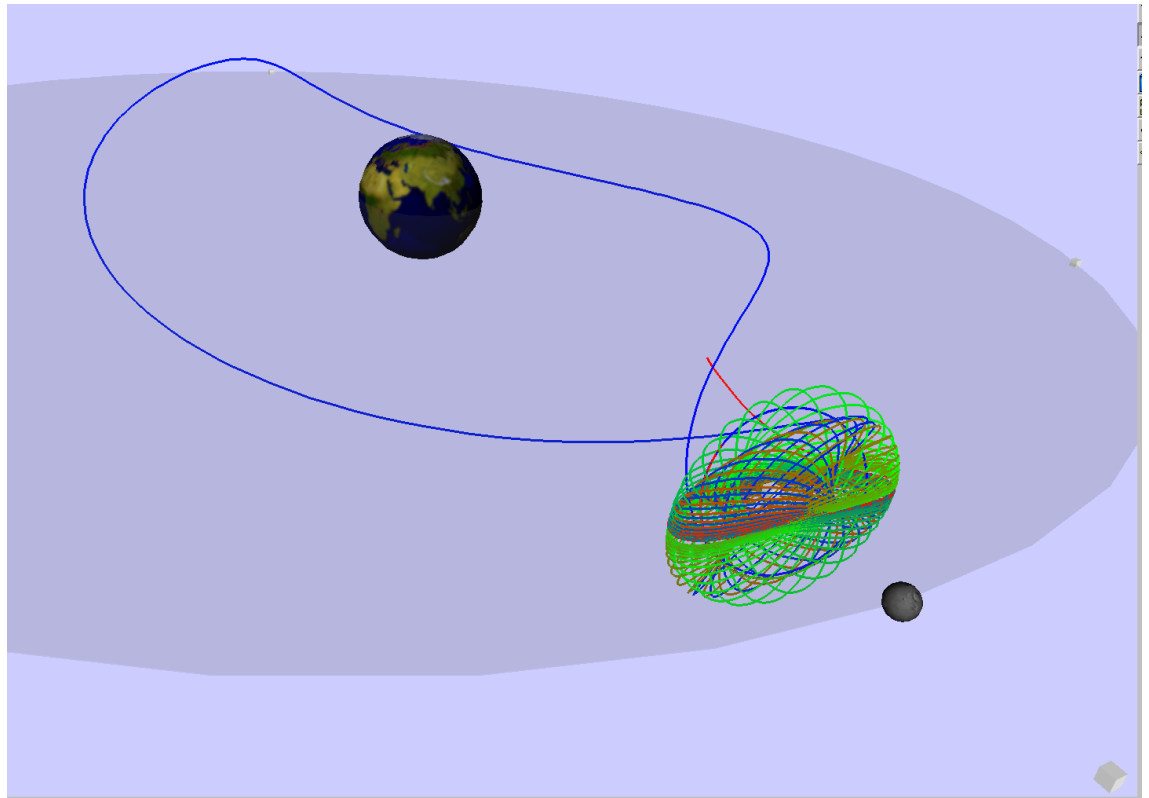
NEW1:Continuation, keeping the endpoint  $x(1)$  fixed.



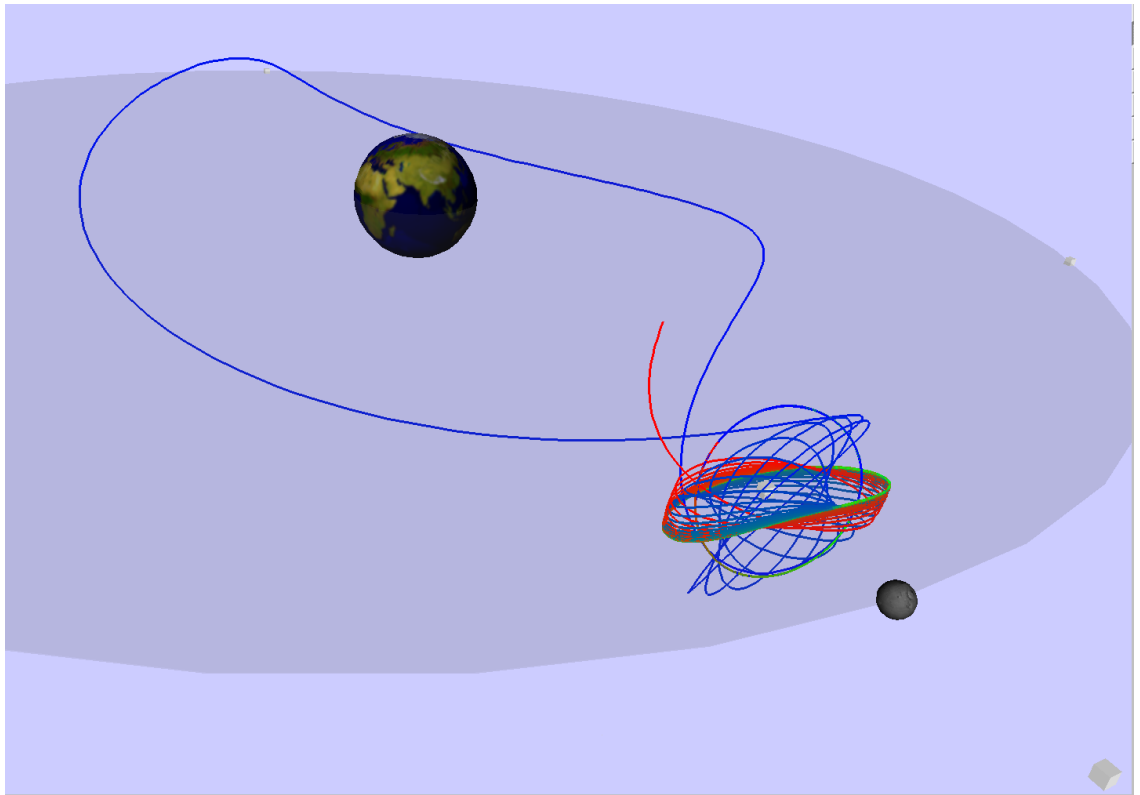
NEW1:Continuation, keeping the endpoint  $x(1)$  fixed.



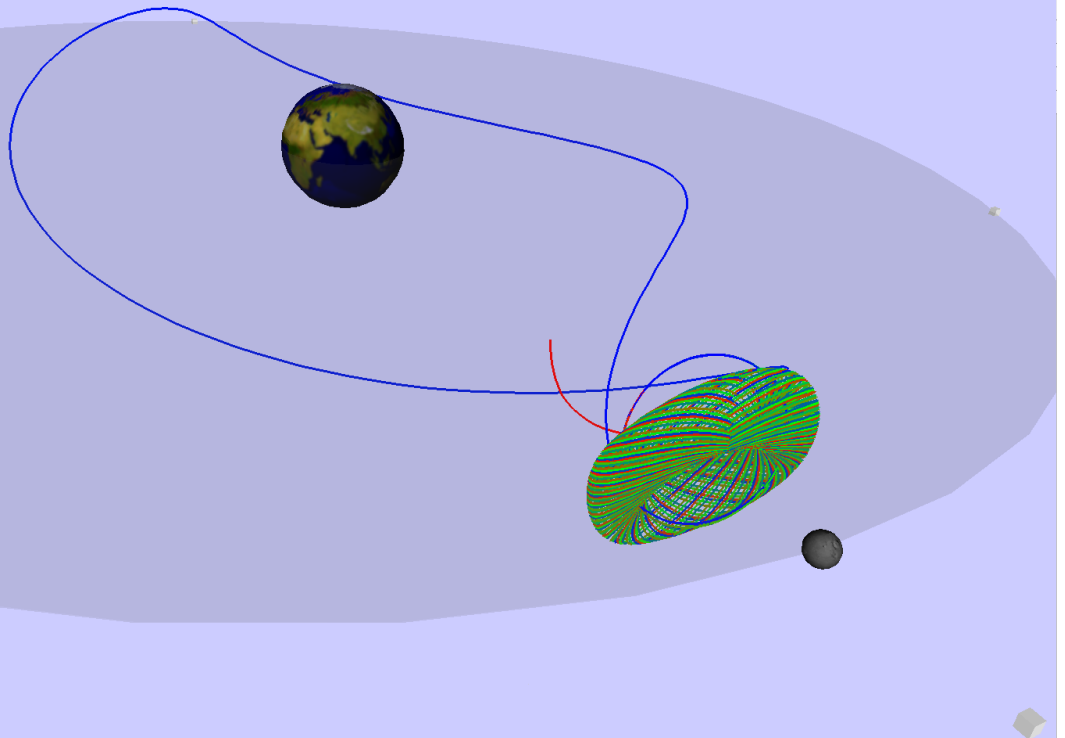
NEW1:Continuation, keeping the endpoint  $x(1)$  fixed.



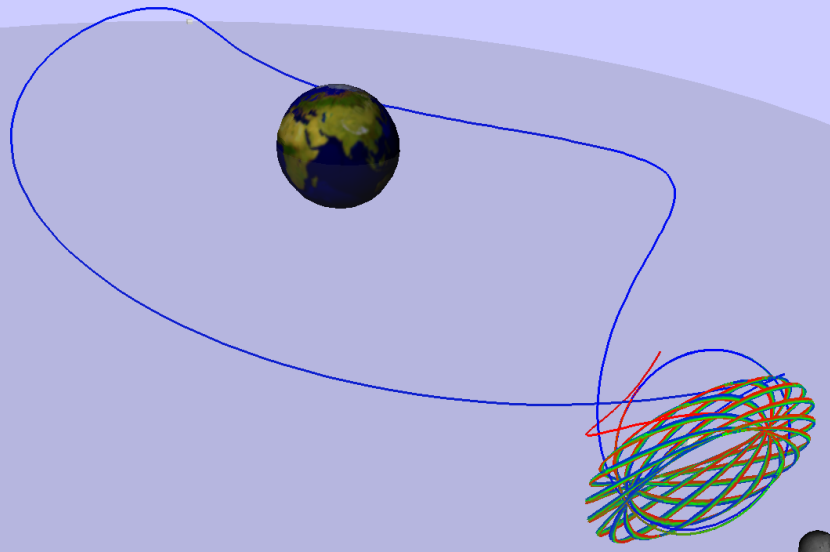
NEW1:Continuation, keeping the endpoint  $x(1)$  fixed.



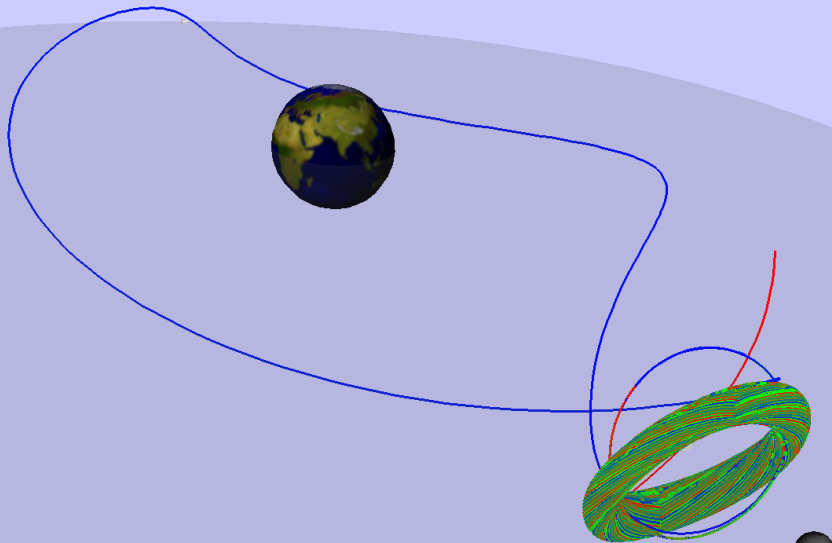
NEW1:Continuation, keeping the endpoint  $x(1)$  fixed.



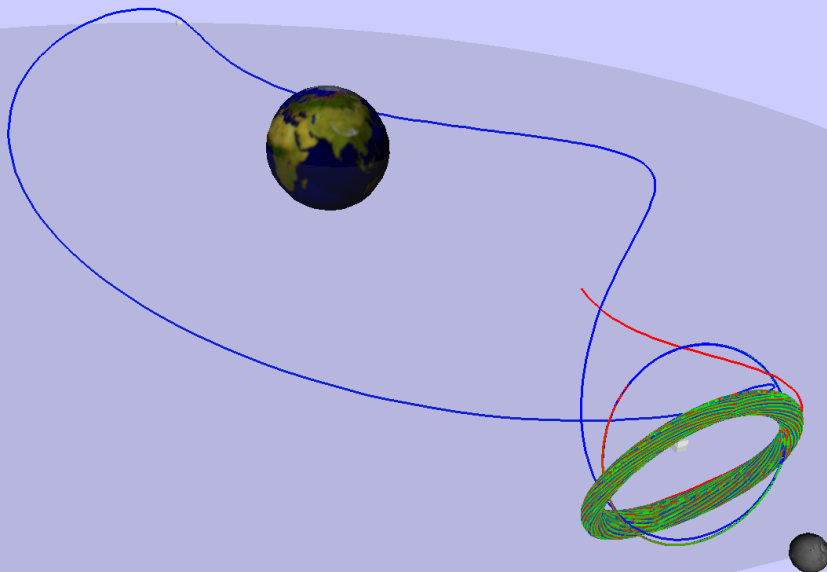
NEW1:Continuation, keeping the endpoint  $x(1)$  fixed.



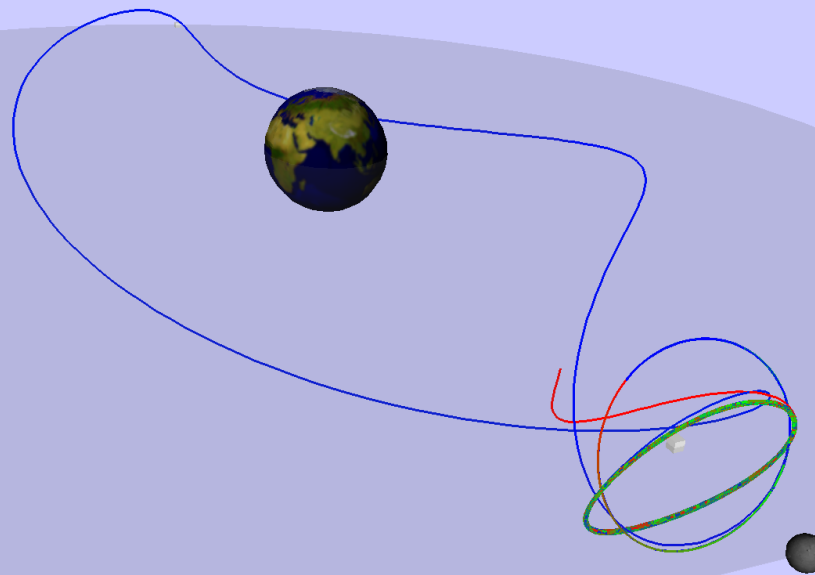
NEW1:Continuation, keeping the endpoint  $x(1)$  fixed.



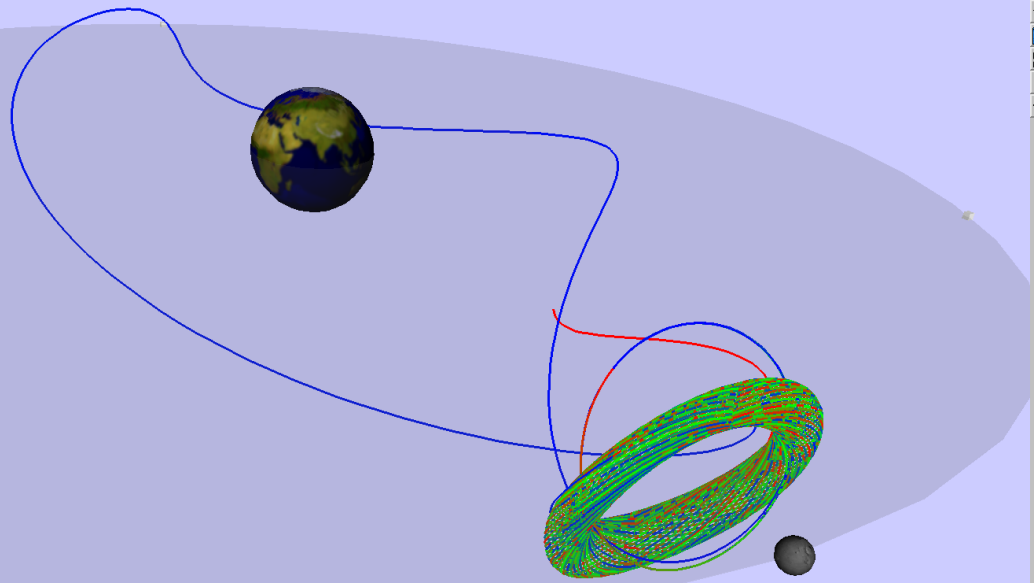
NEW1:Continuation, keeping the endpoint  $x(1)$  fixed.



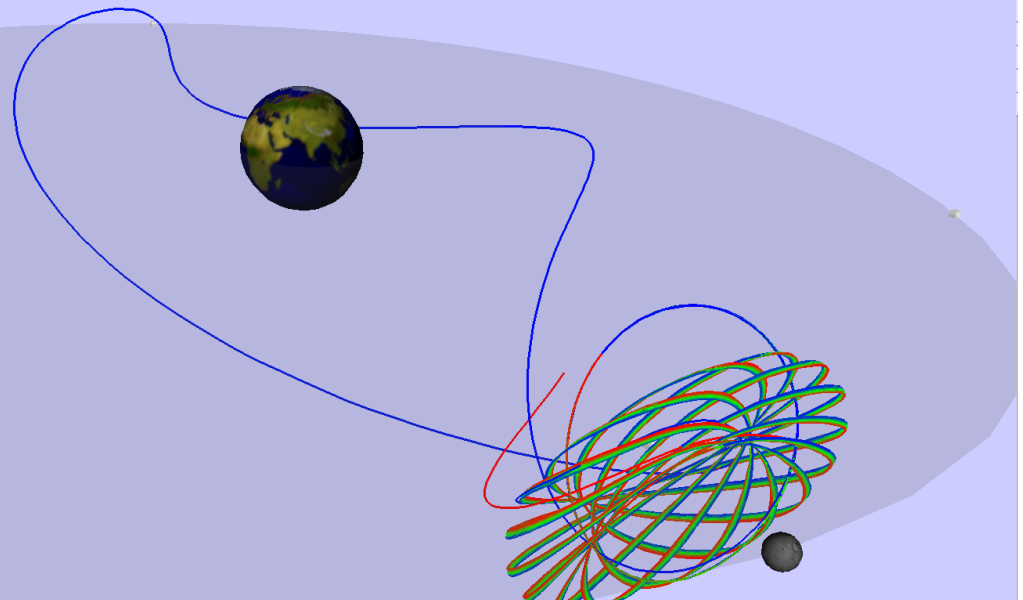
NEW1:Continuation, keeping the endpoint  $x(1)$  fixed.



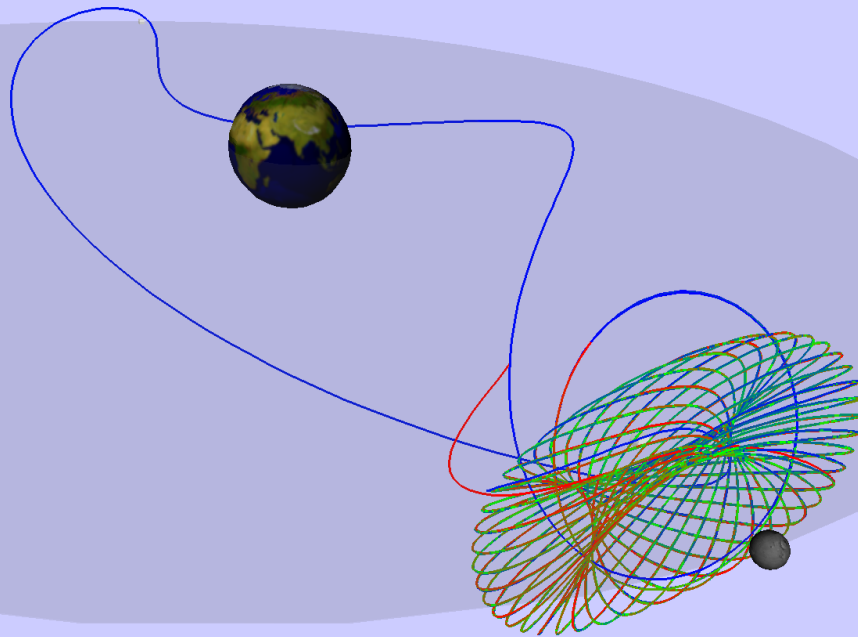
NEW1:Continuation, keeping the endpoint  $x(1)$  fixed.



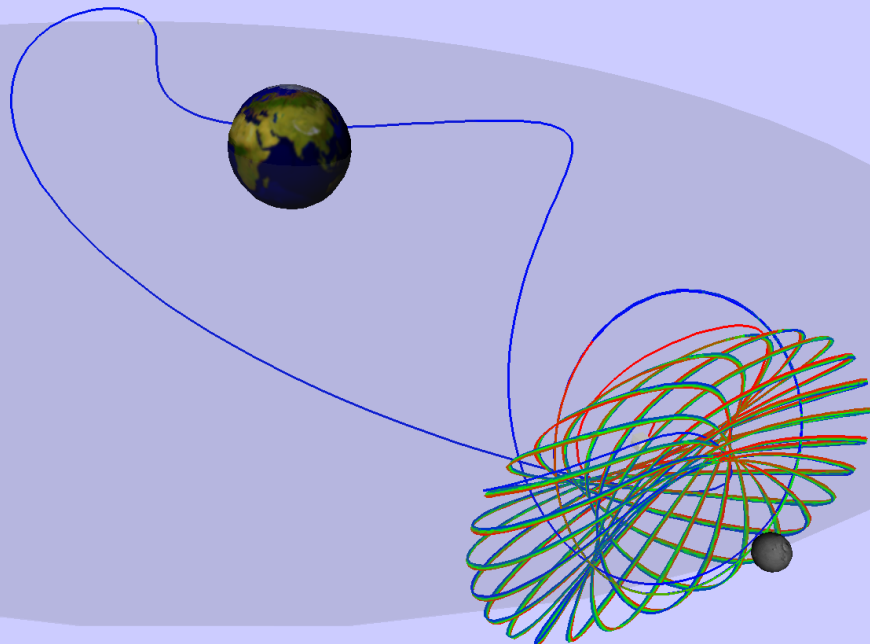
NEW1:Continuation, keeping the endpoint  $x(1)$  fixed.



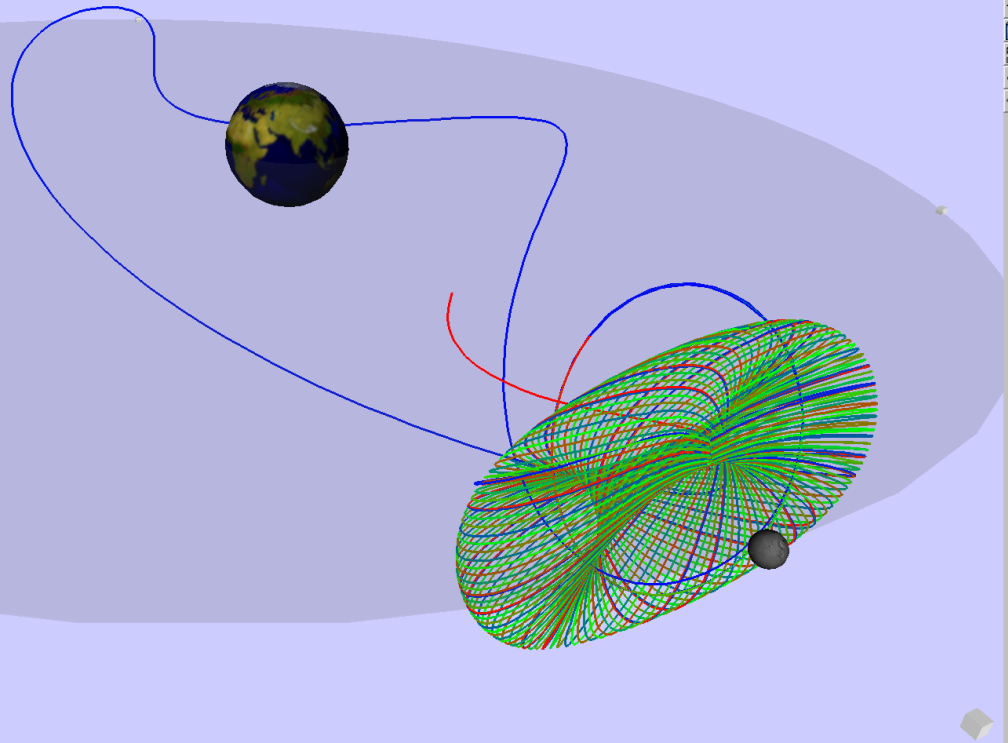
NEW1:Continuation, keeping the endpoint  $x(1)$  fixed.



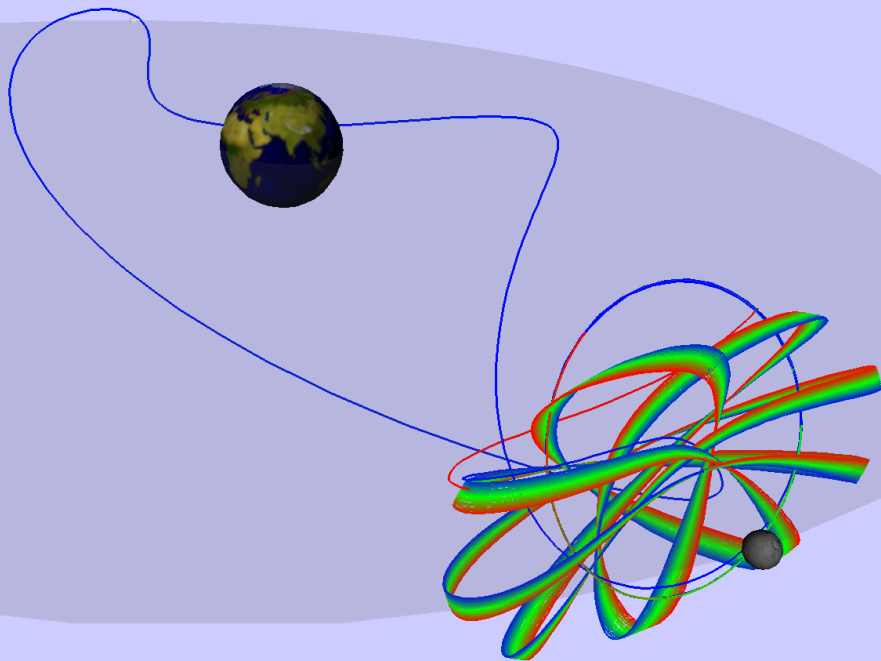
NEW1:Continuation, keeping the endpoint  $x(1)$  fixed.



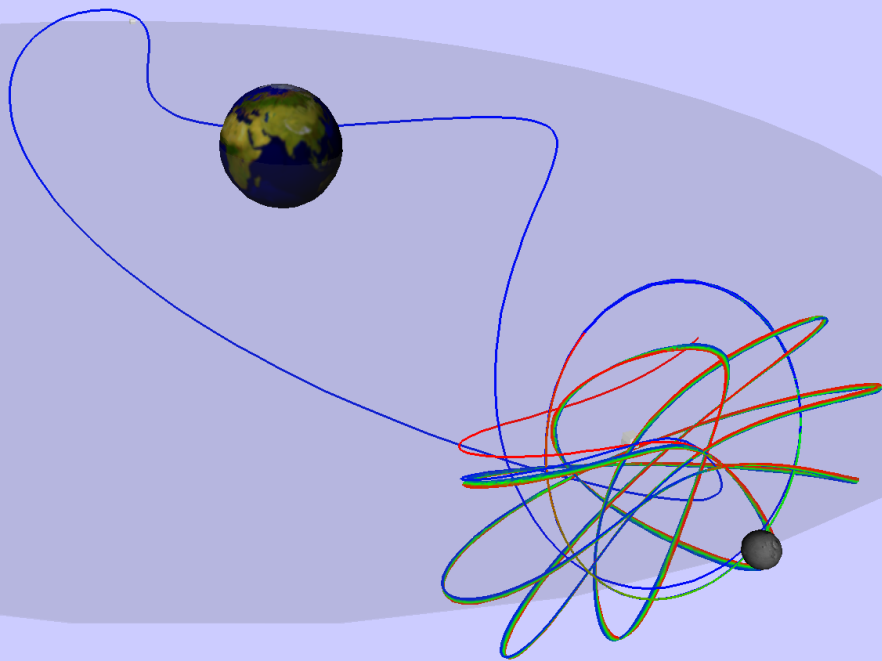
NEW1:Continuation, keeping the endpoint  $x(1)$  fixed.



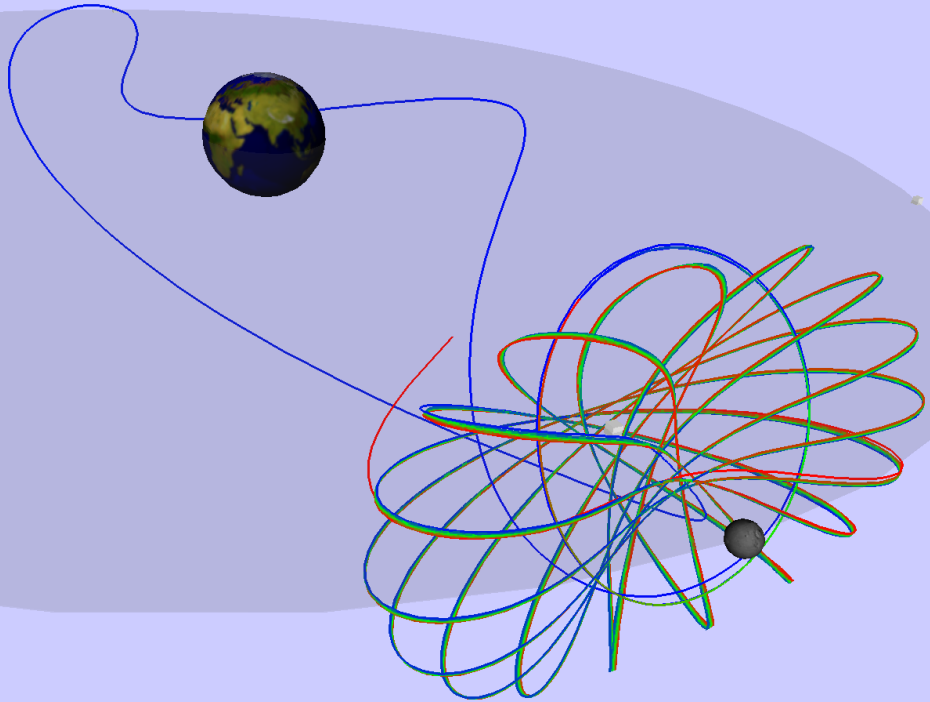
NEW1:Continuation, keeping the endpoint  $x(1)$  fixed.



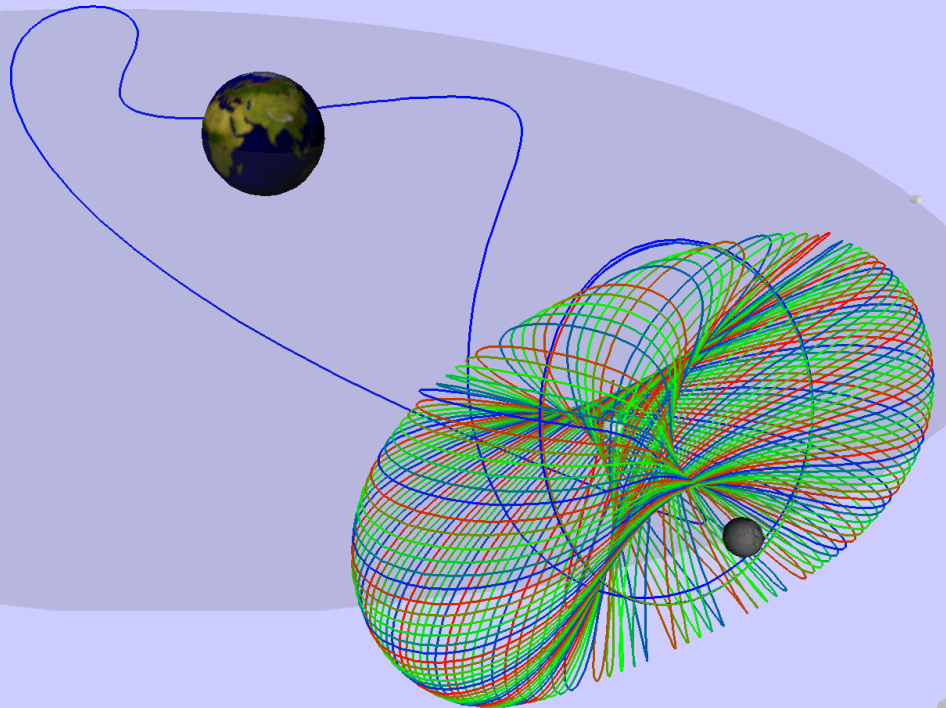
NEW1:Continuation, keeping the endpoint  $x(1)$  fixed.



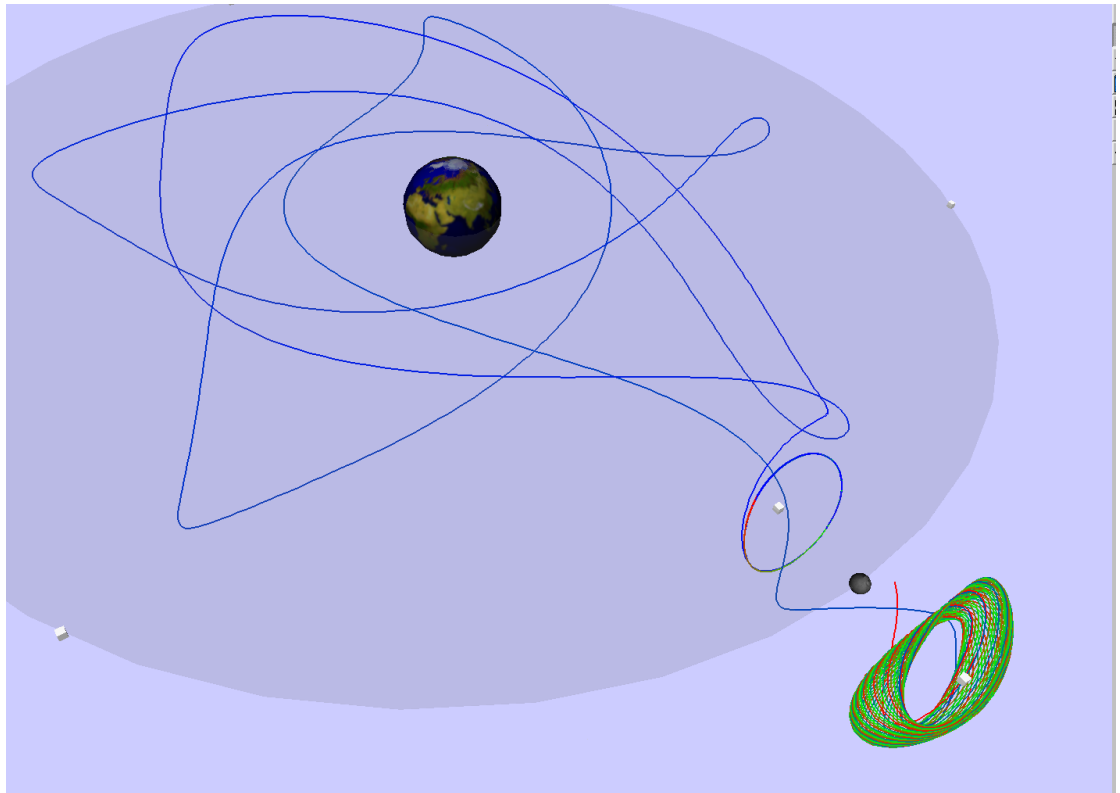
NEW1:Continuation, keeping the endpoint  $x(1)$  fixed.



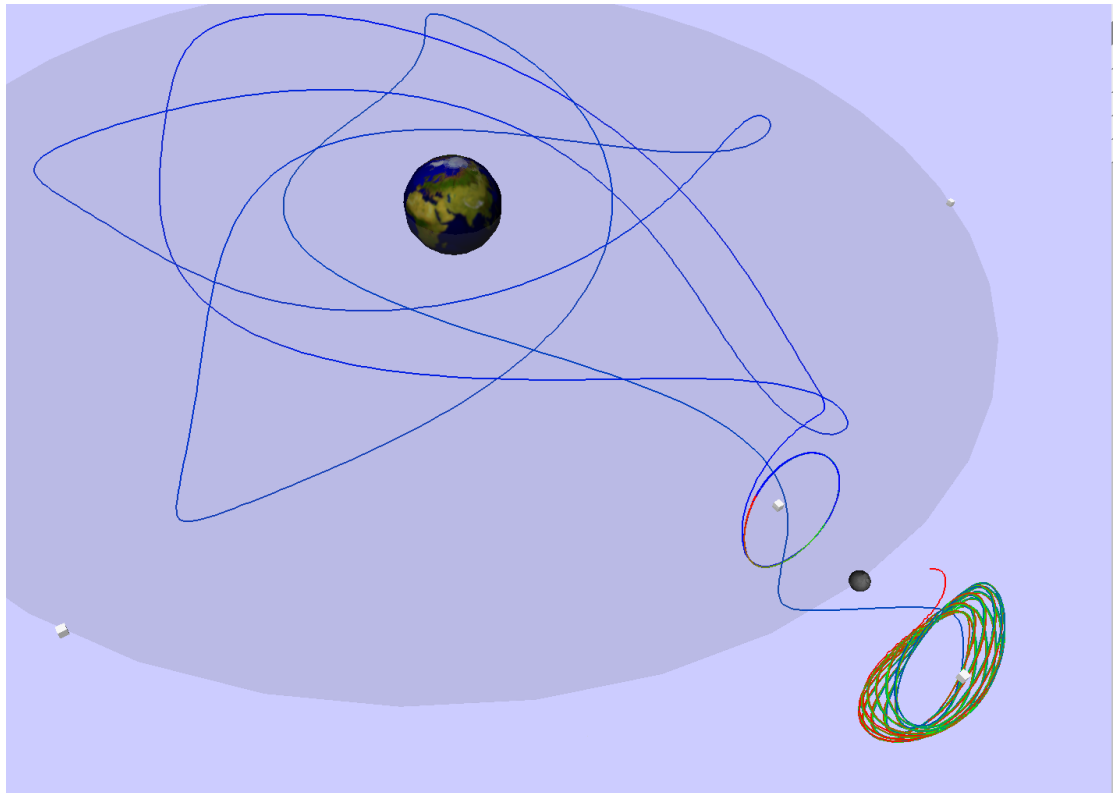
NEW1:Continuation, keeping the endpoint  $x(1)$  fixed.



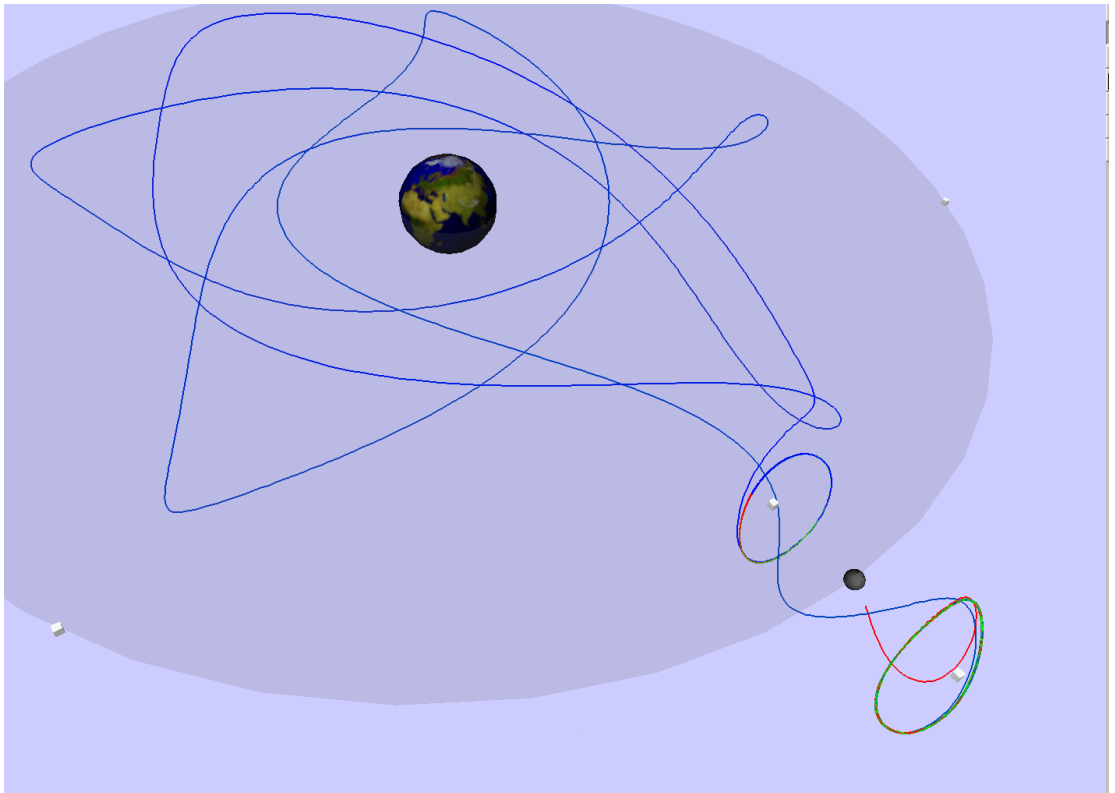
NEW1:Continuation, keeping the endpoint  $x(1)$  fixed.



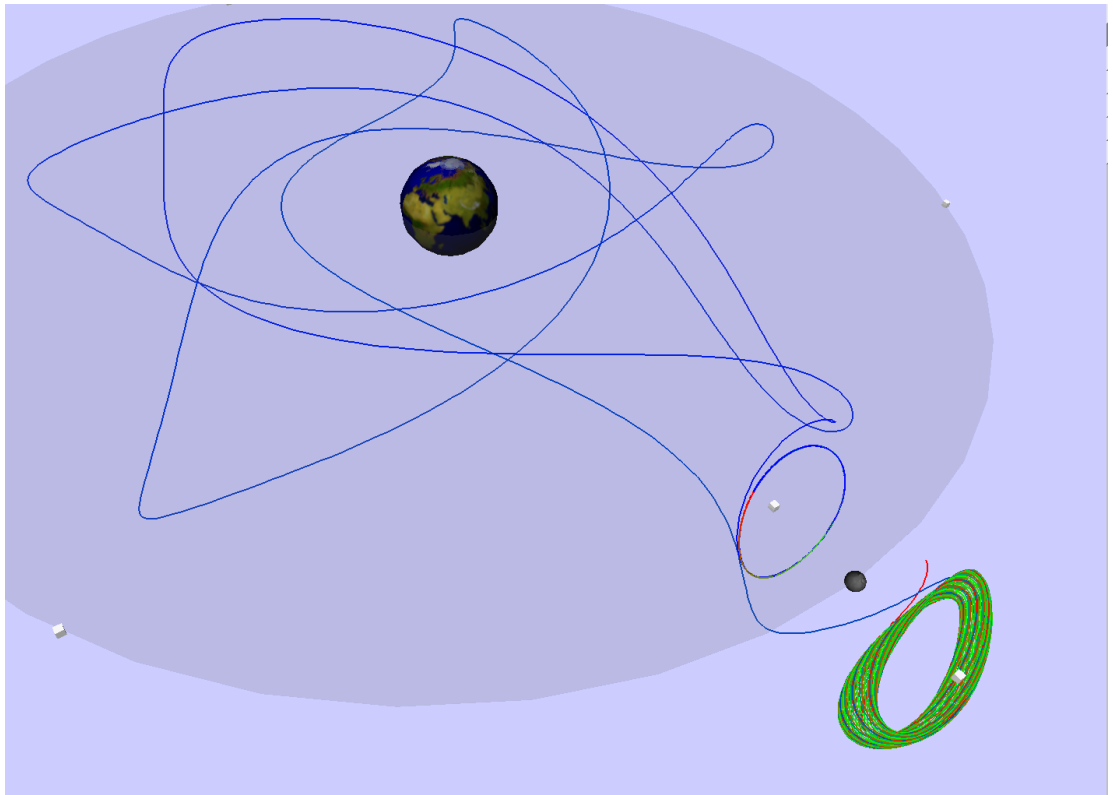
NEW2:Continuation, keeping the endpoint  $x(1)$  fixed.



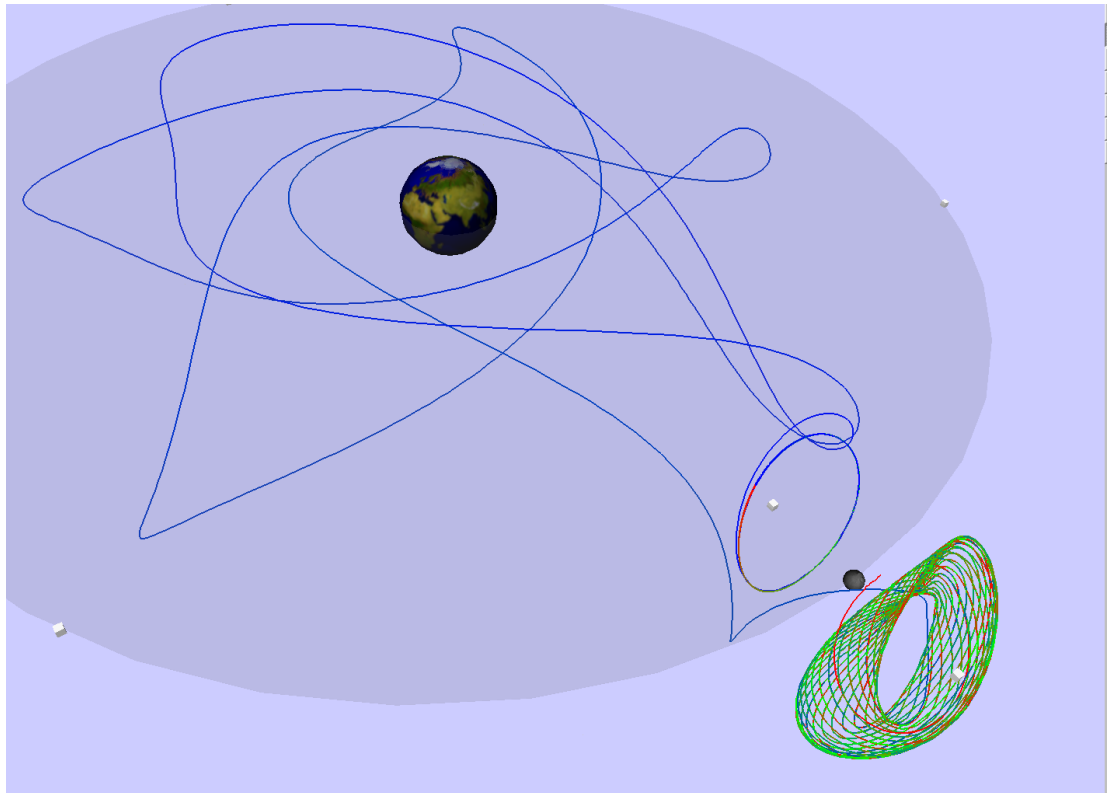
NEW2:Continuation, keeping the endpoint  $x(1)$  fixed.



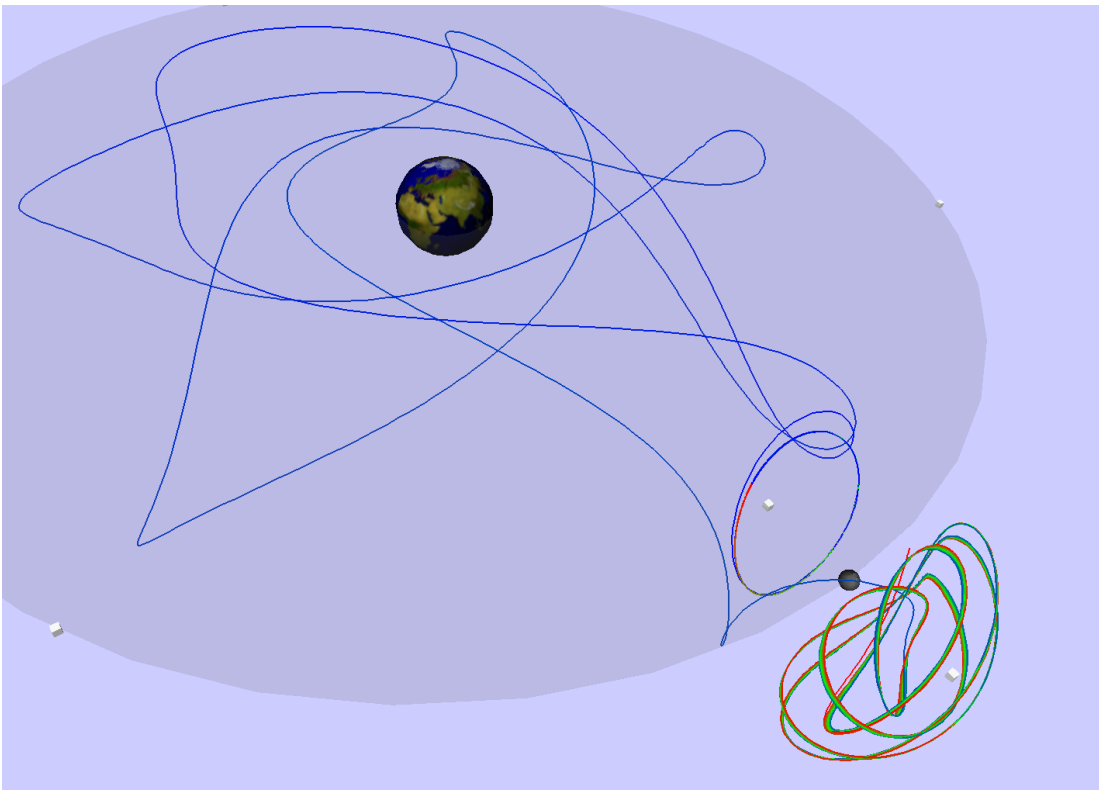
NEW2:Continuation, keeping the endpoint  $x(1)$  fixed.



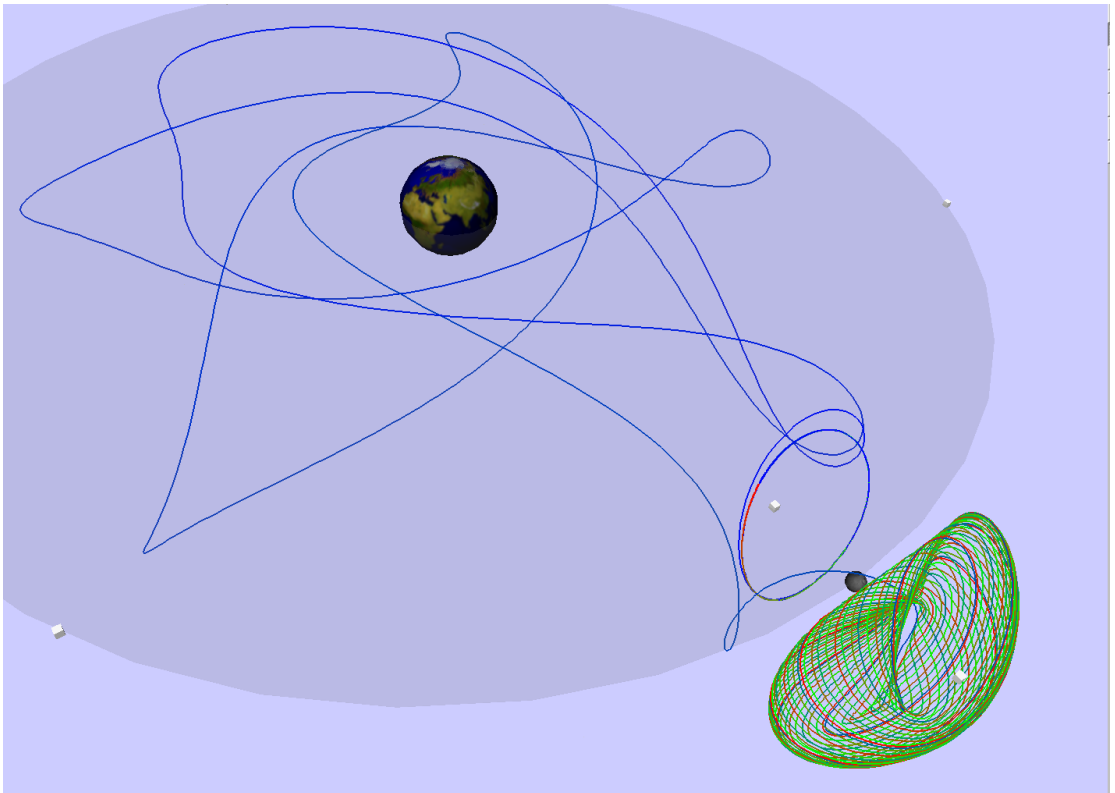
NEW2:Continuation, keeping the endpoint  $x(1)$  fixed.



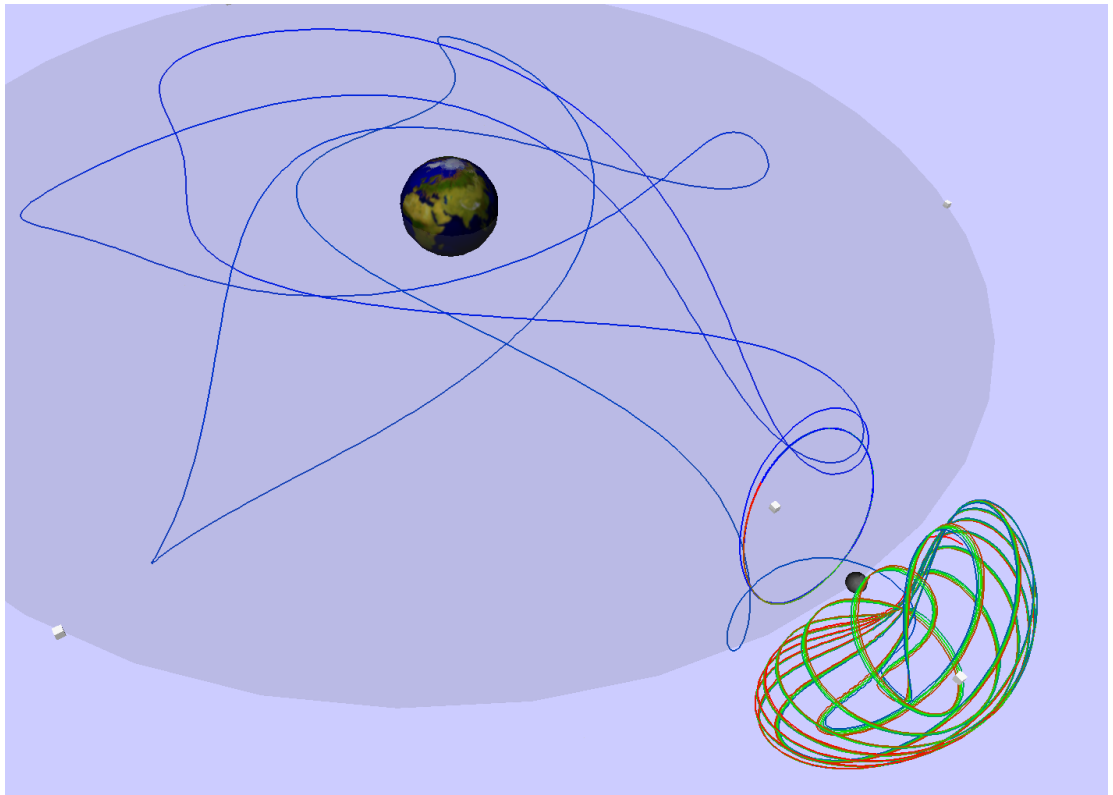
NEW2:Continuation, keeping the endpoint  $x(1)$  fixed.



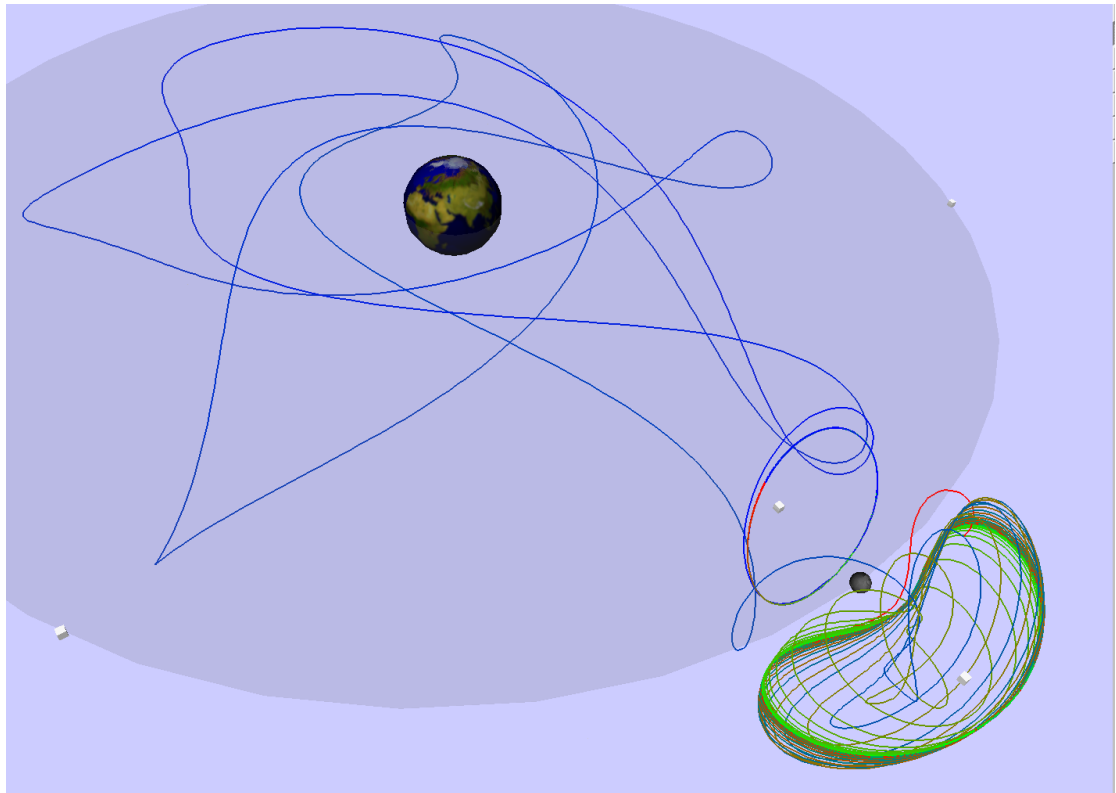
NEW2:Continuation, keeping the endpoint  $x(1)$  fixed.



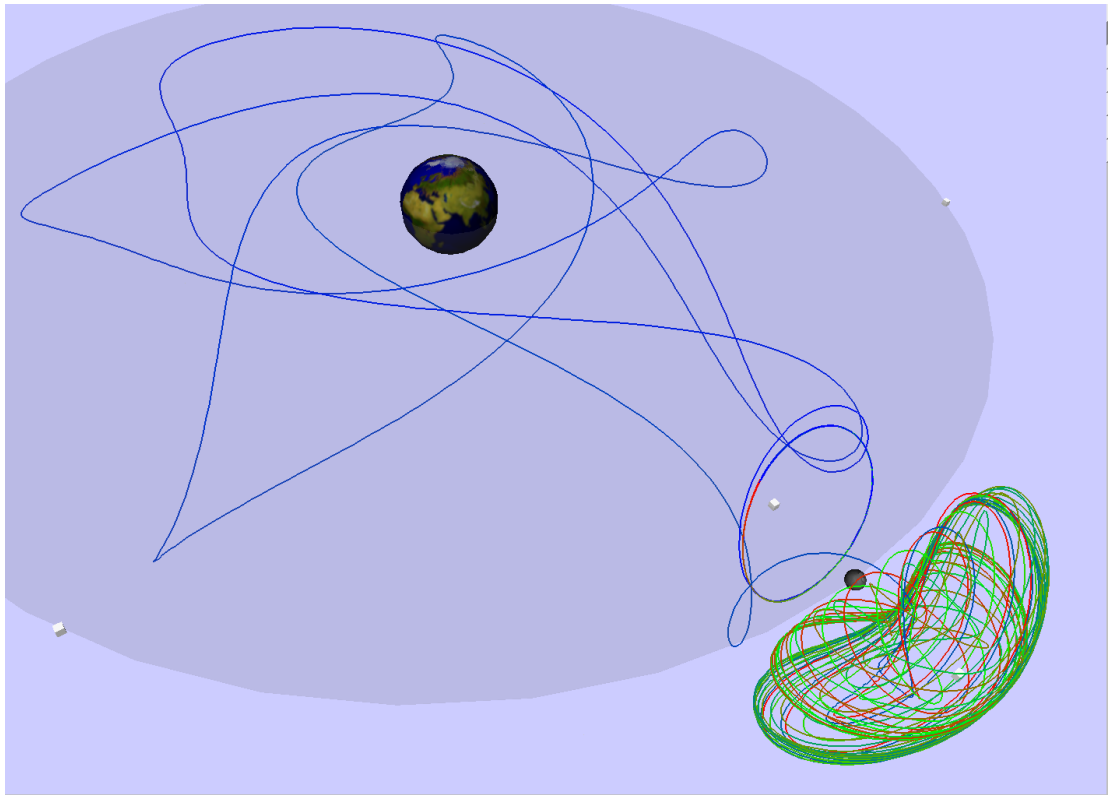
NEW2:Continuation, keeping the endpoint  $x(1)$  fixed.



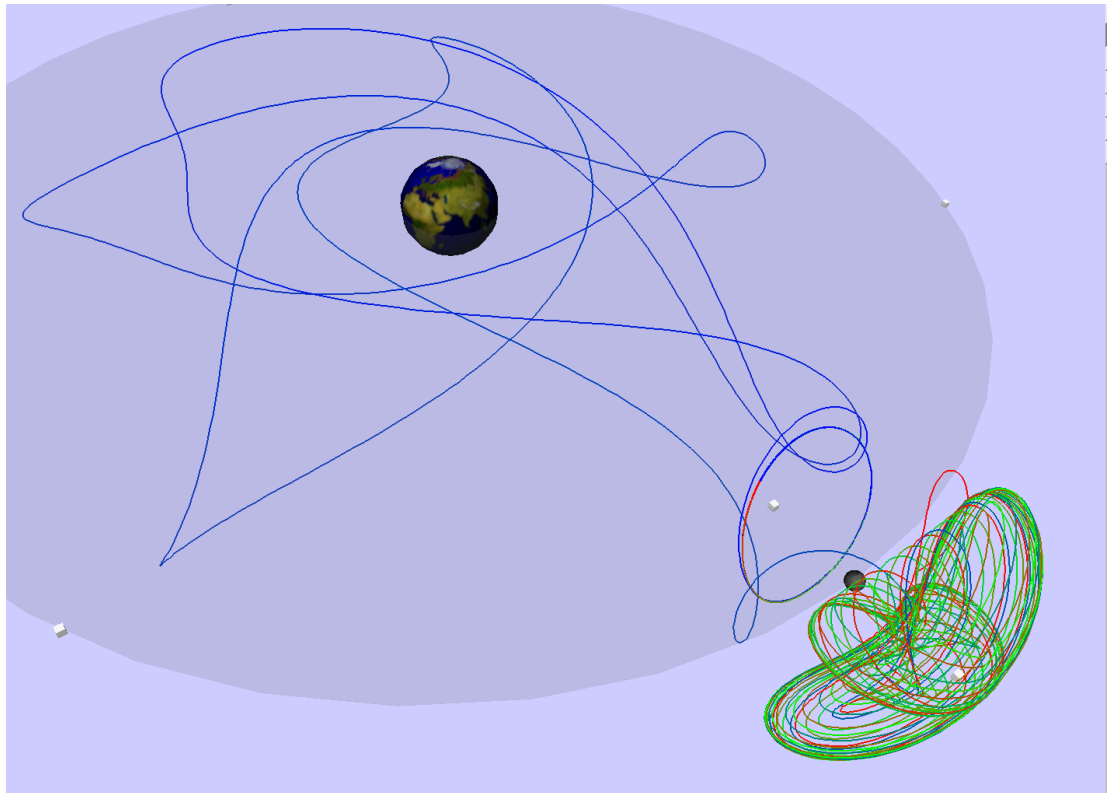
NEW2:Continuation, keeping the endpoint  $x(1)$  fixed.



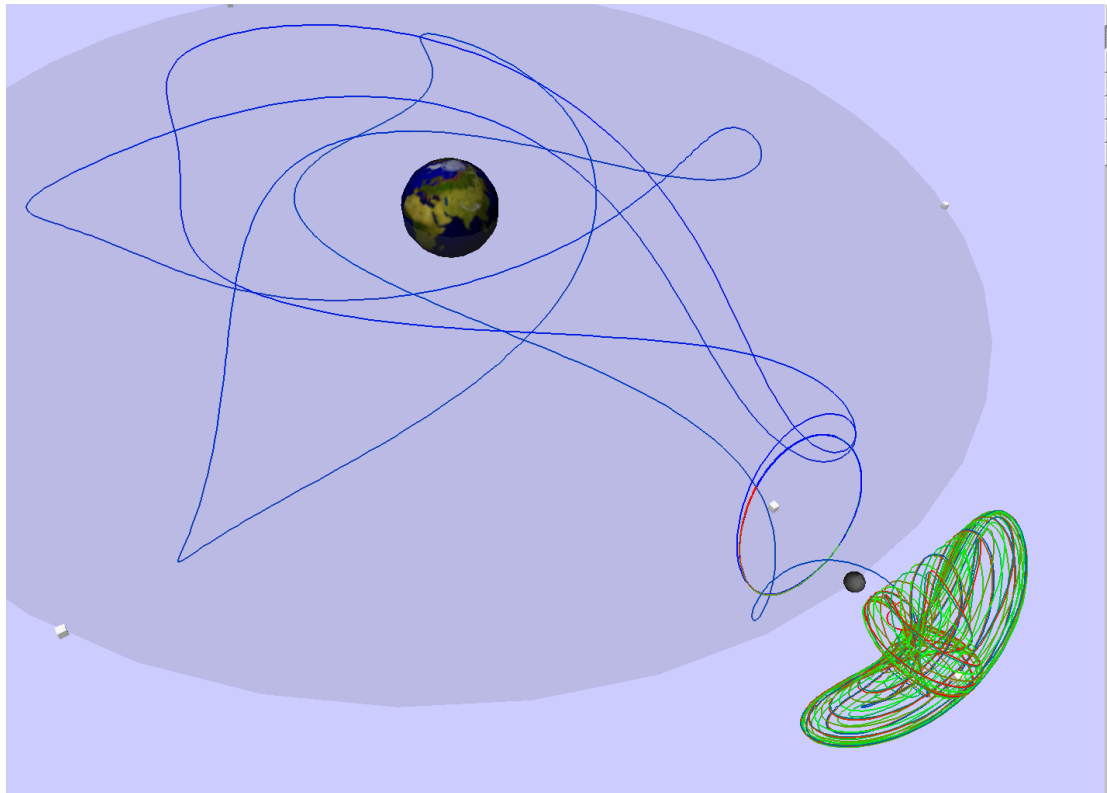
NEW2:Continuation, keeping the endpoint  $x(1)$  fixed.



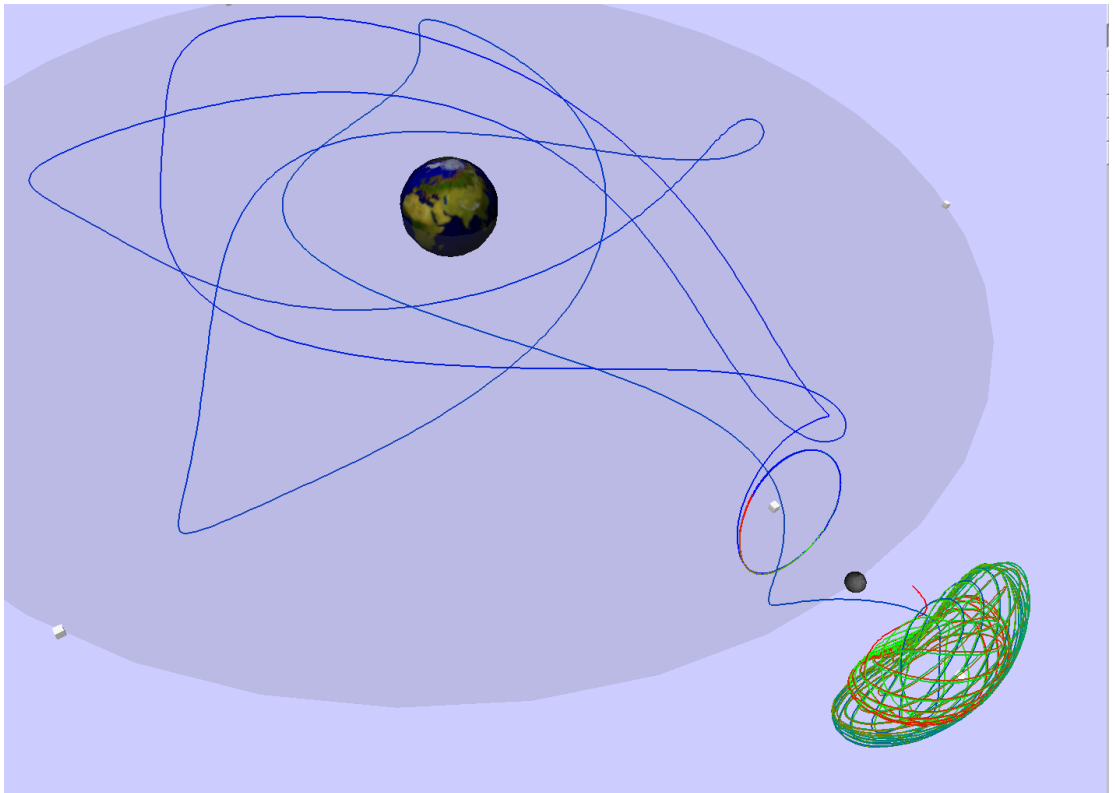
NEW2:Continuation, keeping the endpoint  $x(1)$  fixed.



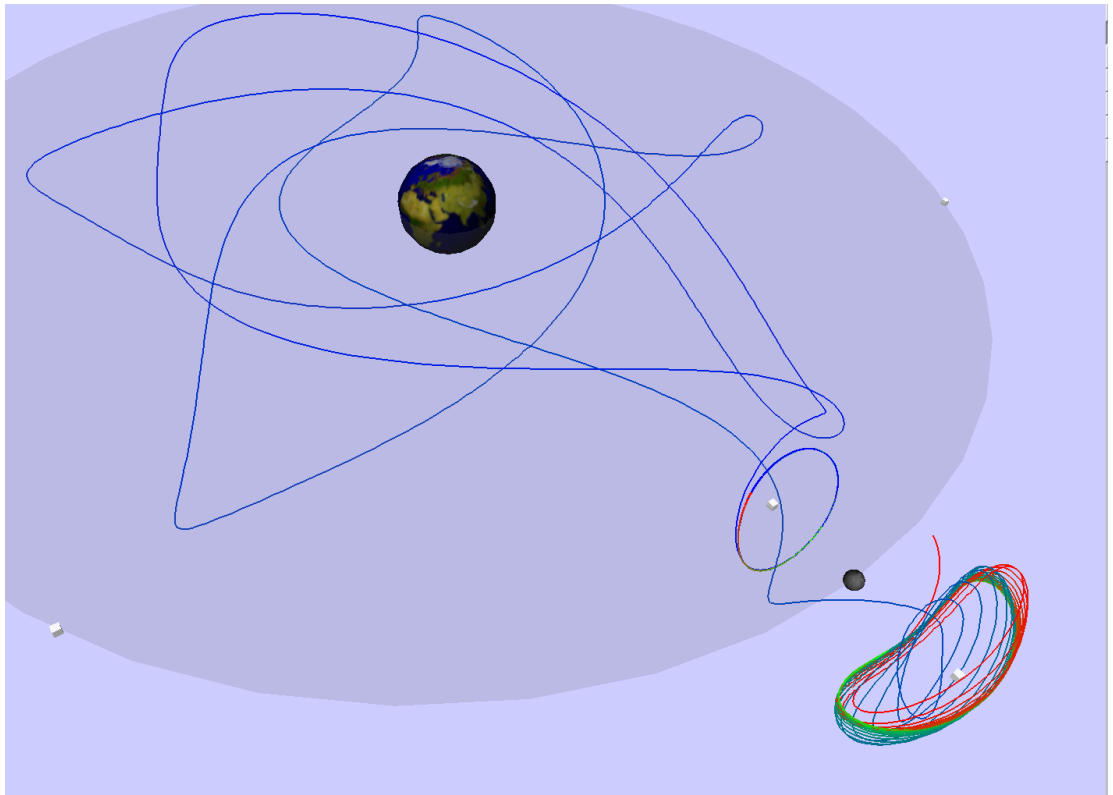
NEW2:Continuation, keeping the endpoint  $x(1)$  fixed.



NEW2:Continuation, keeping the endpoint  $x(1)$  fixed.



NEW2:Continuation, keeping the endpoint  $x(1)$  fixed.



NEW2:Continuation, keeping the endpoint  $x(1)$  fixed.

NOTE:

- Continuation with  $x(1)$  fixed can lead to a Halo-to-torus connection.
- This heteroclinic connection can be continued as a solution to

$$\mathbf{F}(\mathbf{X}_k) = \mathbf{0},$$

$$\langle \mathbf{X}_k - \mathbf{X}_{k-1}, \dot{\mathbf{X}}_{k-1} \rangle - \Delta s = 0.$$

where

$$\mathbf{X} = (\text{Halo orbit}, \text{Floquet function}, \text{connecting orbit}).$$

# Traveling Waves

- One can also use continuation to compute traveling wave phenomena.
- We illustrate this for a particular model from Biology.

# Wave Phenomena in a Distributed System

- We want to find *traveling waves* in a parabolic PDE.
- The PDE has *one* space dimension.
- *Traveling waves* are *periodic solutions* of a "reduced" ODE system.
- *Solitary waves* correspond to *homoclinic orbits* in the reduced system.
- *Moving fronts* are *heteroclinic orbits* in the reduced system.
- Thus ODE continuation techniques can be used.

# An Enzyme Model

- We consider an enzyme catalyzed reaction involving two substrates.
- The reaction takes place inside a single compartment.
- A membrane separates the compartment from an outside reservoir.
- In the reservoir the substrates are kept at a constant level.
- Enzymes are embedded in the membrane.
- The enzymes activate the reaction.

A *simple model* of such a reaction is

$$s'(t) = (s_0 - s) - \rho R(s, a),$$

$$a'((t) = \alpha(a_0 - a) - \rho R(s, a).$$

- $s$  and  $a$  denote the *concentrations* of two chemical species.
- The reaction takes place inside a *compartment*.
- An excess of concentration of  $s$  *inhibits* the reaction.
- $a$  always *activates* the reaction.
- The *reaction rate* is proportional to

$$R(s, a) = \frac{a}{\kappa_1 + a} \frac{s}{1 + s + \kappa_2 s^2}.$$

- $s_0$  and  $a_0$  are the constant concentrations in the *outside reservoir*.
- The reaction is *catalyzed* by an enzyme.

This equation has been used to model a reaction with

substrates *Oxaloacetate* and *NADH* ,  
and *catalyzed* by  
*Malate Deshydrogenase* .

In this case appropriate parameter values are:

$$\kappa_1 = 3.4 \quad , \quad \kappa_2 = 0.023 \quad , \quad \alpha = 0.2 \quad .$$

Thus there are three parameters left, namely,

$$s_0 \quad , \quad a_0 \quad , \quad \rho \quad .$$

First we also fix

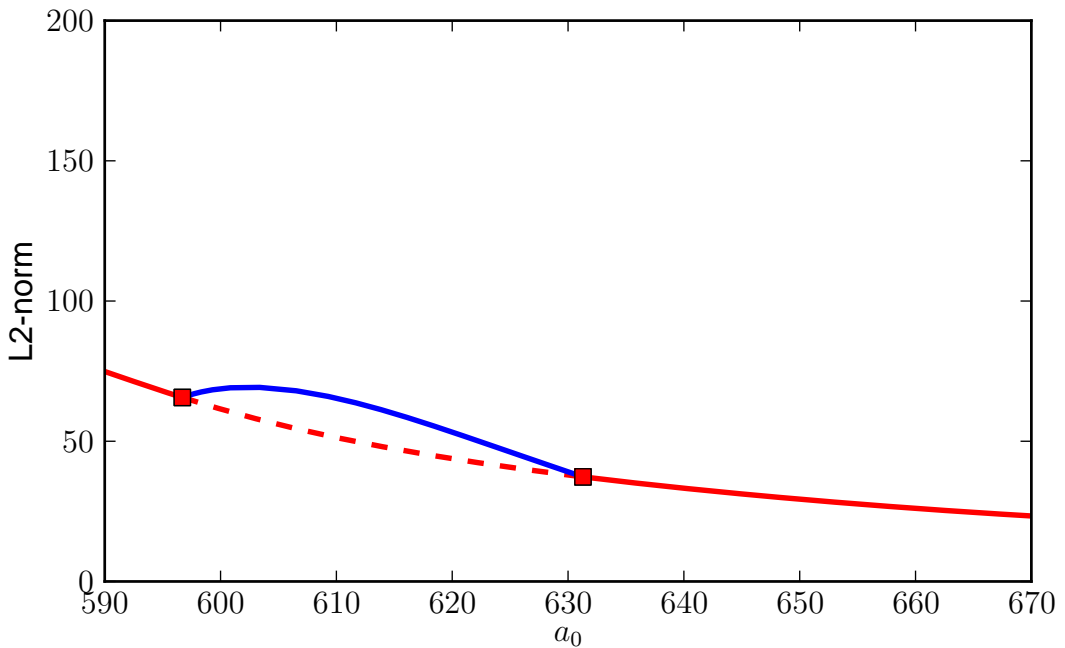
$$\rho = 210 \quad ,$$

and we use

$a_0$  as *bifurcation parameter* ,

for each of the values

$$s_0 = 143.0 \quad , \quad s_0 = 144.5 \quad , \quad s_0 = 145.0 \quad .$$

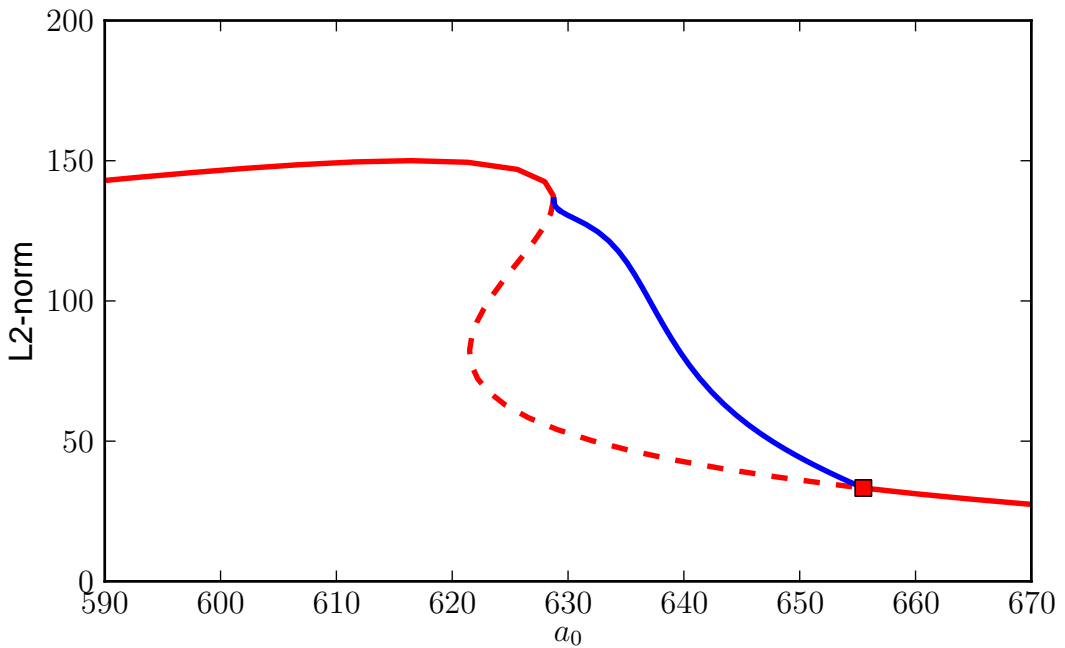


Bifurcation diagram of the ODE for  $s_0 = 143.0$ ,  $\rho = 210$ .

Red: Stationary states ; Blue: Periodic orbits.

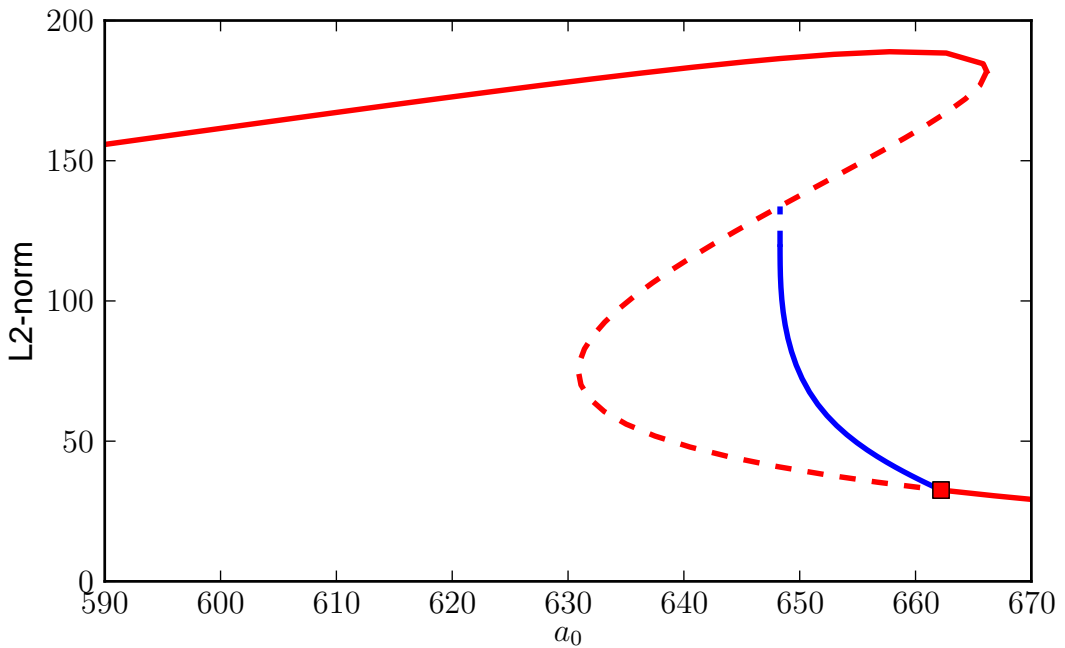
The periodic family connects two *Hopf bifurcations* .

Solid: Stable ; Dashed: Unstable.



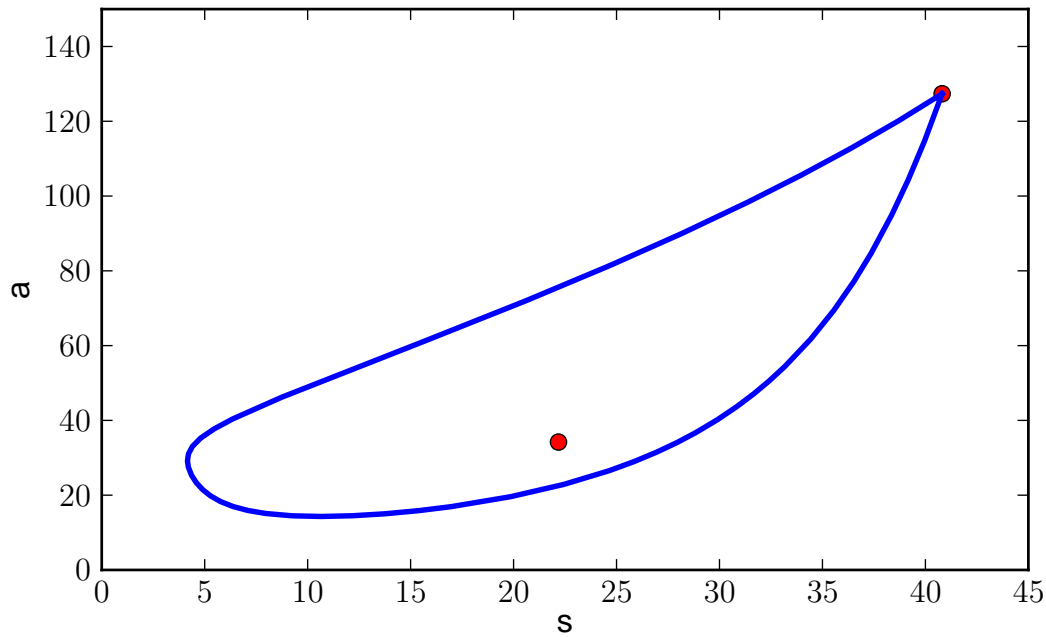
Bifurcation diagram of the ODE for  $s_0 = 144.5$ ,  $\rho = 210$ .

The periodic family ends in a *saddle-node homoclinic orbit*.



Bifurcation diagram of the ODE for  $s_0 = 145.0$ ,  $\rho = 210$ .

The periodic family ends in a *saddle homoclinic orbit*.

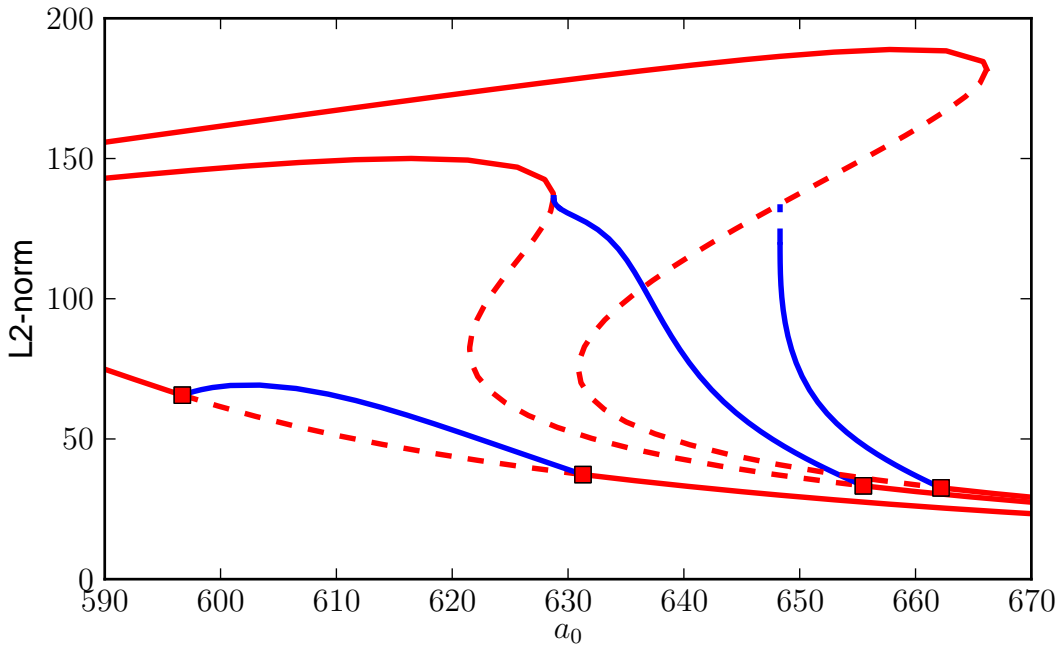


The *saddle homoclinic orbit* that terminates the periodic family.

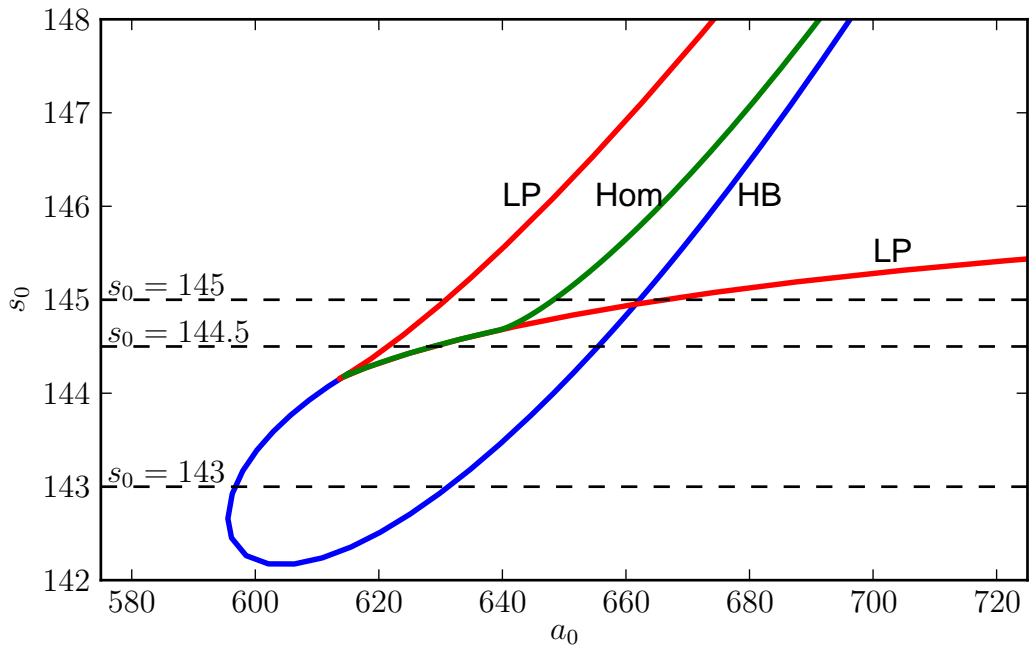
( $s_0 = 145.0$  ; The two stationary points are also indicated.)

NOTE:

- For  $s_0 = 143$  a family of *stable periodic orbits* connects the Hopf points.
- For  $s_0 = 144.5$  there is only *one* Hopf bifurcation.
- At the other end the family ends in a *saddle node homoclinic orbit* .
- For  $s_0 = 145$  there is also only *one* Hopf bifurcation.
- At the other end the family ends in a *saddle homoclinic orbit* .
- The bifurcation diagrams are shown superimposed in the next Figure.



The superimposed bifurcation diagrams.



Loci of folds, Hopf bifurcations, and homoclinic orbits.

NOTE:

- The preceding 2-parameter diagram shows *loci* of "singular points".
- (Loci of *folds*, *Hopf bifurcations*, and *homoclinic orbits*.)
- There is a *cusp* on the locus of folds in the 2-parameter diagram.
- The Hopf bifurcation locus *terminates* on the fold locus near the cusp.
- At this end point the Hopf bifurcation has *infinite period*.
- (The steady state Jacobian has a *double zero eigenvalue* there.)
- (The *geometric multiplicity* of this eigenvalue is 1.)
- This singular point is called a *Takens-Bogdanov* (TB) bifurcation.

NOTE: continued . . .

- The locus of *homoclinic orbits* also emanates from the TB point.
- Part of the locus of homoclinic orbits *follows* the fold locus.
- These homoclinic orbits are called *saddle-node homoclinic orbits* .
- The *stationary point* on these homoclinic orbits is a *fold* point.
- (Thus this stationary point has a *zero eigenvalue* .)
- *Compare* the 2-parameter diagram to the 1-parameter diagrams !

# The Enzyme Model with Diffusion

Now consider the  $s$ - $a$  system with *diffusion*, namely, the PDE

$$s_t = s_{xx} - \lambda[\rho R(s, a) - (s_0 - s)] ,$$

$$a_t = \beta a_{xx} - \lambda[\rho R(s, a) - \alpha(a_0 - a)] ,$$

with, as before,  $a_0$  as a *free parameter*, and

$$\rho = 210 , \quad \kappa_1 = 3.4 , \quad \kappa_2 = 0.023 ,$$

and

$$s_0 = 145 , \quad \beta = 5 , \quad \lambda = 3 .$$

Look for traveling waves:

$$s(x, t) = s(x - ct) , \quad a(x, t) = a(x - ct) .$$

This reduces the PDE to two coupled ODEs:

$$s'' = -cs' + \lambda[\rho R(s, a) - (s_0 - s)] ,$$

$$a'' = -\frac{c}{\beta}a' + \frac{\lambda}{\beta}[\rho R(s, a) - \alpha(a_0 - a)] .$$

Rewrite the *reduced system*

$$s'' = -cs' + \lambda[\rho R(s, a) - (s_0 - s)] ,$$

$$a'' = -\frac{c}{\beta}a' + \frac{\lambda}{\beta}[\rho R(s, a) - \alpha(a_0 - a)] ,$$

as a *first order* system

$$s' = u ,$$

$$u' = -cu + \lambda[\rho R(s, a) - (s_0 - s)] ,$$

$$a' = v ,$$

$$v' = -\frac{c}{\beta}v + \frac{\lambda}{\beta}[\rho R(s, a) - \alpha(a_0 - a)] .$$

The *stationary states* satisfy

$$u = v = 0 ,$$

$$\rho R(s, a) - (s_0 - s) = 0 ,$$

$$\rho R(s, a) - \alpha(a_0 - a) = 0 .$$

NOTE:

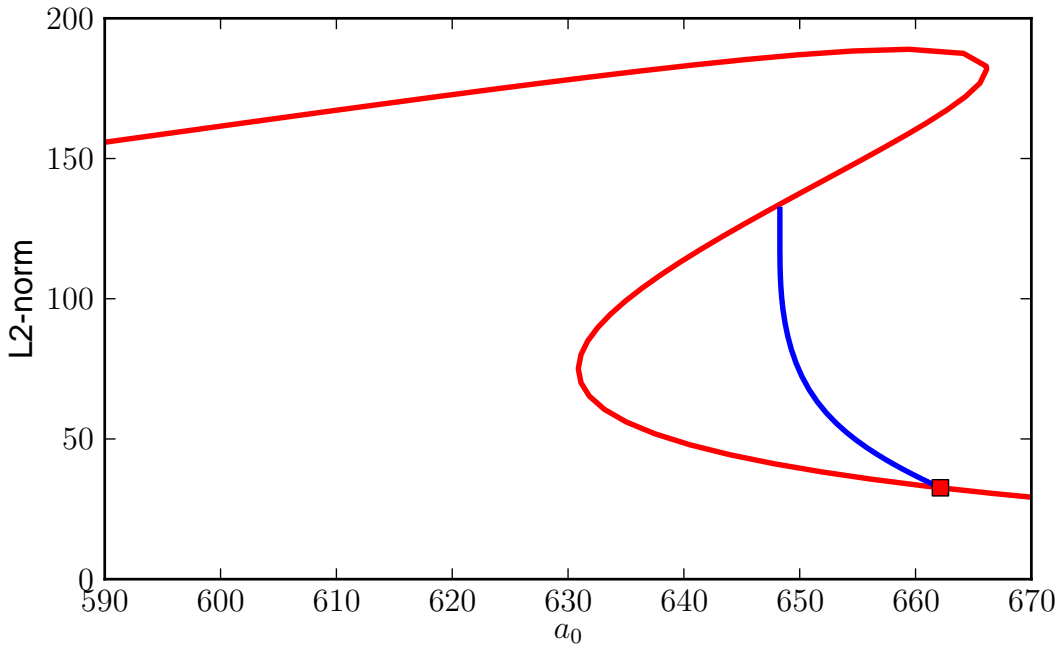
- The stationary states *do not depend* on the wave speed  $c$ .
- The stationary states are those of the system *without diffusion* .
- The Jacobian of the stationary states now *depends on*  $c$ .
- Thus the Hopf bifurcations need *not* be present.
- However, for *large*  $c$  there *must* be a Hopf bifurcation.
- The Hopf bifurcation *approaches* the ODE Hopf as  $c$  gets large.
- Thus there are PDE *wave trains* for large  $c$  , when  $s_0 = 145.$  .
- The ODE homoclinic orbit implies PDE *solitary waves* for large  $c$ .

# Wave Trains and Solitary Waves

For the first bifurcation diagram for the *reduced system* we use  $c = 100$ .

Indeed, we find that

- The stationary states are those of the system *without diffusion*.
- There is a *Hopf bifurcation* near the ODE Hopf bifurcation.
- The family of periodic orbits indeed ends in a *homoclinic orbit*.



Bifurcation diagram of the reduced system for  $c = 100$ .

From the diagram for  $c = 100$  we can conclude that

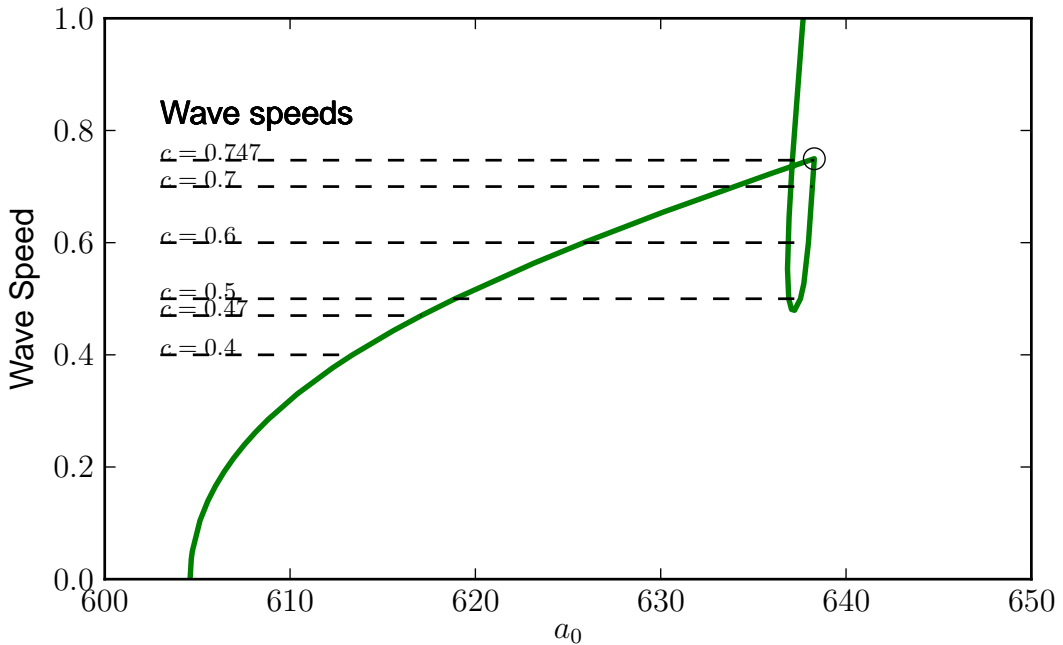
- The PDE has *wave trains* of wave speed  $c = 100$ .
- The PDE has a *solitary wave* of wave speed  $c = 100$ .

Note that

- Stabilities are different from those for the system without diffusion.
- (The diagrams do *not* show stability now.)

Next:

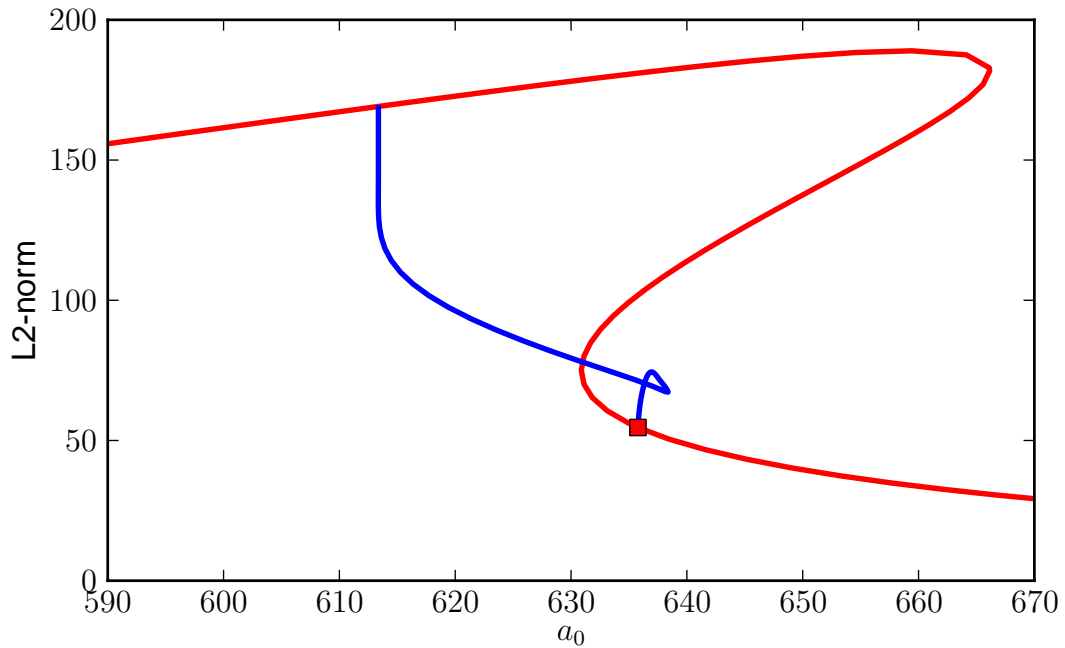
- Are there *low speed* wave trains and *low speed* solitary waves ?
- To find out we compute the *locus of homoclinics* of the *reduced system*.
- As free parameters we use  $a_0$  and the wave speed  $c$ .



The locus of solitary waves. (Shown for smaller values of the wave speed.)

From the preceding diagram we can draw the following *conclusions*:

- For wave speeds between 0.48 and 0.77 there are *three solitary waves*.
- These are at different  $a_0$ -values, but have the *same wave speed*.
- Near  $a_0 = 605$  there is a solitary wave of *wave speed zero*.
- (This is a *stationary wave*.)
- The circled *special point* will be discussed later.
- We first show a *1-parameter diagram* for  $c = 0.4$ .



Bifurcation diagram of the reduced system for  $c = 0.4$ .

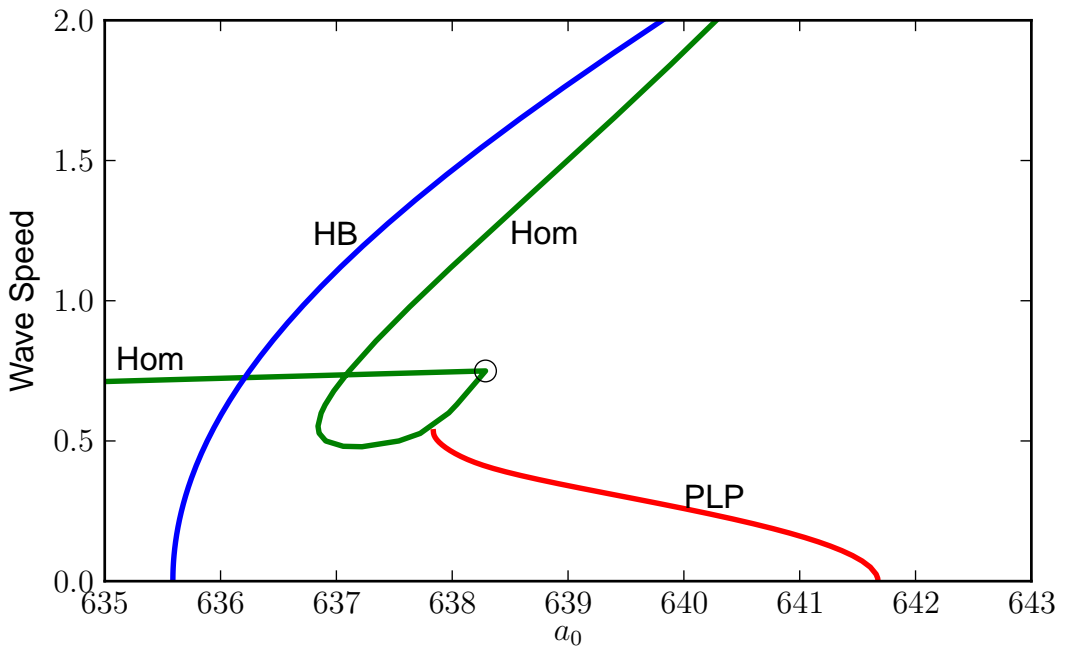
The blue branch represents wave trains.

Its homoclinic end point is a solitary wave.

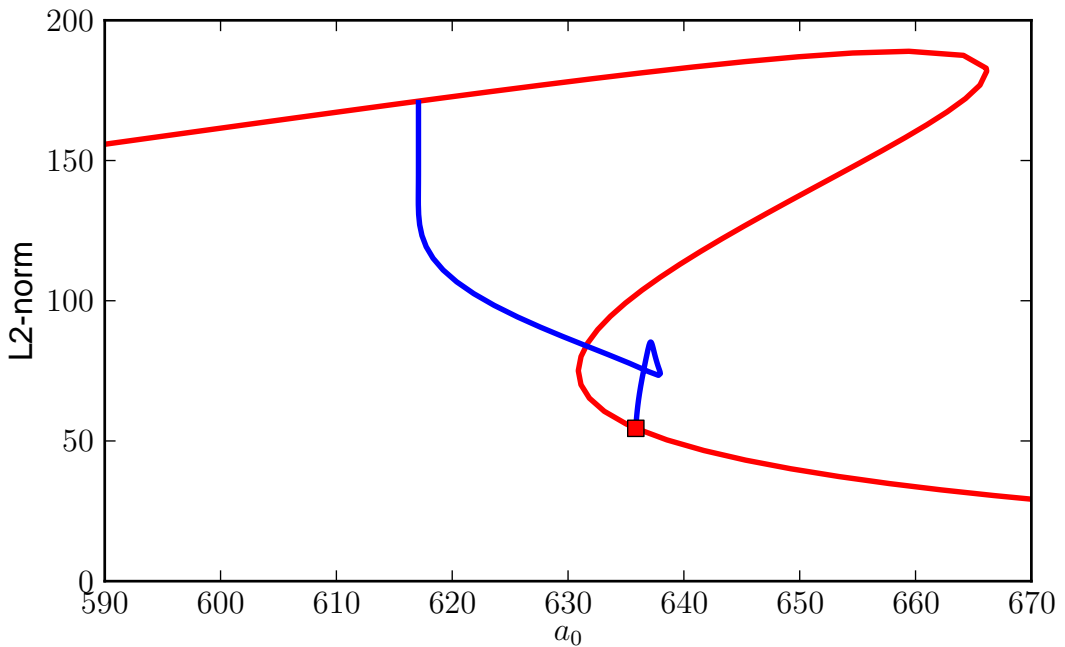
Stability is not shown in this diagram.

For the diagram for  $c = 0.4$  we note that

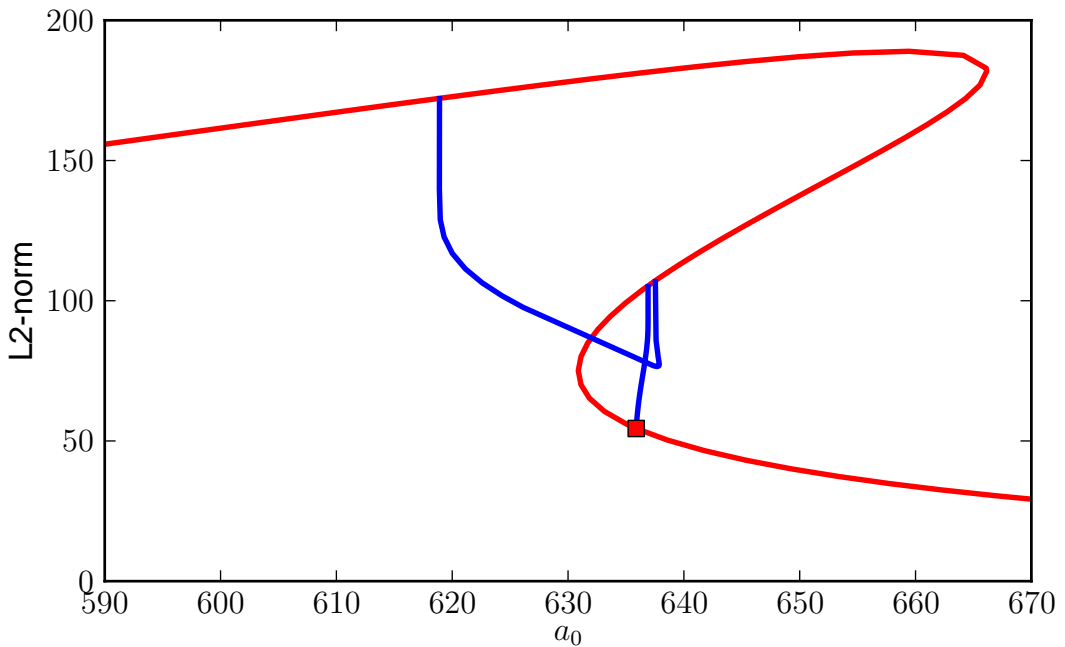
- There is a *fold* on the wave train family.
- We can compute the *locus* of such *folds* for varying  $a_0$  and  $c$ .
- We can also compute the *locus of Hopf points* for varying  $a_0$  and  $c$ .
- We add these loci to the diagram with the *locus of solitary waves*.
- We also show 1-parameter diagrams for more values of  $c$ .



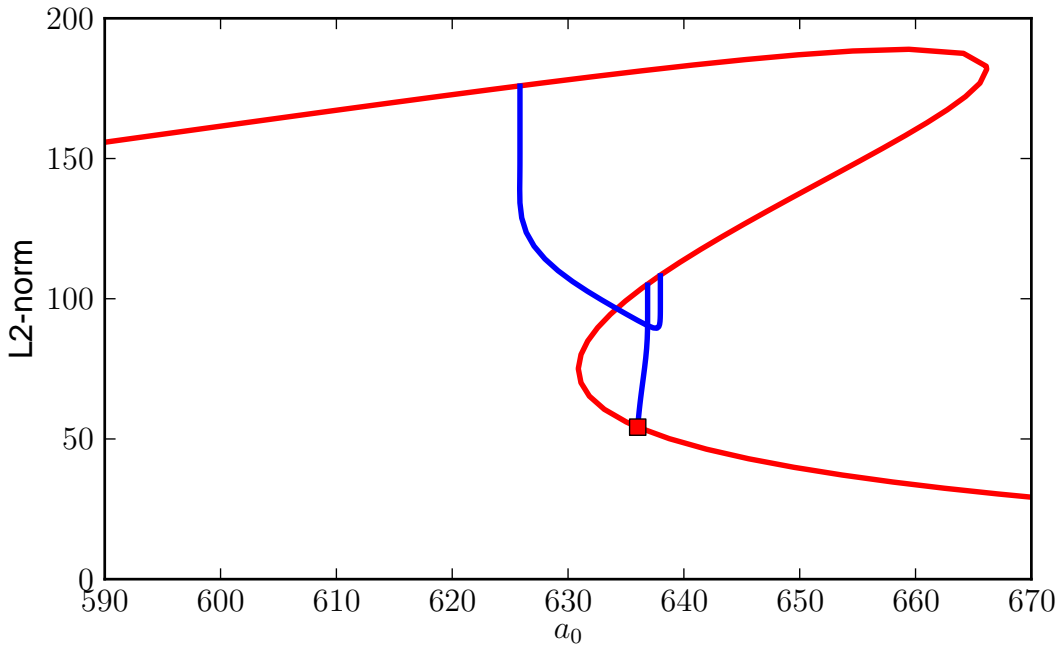
Homoclinic orbits (solitary waves), Hopf bifurcations, and folds.



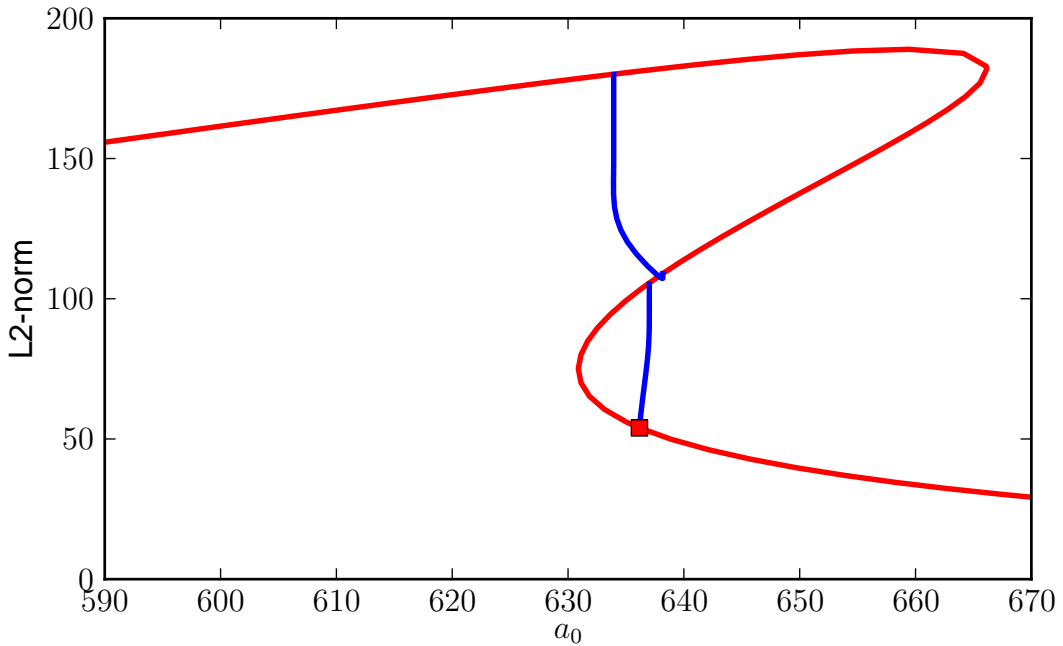
Bifurcation diagram of the reduced system for  $c = 0.47$ .



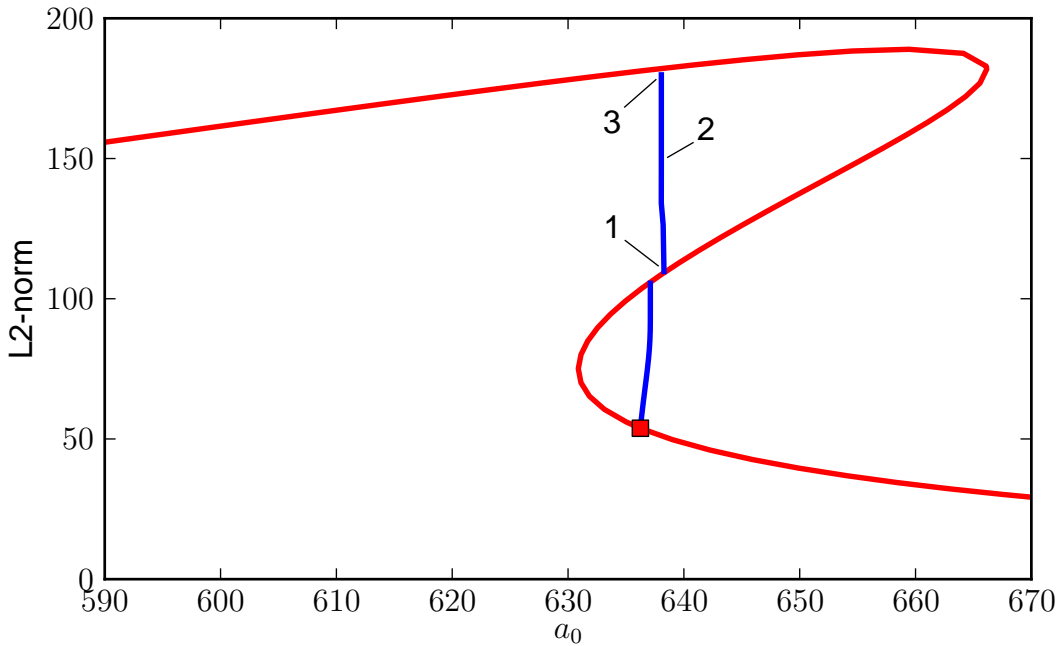
Bifurcation diagram of the reduced system for  $c = 0.5$ .



Bifurcation diagram of the reduced system for  $c = 0.6$ .



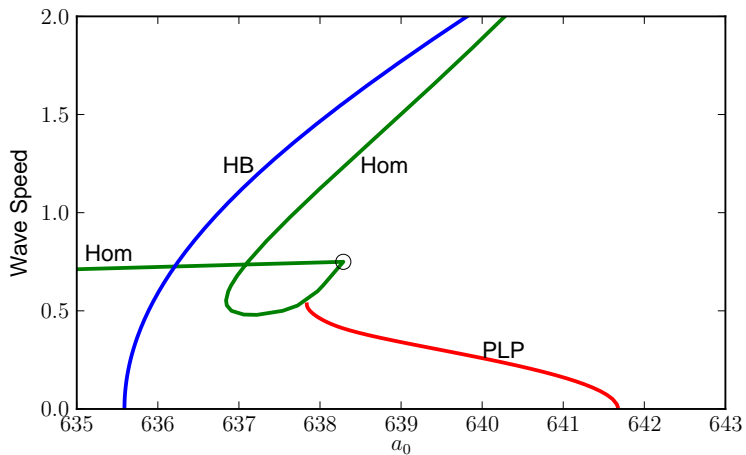
Bifurcation diagram of the reduced system for  $c = 0.7$ .



Bifurcation diagram of the reduced system for  $c = 0.747$ .

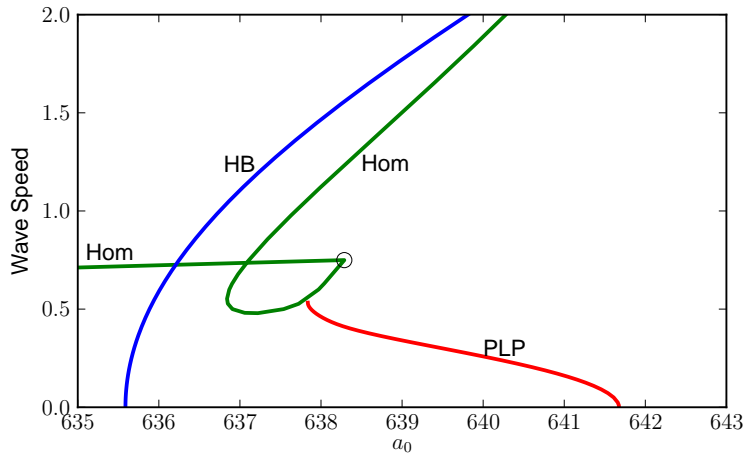
NOTE:

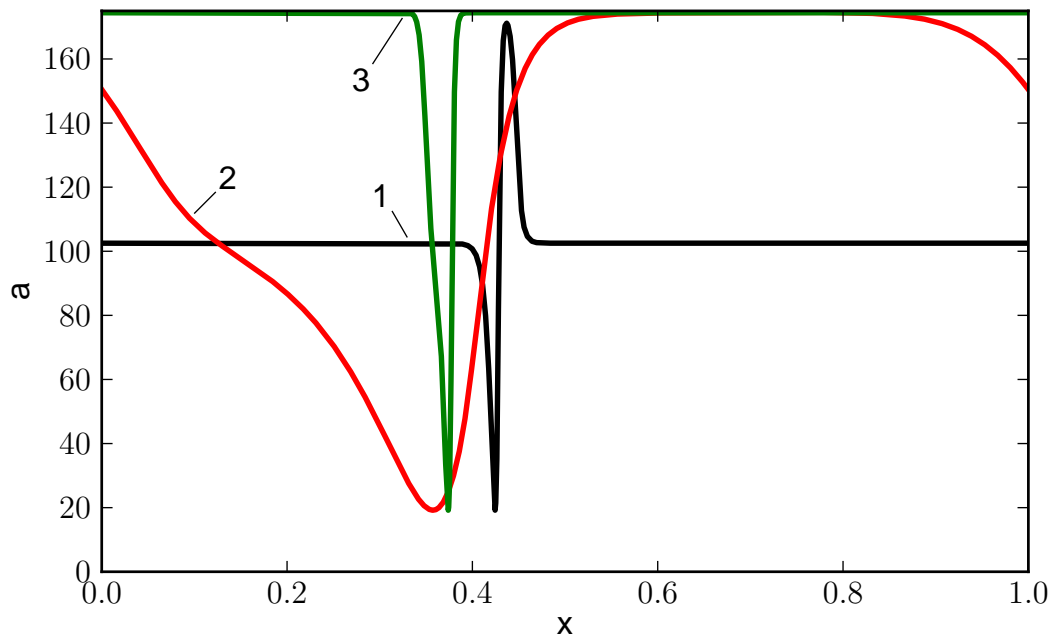
- There is a *fold* w.r.t. the wave speed  $c$  on the solitary wave locus.
- (This fold is near  $c = 0.45$ ,  $a_0 = 637.2$ .)
- Two *new solitary waves* appear at that point.



Now consider the *circled point* near  $a_0 = 638.5$ ,  $c = 0.749$ :

- It then represents a *transition* from one solitary wave to another.
- In the diagram for  $c = 0.747$  note the *near-vertical* family.
- It is a *wave-train family* connecting the solitary waves 1 and 3.
- At the section through the circled point the family is *exactly vertical*.

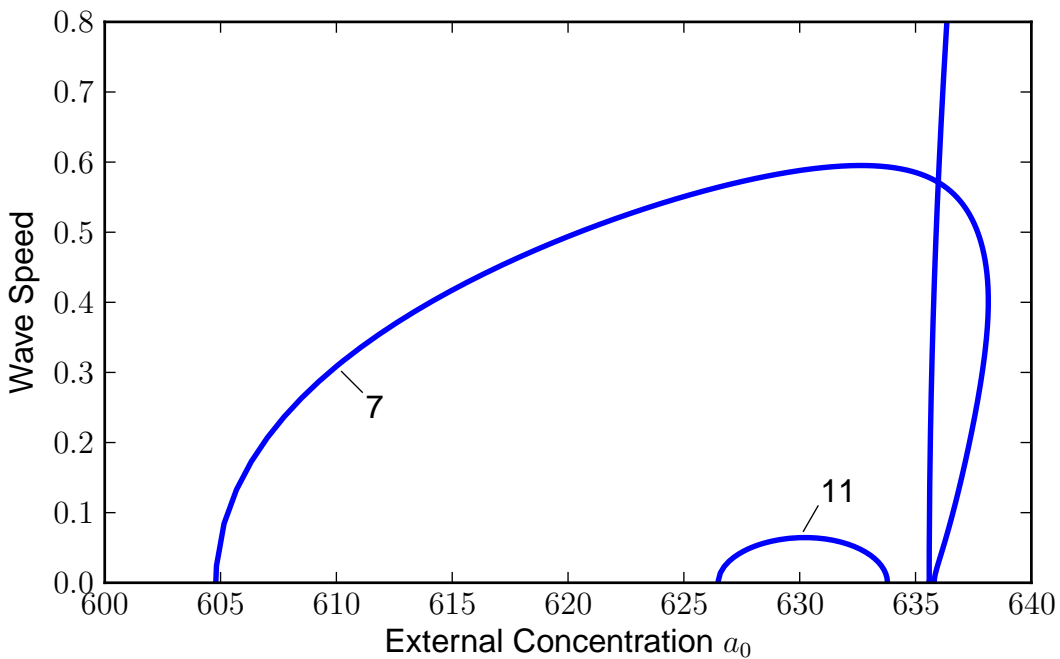




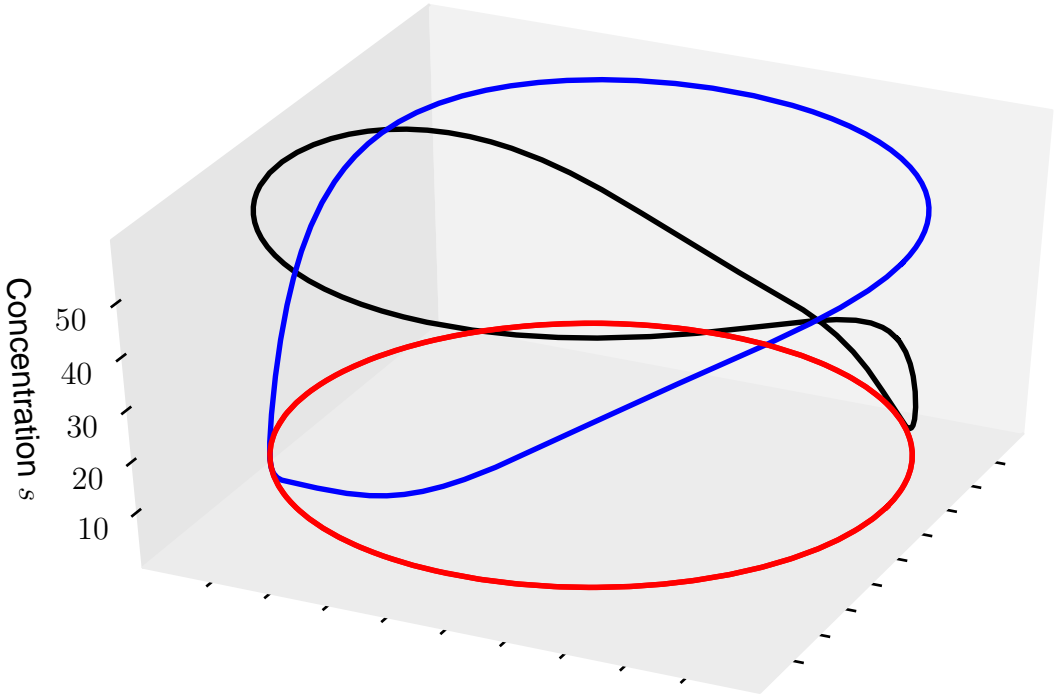
Three periodic solutions that represent solitary waves.  
The independent variable has been scaled to the interval  $[0,1]$ .

# Traveling Waves on a Ring

- We locate traveling wave solutions of *given wave length*  $L$ .
- If necessary we put two or more waves *in series* to get wave length  $L$ .
- For the choice  $L = 22$  we found *five distinct waves* this way.
- We can *continue* these for varying  $a_0$  and  $c$ , with  $L = 22$  *fixed*.
- This corresponds to computing traveling waves on a *ring* of size  $L = 22$ .
- Results are shown projected onto the  $a_0 - c$ -plane in the next diagram.



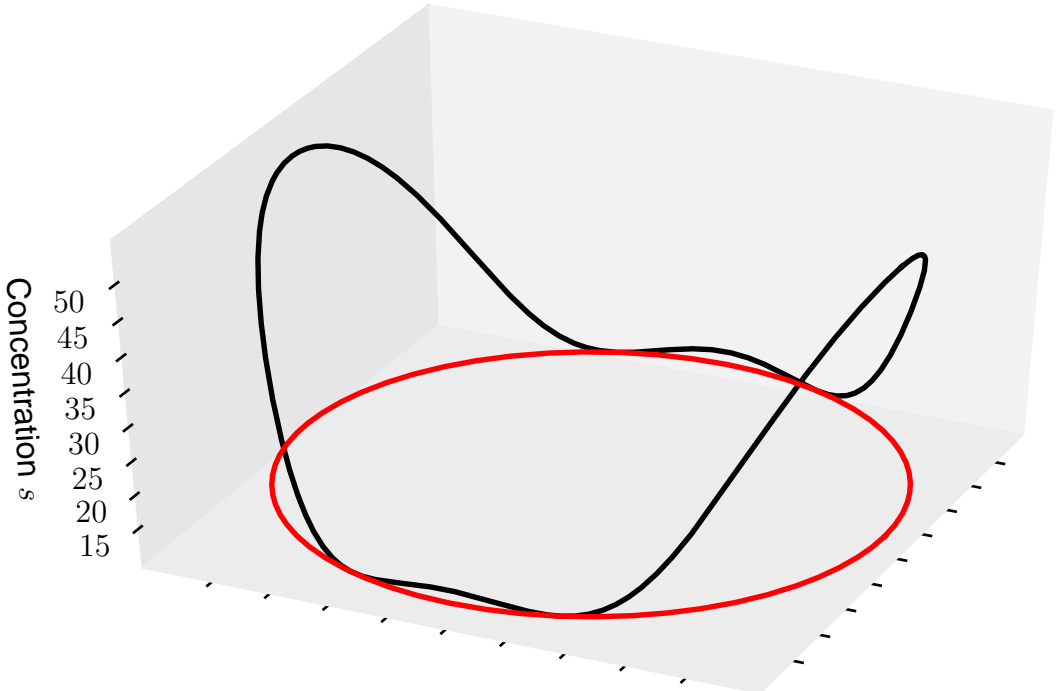
Loci of traveling wave solutions on a ring of size  $L = 22$ .



A traveling wave on the ring. (The solution with label 7.)

# Stationary Waves on a Ring

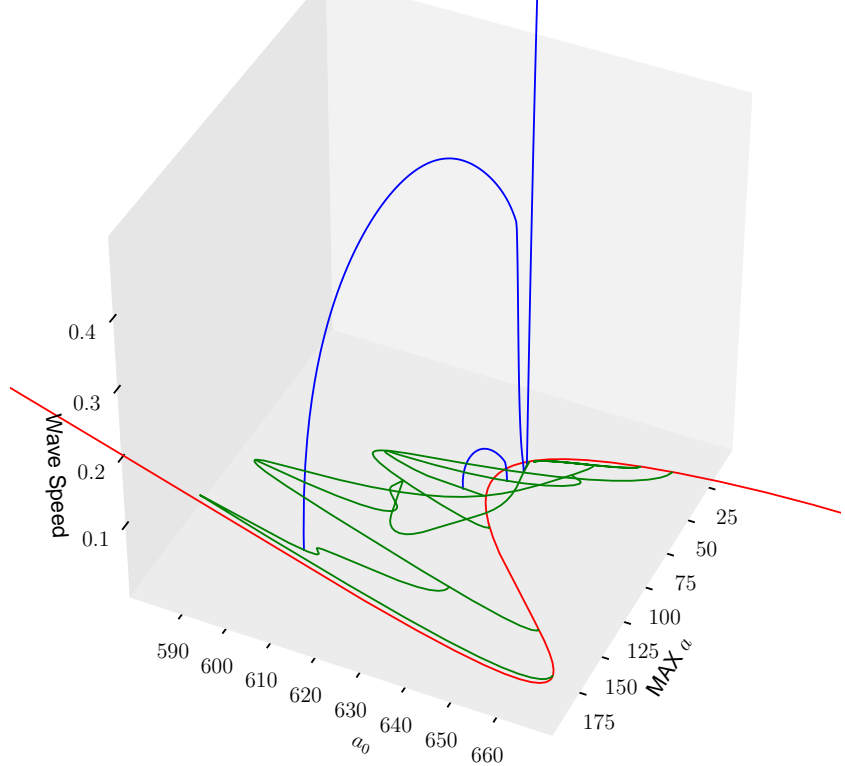
- There are also families of *stationary waves* ("patterns") on the ring.
- Like traveling waves, these are *not unique*.
- (They can be *phase shifted*, i.e., rotated around the ring).
- Such patterns can be found by *time-integrating* unstable traveling waves.
- For example, traveling wave 11 is *unstable*.
- After time integration it approaches a *stationary wave*.
- This stationary wave is shown in the following diagram.



A stationary wave on the ring, obtained after time integration  
of the unstable traveling wave with label 11.

NOTE:

- Stationary waves can be *continued as traveling waves* with  $c = 0$ .
- A *phase condition* is necessary in this continuation.
- (Because stationary waves can be phase-shifted.)
- The next diagram shows a *skeleton* of the solution structure.



Traveling waves, stationary waves and uniform states

NOTE:

- The S-shaped curve with  $c = 0$  represents *spatially uniform states* .
- Other curves in the  $c = 0$  plane represent *stationary waves* .
- Curves that rise above the  $c = 0$  plane represent *traveling waves* .
- Time integration of unstable traveling waves gives *other solutions* .
- For example, waves *bouncing* off each other are found.
- Some of these are stable, while others are *transient* .